11-26-2015 12:00 AM

Pulmonary Imaging to Better Understand Asthma

Sarah Svenningsen
The University of Western Ontario

Supervisor
Grace Parraga
The University of Western Ontario

Graduate Program in Medical Biophysics
A thesis submitted in partial fulfillment of the requirements for the degree in Doctor of Philosophy

PULMONARY IMAGING TO BETTER UNDERSTAND ASTHMA

(Thesis format: Integrated Article)

by

Sarah Svenningsen, BMSc

Graduate Program in Medical Biophysics

Schulich School of Medicine and Dentistry

A thesis submitted in partial fulfillment
of the requirements for the degree of
Doctor of Philosophy

The School of Graduate and Postdoctoral Studies
The University of Western Ontario
London, Ontario, Canada

Abstract

Asthma is characterized using the spirometry measurement of the forced expiratory volume in one second (FEV_1). Simple and inexpensive, FEV_1 provides a global estimate of lung function but this metric cannot regionally identify airways responsible for airflow limitation, asthma symptoms or control. Work that brought about an understanding that airway abnormalities are heterogeneously distributed within the lung in asthma patients has motivated the development of pulmonary imaging approaches, such as hyperpolarized helium-3 (^3He) and xenon-129 (^{129}Xe) magnetic resonance imaging (MRI). These methods provide a way to visualize and quantify lung regions accessed by gas during a breath-hold, as well as those not accessed, referred to as "ventilation defects." Despite the strong foundation for the use of MRI in asthma clinical care, clinical translation has been inhibited in part due to the current limited clinical and physiological understanding of ventilation defects. Accordingly, our objective was to better understand the structural determinants and clinical consequences of MRI ventilation defects observed in asthma and to provide a foundation for imaging to guide clinical decisions and asthma therapy. We evaluated the effect of gas properties on ventilation defects. In asthmatics, we compared hyperpolarized ^3He and ^{129}Xe MRI before and after bronchodilator administration and showed greater gas distribution abnormalities using ^{129}Xe compared to ^3He before bronchodilation. The temporal behavior of asthma ventilation defects was then investigated by generating personalized temporal-spatial pulmonary function maps from ^3He MR images acquired on three occasions. Persistent and intermittent defects were visualized and quantified using this tool and were recognized as potential intermediate endpoints or targets for treatment. We then evaluated clinical and emerging computed tomography-derived airway morphology measurements in asthmatics with and without defects. Ventilation defects were observed in two-thirds of well-controlled asthmatics who had worse lung function, increased airway inflammation, airway hyperresponsiveness and greater airway wall thickness than asthmatics without ventilation defects. Acknowledging that asthma control is the primary goal of asthma treatment, we investigated the relationship, and established a link between worse ventilation and poor control. These findings provide a better understanding of asthma ventilation defects and strongly support their potential as a novel treatment target.

Keywords

Asthma, Computed Tomography, Lung Function, Lung Structure, Magnetic Resonance Imaging, Hyperpolarized ^{3}He, Hyperpolarized ^{129}Xe, Pulmonary Imaging, Ventilation Defect

Co-Authorship Statement

The following thesis contains four manuscripts: three manuscripts have been published in scientific journals and one manuscript has been prepared for submission for publication. As the first author of these peer-reviewed manuscripts, Sarah Svenningsen was a significant contributor to all facets of the studies and in turn, manuscript preparation and submission. Specifically, Sarah made intellectual contributions to all study designs and was responsible for subject recruitment, organization and management of all patient visits. Specific tasks included the acquisition of pulmonary function and MRI data. Following data acquisition, Sarah was responsible for database organization, data analysis and interpretation, clinical/physiological interpretation of the data, drafting and final approval of manuscripts. As the Principal Investigator and Supervisor, Dr. Grace Parraga provided ongoing guidance and was responsible for study conception and experimental design, data acquisition and analysis plan and interpretation, drafting and final revisions and approval of the manuscripts as well as guarantor of integrity of the data as well as responsible for Good Clinical Practice. The management of study visits and acquisition of pulmonary function data was performed under the supervision of Sandra Blamires. Polarization of the ^{3}He and ^{129}Xe gas was performed by Andrew Wheatley and Adam Farag. MRI acquisition was performed by Trevor Szekeres, Heather Biernaski and David Reese. For each manuscript contained in this thesis, all other co-authors approved the final draft of the manuscript and their specific contributions are listed below.

Chapter 2 is an original research article entitled "Hyperpolarized ^{3}He and ^{129}Xe MRI: Differences in Asthma before Bronchodilation," and was published in the *Journal of Magnetic Resonance Imaging* in December 2013. This manuscript was co-authored by Sarah Svenningsen, Miranda Kirby, Danielle Starr, Del Leary, Andrew Wheatley, Geoffrey N Maksym, David G McCormack and Grace Parraga. Miranda Kirby assisted with the acquisition of data, statistical analysis and interpretation. Danielle Starr was responsible for CT airway segmentation, analysis and interpretation. Andrew Wheatley assisted with the acquisition and analysis of the data. Del Leary, Geoffrey N Maksym and David G McCormack were responsible for clinical/physiological interpretation of the data.

Chapter 3 is an original research article entitled "Pulmonary Functional Magnetic Resonance Imaging: Asthma Temporal-Spatial Maps," and was published in the journal *Academic Radiology* in November 2014. This manuscript was co-authored by Sarah Svenningsen, Fumin Guo, Miranda Kirby, Stephen Choy, Andrew Wheatley, David G McCormack and Grace Parraga. Fumin Guo, Stephen Choy and Andrew Wheatley contributed to the development of the algorithm and assisted with data analysis. Miranda Kirby assisted with the algorithm design, statistical analysis of the data and interpretation. David G McCormack was responsible for clinical/physiological interpretation of the data.

Chapter 4 is an original research article entitled "What are Ventilation Defects in Asthma?" and was published in the journal *Thorax* in January 2014. This manuscript was co-authored by Sarah Svenningsen, Miranda Kirby, Danielle Starr, Harvey O Coxson, Nigel AM Paterson, David G McCormack and Grace Parraga. Miranda Kirby assisted with the acquisition of data, statistical analysis and interpretation. Danielle Starr was responsible for CT airway segmentation, analysis and interpretation. Harvey O Coxson assisted with the interpretation of CT data. Nigel AM Paterson and David G McCormack were responsible for clinical/physiological interpretation of the data.

Chapter 5 is an original research article entitled "What do Ventilation Defects reveal about Asthma Control?" and is in preparation to be submitted to the journal *Radiology* in October 2015. This manuscript is co-authored by Sarah Svenningsen, Parameswaran Nair, David G McCormack and Grace Parraga. Parameswaran Nair and David G McCormack were responsible for clinical/physiological interpretation of the data.

To the study participants who made this research possible.

Acknowledgments

I would like to thank my supervisor, Dr. Grace Parraga for providing me with this opportunity as well as continuous hands-on support and guidance throughout this endeavor. Again and again, you pushed me well-beyond my boundaries, resulting in countless opportunities and accomplishments that at one point I truly believed were not within my reach. Your wholehearted compassion for your research and your drive for discovery will forever encourage me to be engaged in work that I love, and for this I am grateful.

I am indebted to thank the members of my advisory committee, Drs. Hanif Ladak, Robert Bartha and Nigel Paterson. Thank you for being engaged in my research and career trajectory; your guidance and criticisms have been imperative to my development as a researcher, leader and communicator. I am especially grateful to Dr. David G McCormack for providing invaluable clinical insight into our research, our countless meetings were always a refreshing opportunity to talk big picture and impact. Furthermore, I am thankful for the professional mentorship, guidance and support that you provided.

Due to past and present staff and trainees, the Parraga lab has been an invaluable platform for me to build friendships, foster professional relationships and develop academic and research excellence. To Sandra Blamires: Thank you for being so excellent at what you do and for sharing your clinical and ethical expertise with me. The skillset that you have provided me with will be invaluable moving forward. To Andrew Wheatley: Thank you for taking care of my interminable computer issues, for always achieving excellent polarization and for your unparalleled organization. To David Reese and Trevor Szekeres: Thank you for your attention to detail and your dedication to obtaining consistently high quality image data. Your positive reception to difficult cases and lengthy imaging protocols was always greatly appreciated. To Miranda Kirby: I couldn't have asked for a more accomplished, caring and patient mentor and role model. Thank you for setting the bar so high and inspiring me to reach for it. You were always there as a friend to coax me through the hard times and laughing with me through the good ones, and for this I will forever be grateful. To Damien Pike and Nikhil Kanhere: We built instant friendships as we started our graduate journey together, coming from very different backgrounds but with similar career aspirations and personal interests. Thank you both for persevering with me

through abstract seasons, manuscript submissions, committee meetings and conference presentations. Your positive outlook through these hurdles was always inspiring, and is something I strive to emulate. To Khadija Sheikh and Dante Capaldi: I am grateful for our many interesting and insightful conversations over daily coffee runs and lunches. Thank you for always being willing to help; your contributions to my personal and academic endeavors were endless and I am very appreciative of this. To Fumin Guo: Thank you for your amusing poetry and late night coding sessions. Additional thanks go to my past and present teammates who were always a pleasure to work alongside: Amir Owrangi, Steve Costella, Daniel Buchanan, Tamas Lindenmaier, Gregory Paulin, Nanxi Zha, Emma Bluemke, Danielle Starr, Alexei Ouriadov, Megan Fennema, Eric Lessard, Rachel Eddy and David Tessier.

Most importantly, I would like to thank John, my family and my friends. Your patience, understanding and continued support have contributed significantly to my success. John: Thank you for holding my hand along this journey. Without you this would not have been a possibility for me. To my parents: Thank you for giving me the chance to pursue academics and providing me with the opportunity to focus on my goals.

Finally, I would like to express my gratitude to the various sources of funding that I have received throughout my graduate studies. I acknowledge funding support from the Canadian Respiratory Research Network, the Natural Sciences and Engineering Research Council of Canada, the Ontario Graduate Scholarship, Lawson Health Research Institute and the Schulich School of Medicine and Dentistry.

Table of Contents

List of Tables

List of Figures

List of Abbreviations

AD	Asthma Defect
ATS	American Thoracic Society
ACQ	Asthma Control Questionnaire
AQLQ	Asthma Quality-of-Life Questionnaire
BT	Bronchial Thermoplasty
BMI	Body Mass Index
CEV	Cumulative Expired Volume
COPD	Chronic Obstructive Pulmonary Disease
COV	Coefficient of Variation
CT	Computed Tomography
ED	Emergency Department
EPR-3	Expert Panel Report 3
FeNO	Fractional Exhaled Nitric Oxide
FEV_1	Forced Expiratory Volume in One Second
FRC	Functional Residual Capacity
FVC	Forced Vital Capacity
GINA	Global Initiative for Asthma
IC	Inspiratory Capacity
LA	Lumen Area
LABA	Long Acting Beta-agonist
LCI	Lung Clearance Index
LTRA	Leukotriene Receptor Antagonist
MBNW	Multiple Breath Nitrogen Washout
MCT	Methacholine Test
MRI	Magnetic Resonance Imaging
ND	No Defect
NHLBI	National Heart, Lung, and Blood Institute
NO	Nitric Oxide
PC_{20}	Provocative Concentration required to decrease FEV_1 by 20%
PET	Positron Emission Tomography
Raw	Airway Resistance
RG	Regional
ROI	Region-Of-Interest
RV	Residual Volume
SD	Standard Deviation
SABA	Short Acting Beta-agonist
SNR	Signal-to-Noise Ratio
SPECT	Single Photon Emission Tomography
sRaw	Specific Airway Resistance
TRE	Target Registration Error
TLC	Total Lung Capacity
VDP	Ventilation Defect Percent
VDP_I	Intermittent Ventilation Defect Percent
VDP_P	Persistent Ventilation Defect Percent

VDV	Ventilation Defect Volume
V_D	Dead Space Volume
V_T	Total Volume
WA%	Wall Area Percent
WL	Whole Lung
WT	Wall Thickness
N_2	Nitrogen
^{1}H	Proton
^{3}He	Helium-3
^{4}He	Helium-4
^{129}Xe	Xenon-129

List of Appendices

CHAPTER 1

Asthma is a chronic and phenotypically heterogeneous disease of intermittent respiratory symptoms and airflow limitation triggered by various stimuli, and is characterized by bronchial hyperresponsiveness and airways inflammation.[1,2]

1 INTRODUCTION

1.1 Motivation and Overview

Asthma is the most common chronic respiratory disease in Canada, accounting for approximately 80% of chronic respiratory disease,[3] affecting 8.1% or 2.4 million Canadians in 2014 (**Figure 1-1)**.[4]

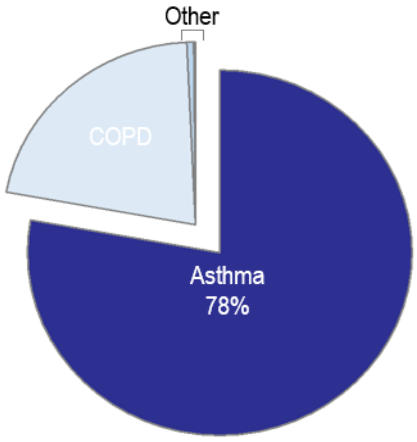

Figure 1-1 Proportion of all respiratory diseases due to specific conditions in Canada. Adapted from Life and Breath: Respiratory Disease in Canada 2008.[5]

Asthma is most common during childhood and affects more than 13% of Canadian children. In 2014, 9.2% of females and 7.0% of males were diagnosed with asthma.[4] In 2009, 228 asthma-related deaths were reported in Canada. Internationally, an estimated 300 million people currently have asthma and this is expected to increase to 400 million by 2025.[6] Asthma is estimated to account for one in 250 deaths worldwide.[6] Due to its high prevalence, asthma has an enormous economic and healthcare burden for the patient and society, with high rates of healthcare resource utilization that vary widely with respect to age and disease severity. Asthma is also a major cause of hospitalization and repeat hospitalization in Canada (**Figure 1-2)**. Annually, the number of patients hospitalized for asthma is comparable to hospitalization due to chronic obstructive pulmonary disease

(COPD) and angina.[7] However, in contrast to COPD and angina, asthma-related hospitalizations are much more common under the age of 19, accounting for approximately 65% of all asthma admissions.[7] Asthma was a contributing factor in approximately 10% of hospital admissions for children under the age of 5 and 8% for those aged 5 to 14 years.[5] In 1990, the estimated cost for asthma in Canada was $504 to $648 million, of which $306 million were direct costs.[8] A study by Ismalia and colleagues indicated that the annual direct cost per asthma patient in Canada ranges from $366 to $647.[9]

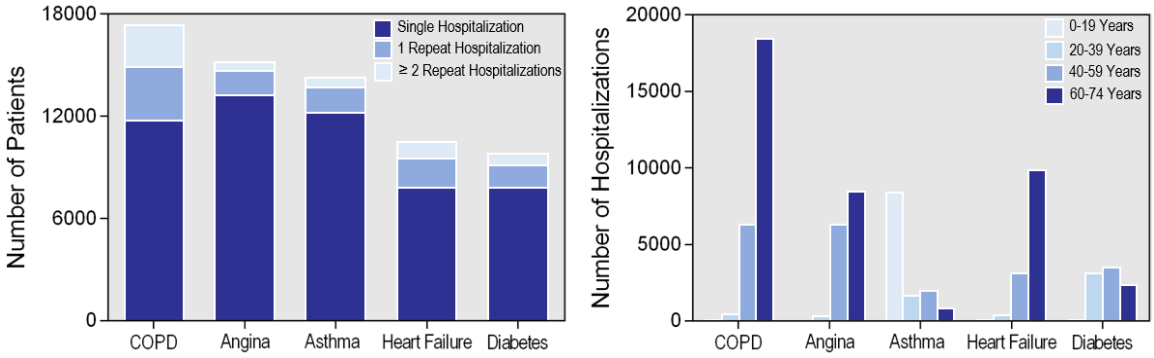

Figure 1-2 Repeat hospitalizations and hospitalization cases by age and condition in Canada.
The left plot shows the number of patients with a single hospitalization, one repeat hospitalization and two or more repeat hospitalization by condition at first admission. The right plot shows the distribution of hospitalization cases by condition and age. Adapted from the Canadian Institute for Health Information's (CIHI) publication entitled Health Indicators 2008.[7]

Despite decades of active research and the staggering societal burden of asthma described above, the mechanism of disease and its distribution within the asthmatic lung are still not fully understood. Imaging and post-mortem evidence allude to the possibility that airway abnormalities in asthma are heterogeneously distributed within the lung. Currently, however, airways disease worsening and response to therapy in asthma are commonly evaluated using the forced expiratory volume in one second (FEV_1) – a simple and inexpensive measurement of airflow obstruction. As a result, current and newly-developed asthma therapies are mainly directed towards improvements in FEV_1, but it is well-known that this global measurement does not capture the regional heterogeneity of airway abnormalities that may be responsible for asthma control and future risk of exacerbations

and lung function decline. In other words, using current clinical tools, there is no way to measure regional lung abnormalities in asthma, making it difficult if not impossible to develop, test and guide regional asthma therapies. Satisfying the uncertain notion that all airways in asthma are equally abnormal and exhibit the same temporal behavior, current therapies are geared to all airways.

Pulmonary functional magnetic resonance imaging (MRI), using inhaled helium-3 (^{3}He) and xenon-129 (^{129}Xe) gas, provides a way to quantify gas distribution *in vivo* and it has the advantage that it shows exactly where functional abnormalities, termed "ventilation defects," are located in the asthmatic lung. In spite of this potential, medical imaging has played a very limited role in asthma research, treatment development and patient care, and for a variety of reasons, the numerous advantages of imaging have not been translated to clinical use. Regardless of the gas used for imaging, the exact etiology of ventilation defects in asthma is poorly understood. A clear understanding of ventilation defects is absolutely necessary prior to the clinical translation of hyperpolarized gas imaging methods. Armed with such an understanding, there is the potential to use functional MRI to guide asthma treatment, predict treatment outcomes, identify new treatment targets and better understand the asthmatic lung regionally and its response to asthma treatment. With the challenges impeding clinical translation in mind, the overarching objective of this thesis was to better understand the underlying structural determinants and clinical consequences of MRI ventilation defects observed in asthma and to provide a foundation for imaging to guide clinical decisions and asthma therapy.

In this Chapter, the relevant background knowledge necessary to understand and motivate the original research presented in Chapters 2 to 5 will be summarized. It will begin with a general overview of the respiratory system's structural and functional responsibilities **(1.2)** before focusing on the pathophysiology and underlying disease mechanisms of asthma **(1.3)**. Subsequently, standard clinical measurements of asthma **(1.4)**, diagnosis and classification schemas **(1.5)** and standard of care treatment regimens **(1.6)** will all be introduced. The benefits and limitations of currently available imaging techniques will be discussed with respect to their influence on better understanding the asthmatic lung and contribution of imaging biomarkers that can be used to guide asthma treatment **(1.7)**. Finally, the specific hypotheses and objectives of this thesis will be introduced **(1.8)**.

1.2 The Respiratory System: Structure and Function

Similar to all organ systems, the functions of the respiratory system are multifaceted and range from protection against inhaled pathogens to gas exchange. While the respiratory system includes the oral and nasal cavities, the lungs, the airways and the muscles responsible for facilitating breathing, here I will elaborate on the structure and function of the airways and the alveoli. The airways are a pipeline which connect the external environment with the alveoli where gas exchange can occur across the blood-gas interface. By the process of ventilation, the main function of the airways and the alveoli is to deliver oxygen and remove carbon dioxide from the blood to maintain normal partial pressure of oxygen and carbon dioxide levels in the arterial blood.

1.2.1 The Airways: Conducting and Respiratory Zones

Inhaled air enters the respiratory system via the nasal or oral passages which converge on the pharynx followed by the larynx. Beyond the upper airways, as shown in **Figure 1-3,** the lower airways are divided into the conducting zone and the respiratory zone based on their structural and functional characteristics. The conducting zone is responsible for carrying inhaled air to the respiratory zone where gas exchange can occur.

Conducting Zone

The conducting zone consists of the first sixteen airway generations, beginning with the trachea (generation zero) and ending with the terminal bronchioles (generation 16).[10] It is important to emphasize that conducting zone airways do not directly participate in gas exchange, but instead their sole function is to conduct and humidify air. Due to its function, this zone is considered anatomic deadspace - approximately 150 mL of air resides here.[10] The trachea is a long, cartilaginous and muscular conduit that follows the larynx that directly supplies air to lungs and bifurcates asymmetrically into the left and right main bronchi that supply the left and right lung respectively. Subsequently, the main bronchi divide into the lobar bronchi that supply the five lobes of the lung, three of which are in the right lung (upper, middle and lower) and two of which are in the left lung (upper and lower). The lobar bronchi then divide into the segmental bronchi that supply air to their corresponding bronchopulmonary segment that is structurally and functionally independent. Bronchi are not individually named distal to the segmental bronchi where

they become narrower, shorter and more numerous as they branch dichotomously to reach all areas of the lung. Secondary lobules or lung sub-segments are supplied by the small bronchi. It is at this point where important structural changes occur. Beyond the small bronchi, the air passages no longer contain cartilage but become embedded in the lung parenchyma for structural support. Terminal bronchioles are the smallest category of air passages without alveoli and are the final conduit of the conducting zone.

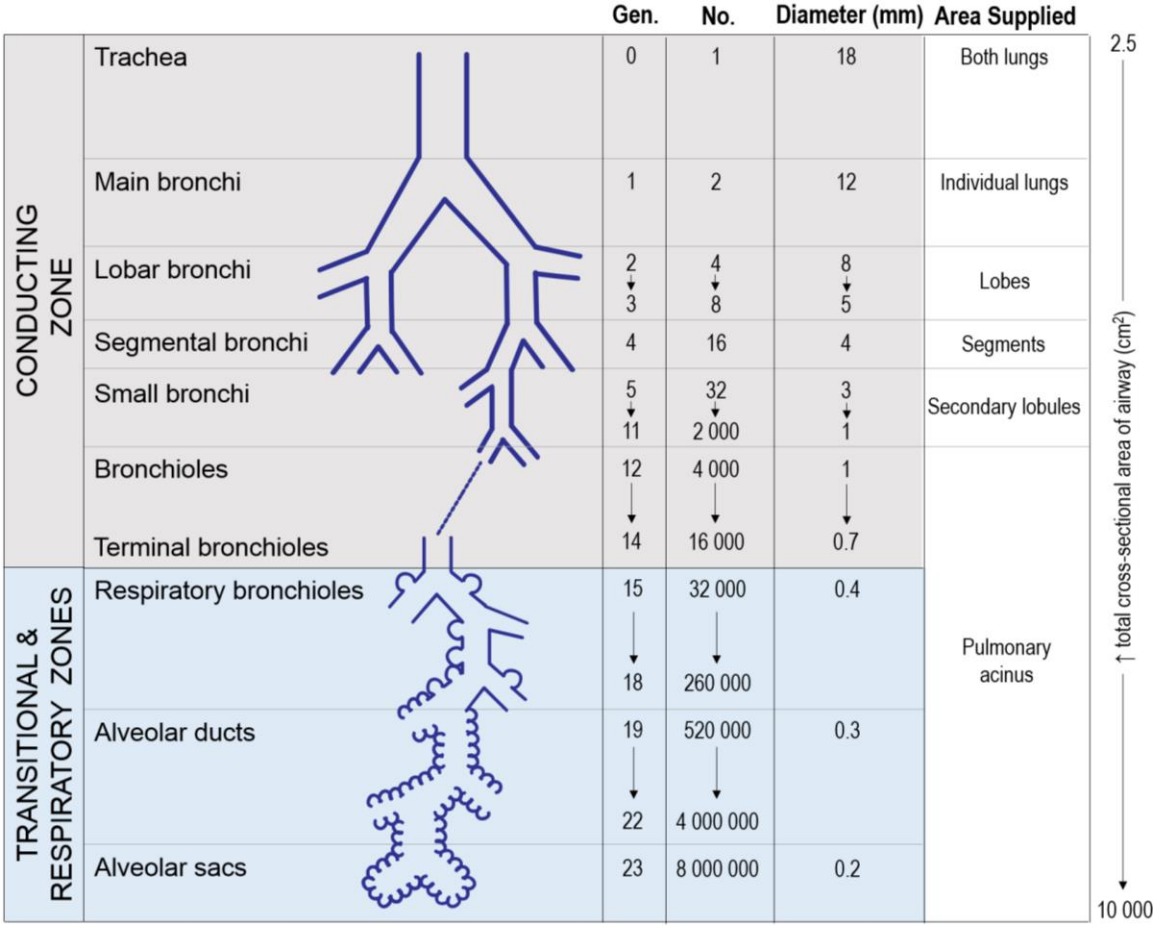

Figure 1-3 Characteristics of the air passages.
Adapted from Lumb A. Nunn's Applied Respiratory Physiology, Fifth edition.[11]

Respiratory Zone

The respiratory zone is the last seven generations (generations 17-23) of the airway tree.[10] In contrast to the conducting zone, the air passages of the respiratory zone contain alveoli which facilitate gas exchange. As shown in **Figure 1-3**, the respiratory bronchioles begin the respiratory zone and have an increasing number of alveoli budding from their muscular walls before giving rise to the alveolar ducts which precede the alveolar sacs that are completely lined with alveoli. A pulmonary acinus is considered a single anatomical unit consisting of a terminal bronchiole and its subsequent respiratory bronchioles, alveolar ducts and sacs. The average human lung contains 30,000 acini,[12] each containing approximately 10,000 alveoli which together make up most of the lung volume, ranging from approximately 2.5 to 3 L at rest.[10]

1.2.2 Site of Gas Exchange: The Alveoli

The alveoli are the site of gas exchange and are the terminal ends of the airway tree found on the respiratory bronchioles, alveolar ducts and alveolar sacs. It has been estimated that 480 million (range: 274-790 million) alveoli exist in the average human lung and that the average size of a single alveolus is 4.2×10^6 μm^3 (range: 3.3-4.8 μm^3) or 200 µm in diameter.[13] The blood-gas interface of the alveoli is comprised of two layers: the alveolar epithelium and the capillary endothelium, which facilitates the movement of oxygen and carbon dioxide between the alveolar airspace and capillary plasma. This interface is extremely thin (0.2-0.3 µm) with a large surface area (50-100 m^2), making it well-suited for efficient exchange of oxygen and carbon dioxide by passive diffusion, according to the principles of Fick's law.

1.2.3 Ventilation

Gas reaches the blood-gas interface by the process of ventilation, which is the exchange of air between the external environment and the alveoli by bulk flow.[10] During ventilation, air flows because of pressure gradients that exist between the atmosphere and alveoli. Inspiration occurs when the inspiratory muscles actively contract and alveolar pressure decreases; whereas expiration occurs when the inspiratory muscles passively relax and alveolar pressure increases. The total amount of air that enters the lungs and resides in the

conducting and respiratory zones upon inspiration is termed tidal volume (V_T) and is approximately 0.5 L. As shown in **Equation 1-1**, total ventilation is the total volume of air leaving the lungs each minute and is calculated as the ventilation rate multiplied by V_T.

Equation 1-1

$$\text{Total ventilation [L/minute]} = \text{Ventilation rate} \times V_T$$

As discussed above, with each exhalation, approximately 0.15 L of "stale" air from the respiratory zone remains in the conducting airways and is first to commute back to the alveoli upon subsequent inspiration. As shown in **Equation 1-2**, alveolar ventilation represents the amount of "fresh" air that reaches the alveoli to participate in gas exchange and it is therefore used to more accurately quantify ventilation efficiency by taking into account the dead space volume (V_D).

Equation 1-2

$$\text{Alveolar ventilation [L/minute]} = \text{Ventilation rate} \times (V_T - V_D)$$

For a healthy adult, the ventilation rate, V_T and V_D are 12-20 breaths/minute, 0.5 L and 0.15 L respectively.[14] At 15 breaths/minute, the total ventilation is 7.50 L/minute and the alveolar ventilation is 5.25 L/minute. This means that although 7.5 L of fresh air enters the respiratory system, only 5.25 L actually reach the alveoli.

1.3 Pathophysiology of Asthma

The word "asthma" originated from the Greek word *aazein*, meaning "to breathe with open mouth or to pant" generalizing that any patient experiencing dyspnea was asthmatic.[15] Given that asthma is as old as antiquity, it is not surprising that the definition and our understanding of the disease has evolved significantly from initial accounts as evidenced by the quotes below. Today, with nearly 300 million asthmatics globally, confusion and controversy continue to surround the definition of asthma.[16]

"Asthma is the inability to breathe without making noise."
Aulus Cornelius, 1st Century BC

"If from running, gymnastic exercises, or any other work, the breathing becomes difficult, it is called Asthma."
Aretaeus the Cappodocian, 2nd Century AD

"Asthma is paroxysmal dyspnea of a peculiar character, generally periodic, with intervals of healthy respiration between attacks."
Henry Hyde Salter, 1860

"Asthma is a special form of inflammation of the small bronchioles."
Sir William Osler, 1892

"Asthma is a disease characterized by an increased responsiveness of the trachea and bronchi to various stimuli and manifested by widespread narrowing of the airways that changes in severity either spontaneously or as a result of therapy.
American Thoracic Society, 1962

1.3.1 Definition of Asthma

In the 2015 Global Initiative for Asthma (GINA) report, the Global Strategy for Asthma Management and Prevention,[1] asthma is defined as: *"A heterogeneous disease usually characterized by chronic airway inflammation. It is defined by a history of respiratory symptoms such as wheeze, shortness of breath, chest tightness and cough that vary over time and in intensity, together with variable expiratory airflow limitation."* This definition consists of four components: symptoms, variable airflow obstruction, airway hyperresponsiveness and airway inflammation.[17] As described in the literature, this relatively broad and non-specific definition encompasses many different asthma phenotypes identified according to environmental triggers, inflammatory processes and clinical features. In a recent review highlighting the heterogeneity of asthma, common clinical phenotypes were classified as trigger-induced phenotypes (occupational asthma, cigarette smoke induced asthma, air pollution induced asthma and exercise induced asthma), symptom-based phenotypes (exacerbation-prone, persistent airflow limitation, cough-variant, adult-onset and the obese asthma) and biomarker-based phenotypes (eosinophilic and neutrophilic asthma).[18] Phenotyping of asthma is becoming more important than ever due to the development of targeted and phenotype specific approaches to asthma therapy.

1.3.2 Causes and Risk

There is no single gene or environmental exposure that causes asthma,[19] although the onset most commonly begins in childhood. Instead, it is widely accepted that host and environmental factors interact to cause asthma.[19] Unfortunately this interplay is complex

and poorly understood. Numerous host factors have been identified that influence the risk of asthma; these include genetic polymorphisms,[20,21] family history of asthma,[22] sex,[23] race[24] and obesity.[25] Similarly, numerous environmental factors have been identified that influence the risk of asthma; these include aeroallergen sensitization,[26] respiratory viruses,[27,28] early life microbial exposures,[29,30] cigarette smoke,[31] air pollution,[32] vitamin D deficiency,[33] antioxidants[34] and stress.[35]

1.3.3 The Asthmatic Lung

Asthma is considered a chronic disorder that is confined to the airways and involves a complex interaction of airflow obstruction, airway hyperresponsiveness and inflammation that results in symptoms.[2] As shown in **Figure 1-4**, as compared to a healthy airway, the airway lumen of an asthmatic is narrowed and obstructed, restricting airflow into and out of the lungs. Characteristic structural abnormalities throughout the airway walls of asthmatics include goblet cell hyperplasia,[36] subepithelial layer thickening,[37] smooth muscle hyperplasia and hypertrophy,[38] submucosal gland hyperplasia and hypersecretion[39] and angiogenesis.[40] Together, these structural abnormalities, in conjunction with inflammatory changes, lead to bronchial thickening and edema as well as increased mucus production and bronchoconstriction, all of which contribute to the airflow obstruction typically found in asthma. The mechanisms that are responsible for airflow obstruction in asthma include bronchoconstriction by airway smooth muscle; luminal obstruction by mucus and debris; and inflammation and remodeling of the airway wall. Bronchoconstriction occurs due to smooth muscle contraction, which results in a reduction in airway caliber by epithelial folding, ultimately increasing airflow resistance. Bronchoconstriction may occur in response to various stimuli that include allergens or irritants such as exercise and cold air. Airway hyperresponsiveness is an "exaggerated" bronchoconstrictor response to various stimuli such as those mentioned above. While airways throughout the bronchial tree can be involved, the magnitude of airway narrowing and resultant airflow obstruction is temporally intermittent but may become persistent.[41]

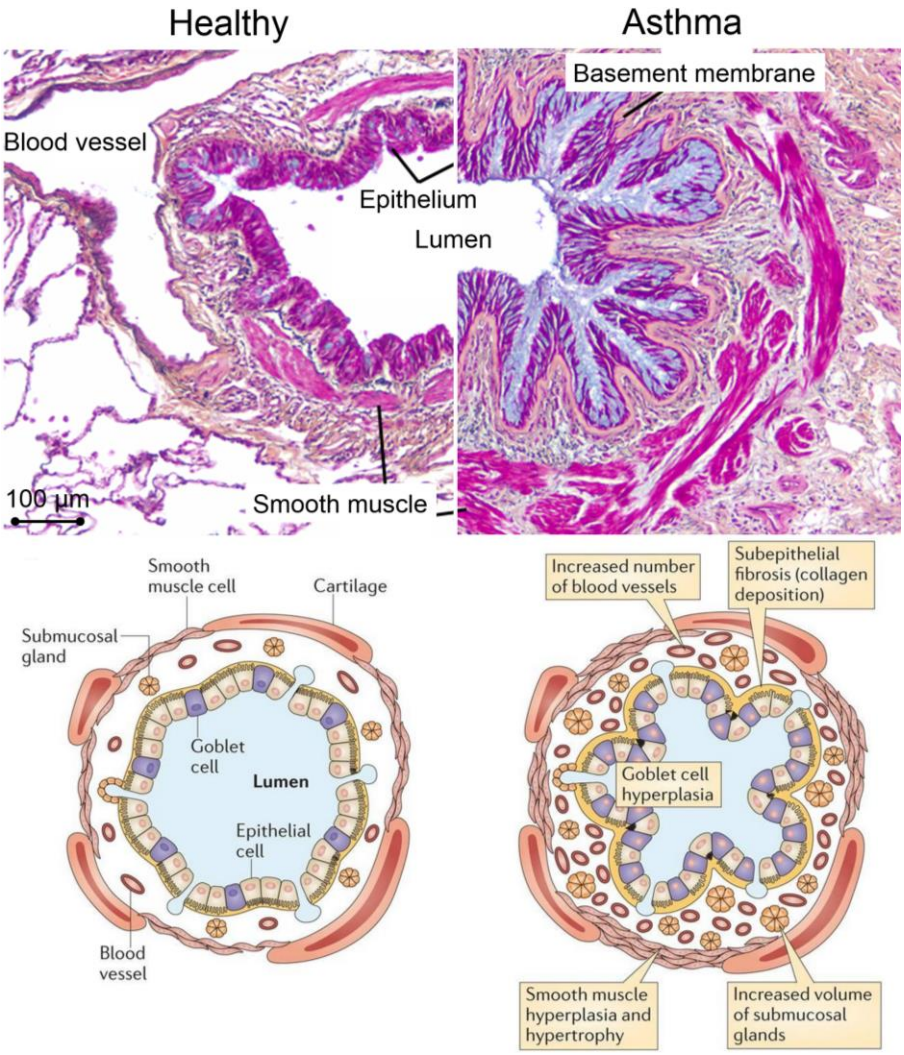

Figure 1-4 Airway pathology in a healthy and an asthmatic airway.
Histological (sectioned and stained using Movat's pentachrome stain) and corresponding schematic representation of airway structures in healthy and asthmatic airways. The asthmatic airway has structural remodeling, including goblet cell hyperplasia, subepithelial fibrosis and increased smooth muscle.
Adapted from JV Fahy Nature Reviews 2015.[42]

Airway inflammation has a fundamental role in the pathophysiology of asthma and involves the interaction of many cell types and mediators. Although the cellular mechanisms behind airway inflammation are beyond the scope of this thesis, important inflammatory cells include lymphocytes, mast cells, eosinophils, neutrophils, dendritic cells, macrophages and epithelial cells. Additionally, important inflammatory mediators include chemokines, cytokines, cysteinyl-leukotrienes and nitric oxide. Immunoglobulin

E (IgE) is the antibody responsible for activation of allergic reactions and is important in the development of persistent inflammation.

1.4 Clinical Measurements of Asthma

Clinical measurements of asthma play an important role in diagnosis, categorizing disease severity and evaluating the effectiveness of medications to manage disease. Currently, no single clinical tool can be used to adequately diagnose and manage asthma. Instead, an integrated approach is employed which combines objective measurements of pulmonary function, bronchial responsiveness, airway inflammation and subjective symptom and quality-of-life questionnaires.

1.4.1 Global Measurements of Pulmonary Function

In a physician's office and hospital pulmonary function laboratory, various aspects of lung function can be evaluated by performing cost-effective pulmonary function testing. Global spirometry measurements and lung volumes play an important role in the diagnosis and management of asthma. It is important to acknowledge that pulmonary function tests are dependent on patient effort, limiting their use in children and cognitively impaired populations. With appropriate coaching by a trained pulmonary function technologist, the majority of patients can perform adequate pulmonary function manoeuvres for which acceptability and reproducibility criteria have been published.

1.4.1.1 *Spirometry*

Spirometry, the gold standard measurement of lung function, is an important diagnostic and disease monitoring test that measures volume and flow of air during inhalation and exhalation manoeuvres. As shown in **Figure 1-5**, spirometry is often performed using a hand-held spirometer (**Figure 1-5A**) and the most commonly performed manoeuvre is the forced exhalation manoeuvre (**Figure 1-5B**). This is performed by having a participant breathe normally and then inspire fully, filling their lungs completely, followed by a hard and fast forced exhalation. It is important that the participant exhale as hard and as fast as they can and that they continue exhaling until they cannot expel any more air. At this point, the end of test criteria has been met. The duration of exhalation may extend well beyond 15 seconds, depending on the severity of the participants airflow obstruction. The most

widely reported indices derived from the forced exhalation manoeuvre are the forced vital capacity (FVC), the FEV_1 and the ratio of FEV_1 to FVC (FEV_1/FVC). As shown in **Figure 1-5B**, FVC is a measure of the total volume of air that can be forcefully exhaled from full inspiration, whereas FEV_1 is a measure of the maximum volume of air that can be forcefully exhaled in the first second of the manoeuvre. Both FVC and FEV_1 are measured in litres and are also commonly expressed as a percentage of the reference value based on the patient's age, height, sex and ethnicity. Extensive spirometry standardization criteria have been compiled by the ATS/ERS Task Force and are now widely applied.[43]

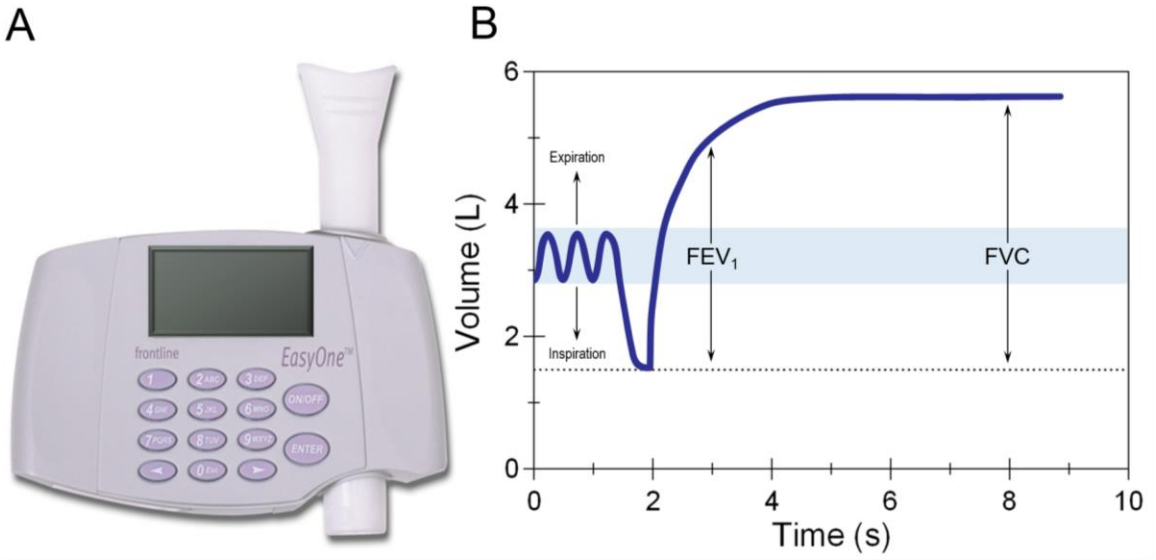

Figure 1-5 Handheld spirometer and typical volume-time spirogram tracing.
FEV_1=forced expiratory volume in one second; FVC=forced vital capacity.

1.4.1.2 *Lung Volumes and Capacities*

Static lung volumes and capacities are identified on a typical volume-time spirogram tracing as shown in **Figure 1-6B**. While the majority of these can be directly measured by spirometry (tidal volume (TV), inspiratory reserve volume (IRV), expiratory reserve volume (ERV), vital capacity (VC) and inspiratory capacity (IC)), this tes0t cannot determine the functional residual capacity (FRC), residual volume (RV) or total lung capacity (TLC). All lung volumes are defined as follows: TV is the volume of gas exchanged at mouth during a normal inhalation or exhalation during tidal breathing; IRV is the volume of gas that can be inhaled from the end of a normal inhalation during tidal

breathing; ERV is the volume of gas that can be exhaled from the end of a normal exhalation during tidal breathing; VC is the volume of gas exchanged at the mouth between a full inspiration and full exhalation; IC is the volume of gas that can be inhaled from the end of a normal exhalation while tidal breathing; FRC is the volume of gas remaining in the lungs at the end of a normal exhalation while tidal breathing; RV is the volume of gas remaining in the lungs at the end of a full exhalation; and TLC is the volume of gas in the lungs at the end of a full inhalation.

As previously alluded to, alternative nitrogen washout, gas dilution or body plethysmography techniques are required to measure FRC, from which RV and TLC can subsequently be derived by performing "linked" spirometry manoeuvres.[44] As shown in **Figure 1-6A**, a body plethysmograph is an airtight chamber that can accommodate the patient comfortably inside. Briefly, the linked manoeuvre is performed by having the participant breathe normally and then perform a series of gentle pants against a closed shutter initiated at FRC. After sufficient panting has been achieved the shutter will open and the participant can then resume tidal breathing followed by a full inhalation and slow full exhalation from which ERV and IVC can be measured. FRC is obtained by applying the principles of Boyle's law relating pressure and volume in an isothermal environment.[44] RV can then be calculated as FRC minus ERV, and TLC can be calculated as the sum of FRC and IC.

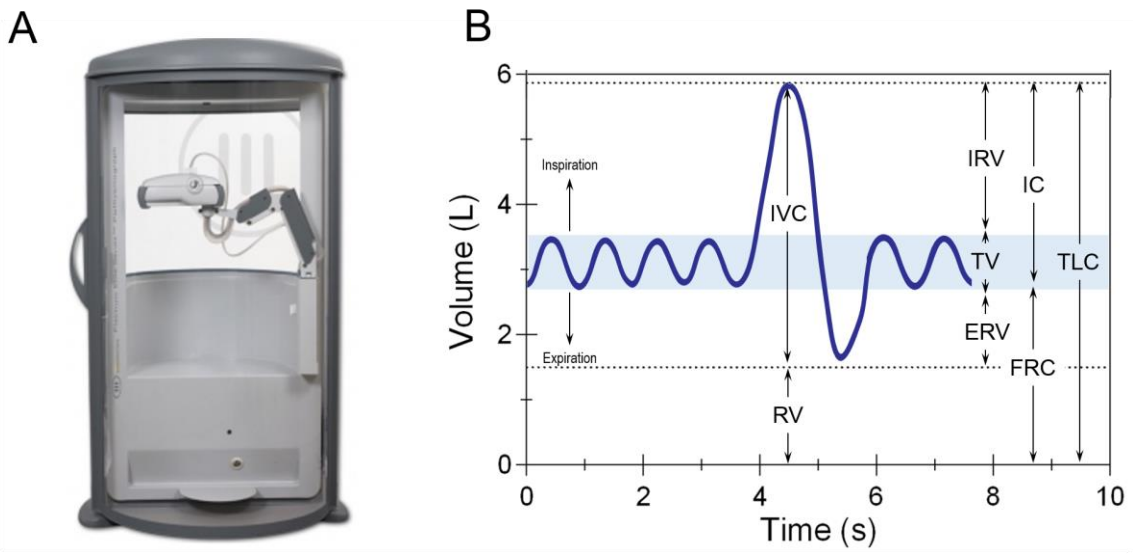

Figure 1-6 Body plethysmograph and typical volume-time spirogram tracing identifying lung volumes.
TV=tidal volume; IRV=inspiratory reserve volume; ERV=expiratory reserve volume; VC=vital capacity; IC=inspiratory capacity; FRC=functional residual capacity; RV=residual volume; TLC=total lung capacity.

1.4.1.3 *Airway Resistance*

Airway resistance (Raw) is a measure of the resistance to flow within the airways and is defined in **Equation 1-3** as the ratio of the driving force of airflow (difference in alveolar and mouth pressure) to the flow rate (measured at the mouth) and can be quantified using several techniques. Raw is influenced by resistance in the mouth, pharynx, larynx, large airways and small airways[11] and is most commonly indirectly quantified using whole body plethysmography.[45] Raw can be derived from the specific airway resistance (sRaw) and FRC as shown in **Equation 1-4**, both of which can be directly measured using plethysmography. sRaw is a corrected index that describes airway resistance regardless of lung volume.[46] Following open shutter panting, the inverse slope of the plot of flow rate versus box pressure is sRaw. In healthy adults, Raw typically falls within 0.6-2.4 $cmH_2O \cdot s \cdot L^{-1}$.[47] Both Raw and sRaw are increased in the presence of inflammation, mucus secretion, and bronchoconstriction.[47]

Equation 1-3

$$\text{Airway resistance (Raw) } [cmH_2O \cdot s \cdot L^{-1}] = \frac{\text{Alveolar pressure - Mouth pressure } [cmH_2O]}{\text{Flow rate } (\dot{V}) \ [L \cdot s^{-1}]}$$

Equation 1-4

$$\text{Airway resistance (Raw) } [cmH_2O \cdot s \cdot L^{-1}] = \frac{\text{Specific airway resistance (sRaw) } [cmH_2O \cdot s]}{\text{Functional residual capacity (FRC) [L]}}$$

1.4.1.4 *Inert Gas Washout*

Single-breath[48] and multiple-breath[49] inert gas washout techniques (SBW and MBW, respectively) were first employed more than 65 years ago to measure lung volumes and ventilation heterogeneity. Although both tests are relatively simple, the MBW test is more informative and has been more commonly used. MBW involves measuring the washout concentration of an inert tracer gas from the lungs during normal tidal breathing. The tracer gas can be endogenous, such as nitrogen (N_2), and washed-out of lungs by breathing 100% oxygen. Alternatively, if the tracer gas is exogenous, such as sulfur hexafluoride (SF_6) or helium (He), it must be washed-in prior to being washed out of the lung by breathing room air. As shown in **Figure 1-7**, with each tidal breath of the washout phase, there is a decrease in the concentration of the exhaled tracer gas (N_2 in this example) and when the gas concentration has decreased to 1/40th of the starting concentration, the test is complete. The manoeuvre is generally completed with the participant sitting upright and breathing through a mouthpiece while wearing nose clips.

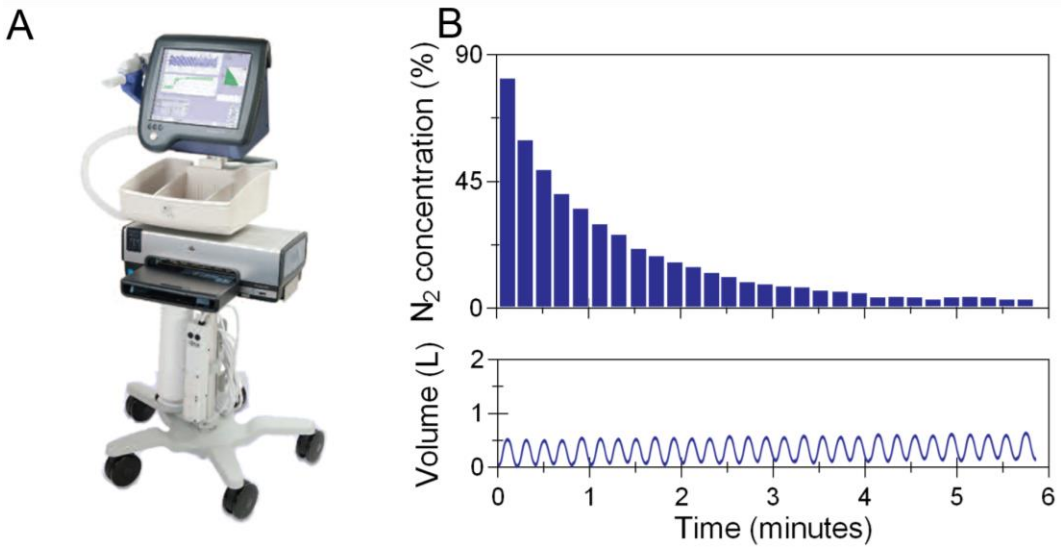

Figure 1-7 Example of a typical inert gas washout machine and inert gas multiple breath washout tracing.
The MBW tracings display tidal volume (lower plot) and the corresponding nitrogen gas (N_2) concentration (upper plot). With each breath there is a decrease in the peak expiratory N_2 concentration.

The most commonly reported MBW derived measurement is the lung clearance index (LCI), which is thought to be representative of whole lung ventilation heterogeneity.[50] LCI is the number of FRC lung turnovers needed to clear the lungs of the inert marker gas and it is calculated as the cumulative expired gas volume (CEV) divided by FRC.[51] Additional metrics that reflect ventilation heterogeneity in the conductive and acinar lung zones (Scond and Sacin, respectively) can be derived using sophisticated phase III slope analysis of the MBW tracing.[52] Additional outcomes include FRC, trapped gas volume and closing capacity.

Inert gas washout measurements are becoming particularly attractive due to their feasibility in the pediatric population[53,54] and increased sensitivity to early disease changes[55,56] while offering complementary information to standard pulmonary function tests. Taken together, MBW indices of ventilation heterogeneity in asthmatics are elevated in comparison to healthy controls;[57-59] are independent determinants of airway hyperresponsiveness;[60] improve with bronchodilation[57,61] and inhaled corticosteroids;[62,63] and worsen during exacerbations.[64] Unfortunately, these measurements cannot regionally localize the site of functional abnormalities.

1.4.2 Bronchial Responsiveness

Reversibility of airflow obstruction and bronchial hyperresponsiveness are features of asthma airway pathophysiology that can be objectively evaluated. The assessment of these disease characteristics are important for diagnosing asthma, categorizing disease severity and evaluating the effectiveness of asthma medications to manage disease.

1.4.2.1 *Assessing Bronchodilator Reversibility*

Evidence of reversible airflow obstruction is a key consideration when establishing a diagnosis of asthma. The primary objective of reversibility testing is to determine whether a participant's lung function is improved following bronchodilation, assessed by performing spirometry pre- and post-bronchodilator administration. Baseline spirometry is performed after the participant has withheld their medications for an appropriate duration as advised by the ATS/ERS Task Force.[43] Subsequently, an inhaled short-acting beta-agonist (four 100μg doses of albuterol/salbutamol) is delivered to the participant prior to performing post-bronchodilator spirometry 15 minutes later. Reversibility is commonly

expressed as the absolute change in FEV_1 and FVC or as a percent of the pre-bronchodilator value, as shown in **Equation 1-5**. It is generally accepted that a clinically-relevant positive bronchodilator response is warranted when the post-bronchodilator increase in FVC and/or FEV_1 is $\geq$ 12% and 200mL from baseline.[65]

Equation 1-5

$$\%\ \text{reversibility} = \left[\frac{(\text{Post-bronchodilator value}) - (\text{Pre-bronchodilator value})}{(\text{Pre-bronchodilator value})}\right] \times 100$$

1.4.2.2 *Assessing Airway Hyperresponsiveness*

In addition to bronchodilator reversibility, airway hyperresponsiveness is another defining characteristic of asthma.[66] Methacholine and exercise challenge testing are two of the most widely used methods to assess airway hyperresponsiveness for which standardized guidelines have been published.[67]

Methacholine Challenge

Methacholine induces bronchoconstriction by acting on airway smooth muscle receptors. Similar to reversibility testing, a methacholine test (MCT) should be performed after the participant has withheld their medications for an appropriate duration as advised by ATS guidelines.[67] Aerosolized methacholine is inhaled through a nebulizer and the MCT is completed according to the established two-minute tidal breathing or five-breath dosimeter protocol described in detail by ATS.[67] Briefly, baseline spirometry is first performed to assess pre-MCT FEV_1 and subsequently the diluent or first dose of methacholine (0.03mg/mL) is administered. After the nebulization has been completed, spirometry is repeated. If FEV_1 has not declined by 20%, the next highest concentration of methacholine should be delivered. This procedure is repeated with increasing concentrations of methacholine until FEV_1 has declined by more than 20% of baseline or until the highest concentration of methacholine (16mg/mL) has been reached.

The primary outcome measure for the MCT is the provocative concentration of methacholine that causes a 20% decrease in FEV_1 (PC_{20}), from which the degree of airway hyperresponsiveness can be interpreted clinically. Calculated according to **Equation 1-6**, PC_{20} $\geq$16mg/mL is indicative of normal airway hyperresponsiveness, whereas a PC_{20}

≤4mg/mL is indicative of abnormal airway hyperresponsiveness.[67] Intermediate values (< 16 and >4 mg/mL) indicate borderline airway hyperresponsiveness and should be interpreted with caution.[67]

Equation 1-6

$$PC_{20}\ [mg/mL]=\text{antilog}\left[\log C_1+\frac{(\log C_2-\log C_1)(20-R_1)}{R_2-R_1}\right]$$

C_1 = second-to-last methacholine concentration; C_2 = last methacholine concentration; R_1 = percent fall in FEV_1 after C_1; R_2 = percent fall in FEV_1 after C_2.

Exercise Challenge

Exercise induces bronchoconstriction in approximately 80% of asthmatics.[68] In contrast to methacholine, exercise is an indirect activator of smooth muscle constriction induced by airway dehydration and subsequent mediator release.[69] Exercise challenge testing is preferentially performed using a treadmill or cycle ergometer as described in detail by ATS, although the protocols are not well standardized or uniformly implemented.[67] Briefly, 6-8 minutes of exercise (4-6 minutes at a pre-determined target intensity) should be completed while breathing cool (<25ºC) dry air. The primary outcome measure for an exercise challenge is FEV_1. A post-exercise decreased in FEV_1 >10% is considered abnormal and a decrease >15% is indicative of exercise-induced bronchoconstriction.

1.4.3 Inflammation

1.4.3.1 *FeNO*

Nitric oxide (NO) is produced in the lungs and can be detected in the exhaled breath of humans, as first described in 1991.[70] Although the exact pathophysiological role of NO in the lung is complex and poorly understood, its production increases in the presence of inflammation.[71] The relationship between NO and eosinophilic airway inflammation has been extensively studied and has been correlated with blood eosinophils and eosinophils present in induced sputum, bronchoalveolar lavage and biopsies.[72-77] Fractional exhaled nitric oxide (FeNO) is a well-established, simple, noninvasive and highly reproducible quantitative biomarker of eosinophilic airway inflammation that is ideally suited for serial monitoring of patients with airways disease. Among the most important clinical

applications of FeNO are its ability to aid in the diagnosis of eosinophilic asthma and to predict corticosteroids-responsiveness. Asthmatics have higher levels of NO in their exhaled breath as compared to healthy controls.[78,79] Although not all asthmatics have eosinophilic inflammation, those who do tend to have elevated FeNO levels and are much more likely to benefit from inhaled corticosteroid (ICS) therapy than those with normal FeNO levels.[80] According to the 2011 ATS recommendations, FeNO < 25 ppb indicates that eosinophilic inflammation and responsiveness to corticosteroids are unlikely, whereas FeNO > 50 ppb indicates that eosinophilic inflammation and responsiveness to corticosteroids is likely.[81] Intermediate values (≥ 25 and ≤ 50 ppb) should be interpreted with caution. Currently, a clinically important difference in FeNO levels has not been determined. Standardized for clinical use, ATS/ERS guidelines for the measurement of FeNO have been published.[82,83]

1.4.4 Validated Questionnaires

1.4.4.1 *Asthma Control Questionnaire*

The Asthma Control Questionnaire (ACQ)[84] was designed to measure asthma control and the change in asthma control over time or in response to treatment. It has been widely adopted as a clinical trial endpoint.[85-87] The questionnaire evaluates control during the previous week and contains five symptom-related questions (night awakenings by symptoms, symptoms on waking, activity limitation, dyspnea and wheeze), pre-bronchodilator $FEV_1\%_{pred}$ and daily rescue bronchodilator use, each scored on a seven-point scale. The ACQ score is calculated as the mean of five, six or seven questions to generate the ACQ-5 score (pre-bronchodilator $FEV_1\%_{pred}$ and daily rescue bronchodilator use omitted), ACQ-6 score (pre-bronchodilator $FEV_1\%_{pred}$ omitted) and ACQ-7 score respectively. Scores range from zero (totally controlled) to six (severely uncontrolled). Asthmatics whose score ranges from 0.0 to 0.75 are considered well-controlled and those whose score is >1.5 are poorly-controlled.[88] The cross-over point between well-controlled and poorly-controlled asthma is near 1.0, therefore asthmatics whose score ranges from 0.75 to 1.5 fall into a 'grey zone' and should be interpreted with caution.[88] The minimum clinically-important difference is 0.5.[89]

In addition to the ACQ, there are numerous additional questionnaires used to evaluate asthma control. Some of the more common questionnaires are the Asthma Control Test (ACT), the Asthma Control Scoring System (ACSS), the Asthma Therapy Assessment Questionnaire (ATAQ), the 30-Second Asthma Test and Lara Asthma Symptom Scale (LASS).

1.4.4.2 *Standardized Asthma Quality of Life Questionnaire*

The Standardized Asthma Quality-of-Life Questionnaire (AQLQ(S))[90] was designed to measure asthma-related quality-of-life. The questionnaire evaluates quality-of-life during the previous two weeks and consists of 32 questions encompassing four subscore domains (12 questions on symptoms; 11 questions on activity limitation; 5 questions on emotional function and 4 questions on exposure to environmental stimuli). A range of matters are assessed including activity limitation, amount of discomfort due to chest tightness, concern about having asthma, fear of not having access to asthma medication and symptoms from exposure to cigarette smoke. Four different seven-point Likert-type response scales are used, ranging from one (totally limited/a very great deal/all of the time/severely limited, most not done) to seven (not at all limited/none/none of the time/not limited, have done all). The AQLQ total score is calculated as the mean of all 32 questions and the domain subscores are the mean of the questions in the domain. The minimum clinically-important difference is 0.5,[91] although the validity of this threshold is still being discussed. Importantly, the AQLQ(S) has been widely adopted as a clinical trial endpoint.[92]

The AQLQ preceded the AQLQ(S) and there are now additional variations including the Mini Asthma Quality of Life Questionnaire (Mini AQLQ) and Acute Asthma Quality of Life Questionnaire (Acute AQLQ). In addition to the various AQLQ instruments, there are numerous additional questionnaires used to evaluate asthma-related quality-of-life. Some of the more common questionnaires are the Asthma Bother Profile (ABP), Asthma Impact Survey (AIS-6), Living with Asthma Questionnaire (LWAQ), Modified Asthma Quality of Life-Marks (M-AQLQ-Marks), Asthma Short Form (ASF), St. George's Respiratory Questionnaire (SGRQ) and Airways Questionnaire-20 (AQ-20).

1.4.4.3 *Dyspnea*

Dyspnea is a common symptom of asthma and the Modified Medical Research Council (mMRC)[93] and Borg dyspnea scales[94] are commonly used to assess it severity. The Modified Medical Research Council dyspnea scale is one of the most commonly used questionnaires to assess dyspnea. It uses a simple five-point scale which assesses the impact or burden of dyspnea on the patient. Scores range from zero (breathless with strenuous exercise) to four (too breathless to leave the house, or breathless when dressing). Similarly, the modified 0-10 Borg dyspnea scale assesses how patients perceive their severity of dyspnea using a simple 10-point scale, with scores ranging from zero (nothing at all) to ten (maximal).

1.5 Diagnosis and Classification of Asthma

Asthma is particularly challenging to diagnose and classify due to its multiple overlapping pathologies that are heterogeneous between individuals (**Figure 1-8**).[95] Although spirometry is most often employed to diagnose asthma, it is difficult to use spirometry to further classify asthma into respective phenotypic categories. With the advent of novel biomarkers, such as FeNO, accurate classification of asthma sub-phenotypes is possible.[95] As depicted schematically in **Figure 1-8**, a multifaceted approach and a gamut of biomarkers is required to accurately diagnose and subsequently classify asthma.[96]

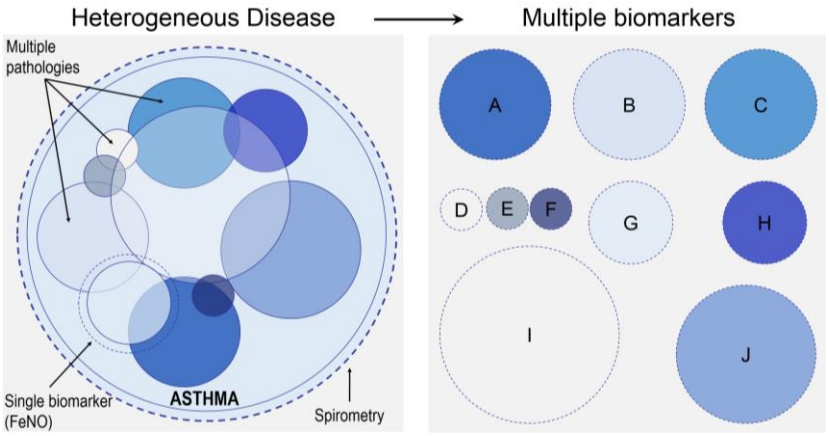

Figure 1-8 Asthma is a heterogeneous disease consisting of several overlapping pathologies necessitating multiple biomarkers to accurately diagnose and phenotype patients.
Adapted from SJ Wadsworth, J Asthma Allergy 2011.

1.5.1 Asthma Diagnosis

A history of variable respiratory symptoms, the presence of airflow obstruction or hyperresponsiveness, reversibility of obstruction and exclusion of alternative diagnoses constitutes a positive diagnosis of asthma.[1,2] Respiratory symptoms indicative of asthma include a combination of wheeze, dyspnea, chest tightness and cough that are temporally intermittent and tend to worsen at night.[1,2] In reality, asthma is still commonly diagnosed on the basis of symptoms alone. In Ontario, Canada, only 43% of asthmatics diagnosed by a physician performed spirometry.[97] Failure to include objective assessments in the diagnostic process is likely contributing to overdiagnosis; evidence of this was observed in a longitudinal study across eight Canadian cities that concluded approximately 33% of individuals with a physician diagnosis of asthma did not have asthma when objectively assessed.[98] Ideally, a diagnosis should be rendered through evaluation of the patient's respiratory symptoms, medical history, physical examination and spirometry.[1,2] Independently, symptoms, medical history and physical exams cannot accurately exclude and/or confirm a diagnosis of asthma. Spirometry is absolutely required to objectively assess airflow obstruction, its severity and reversibility.[96] Accordingly, spirometry should be performed prior to and following inhalation of a short-acting bronchodilator to indicate the degree of obstruction and reversibility according to ATS/ERS standards.[65]

Common differential diagnoses include chronic obstructive pulmonary disease, alternative upper airway diseases (e.g. rhinitis) and obstructions involving the large (e.g. vocal cord dysfunction) and small airways (e.g. bronchiolitis).[2]

1.5.2 Asthma Control

Asthma control refers to the extent that symptoms of asthma can been reduced or removed by treatment.[17] Control encompasses two domains: current clinical control and future risk of exacerbations and lung function decline.[17] Symptom control is gauged by evaluating the frequency of day-time symptoms, night-time symptoms, short-acting beta-agonist (SABA) use and activity limitation. Risk is gauged by evaluating the frequency and severity of previous exacerbations. Taken together, a patient's asthma is considered to be well-controlled if he/she is symptom free without activity limitation or exacerbations and does not experience variable lung function. As described above, multiple standardized

questionnaires have been designed to assess the degree of asthma control. Some of the most commonly used questionnaires are the ACQ and ACT. There is no general consensus between national and international guidelines regarding degrees of asthma control. For example, the GINA report of 2015 used categories of "well-controlled," "partly-controlled" and "uncontrolled;"[1] whereas the National Heart, Lung, and Blood Institute (NHLBI) ERP3 used "well-controlled," "not well-controlled" and "very poorly-controlled."[2] Regardless, the primary goal of asthma treatment is the achievement and maintenance of disease control.

1.5.3 Asthma Severity

Asthma severity can be defined by the intensity of treatment required to control asthma.[17,99] Severity can be classified as intermittent, mild, moderate and severe according to the lowest level of treatment required to achieve asthma control. Shown below in **Table 1-1**, intermittent, mild, moderate and severe asthma is asthma that is well-controlled while receiving the indicated treatment regimen. The indicated treatment regimens can be extrapolated to reflect the six-step and five-step treatment strategies proposed by the NHLBI[100] and GINA,[1] respectively. Severe asthma is defined as asthma which requires treatment with high dose ICS and LABA (and/or OCS) to achieve asthma control, or asthma that remains uncontrolled despite maximum therapy.[101] As defined, asthma severity can only be assessed after a patient has been on regular controller treatment for several months.

Table 1-1 Classification of asthma severity.

	Intermittent	Mild	Moderate	Severe
Lowest level of treatment required to achieve control	SABA as needed	Low-dose ICS or other low intensity treatment	Low- to moderate-dose ICS and LABA	High dose ICS and LABA ± OCS
Treatment strategy Step Allocation				
NHLBI EPR3[100]	1	2	3 or 4	5 or 6
GINA[1]	-	1 or 2	3	4 or 5

NHLB, Expert Panel Report 3 of the National Heart, Lung and Blood Institute; GINA, Global Initiative for Asthma; ICS, inhaled corticosteroids; LABA, long acting beta-agonists; OCS, oral corticosteroids. Adapted from DR Taylor, Eur Respir J 2008.[99]

1.6 Treating Asthma

Similar to the majority of chronic lung diseases, no existing asthma treatments are preventative or curative. Accordingly, the primary goal of asthma treatment is the achievement and maintenance of disease control while minimizing the risk of future exacerbations or lung function decline. The majority of asthma can be well-controlled using a SABA for rescue during acute onset bronchoconstriction and ICS for chronic control. However, as asthma severity is increased, treatment becomes more complex and requires personalized, phenotype-specific additive therapies.

Towards the goal of asthma treatment, evidence-based stepwise approaches have been developed by the NHLBI[100] and GINA[1] (**Figure 1-9**) to guide treatment decisions. Both guidelines suggest that a continuous control-based management cycle (**Figure 1-9**), consisting of iterative patient assessment, treatment and review is necessary to ensure asthma is adequately treated. Following each assessment, treatment can be "stepped-up" when asthma in not well-controlled and "stepped-down" when asthma is well-controlled.[102] The breadth of asthma medications can be categorized as controllers, relievers and add-on therapies. Corticosteroids, beta-agonist bronchodilators, theophylline, leukotriene receptor antagonists, immunomodulators and bronchial thermoplasty are briefly described below.

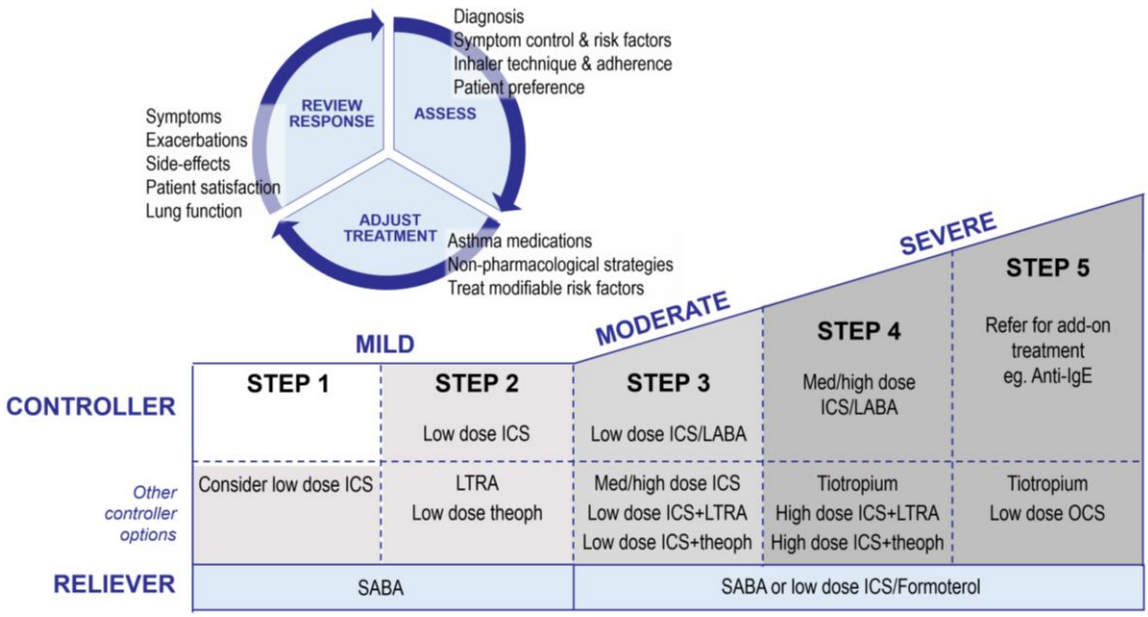

Figure 1-9 2015 GINA stepwise approach to asthma treatment.
ICS, inhaled corticosteroids; SABA, short-acting beta$_2$-agonists; LABA, long-acting beta-agonists; OCS, oral corticosteroids; anti-IgE, anti-immunoglobin E therapy; theoph, theophylline; LTRA, leukotriene receptor antagonists.
Adapted from GINA Global Strategy for Asthma Management and Prevention, 2015.[1]

1.6.1 Controller & Reliever Treatment

1.6.1.1 *Corticosteroids*

Corticosteroid anti-inflammatory therapy is the most effective therapy for asthma.[1,2] Corticosteroids block various inflammatory pathways, suppressing cytokine production, recruitment of eosinophils and the release of inflammatory mediators.[41] In the 1990s, their efficacy was evidenced by their ability to safely reduce airflow obstruction, symptoms, emergency department visits, hospitalizations and asthma-related deaths, to improve asthma control and quality-of-life and to decrease airway hyperresponsiveness and exacerbation frequency.[103-107] Response to this treatment is variable between asthmatics and is related to the type of underlying inflammation. Asthmatics with neutrophilic predominant inflammation are commonly corticosteroid-resistant;[108] whereas asthmatics with eosinophilic predominant inflammation are predominantly corticosteroid-responsive. As an independent controller medication, ICS demonstrate superiority over other controller

medications in placebo-controlled trials.[109,110] Commonly used ICS include beclomethasone, budesonide, ciclesonide, fluticasone, mometasone and triamcinalone.

As many as 30% of severe asthmatics require daily oral systemic corticosteroids (OCS) as additive maintenance therapy, with 50% requiring more than three bursts of OCS annually.[111] Due to the well-documented negative side-effects of chronic OCS use, they are only recommended as an add-on treatment for severe asthmatics who remain poorly controlled despite high-dose ICS and long-acting beta-agonists (LABA).[1,2] OCS are more commonly used in short bursts (3-7 days) during an exacerbation to gain control of symptoms as they speed the resolution and prevent relapse of exacerbations.[112,113]

1.6.1.2 *Beta-agonist Bronchodilators*

Short-acting and long-acting beta-agonists (SABA and LABA, respectively) are the most commonly used bronchodilators for treating asthma. SABAs, such as salbutamol, are a highly-effective reliever of acute bronchoconstriction in mild, moderate and severe asthma. LABAs, salmeterol and formoterol, cause bronchodilation for greater than 12 hours[114] and are used in combination with ICS for long-term control in moderate and severe asthma. The clinical benefit of monotherapy therapy with SABA and LABAs is inferior to that of ICS and has been linked to adverse outcomes,[115] accordingly LABAs are rarely used independently. When used in combination with ICS, LABAs have an additive effect, improving lung function and symptom control.[116,117] The effects of beta-agonists are the result of their binding to beta-adrenoceptors, present on airway smooth muscle, epithelial and inflammatory cells. Its major mechanism of action is initiated when beta-adrenoceptors on the airway smooth muscle are stimulated, increasing cyclic AMP, which causes the smooth muscle to relax. The variable rate of onset and the duration of effect between SABAs and LABAs is due to their hydrophilic and lipophilic characteristics that govern their interaction with beta-adrenoceptors.[114]

1.6.2 Add-on Treatments

1.6.2.1 *Theophylline*

Low-dose theophylline, is a relatively weak bronchodilator that may have an anti-inflammatory and immunomodulatory effect.[41] Due to the availability of safer and more

effective treatments, such as ICS and beta-agonists, theophylline is considered an alternative controller option or add-on treatment.[1,2,118] The clinical benefit of adding theophylline to ICS treatment was found to only minimally improve lung function.[119] The clinical utility of theophylline is complicated due to its toxicity and associated side-effects at effective doses, which is particularly problematic as its bronchodilator effect is dose-dependent. Despite guideline recommendations, theophylline is one of the most prescribed medications for asthma internationally because of its low cost. This relates to its use in developing nations where access to superior and more expensive alternatives is limited.

1.6.2.2 *Leukotriene Receptor Antagonists (LTRAs)*

LTRAs reduce bronchoconstriction and inflammation in response to various stimuli; they are considered an alternative first-line therapy, but are most commonly used as add-on treatment.[1,2] Leukotrienes are biochemical mediators that are released from inflammatory cells such as mast cells, eosinophils and macrophages in response to various stimuli.[41,120] Binding of cysteinyl-leukotrienes to cysteinyl-leukotrienes receptors results in smooth muscle constriction, mucus secretion, edema and inflammation.[41,120] For the treatment of asthma, montelukast (Singulair) is the most commonly used LTRA, blocking the effect of cysteinyl-leukotrienes receptors. LTRAs are considered an alternative first-line therapy as they are less effective than ICS when used independently.[121] In a multicentre, randomized, double-blind, placebo-controlled trial, montelukast improved airway obstruction, exacerbations, control and blood eosinophils in stable asthma.[122] In a subsequent trial, the clinical benefit of adding montelukast to ICS treatment was found to be as effective as doubling the ICS dose.[123] Multiple studies have concluded that adding LTRA to ICS results in comparable[124] or worse outcomes[125,126] than achieved by adding LABA to ICS.[127]

1.6.2.3 *Anticholinergic bronchodilators*

Anticholinergic bronchodilators are considered a clinically valuable add-on treatment for the treatment of asthma. Anticholinergic agents inhibit cholinergic activity by competing with acetylcholine at muscarinic receptors to permit dilation of the airways.[41] Acetylcholine, which acts through muscarinic receptors, is a key player in the regulation of airway smooth muscle tone and mucus gland secretion.[128] Studies evaluating the efficacy of Tiotropium Bromide (Spiriva), a long-acting muscarinic antagonist, reported

improved lung function and symptoms, reduced frequency of SABA use and reduced risk of future exacerbations in asthmatics taking ICSs and LABAs.[129-131]

1.6.2.4 *Immunomodulators*

Immunomodulator is an umbrella term used to encompass many different pharmaceutical agents aimed at modulating cell signalling and the immunologic responses in asthma. Omalizumab, a monoclonal antibody that interrupts the allergic cascade by binding free immunoglobulin E (IgE), is considered a phenotype-guided add-on treatment for allergic asthma that cannot be well-controlled with ICS.[1,2] In patients with moderate-to-severe allergic asthma, large-scale clinical trials have proven omalizumab reduces exacerbations and symptoms, improves quality-of-life and has a steroid-sparing effect.[132-135] In subsequent trials, adding omalizumab to ICS treatment was proven clinically beneficial due to further improved lung function and a reduction in exacerbations. While omalizumab is the only immunomodulator currently integrated into treatment guidelines, numerous clinical trials have emerged to evaluate novel pharmaceutical agents engineered to target various pathways important to the pathogenesis of asthma. Potential new treatments include: anti-interleukin 5 (IL-5) antibodies, mepolizumab[136] and reslizumab;[87] anti-IL-13 antibodies, lebrikizumab[137] and tralokinumab;[138] anti-TNF-α antibody, golimumab;[139] tyrosine kinase inhibitor, masitinib;[140] IL-2Rα antibody, daclizumab;[141] and CXCR2 antagonist, SCH527123.[142]

1.6.2.5 *Bronchial Thermoplasty*

Bronchial thermoplasty is a novel nonpharmacological outpatient treatment procedure for severe asthma. During three bronchoscopy sessions, radiofrequency energy is delivered to all of the bronchopulmonary segments to disrupt bronchial smooth muscle.[143] The effect of this procedure is a reduction in airway smooth muscle mass in the treated airways, resulting in a reduced potential for bronchoconstriction.[144,145] The safety and efficacy of bronchial thermoplasty have been evaluated in numerous clinical trials, including a multi-centre, randomized, double-blinded, sham-controlled trial, that together demonstrated improved asthma control, quality-of-life, and decreased exacerbation frequency, hospitalizations and ED visits following treatment.[86,146,147] The long-term effectiveness was recently evaluated and reduced hospitalizations and exacerbation frequency were

shown to persist five years after treatment.[148,149] Despite its excellent safety and efficacy profile, the worldwide literature consists of only about 200 patients who have received this treatment.

1.7 Imaging Asthma

Currently, the clinical use of imaging in asthma is minimal and largely confined to chest radiography and x-ray computed tomography (CT). Through research initiatives, novel imaging biomarkers of lung structure and function have been developed, many of which have the potential to impact asthma diagnosis, management and evaluation of treatment effect. X-ray CT, single photon emission computed tomography (SPECT), positron emission tomography (PET) and MRI based techniques can be used to non-invasively evaluate regional ventilation. Imaging has provided valuable insight into the underlying disease mechanisms of asthma, and will be discussed below.

1.7.1 Plain X-ray

The chest radiograph **(Figure 1-10)** is the oldest and most common type of image used to evaluate the lung as it is relatively inexpensive and fast. Unfortunately, the utility of chest radiographs is limited as they are two-dimensional projection images of the three-dimensional anatomy and are therefore limited by tissue superimposition. A posterior-anterior chest radiograph is obtained with the patient standing upright, with the x-ray source positioned behind them so that the x-ray beam enters from the posterior side and exits the anterior side of the patient.[150] Different anatomical structures absorb x-rays to different extents and this is termed attenuation, the principle behind the contrast in an x-ray image.[150] Highly attenuating tissues such as bone absorb many x-rays and appear white on an x-ray image. In contrast, low attenuating tissues such as lung parenchyma absorb very few x-rays and therefore appear black on an x-ray image. The radiation dose associated with a typical posterior-anterior chest radiograph is 0.01 mSv,[151] approximately equivalent to 0.6% of the annual background radiation in Toronto, Canada (1.6 mSv).

Chest radiographs are rarely useful in the diagnosis and management of asthma as they are often normal. However, their strength lies in the ability to reveal complications or alternative causes of "asthma-like symptoms." A study by Paganin and colleagues concluded that only 38% of chest radiographs were abnormal in adults with chronic

asthma.[152] Radiographic findings associated with asthma are generally subtle and they include increased lung volume, increased lung lucency and bronchial wall thickening.[153] Increased lung volume or hyperinflation is the most common radiographic observation and is seen as increased lung length and flattening of the diaphragm (**Figure 1-10**).[41] The prevalence of bronchial wall thickening identified on chest radiographs has been related to asthma severity.[152]

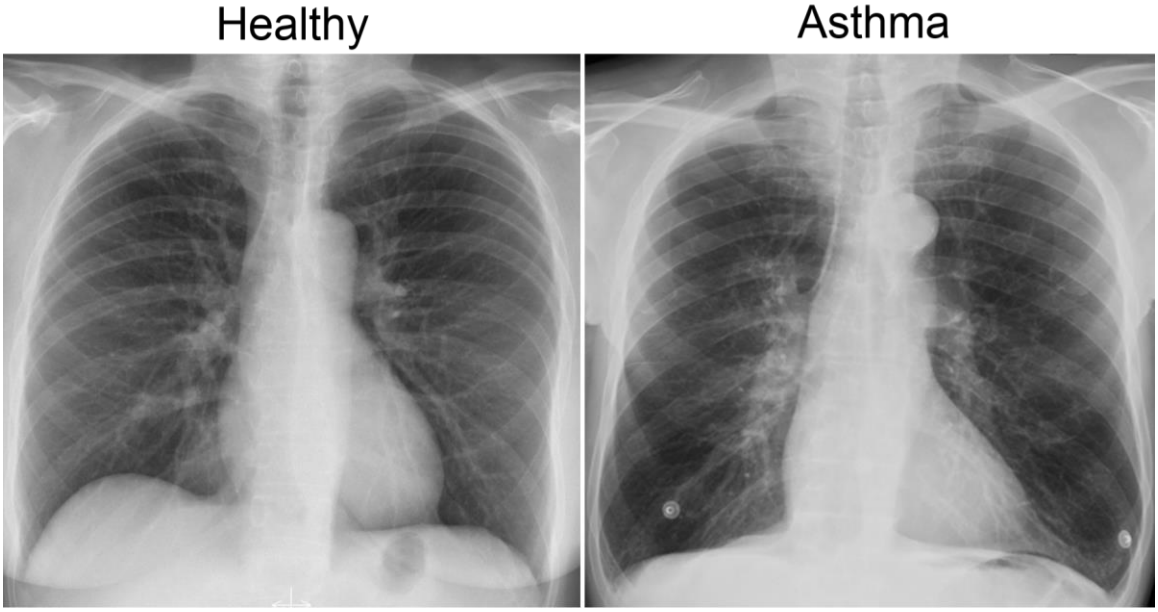

Figure 1-10 Representative posterior-anterior chest radiograph of a healthy volunteer and an asthmatic subject.
In asthma, diaphragm flattening is indicative of hyperinflation. Healthy case courtesy of Dr. Usman Bashir, Radiopaedia.org, rID: 18394; Asthma case courtesy of Dr. Garth Kruger, Radiopaedia.org, rID: 21812.

1.7.2 X-ray Computed Tomography

Since its advent in the 1970s, x-ray CT has become the imaging modality of choice for the evaluation of pulmonary disease. Through technological advancements, the entire lung volume can now be captured with sub-millimetre isotropic spatial resolution in a single breath-hold using multiple-row detector CT scanners.[154] This increased spatial resolution and the potential for isotropic voxels permit multi-planar and three-dimensional reconstructions.[155] Similar to plain radiography, the attenuation properties of tissues govern image contrast in x-ray CT. In CT however, attenuation values are measured in

Hounsfield units (HU) and range from -1000 HU for air, 0 HU for water and to approximately 700 HU for bone.[155]

CT of asthmatic subjects have shown abnormal findings such as bronchial wall thickening, bronchial wall dilation, luminal narrowing, bronchiectasis, mosaic lung attenuation, mucus plugging and atelectasis **(Figure 1-11)**.[152,156] In asthma research studies, CT has been used extensively to directly evaluate the large airways and to indirectly evaluate the small airways (<2mm). As detailed below, CT-derived metrics are correlated with clinical symptoms and are highly sensitive to treatment response. Gupta and colleagues used CT to evaluate 185 severe asthmatics and reported that abnormalities were present in 80% of study participants.[157]

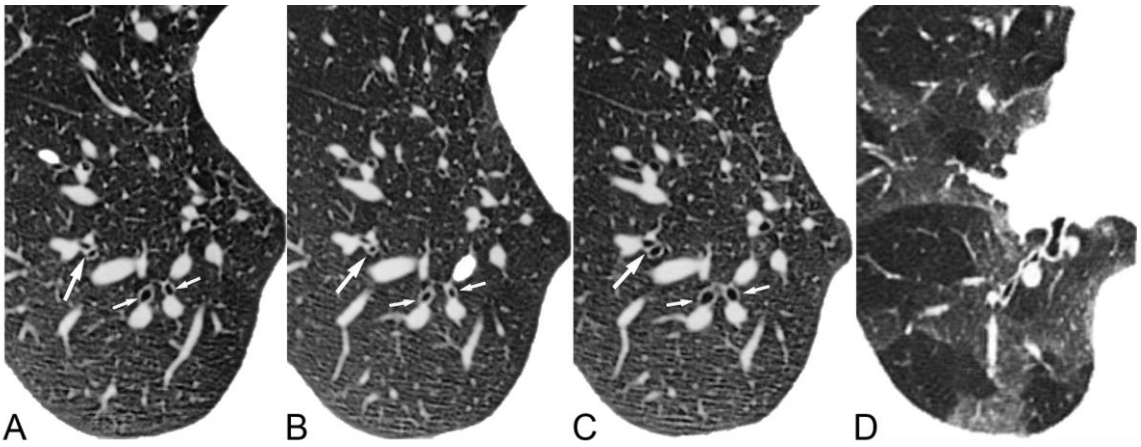

Figure 1-11 Axial CT of the right lower lobe in two representative asthmatics.
At baseline (panel A), after inhalation of methacholine (panel B) and then salbutamol (panel C) there are visually obvious variations in bronchial lumen diameters (highlighted by white arrow) consistent with bronchoconstriction and subsequent bronchodilation.[158] In a separate asthmatic (panel D) mosaic attenuation due to air-trapping is observed.[159]
Reproduced with permission from Beigelman-aubry et al (2002)[158] and Sung et al (2007).[159]

The architecture of the large airways is assessed by quantifying metrics similar to those employed in histological studies such as the airway wall area percent **(Equation 1-7)**, airway wall thickness percent **(Equation 1-8)** and airway lumen area. Initial airway quantification techniques relied on manual tracing; however, due to the obvious limitations of this approach, semi-automated and automated computer-based approaches have since been developed. Three-dimensional approaches enable up to ten generations of the airway

tree to be segmented, and reliable quantification can be achieved for first to sixth generation airways.[154,160] Furthermore, automated three-dimensional approaches allow for the identification of airways using standardized clinical nomenclature, as demonstrated in **Figure 1-12**.[160] Awadh and colleagues were the first to quantify airway wall thickness in the segmental and sub-segmental airways of asthmatics and healthy controls using a manual approach. They reported that asthmatics had a greater airway wall thickness as compared to controls and that wall thickness was increased with increasing asthma severity.[161] Subsequent investigations have compared airway measurements in normal and asthmatic subjects using various quantification techniques and their results support the initial findings by Awadh et al.[162-167] Furthermore, CT airway measurements have been correlated with asthma severity,[167-169] airflow obstruction,[162,164,167,168,170] airway hyperresponsiveness[163,168,171] and pathology.[168] Following interventions such as deep inspiration,[172] methacholine challenge[166] and ICS therapy,[165,173,174] the airways have been shown to behave in the expected direction.

Equation 1-7

$$\text{Wall Area Percent [\%]} = \frac{\text{Airway wall area}}{\text{Total airway area}} \times 100$$

Equation 1-8

$$\text{Wall Thickness Percent [\%]} = \frac{\text{Airway wall thickness}}{\text{Airway outer diameter}} \times 100$$

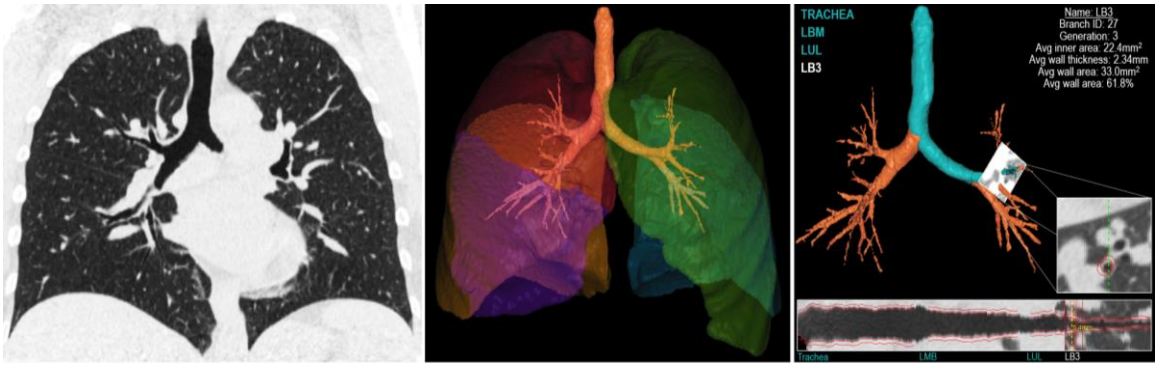

Figure 1-12 Three-dimensional quantitative CT of the lungs and airways in asthma. Coronal CT (left panel) and the corresponding three-dimensional rendering of the lung and airway tree using Pulmonary Workstation 2.0 (VIDA) (middle panel). The trachea, left

main bronchus and left upper lobe bronchus pathway is highlighted (in blue) and the segmental LB3 airway is quantified (right panel). In cross-section, the pathway and LB3 airway boundaries are outlined in red.

The small airways (<2mm) cannot be directly evaluated using CT as they are beyond the current spatial resolution limit of the technique. However, air trapping in asthma is thought to be an indirect measure of small airway obstruction and can be visualized as heterogeneous regions of low attenuation on CT **(Figure 1-11)**. As expected, regions of low attenuation are more apparent on expiratory as compared to inspiratory scans. Various metrics have been used to quantify the extent of air trapping on CT and these include scoring systems, threshold and percentile techniques and lung density expiratory to inspiratory ratios. Threshold techniques use a specific threshold of HU (e.g. -950 HU, -910 HU, -856 HU) and the percentage of the lung less than this threshold is calculated.[175] Percentile techniques require a specific percentile point (e.g. lowest 15th percentile) to be selected and the HU value for the corresponding percentile is determined.[175] Using various CT-derived gas trapping metrics, investigators have observed significantly elevated gas trapping in asthmatics over healthy controls.[158,176] Other investigators correlated CT measurements of gas trapping in asthma with asthma severity,[177] airflow obstruction,[170,176,178] airway hyperresponsiveness and disease duration.[178] Zeidler and colleagues performed a double-blinded, cross-over study to compare the effect of montelukast versus placebo on small airway function in mild-to-moderate asthma. Compared to placebo, montelukast resulted in significantly less air trapping on CT.[179] Moreover, other interventional studies have shown that air trapping on CT worsens following methacholine[158] and improves following treatment with ICS.[180,181] These studies similarly concluded that CT is a more sensitive method to assess treatment response in the small airways than conventional lung function tests.

In addition to providing rich qualitative and quantitative structural information regarding the airways and lung parenchyma, functional assessments of ventilation and perfusion are also possible with novel CT techniques. Introduced in the late 1980s, xenon ventilation CT[182] is a technique used to non-invasively measure regional pulmonary ventilation in lung diseases. CT is performed after the participant inhales radiodense xenon and ventilation can in turn be assessed because the airspaces that contain xenon have increased CT density

in comparison to those that do not.[183] However, this technique is limited as xenon enhancement is poor and this has motivated xenon ventilation imaging using a dual-energy CT based approach. Using dual-energy CT, Chea and colleagues observed ventilation defects in 80% of stable asthmatics who had significantly worse airflow obstruction and thicker airway walls than asthmatics without defects.[183] Using the same approach, another group of investigators observed an increase in xenon ventilation defects following methacholine that resolved following salbutamol inhalation.[184]

Despite the rich qualitative and quantitative structural and functional information that CT can provide, it is disadvantaged due to its use of ionizing radiation. The radiation dose associated a clinical chest CT is approximately 8 mSv,[151] equivalent to roughly five years of background radiation in Toronto, Canada (1.6 mSv) or 400 plain chest radiographs. This becomes a major concern in asthma research and patient care as serial imaging capabilities are necessary for disease management and the evaluation of response to treatment or intervention.

1.7.3 Nuclear Medicine

Gamma Scintigraphy & Single Photon Emission Computed Tomography (SPECT)

Scintigraphy and SPECT can be used to regionally evaluate perfusion and ventilation in the lungs. Following the injection or inhalation of a radionuclide tracer, gamma radiation is used to form an image of radioactivity within the body. Radionuclide tracers emit gamma rays at a specific energy that can be detected by a gamma camera that converts absorbed energy into an electrical signal that can be displayed as an image. Accordingly, regions of high radionuclide concentration appear as hot spots on the image. Similar to how x-ray CT compares to plain x-ray, SPECT compares to scintigraphy.[185] Scintigraphy uses gamma radiation to form two-dimensional images of radioactivity within the body, whereas SPECT offers a three-dimensional image.

A tracer that is radioactive itself or labelled with a radionuclide is required.[185] For regional imaging of ventilation, radioactive gases, radioactively-labelled aerosols and Technegas can be used.[185] The most commonly used radioactive gases are xenon-133 (^{133}Xe) and krypton-81m (^{81m}Kr). The radionuclide technetium-99m (^{99m}Tc) is used as ^{99m}Tc-

diethylene-triamine pentaacetate (DTPA) aerosol and Technegas.[185] The inhaled deposition of Technegas has been shown to be similar to the distribution of inhaled ^{133}Xe gas, and is preferred as its deposition within the lungs remains unchanged for more than 20 minutes.[186]

Scintigraphy using inhaled ^{133}Xe gas was the first method to identify regional ventilation abnormities in asthma.[187,188] Engel and colleagues were the first investigators to show the effect of methacholine-induced bronchoconstriction on regional ventilation.[189] Nearly ten years later, the effect of histamine-induced bronchoconstriction on ventilation was observed.[190] In the late 1990s, King and colleagues began to measure ventilation in asthma using SPECT and an inhaled bolus of Technegas. As hypothesized based on previous scintigraphy studies, ventilation was compromised in asthmatics compared to healthy controls.[191] Using the same technique, the investigators subsequently observed increased ventilation abnormalities following methacholine challenge in asthma.[192] Importantly, the team demonstrated a link between ventilation defects and peripheral airways disease measured by MBNW.[192] Not necessarily representative of ventilation, SPECT has been used extensively in research to investigate the regional deposition of inhaled aerosols when labelled with the radionuclide ^{99m}Tc.[193,194]

Similar to x-ray based imaging methods, an obvious limitation of SPECT is its radionuclide-dependent radiation exposure. A lung ventilation-perfusion study using ^{99m}Tc exposes the subject to an effective dose of 2-3mSv.[185] Furthermore, SPECT suffers from poor spatial resolution (~15mm) and motion artifact due to long acquisition times.

Positron Emission Tomography (PET)

Similar to SPECT, PET offers three-dimensional images of radioactivity and requires the injection or inhalation of a positron-emitting radioisotope. As the radioisotope decays within the patient, positrons are emitted and then quickly annihilated when they come into contact with an electron. As a result, two photons are emitted approximately 180º to one another.[195] The emitted photons can be detected and a three-dimensional map of radioactivity can be reconstructed to generate a PET image.[195]

Regional ventilation, perfusion and ventilation/perfusion matching can be assessed with nitrogen-13 (^{13}NN) PET following bolus injection or inhalation of ^{13}NN. ^{13}NN has a half-

life of ten minutes and is not soluble in blood or tissue.[195] The bolus injection technique is used to deliver ^{13}NN to the lung via the bloodstream. Accordingly, unventilated lung regions, termed ventilation defects, retain the tracer due to gas trapping whereas the tracer is quickly washed out of ventilated lung regions. Conversely, when the alternative inhalation technique is used, the tracer does not reach poorly-ventilated regions of the lungs. Intravenous bolus injection of ^{13}NN was used by Venegas and colleagues in a study evaluating the effect of methacholine-induced bronchoconstriction on regional ventilation in mild-to-moderate asthmatics.[196] Following bronchoconstriction, the investigators observed regions of poor ventilation.[196] Using the same technique, similar results were observed in mild asthmatics but in a subsequent study, lung perfusion was shown to redistribute away from ventilation defects.[197] The effect of omalizumab treatment on ventilation and ventilation/perfusion matching metrics was assessed in a small group of uncontrolled allergic asthmatics but no effect was observed.[198]

^{18}F-fluorodeoxyglucose (FDG) is the most commonly used PET tracer in clinical practice due to its high uptake by metabolically active cells, such as cancer cells.[154] Interest has surrounded the utility of FDG-PET as a biomarker of eosinophilic and neutrophilic inflammation in the lungs of asthmatics.[199,200] Future work is required to determine the utility of this approach in asthma.

1.7.4 Magnetic Resonance Imaging

MRI does not require ionizing radiation and, due to this obvious advantage, the past 25 years have seen an accelerated development of pulmonary MRI. However, conventional ^{1}H MRI has numerous inherent limitations that have motivated the development of alternative inhaled gas contrast methods since the 1990s. Oxygen-enhanced, fluorinated gas and hyperpolarized gas MRI are capable of imaging lung structure and function. Of these techniques, hyperpolarized gas MRI has been most widely applied in pulmonary research; however, despite its utility, clinical translation has been slow.

1.7.4.1 *Conventional ^{1}H MRI*

Conventional ^{1}H MRI is challenging due to the lung's inherent properties. Primarily consisting of air, the density of the human lung is approximately 0.1 g/cm^3, making it the least dense organ in the body[201]. Accordingly, the lungs inherently low ^{1}H density

translates to low ^{1}H MRI signal intensity. Furthermore, the lung consists of millions of alveoli or air-tissue interfaces. These numerous air-tissue interfaces create significant local magnetic field inhomogeneities referred to as susceptibility artifacts, further inducing ^{1}H MRI signal loss.[201] Finally, due to cardiac and respiratory motion, the images are highly susceptible to motion artifacts. Due to these limitations, as shown in **Figure 1-13**, the lungs appear as black holes and resultantly healthy and asthmatic lungs are relatively indistinguishable using conventional ^{1}H MRI sequences.

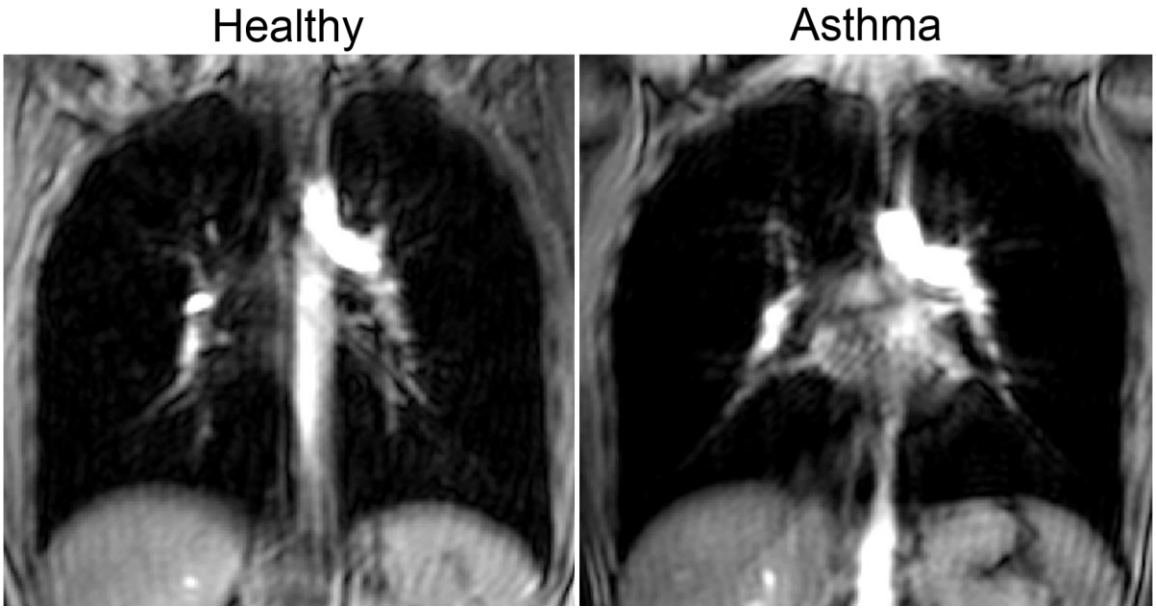

Figure 1-13 Representative coronal conventional ^{1}H MRI of a healthy volunteer and an asthmatic subject.
Due to the low ^{1}H density within the lung, ^{1}H MRI cannot visually distinguish structural abnormalities inherent to the asthmatic lung.

Despite these shortcomings, alternative and potentially more sensitive ^{1}H MRI techniques such as ultra-short echo time (UTE),[202] oxygen-enhanced[203] and Fourier decomposition[204] methods have been developed. Advantageously, both oxygen-enhanced and Fourier decompositions methods provide functional information, offering insight into ventilation and perfusion characteristics. Even with the advent of these alternative techniques, the application of ^{1}H MRI in asthma has been limited. Static and dynamic oxygen-enhanced MRI methods have been used to assess oxygen delivery, uptake and washout in asthma.[205-208] Oxygen-enhanced MRI metrics are sensitive to asthma severity[205-207] and correlate with

FEV_1.[207] Most recently, the oxygen transfer function has been shown to decrease in asthma subjects after a segmental endobronchial allergen challenge and was correlated with bronchoalveolar lavage eosinophil counts.[208] Although yet to be evaluated in asthma, Fourier decomposition MRI allows lung perfusion and ventilation to be assessed, and preliminary studies have demonstrated excellent feasibility and reproducibility in healthy volunteers and subjects with respiratory disease.[204,209-211] Similarly, UTE methods have not been evaluated in subjects with asthma. However, in a murine asthma model UTE ^{1}H MRI was used to quantify peribronchial eosinophilic inflammation that correlated with lung function parameters.[212]

1.7.4.2 *Inhaled Gas MRI*

Over the past two decades, MRI using inhaled hyperpolarized and fluorinated gases has been used to investigate lung function and structure in healthy volunteers and subjects with pulmonary disease. Thus far, the field of inhaled gas MRI has been dominated by hyperpolarized gas techniques, using ^{129}Xe and ^{3}He. Unlike conventional ^{1}H MRI, specialized polarizer equipment and multinuclear radio-frequency hardware are necessary. Furthermore, this approach requires the subject to inhale an anoxic gas mixture and perform a short breath-hold (8-14 seconds) during image acquisition. The field slowly began to take shape following the seminal investigation by Albert and colleagues who produced the first hyperpolarized ^{129}Xe MR images of excised mouse lungs.[213] Using spin-exchange optical pumping, Albert and colleagues recognized that the longitudinal polarization of ^{3}He and ^{129}Xe gas nuclei could be increased by approximately 100,000 times.[214] This strong signal makes it possible to acquire data from the hyperpolarized gas itself once inhaled by the patient.

The process of polarization is achieved by spin-exchange optical pumping, circularly polarized light bombards a glass cell housing rubidium and a noble gas situated within a helmholtz coil.[215] The circularly polarized light is absorbed by the rubidium atoms, resulting in spin-polarization of its valence electrons. Subsequent collisions between the noble gas and polarized rubidium atoms result in the transfer of angular momentum from rubidium electrons to the noble gas nucleus, thereby increasing its nuclear-spin polarization.[215]

While initial investigations used hyperpolarized ^{129}Xe gas, the field quickly transitioned to hyperpolarized ^{3}He gas due to its three-fold higher nuclear gyromagnetic ratio (^{129}Xe: 11.78 MHz/T; ^{3}He: 33.43 MHz/T) and greater achievable polarization (^{129}Xe: 8-25%; ^{3}He: 30-40%) – both of which contribute to the greater MRI signal achieved with ^{3}He than ^{129}Xe gas.[215] More recently, the limited quantity and resultant high cost of ^{3}He gas has motivated the field to shift its focus back towards ^{129}Xe gas as it is widely available and a less expensive alternative.[216,217] Notably, advances in polarizer technology have resulted in improved ^{129}Xe polarization that has improved the overall MRI signal. It is important to acknowledge that excellent safety and tolerability of both ^{3}He and ^{129}Xe MRI has been demonstrated in healthy volunteers and subjects with pulmonary disease.[218,219] Studies have shown no clinically significant adverse effects of ^{3}He or ^{129}Xe inhalation.[218,219] With this method, regional ventilation, lung microstructure and gas exchange have been qualitatively and quantitatively evaluated in clinical research.

Ventilation Imaging

Spin density imaging of hyperpolarized ^{3}He or ^{129}Xe, acquired during breath-hold, provides an opportunity to visualize with high spatial resolution those areas of the lung that participate in gas distribution and those that do not. As shown in **Figure 1-14**, in healthy young adults, inhalation of hyperpolarized gas results in homogeneous signal suggesting that all areas of the lung are participating equally in ventilation. In contrast, characteristic regions of signal void are observed in asthma **(Figure 1-14)**, corresponding to areas of the lungs that are not ventilated within the time-course of a breath-hold scan. Regions of signal void, termed ventilation defects, have also been observed in cystic fibrosis, COPD, bronchiectasis, lung cancer and the healthy elderly.

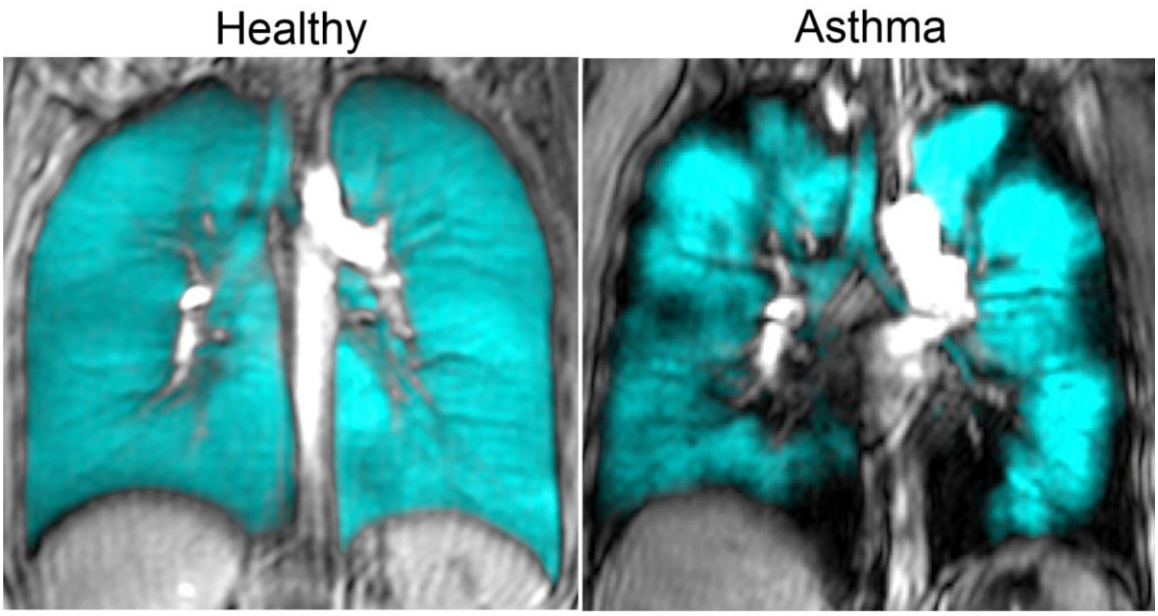

Figure 1-14 Representative coronal centre slice hyperpolarized ^{3}He MRI of a healthy volunteer and an asthmatic subject.
^{3}He MRI gas distribution (in blue) registered to the ^{1}H MRI of the thorax (in grey-scale). Unlike the representative healthy volunteer, the asthmatic subject has visually obvious ventilation defects.

The presence of ventilation abnormalities were initially quantified using visual scoring and manual segmentation, but semi-automated[220,221] and automated[222] segmentation approaches are now more commonly employed. Quantitative MRI-derived metrics include the ventilation defect volume,[223,224] ventilated volume,[225] ventilation coefficient of variation[226,227] and the ventilation defect percent (VDP). VDP is a measure of the ventilation defect volume normalized to the thoracic cavity volume, as shown in **Equation 1-9**. VDP is now a widely disseminated biomarker[220,221,225] due to its demonstrated reproducibility,[220] relation to standard measurements of lung function[228] and its sensitivity to disease severity and treatment response.[229]

Equation 1-9

$$\text{Ventilation Defect Percent (VDP) [\%]} = \frac{\text{Ventilation defect volume}}{\text{Thoracic cavity volume}} \times 100$$

Many clinical research studies using hyperpolarized gas MRI have been performed in asthma to evaluate ventilation heterogeneity.[224,226,230-239] In 2001, Altes and colleagues were the first to observe heterogeneous ventilation in non-symptomatic asthmatic adults

with normal lung function using hyperpolarized ^{3}He MRI.[235] In addition to this seminal study, numerous others have observed worse ventilation in asthmatics compared to healthy controls **(Figure 1-14)**.[226,233,235,237] While the majority of investigational studies to date have evaluated adults, a recent study by Cadmen and colleagues imaged asthmatic children for the first time.[239] Similar to previous observations in adults, a greater number and larger size of ventilation defects were observed in children with asthma than those without asthma.[239] In one of the largest studies evaluating 58 asthmatics with varying disease severity, ventilation worsened with the increase of disease severity.[233] With respect to lung function, the number of ventilation defects[224,236] and the number of ventilation defects per slice[232,233] were inversely correlated with FEV_1, but not ventilation volume[234] or VDP.[237] VDP was, however, correlated with airways resistance, FeNO and dyspnea.[237]

Without ionizing radiation, there is enormous potential for serial and longitudinal treatment evaluation studies using hyperpolarized gas MRI. Accordingly, and for obvious reasons, interest has surrounded the temporal variability of focal MRI ventilation defects in asthma. In a 30-minute scan-rescan study, all defects were found to be persistent.[235] Another study concluded that approximately 75% of defects remained in the same location when evaluated twice in the same day.[231] Over longer periods of time (7-476 days) many ventilation defects were persistent or reoccurred in the same location.[230-232] Similarly, following repeat bronchoconstriction on separate days, the majority of defects were also induced in the same locations.[232] With methacholine[226,232,236,237] and exercise[230,236] induced bronchoconstriction, numerous new ventilation defects and more heterogeneous ventilation patterns have been observed. Alternatively, salbutamol-induced bronchodilation has been shown to improve, but not completely reverse, induced ventilation abnormalities.[232,234,236,237] **Figure 1-15** shows the ventilation distribution for a representative asthmatic at baseline, post-methacholine challenge and post-salbutamol inhalation. A double-blinded, placebo-controlled, multi-institutional study assessed the response of ^{3}He MRI ventilation to montelukast therapy in exercise-induced bronchoconstriction.[234] Following exercise, the authors observed a larger drop in ventilation volume while receiving placebo than while receiving treatment.[234] These studies demonstrate the sensitivity of MRI ventilation to bronchoconstriction and treatment.

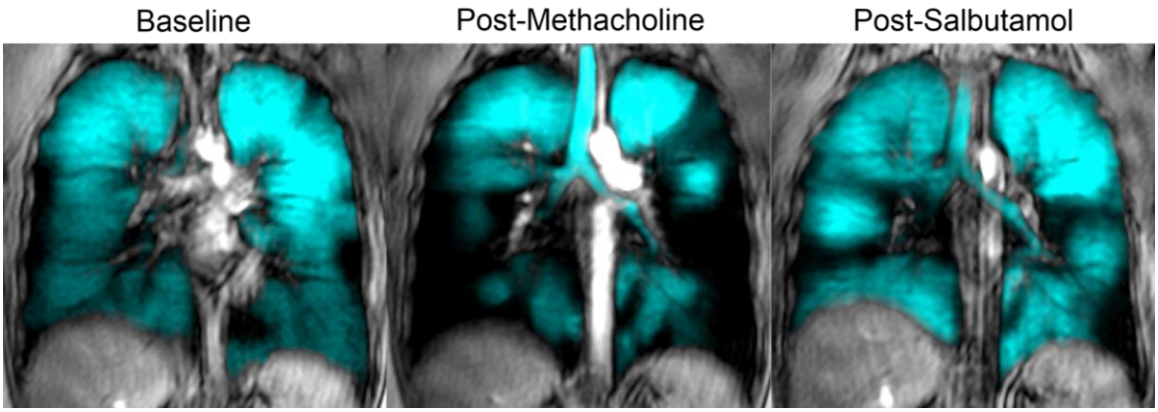

Figure 1-15 Representative coronal centre slice hyperpolarized ^{3}He MRI of an asthmatic subject at baseline, post-methacholine and post-salbutamol.
^{3}He MRI gas distribution (in blue) registered to the ^{1}H MRI of the thorax (in grey-scale). Ventilation abnormalities are present at baseline that become worse following methacholine-induced bronchoconstriction. Post-salbutamol, ventilation is improved but abnormalities are not completely resolved.

It is probable that ventilation defects in asthma are the result of gas trapping and airway obstruction, although their etiology remains to be investigated. In an attempt to evaluate the structural determinants of ventilation defects in asthma, Fain and colleagues evaluated ^{3}He MRI in conjunction with CT and bronchoalveolar lavage.[224] It was concluded that global metrics of ventilation volume were not related to inflammatory markers. However, subsequent regional analysis suggested that ventilation defects may be associated with abnormal inflammation as poorly-ventilated lobes had elevated neutrophils as compared to well-ventilated lobes in the same patient. [224] Furthermore, in the same asthmatics, a spatial relationship between ventilation defects and CT hyperlucency was observed.[224]

Taken together, these studies suggest that in asthma, ventilation defects are related to airways disease, are regionally heterogeneous, temporally variable and responsive to therapy and provocation. MRI ventilation defects vary in size, ranging from tiny focal hypo-ventilated spots to lobar in nature, and are often observed in asthmatics despite normal lung function. Most importantly, these studies suggest that asthma is a disease that involves selected airways focally rather than diffusely, a concept that could revolutionize asthma management and treatment. With the field's imminent transition to ^{129}Xe MRI, asthma has yet to be evaluated using this alternative approach. While it can be

hypothesized that the knowledge gained from ^{3}He MRI investigations will be transferable, direct comparisons are required.

Diffusion-weighted Imaging

Another type of hyperpolarized gas MR image that has been commonly acquired uses diffusion-weighted MRI, providing a sensitive and rapid approach for evaluating the lung microstructure.[240] Within the lungs, movement of gas atoms is restricted by tissue boundaries. Therefore, a quantitative apparent diffusion coefficient (ADC) map can be generated that is representative of airspace size.[241] While both ^{3}He and ^{129}Xe ADC measurements have been obtained in the lung, ^{3}He ADC has been more extensively studied demonstrating high reproducibility[242-244] and correlation with histology measurements of airspace size.[245] For obvious reasons, ADC studies have been most commonly employed in COPD, while to date there have only been a few investigations in asthma.[237,239,246,247] While heterogeneous gas diffusion coefficients have been observed throughout the asthmatic lung, contradiction surrounds the differences in whole lung microstructure between asthmatics and healthy controls. One study has shown increased gas diffusion coefficients in asthma compared to healthy controls,[246] whereas another study observed no difference.[237] In the only study evaluating gas diffusion in asthmatic children, Cadmen and colleagues reported a greater degree of restricted diffusion in children with asthma compared to children without asthma.[239] In the only treatment study, ADC in asthma was quantified at baseline, post-methacholine challenge and following salbutamol inhalation.[237] An increased ADC was observed following methacholine, indicative of gas trapping, which was subsequently reduced followed salbutamol inhalation.[237] A recent study indicated ADC in asthma is related to the acinar component of ventilation heterogeneity due to its relationship with the MBNW derived metric Scond. The same authors also observed that ADC was strongly related to FVC and a CT marker of gas trapping.[247]

1.8 Thesis Hypotheses and Objectives

The overarching objective of this thesis was to develop and apply novel pulmonary imaging methods to better understand asthma and to provide a foundation for functional imaging to guide clinical decisions and treatment in patients with asthma. The specific objectives and hypotheses tested in each chapter of this thesis are introduced below.

In Chapter 2, our objective was to quantitatively compare hyperpolarized ^{3}He and ^{129}Xe MRI within a five-minute period before and after bronchodilator administration in a small group of well-controlled asthmatic adults. We wanted to understand the effect of the gas physical properties on ventilation defects in asthma. The transition from ^{3}He to ^{129}Xe gas is a necessary step to facilitate broad clinical integration of hyperpolarized gas MRI. Due to the higher density and viscosity of ^{129}Xe gas, we hypothesized that ^{129}Xe MRI would reveal more ventilation abnormalities pre-bronchodilator than ^{3}He MRI and that these differences would be diminished post-bronchodilator.

In Chapter 3, our objective was to exploit the inherent temporal and spatial pulmonary function information provided by hyperpolarized ^{3}He MRI and develop image processing methods to regionally identify temporally persistent and intermittent ventilation defects that could be used to measure, optimize and guide asthma treatment. In this proof-of-concept study, seven asthmatic subjects underwent MR imaging at three timepoints over a two-week period. We hypothesized that patient-specific temporal-spatial pulmonary function maps could be generated from ^{3}He MRI to visualize and quantify temporally persistent and intermittent ventilation defects.

In Chapter 4, our objective was to determine the underlying structural and clinical determinants of asthma ventilation defects by evaluating well-established clinical and emerging imaging (hyperpolarized ^{3}He MRI and CT) measurements in healthy volunteers and subjects with well-controlled asthma. In addition to evaluating the relationship between airway structure and lung function, we asked the question: *Are asthmatics with ventilation defects different from asthmatics without ventilation defects?* We hypothesized that there would be a quantitative and spatial relationship between MRI ventilation defects and abnormal airways and that ventilation defects would be related to well-established clinical measurements of asthma.

In Chapter 5, our objective was to evaluate the relationship between MBNW and MRI measurements of ventilation, and to better understand their link to asthma control. Multiple-breath gas washout studies have previously demonstrated a link between poor asthma control and increased ventilation abnormalities, and this led to the questions: *What is the relationship between in vivo ventilation defects quantified using MRI and asthma*

control? Can ventilation defects serve as an intermediate endpoint of outcomes like exacerbations, quality-of-life and asthma control? We wanted to understand this relationship because the primary goal of asthma treatment is the achievement and maintenance of disease control. Accordingly, we hypothesized that MRI and MBNW measurements of ventilation would be related, and contribute to poor asthma control.

In Chapter 6, an overview and summary of the important findings and conclusions of Chapters 2-5 will be provided. The study specific limitations as well as general limitations of the hyperpolarized gas MRI studies presented will be discussed, and some potential solutions will be offered. The thesis ends with a roadmap for future studies that could build on the foundation of knowledge generated by this work.

1.9 References

(1) Global Initiative for Asthma: Global Strategy for Asthma Management and Prevention, 2015. http://www.ginasthma.org (accessed July 2015).

(2) Busse WW. National Asthma Education and Prevention Program Expert Panel Report 3: Guidelines for the Diagnosis and Management of Asthma, Summary Report 2007. *J Allergy Clin Immunol* 2007;120:S93-S140.

(3) To T, Gershon A, Cicutto L, *et al.* The burden of asthma: can it be eased? The Ontario record. *Healthc Q* 2007;10:22-4.

(4) Canada S. Health Trends. Statistics Canada Catalogue No. 82-213-XWE, 2014.

(5) Public Health Agency of C. Life and breath: respiratory disease in Canada. Ottawa [Ont.]: Public Health Agency of Canada, 2007.

(6) Masoli M, Fabian D, Holt S, *et al.* The global burden of asthma: executive summary of the GINA Dissemination Committee report. *Allergy* 2004;59:469-78.

(7) Canadian Institute for Health Information. *Health Indicators 2008*: Canadian Institute for Health Information 2008.

(8) Krahn MD, Berka C, Langlois P, *et al.* Direct and indirect costs of asthma in Canada, 1990. *CMAJ* 1996;154:821-31.

(9) Ismaila AS, Sayani AP, Marin M, *et al.* Clinical, economic, and humanistic burden of asthma in Canada: a systematic review. *BMC Pulm Med* 2013;13:70.

(10) West JB. *Respiratory physiology: the essentials*. Philadelphia: Wolters Kluwer Health/Lippincott Williams & Wilkins, 2012.

(11) Lumb AB, Nunn JF. *Nunn's applied respiratory physiology*. Oxford; Boston: Butterworth-Heinemann, 2000.

(12) Haefeli-Bleuer B, Weibel ER. Morphometry of the human pulmonary acinus. *Anat Rec* 1988;220:401-14.

(13) Ochs M, Nyengaard JR, Jung A, *et al.* The number of alveoli in the human lung. *Am J Respir Crit Care Med* 2004;169:120-4.

(14) Silverthorn D. *Human Physiology:An Integrated Approach*: Prentice Hall PTR, 2003.

(15) Holgate ST. A brief history of asthma and its mechanisms to modern concepts of disease pathogenesis. *Allergy Asthma Immunol Res* 2010;2:165-71.

(16) Hargreave FE, Nair P. The definition and diagnosis of asthma. *Clin Exp Allergy* 2009;39:1652-8.

(17) Reddel HK, Taylor DR, Bateman ED, *et al.* An official American Thoracic Society/European Respiratory Society statement: asthma control and exacerbations: standardizing endpoints for clinical asthma trials and clinical practice. *Am J Respir Crit Care Med* 2009;180:59-99.

(18) Hekking PP, Bel EH. Developing and emerging clinical asthma phenotypes. *J Allergy Clin Immunol Pract* 2014;2:671-80; quiz 81.

(19) Jackson DJ, Hartert TV, Martinez FD, *et al.* Asthma: NHLBI Workshop on the Primary Prevention of Chronic Lung Diseases. *Ann Am Thorac Soc* 2014;11 Suppl 3:S139-45.

(20) Moffatt MF, Gut IG, Demenais F, *et al.* A large-scale, consortium-based genomewide association study of asthma. *N Engl J Med* 2010;363:1211-21.

(21) Torgerson DG, Ampleford EJ, Chiu GY, *et al.* Meta-analysis of genome-wide association studies of asthma in ethnically diverse North American populations. *Nat Genet* 2011;43:887-92.

(22) Litonjua AA, Carey VJ, Burge HA, *et al.* Parental history and the risk for childhood asthma. Does mother confer more risk than father? *Am J Respir Crit Care Med* 1998;158:176-81.

(23) Almqvist C, Worm M, Leynaert B, *et al.* Impact of gender on asthma in childhood and adolescence: a GA2LEN review. *Allergy* 2008;63:47-57.

(24) Akinbami LJ, Moorman JE, Bailey C, *et al.* Trends in asthma prevalence, health care use, and mortality in the United States, 2001-2010. *NCHS Data Brief* 2012:1-8.

(25) Ali Z, Ulrik CS. Obesity and asthma: a coincidence or a causal relationship? A systematic review. *Respir Med* 2013;107:1287-300.

(26) Simpson A, Tan VY, Winn J, *et al.* Beyond atopy: multiple patterns of sensitization in relation to asthma in a birth cohort study. *Am J Respir Crit Care Med* 2010;181:1200-6.

(27) Krishnamoorthy N, Khare A, Oriss TB, *et al.* Early infection with respiratory syncytial virus impairs regulatory T cell function and increases susceptibility to allergic asthma. *Nat Med* 2012;18:1525-30.

(28) Jackson DJ. The role of rhinovirus infections in the development of early childhood asthma. *Curr Opin Allergy Clin Immunol* 2010;10:133-8.

(29) Ege MJ, Mayer M, Normand AC, *et al.* Exposure to environmental microorganisms and childhood asthma. *N Engl J Med* 2011;364:701-9.

(30) Riedler J, Braun-Fahrlander C, Eder W, *et al.* Exposure to farming in early life and development of asthma and allergy: a cross-sectional survey. *Lancet* 2001;358:1129-33.

(31) Cohen RT, Raby BA, Van Steen K, *et al.* In utero smoke exposure and impaired response to inhaled corticosteroids in children with asthma. *J Allergy Clin Immunol* 2010;126:491-7.

(32) Laumbach RJ, Kipen HM. Respiratory health effects of air pollution: update on biomass smoke and traffic pollution. *J Allergy Clin Immunol* 2012;129:3-11; quiz 12-3.

(33) Lange NE, Litonjua A, Hawrylowicz CM, *et al.* Vitamin D, the immune system and asthma. *Expert Rev Clin Immunol* 2009;5:693-702.

(34) Devereux G, Seaton A. Diet as a risk factor for atopy and asthma. *J Allergy Clin Immunol* 2005;115:1109-17; quiz 18.

(35) Yonas MA, Lange NE, Celedon JC. Psychosocial stress and asthma morbidity. *Curr Opin Allergy Clin Immunol* 2012;12:202-10.

(36) Fahy JV. Goblet cell and mucin gene abnormalities in asthma. *Chest* 2002;122:320S-26S.

(37) Roche WR, Beasley R, Williams JH, *et al.* Subepithelial fibrosis in the bronchi of asthmatics. *Lancet* 1989;1:520-4.

(38) James AL, Elliot JG, Jones RL, *et al.* Airway smooth muscle hypertrophy and hyperplasia in asthma. *Am J Respir Crit Care Med* 2012;185:1058-64.

(39) Dunnill MS, Massarella GR, Anderson JA. A comparison of the quantitative anatomy of the bronchi in normal subjects, in status asthmaticus, in chronic bronchitis, and in emphysema. *Thorax* 1969;24:176-9.

(40) Barbato A, Turato G, Baraldo S, *et al.* Epithelial damage and angiogenesis in the airways of children with asthma. *Am J Respir Crit Care Med* 2006;174:975-81.

(41) Barnes PJ. *Asthma and COPD: basic mechanisms and clinical management*. Amsterdam; Boston: Academic Press, 2002.

(42) Fahy JV. Type 2 inflammation in asthma--present in most, absent in many. *Nat Rev Immunol* 2015;15:57-65.

(43) Miller MR, Hankinson J, Brusasco V, *et al.* Standardisation of spirometry. *Eur Respir J* 2005;26:319-38.

(44) Wanger J, Clausen JL, Coates A, *et al.* Standardisation of the measurement of lung volumes. *Eur Respir J* 2005;26:511-22.

(45) Criee CP, Sorichter S, Smith HJ, *et al.* Body plethysmography--its principles and clinical use. *Respir Med* 2011;105:959-71.

(46) Piatti G, Fasano V, Cantarella G, *et al.* Body plethysmographic study of specific airway resistance in a sample of healthy adults. *Respirology* 2012;17:976-83.

(47) Ruppel G. *Manual of pulmonary function testing*. St. Louis, Mo: Mosby Elsevier, 2009.

(48) Fowler WS. Lung function studies; uneven pulmonary ventilation in normal subjects and in patients with pulmonary disease. *J Appl Physiol* 1949;2:283-99.

(49) Robertson JS, Siri WE, Jones HB. Lung ventilation patterns determined by analysis of nitrogen elimination rates; use of mass spectrometer as a continuous gas analyzer. *J Clin Invest* 1950;29:577-90.

(50) Becklake MR. A new index of the intrapulmonary mixture of inspired air. *Thorax* 1952;7:111-6.

(51) Robinson PD, Latzin P, Verbanck S, *et al.* Consensus statement for inert gas washout measurement using multiple- and single- breath tests. *Eur Respir J* 2013;41:507-22.

(52) Verbanck S, Schuermans D, Van Muylem A, *et al.* Ventilation distribution during histamine provocation. *J Appl Physiol* 1997;83:1907-16.

(53) Aurora P, Bush A, Gustafsson P, *et al.* Multiple-breath washout as a marker of lung disease in preschool children with cystic fibrosis. *Am J Respir Crit Care Med* 2005;171:249-56.

(54) Hulskamp G, Lum S, Stocks J, *et al.* Association of prematurity, lung disease and body size with lung volume and ventilation inhomogeneity in unsedated neonates: a multicentre study. *Thorax* 2009;64:240-5.

(55) Gustafsson PM, Aurora P, Lindblad A. Evaluation of ventilation maldistribution as an early indicator of lung disease in children with cystic fibrosis. *Eur Respir J* 2003;22:972-9.

(56) Aurora P, Stanojevic S, Wade A, *et al.* Lung clearance index at 4 years predicts subsequent lung function in children with cystic fibrosis. *Am J Respir Crit Care Med* 2011;183:752-8.

(57) Gustafsson PM. Peripheral airway involvement in CF and asthma compared by inert gas washout. *Pediatr Pulmonol* 2007;42:168-76.

(58) Zwitserloot A, Fuchs SI, Muller C, *et al.* Clinical application of inert gas Multiple Breath Washout in children and adolescents with asthma. *Respir Med* 2014;108:1254-9.

(59) Macleod KA, Horsley AR, Bell NJ, *et al.* Ventilation heterogeneity in children with well controlled asthma with normal spirometry indicates residual airways disease. *Thorax* 2009;64:33-7.

(60) Downie SR, Salome CM, Verbanck S, *et al.* Ventilation heterogeneity is a major determinant of airway hyperresponsiveness in asthma, independent of airway inflammation. *Thorax* 2007;62:684-9.

(61) Verbanck S, Schuermans D, Paiva M, *et al.* Nonreversible conductive airway ventilation heterogeneity in mild asthma. *J Appl Physiol* 2003;94:1380-6.

(62) Verbanck S, Schuermans D, Paiva M, *et al.* The functional benefit of anti-inflammatory aerosols in the lung periphery. *J Allergy Clin Immunol* 2006;118:340-6.

(63) Farah CS, King GG, Brown NJ, *et al.* Ventilation heterogeneity predicts asthma control in adults following inhaled corticosteroid dose titration. *J Allergy Clin Immunol* 2012;130:61-8.

(64) Thompson BR, Douglass JA, Ellis MJ, *et al.* Peripheral lung function in patients with stable and unstable asthma. *J Allergy Clin Immunol* 2013;131:1322-8.

(65) Pellegrino R, Viegi G, Brusasco V, *et al.* Interpretative strategies for lung function tests. *EurRespirJ* 2005;26:948-68.

(66) Hargreave FE, Ryan G, Thomson NC, *et al.* Bronchial responsiveness to histamine or methacholine in asthma: measurement and clinical significance. *J Allergy Clin Immunol* 1981;68:347-55.

(67) Crapo RO, Casaburi R, Coates AL, *et al.* Guidelines for methacholine and exercise challenge testing-1999. This official statement of the American Thoracic Society was adopted by the ATS Board of Directors, July 1999. *Am J Respir Crit Care Med* 2000;161:309-29.

(68) Anderson SD. Exercise-induced bronchoconstriction in the 21st century. *J Am Osteopath Assoc* 2011;111:S3-10.

(69) Anderson SD. Indirect challenge tests: Airway hyperresponsiveness in asthma: its measurement and clinical significance. *Chest* 2010;138:25S-30S.

(70) Gustafsson LE, Leone AM, Persson MG, *et al.* Endogenous nitric oxide is present in the exhaled air of rabbits, guinea pigs and humans. *Biochem Biophys Res Commun* 1991;181:852-7.

(71) Guo FH, Comhair SA, Zheng S, *et al.* Molecular mechanisms of increased nitric oxide (NO) in asthma: evidence for transcriptional and post-translational regulation of NO synthesis. *J Immunol* 2000;164:5970-80.

(72) Zietkowski Z, Bodzenta-Lukaszyk A, Tomasiak MM, *et al.* Comparison of exhaled nitric oxide measurement with conventional tests in steroid-naive asthma patients. *J Investig Allergol Clin Immunol* 2006;16:239-46.

(73) Warke TJ, Fitch PS, Brown V, *et al.* Exhaled nitric oxide correlates with airway eosinophils in childhood asthma. *Thorax* 2002;57:383-7.

(74) Payne DN, Adcock IM, Wilson NM, *et al.* Relationship between exhaled nitric oxide and mucosal eosinophilic inflammation in children with difficult asthma, after treatment with oral prednisolone. *Am J Respir Crit Care Med* 2001;164:1376-81.

(75) Berlyne GS, Parameswaran K, Kamada D, *et al.* A comparison of exhaled nitric oxide and induced sputum as markers of airway inflammation. *J Allergy Clin Immunol* 2000;106:638-44.

(76) Jatakanon A, Lim S, Kharitonov SA, *et al.* Correlation between exhaled nitric oxide, sputum eosinophils, and methacholine responsiveness in patients with mild asthma. *Thorax* 1998;53:91-5.

(77) Lim S, Jatakanon A, Meah S, *et al.* Relationship between exhaled nitric oxide and mucosal eosinophilic inflammation in mild to moderately severe asthma. *Thorax* 2000;55:184-8.

(78) Alving K, Weitzberg E, Lundberg JM. Increased amount of nitric oxide in exhaled air of asthmatics. *Eur Respir J* 1993;6:1368-70.

(79) Kharitonov SA, Yates D, Robbins RA, *et al.* Increased nitric oxide in exhaled air of asthmatic patients. *Lancet* 1994;343:133-5.

(80) Smith AD, Cowan JO, Brassett KP, *et al.* Exhaled nitric oxide: a predictor of steroid response. *Am J Respir Crit Care Med* 2005;172:453-9.

(81) Dweik RA, Boggs PB, Erzurum SC, *et al.* An official ATS clinical practice guideline: interpretation of exhaled nitric oxide levels (FENO) for clinical applications. *Am J Respir Crit Care Med* 2011;184:602-15.

(82) American Thoracic S, European Respiratory S. ATS/ERS recommendations for standardized procedures for the online and offline measurement of exhaled lower respiratory nitric oxide and nasal nitric oxide, 2005. *Am J Respir Crit Care Med* 2005;171:912-30.

(83) Recommendations for standardized procedures for the on-line and off-line measurement of exhaled lower respiratory nitric oxide and nasal nitric oxide in adults and children-1999. This official statement of the American Thoracic Society was adopted by the ATS Board of Directors, July 1999. *Am J Respir Crit Care Med* 1999;160:2104-17.

(84) Juniper EF, O'Byrne PM, Guyatt GH, *et al.* Development and validation of a questionnaire to measure asthma control. *Eur Respir J* 1999;14:902-7.

(85) Sutherland ER, King TS, Icitovic N, *et al.* A trial of clarithromycin for the treatment of suboptimally controlled asthma. *J Allergy Clin Immunol* 2010;126:747-53.

(86) Cox G, Thomson NC, Rubin AS, *et al.* Asthma control during the year after bronchial thermoplasty. *N Engl J Med* 2007;356:1327-37.

(87) Castro M, Mathur S, Hargreave F, *et al.* Reslizumab for poorly controlled, eosinophilic asthma: a randomized, placebo-controlled study. *Am J Respir Crit Care Med* 2011;184:1125-32.

(88) Juniper EF, Bousquet J, Abetz L, *et al.* Identifying 'well-controlled' and 'not well-controlled' asthma using the Asthma Control Questionnaire. *Respir Med* 2006;100:616-21.

(89) Juniper EF, Svensson K, Mork AC, *et al.* Measurement properties and interpretation of three shortened versions of the asthma control questionnaire. *Respir Med* 2005;99:553-8.

(90) Juniper EF, Buist AS, Cox FM, *et al.* Validation of a standardized version of the Asthma Quality of Life Questionnaire. *Chest* 1999;115:1265-70.

(91) Juniper EF, Guyatt GH, Willan A, *et al.* Determining a minimal important change in a disease-specific Quality of Life Questionnaire. *J Clin Epidemiol* 1994;47:81-7.

(92) Hanania NA, Alpan O, Hamilos DL, *et al.* Omalizumab in severe allergic asthma inadequately controlled with standard therapy: a randomized trial. *Ann Intern Med* 2011;154:573-82.

(93) Fletcher CM, Elmes PC, Fairbairn AS, *et al.* The significance of respiratory symptoms and the diagnosis of chronic bronchitis in a working population. *Br Med J* 1959;2:257-66.

(94) Borg GA. Psychophysical bases of perceived exertion. *Med Sci Sports Exerc* 1982;14:377-81.

(95) Wadsworth S, Sin D, Dorscheid D. Clinical update on the use of biomarkers of airway inflammation in the management of asthma. *J Asthma Allergy* 2011;4:77-86.

(96) Li JT, O'Connell EJ. Clinical evaluation of asthma. *Ann Allergy Asthma Immunol* 1996;76:1-13; quiz 13-5.

(97) Gershon AS, Victor JC, Guan J, *et al.* Pulmonary function testing in the diagnosis of asthma: a population study. *Chest* 2012;141:1190-6.

(98) Aaron SD, Vandemheen KL, Boulet LP, *et al.* Overdiagnosis of asthma in obese and nonobese adults. *CMAJ* 2008;179:1121-31.

(99) Taylor DR, Bateman ED, Boulet LP, *et al.* A new perspective on concepts of asthma severity and control. *Eur Respir J* 2008;32:545-54.

(100) National Asthma E, Prevention P. Expert Panel Report 3 (EPR-3): Guidelines for the Diagnosis and Management of Asthma-Summary Report 2007. *J Allergy Clin Immunol* 2007;120:S94-138.

(101) Chung KF, Wenzel SE, Brozek JL, *et al.* International ERS/ATS guidelines on definition, evaluation and treatment of severe asthma. *Eur Respir J* 2014;43:343-73.

(102) Thomas A, Lemanske RF, Jr., Jackson DJ. Approaches to stepping up and stepping down care in asthmatic patients. *J Allergy Clin Immunol* 2011;128:915-24; quiz 25-6.

(103) Barnes NC, Marone G, Di Maria GU, *et al.* A comparison of fluticasone propionate, 1 mg daily, with beclomethasone dipropionate, 2 mg daily, in the treatment of severe asthma. International Study Group. *Eur Respir J* 1993;6:877-85.

(104) Dahl R, Lundback B, Malo JL, *et al.* A dose-ranging study of fluticasone propionate in adult patients with moderate asthma. International Study Group. *Chest* 1993;104:1352-8.

(105) Fabbri L, Burge PS, Croonenborgh L, *et al.* Comparison of fluticasone propionate with beclomethasone dipropionate in moderate to severe asthma treated for one year. International Study Group. *Thorax* 1993;48:817-23.

(106) Gustafsson P, Tsanakas J, Gold M, *et al.* Comparison of the efficacy and safety of inhaled fluticasone propionate 200 micrograms/day with inhaled beclomethasone dipropionate 400 micrograms/day in mild and moderate asthma. *Arch Dis Child* 1993;69:206-11.

(107) Suissa S, Ernst P, Benayoun S, *et al.* Low-dose inhaled corticosteroids and the prevention of death from asthma. *N Engl J Med* 2000;343:332-6.

(108) Green RH, Brightling CE, Woltmann G, *et al.* Analysis of induced sputum in adults with asthma: identification of subgroup with isolated sputum neutrophilia and poor response to inhaled corticosteroids. *Thorax* 2002;57:875-9.

(109) Garcia Garcia ML, Wahn U, Gilles L, *et al.* Montelukast, compared with fluticasone, for control of asthma among 6- to 14-year-old patients with mild asthma: the MOSAIC study. *Pediatrics* 2005;116:360-9.

(110) Zeiger RS, Szefler SJ, Phillips BR, *et al.* Response profiles to fluticasone and montelukast in mild-to-moderate persistent childhood asthma. *J Allergy Clin Immunol* 2006;117:45-52.

(111) Moore WC, Bleecker ER, Curran-Everett D, *et al.* Characterization of the severe asthma phenotype by the National Heart, Lung, and Blood Institute's Severe Asthma Research Program. *J Allergy Clin Immunol* 2007;119:405-13.

(112) Edmonds ML, Milan SJ, Camargo CA, Jr., *et al.* Early use of inhaled corticosteroids in the emergency department treatment of acute asthma. *Cochrane Database Syst Rev* 2012;12:CD002308.

(113) Rowe BH, Spooner CH, Ducharme FM, *et al.* Corticosteroids for preventing relapse following acute exacerbations of asthma. *Cochrane Database Syst Rev* 2007:CD000195.

(114) Kips JC, Pauwels RA. Long-acting inhaled beta(2)-agonist therapy in asthma. *Am J Respir Crit Care Med* 2001;164:923-32.

(115) Simons FE. A comparison of beclomethasone, salmeterol, and placebo in children with asthma. Canadian Beclomethasone Dipropionate-Salmeterol Xinafoate Study Group. *N Engl J Med* 1997;337:1659-65.

(116) Greening AP, Ind PW, Northfield M, *et al.* Added salmeterol versus higher-dose corticosteroid in asthma patients with symptoms on existing inhaled corticosteroid. Allen & Hanburys Limited UK Study Group. *Lancet* 1994;344:219-24.

(117) Woolcock A, Lundback B, Ringdal N, *et al.* Comparison of addition of salmeterol to inhaled steroids with doubling of the dose of inhaled steroids. *Am J Respir Crit Care Med* 1996;153:1481-8.

(118) Dahl R, Larsen BB, Venge P. Effect of long-term treatment with inhaled budesonide or theophylline on lung function, airway reactivity and asthma symptoms. *Respir Med* 2002;96:432-8.

(119) Lim S, Jatakanon A, Gordon D, *et al.* Comparison of high dose inhaled steroids, low dose inhaled steroids plus low dose theophylline, and low dose inhaled steroids alone in chronic asthma in general practice. *Thorax* 2000;55:837-41.

(120) Matsuse H, Kohno S. Leukotriene receptor antagonists pranlukast and montelukast for treating asthma. *Expert Opin Pharmacother* 2014;15:353-63.

(121) Ducharme FM. Inhaled glucocorticoids versus leukotriene receptor antagonists as single agent asthma treatment: systematic review of current evidence. *BMJ* 2003;326:621.

(122) Reiss TF, Chervinsky P, Dockhorn RJ, *et al.* Montelukast, a once-daily leukotriene receptor antagonist, in the treatment of chronic asthma: a multicenter, randomized, double-blind trial. Montelukast Clinical Research Study Group. *Arch Intern Med* 1998;158:1213-20.

(123) Price DB, Hernandez D, Magyar P, *et al.* Randomised controlled trial of montelukast plus inhaled budesonide versus double dose inhaled budesonide in adult patients with asthma. *Thorax* 2003;58:211-6.

(124) Price D, Musgrave SD, Shepstone L, *et al.* Leukotriene antagonists as first-line or add-on asthma-controller therapy. *N Engl J Med* 2011;364:1695-707.

(125) Ringdal N, Eliraz A, Pruzinec R, *et al.* The salmeterol/fluticasone combination is more effective than fluticasone plus oral montelukast in asthma. *Respir Med* 2003;97:234-41.

(126) Fish JE, Israel E, Murray JJ, *et al.* Salmeterol powder provides significantly better benefit than montelukast in asthmatic patients receiving concomitant inhaled corticosteroid therapy. *Chest* 2001;120:423-30.

(127) Lougheed MD, Lemiere C, Ducharme FM, *et al.* Canadian Thoracic Society 2012 guideline update: diagnosis and management of asthma in preschoolers, children and adults. *Can Respir J* 2012;19:127-64.

(128) Soler X, Ramsdell J. Anticholinergics/antimuscarinic drugs in asthma. *Curr Allergy Asthma Rep* 2014;14:484.

(129) Kerstjens HA, Engel M, Dahl R, *et al.* Tiotropium in asthma poorly controlled with standard combination therapy. *N Engl J Med* 2012;367:1198-207.

(130) Kerstjens HA, Disse B, Schroder-Babo W, *et al.* Tiotropium improves lung function in patients with severe uncontrolled asthma: a randomized controlled trial. *J Allergy Clin Immunol* 2011;128:308-14.

(131) Peters SP, Kunselman SJ, Icitovic N, *et al.* Tiotropium bromide step-up therapy for adults with uncontrolled asthma. *N Engl J Med* 2010;363:1715-26.

(132) Soler M, Matz J, Townley R, *et al.* The anti-IgE antibody omalizumab reduces exacerbations and steroid requirement in allergic asthmatics. *Eur Respir J* 2001;18:254-61.

(133) Humbert M, Beasley R, Ayres J, *et al.* Benefits of omalizumab as add-on therapy in patients with severe persistent asthma who are inadequately controlled despite best available therapy (GINA 2002 step 4 treatment): INNOVATE. *Allergy* 2005;60:309-16.

(134) Busse W, Corren J, Lanier BQ, *et al.* Omalizumab, anti-IgE recombinant humanized monoclonal antibody, for the treatment of severe allergic asthma. *J Allergy Clin Immunol* 2001;108:184-90.

(135) Ayres JG, Higgins B, Chilvers ER, *et al.* Efficacy and tolerability of anti-immunoglobulin E therapy with omalizumab in patients with poorly controlled (moderate-to-severe) allergic asthma. *Allergy* 2004;59:701-8.

(136) Nair P, Pizzichini MM, Kjarsgaard M, *et al.* Mepolizumab for prednisone-dependent asthma with sputum eosinophilia. *N Engl J Med* 2009;360:985-93.

(137) Corren J, Lemanske RF, Hanania NA, *et al.* Lebrikizumab treatment in adults with asthma. *N Engl J Med* 2011;365:1088-98.

(138) Piper E, Brightling C, Niven R, *et al.* A phase II placebo-controlled study of tralokinumab in moderate-to-severe asthma. *Eur Respir J* 2013;41:330-8.

(139) Wenzel SE, Barnes PJ, Bleecker ER, *et al.* A randomized, double-blind, placebo-controlled study of tumor necrosis factor-alpha blockade in severe persistent asthma. *Am J Respir Crit Care Med* 2009;179:549-58.

(140) Humbert M, de Blay F, Garcia G, *et al.* Masitinib, a c-kit/PDGF receptor tyrosine kinase inhibitor, improves disease control in severe corticosteroid-dependent asthmatics. *Allergy* 2009;64:1194-201.

(141) Busse WW, Israel E, Nelson HS, *et al.* Daclizumab improves asthma control in patients with moderate to severe persistent asthma: a randomized, controlled trial. *Am J Respir Crit Care Med* 2008;178:1002-8.

(142) Nair P, Gaga M, Zervas E, *et al.* Safety and efficacy of a CXCR2 antagonist in patients with severe asthma and sputum neutrophils: a randomized, placebo-controlled clinical trial. *Clin Exp Allergy* 2012;42:1097-103.

(143) Cox PG, Miller J, Mitzner W, *et al.* Radiofrequency ablation of airway smooth muscle for sustained treatment of asthma: preliminary investigations. *Eur Respir J* 2004;24:659-63.

(144) Pretolani M, Dombret MC, Thabut G, *et al.* Reduction of airway smooth muscle mass by bronchial thermoplasty in patients with severe asthma. *Am J Respir Crit Care Med* 2014;190:1452-4.

(145) Miller JD, Cox G, Vincic L, *et al.* A prospective feasibility study of bronchial thermoplasty in the human airway. *Chest* 2005;127:1999-2006.

(146) Pavord ID, Cox G, Thomson NC, *et al.* Safety and efficacy of bronchial thermoplasty in symptomatic, severe asthma. *Am J Respir Crit Care Med* 2007;176:1185-91.

(147) Castro M, Rubin AS, Laviolette M, *et al.* Effectiveness and safety of bronchial thermoplasty in the treatment of severe asthma: a multicenter, randomized, double-blind, sham-controlled clinical trial. *Am J Respir Crit Care Med* 2010;181:116-24.

(148) Wechsler ME, Laviolette M, Rubin AS, *et al.* Bronchial thermoplasty: Long-term safety and effectiveness in patients with severe persistent asthma. *J Allergy Clin Immunol* 2013;132:1295-302.

(149) Pavord ID, Thomson NC, Niven RM, *et al.* Safety of bronchial thermoplasty in patients with severe refractory asthma. *Ann Allergy Asthma Immunol* 2013;111:402-7.

(150) Joarder R, Crundwell N, SpringerLink. *Chest X-Ray in Clinical Practice*. London: Springer Verlag London Limited, 2009.

(151) Brenner DJ, Hall EJ. Computed tomography--an increasing source of radiation exposure. *N Engl J Med* 2007;357:2277-84.

(152) Paganin F, Trussard V, Seneterre E, *et al.* Chest radiography and high resolution computed tomography of the lungs in asthma. *Am Rev Respir Dis* 1992;146:1084-7.

(153) Webb WR, Higgins CB. *Thoracic imaging: pulmonary and cardiovascular radiology*. Philadelphia: Wolters Kluwer Health/Lippincott Williams & Wilkins, 2011.

(154) Castro M, Fain SB, Hoffman EA, *et al.* Lung imaging in asthmatic patients: the picture is clearer. *J Allergy Clin Immunol* 2011;128:467-78.

(155) Desai S. *Pulmonary imaging: contributions to key clinical questions*. London;Boca Raton, FL;: Informa Healthcare, 2007.

(156) Lynch DA, Newell JD, Tschomper BA, *et al.* Uncomplicated asthma in adults: comparison of CT appearance of the lungs in asthmatic and healthy subjects. *Radiology* 1993;188:829-33.

(157) Gupta S, Siddiqui S, Haldar P, *et al.* Qualitative analysis of high-resolution CT scans in severe asthma. *Chest* 2009;136:1521-8.

(158) Beigelman-Aubry C, Capderou A, Grenier PA, *et al.* Mild intermittent asthma: CT assessment of bronchial cross-sectional area and lung attenuation at controlled lung volume. *Radiology* 2002;223:181-7.

(159) Sung A, Naidich D, Belinskaya I, *et al.* The role of chest radiography and computed tomography in the diagnosis and management of asthma. *Curr Opin Pulm Med* 2007;13:31-6.

(160) Tschirren J, Hoffman EA, McLennan G, *et al.* Intrathoracic airway trees: segmentation and airway morphology analysis from low-dose CT scans. *IEEE Trans Med Imaging* 2005;24:1529-39.

(161) Awadh N, Muller NL, Park CS, *et al.* Airway wall thickness in patients with near fatal asthma and control groups: assessment with high resolution computed tomographic scanning. *Thorax* 1998;53:248-53.

(162) Kasahara K, Shiba K, Ozawa T, *et al.* Correlation between the bronchial subepithelial layer and whole airway wall thickness in patients with asthma. *Thorax* 2002;57:242-46.

(163) Siddiqui S, Gupta S, Cruse G, *et al.* Airway wall geometry in asthma and nonasthmatic eosinophilic bronchitis. *Allergy* 2009;64:951-8.

(164) Gupta S, Siddiqui S, Haldar P, *et al.* Quantitative analysis of high-resolution computed tomography scans in severe asthma subphenotypes. *Thorax* 2010;65:775-81.

(165) Niimi A, Matsumoto H, Amitani R, *et al.* Effect of short-term treatment with inhaled corticosteroid on airway wall thickening in asthma. *Am J Med* 2004;116:725-31.

(166) Okazawa M, Muller N, McNamara AE, *et al.* Human airway narrowing measured using high resolution computed tomography. *Am J Respir Crit Care Med* 1996;154:1557-62.

(167) Niimi A, Matsumoto H, Amitani R, *et al.* Airway wall thickness in asthma assessed by computed tomography. Relation to clinical indices. *Am J Respir Crit Care Med* 2000;162:1518-23.

(168) Aysola RS, Hoffman EA, Gierada D, *et al.* Airway remodeling measured by multidetector CT is increased in severe asthma and correlates with pathology. *Chest* 2008;134:1183-91.

(169) Little SA, Sproule MW, Cowan MD, *et al.* High resolution computed tomographic assessment of airway wall thickness in chronic asthma: reproducibility and relationship with lung function and severity. *Thorax* 2002;57:247-53.

(170) Gono H, Fujimoto K, Kawakami S, *et al.* Evaluation of airway wall thickness and air trapping by HRCT in asymptomatic asthma. *Eur Respir J* 2003;22:965-71.

(171) Niimi A, Matsumoto H, Takemura M, *et al.* Relationship of airway wall thickness to airway sensitivity and airway reactivity in asthma. *Am J Respir Crit Care Med* 2003;168:983-8.

(172) Brown RH, Scichilone N, Mudge B, *et al.* High-resolution computed tomographic evaluation of airway distensibility and the effects of lung inflation on airway caliber in healthy subjects and individuals with asthma. *Am J Respir Crit Care Med* 2001;163:994-1001.

(173) Lee YM, Park JS, Hwang JH, *et al.* High-resolution CT findings in patients with near-fatal asthma: comparison of patients with mild-to-severe asthma and normal control subjects and changes in airway abnormalities following steroid treatment. *Chest* 2004;126:1840-8.

(174) Kurashima K, Kanauchi T, Hoshi T, *et al.* Effect of early versus late intervention with inhaled corticosteroids on airway wall thickness in patients with asthma. *Respirology* 2008;13:1008-13.

(175) Washko GR, Parraga G, Coxson HO. Quantitative pulmonary imaging using computed tomography and magnetic resonance imaging. *Respirology* 2012;17:432-44.

(176) Newman KB, Lynch DA, Newman LS, *et al.* Quantitative computed tomography detects air trapping due to asthma. *Chest* 1994;106:105-9.

(177) Mitsunobu F, Mifune T, Ashida K, *et al.* Influence of age and disease severity on high resolution CT lung densitometry in asthma. *Thorax* 2001;56:851-56.

(178) Busacker A, Newell JD, Jr., Keefe T, *et al.* A multivariate analysis of risk factors for the air-trapping asthmatic phenotype as measured by quantitative CT analysis. *Chest* 2009;135:48-56.

(179) Zeidler MR, Kleerup EC, Goldin JG, *et al.* Montelukast improves regional air-trapping due to small airways obstruction in asthma. *Eur Respir J* 2006;27:307-15.

(180) Tunon-de-Lara JM, Laurent F, Giraud V, *et al.* Air trapping in mild and moderate asthma: effect of inhaled corticosteroids. *J Allergy Clin Immunol* 2007;119:583-90.

(181) Goldin JG, Tashkin DP, Kleerup EC, *et al.* Comparative effects of hydrofluoroalkane and chlorofluorocarbon beclomethasone dipropionate inhalation on small airways: assessment with functional helical thin-section computed tomography. *J Allergy Clin Immunol* 1999;104:S258-67.

(182) Murphy DM, Nicewicz JT, Zabbatino SM, *et al.* Local pulmonary ventilation using nonradioactive xenon-enhanced ultrafast computed tomography. *Chest* 1989;96:799-804.

(183) Chae EJ, Seo JB, Lee J, *et al.* Xenon ventilation imaging using dual-energy computed tomography in asthmatics: initial experience. *Invest Radiol* 2010;45:354-61.

(184) Jung JW, Kwon JW, Kim TW, *et al.* New insight into the assessment of asthma using xenon ventilation computed tomography. *Ann Allergy Asthma Immunol* 2013;111:90-95 e2.

(185) Petersson J, Sanchez-Crespo A, Larsson SA, *et al.* Physiological imaging of the lung: single-photon-emission computed tomography (SPECT). *J Appl Physiol (1985)* 2007;102:468-76.

(186) Amis TC, Crawford AB, Davison A, *et al.* Distribution of inhaled 99mtechnetium labelled ultrafine carbon particle aerosol (Technegas) in human lungs. *Eur Respir J* 1990;3:679-85.

(187) Bentivoglio LG, Beerel F, Bryan AC, *et al.* Regional Pulmonary Function Studied with Xenon in Patients with Bronchial Asthma. *J Clin Invest* 1963;42:1193-200.

(188) Heckscher T, Bass H, Oriol A, *et al.* Regional lung function in patients with bronchial asthma. *J Clin Invest* 1968;47:1063-70.

(189) Engel LA, Landau L, Taussig L, *et al.* Influence of bronchomotor tone on regional ventilation distribution at residual volume. *J Appl Physiol* 1976;40:411-16.

(190) Clague H, Ahmad D, Chamberlain MJ, *et al.* Histamine bronchial challenge: effect on regional ventilation and aerosol deposition. *Thorax* 1983;38:668-75.

(191) King GG, Eberl S, Salome CM, *et al.* Differences in airway closure between normal and asthmatic subjects measured with single-photon emission computed tomography and technegas. *Am J Respir Crit Care Med* 1998;158:1900-06.

(192) Farrow CE, Salome CM, Harris BE, *et al.* Airway closure on imaging relates to airway hyperresponsiveness and peripheral airway disease in asthma. *J Appl Physiol* 2012;113:958-66.

(193) Leach CL, Kuehl PJ, Chand R, *et al.* Characterization of respiratory deposition of fluticasone-salmeterol hydrofluoroalkane-134a and hydrofluoroalkane-134a beclomethasone in asthmatic patients. *Ann Allergy Asthma Immunol* 2012;108:195-200.

(194) Newman S, Salmon A, Nave R, *et al.* High lung deposition of 99mTc-labeled ciclesonide administered via HFA-MDI to patients with asthma. *Respir Med* 2006;100:375-84.

(195) Musch G, Venegas JG. Positron emission tomography imaging of regional lung function. *Minerva Anestesiol* 2006;72:363-7.

(196) Venegas JG, Winkler T, Musch G, *et al.* Self-organized patchiness in asthma as a prelude to catastrophic shifts. *Nature* 2005;434:777-82.

(197) Harris RS, Winkler T, Tgavalekos N, *et al.* Regional pulmonary perfusion, inflation, and ventilation defects in bronchoconstricted patients with asthma. *Am J Respir Crit Care Med* 2006;174:245-53.

(198) Kelmenson DA, Kelly VJ, Winkler T, *et al.* The effect of omalizumab on ventilation and perfusion in adults with allergic asthma. *Am J Nucl Med Mol Imaging* 2013;3:350-60.

(199) Chen DL, Schuster DP. Imaging pulmonary inflammation with positron emission tomography: a biomarker for drug development. *Mol Pharm* 2006;3:488-95.

(200) Harris RS, Venegas JG, Wongviriyawong C, *et al.* 18F-FDG uptake rate is a biomarker of eosinophilic inflammation and airway response in asthma. *J Nucl Med* 2011;52:1713-20.

(201) Bergin CJ, Glover GM, Pauly J. Magnetic resonance imaging of lung parenchyma. *J Thorac Imaging* 1993;8:12-7.

(202) Bergin CJ, Pauly JM, Macovski A. Lung parenchyma: projection reconstruction MR imaging. *Radiology* 1991;179:777-81.

(203) Edelman RR, Hatabu H, Tadamura E, *et al.* Noninvasive assessment of regional ventilation in the human lung using oxygen-enhanced magnetic resonance imaging. *Nat Med* 1996;2:1236-9.

(204) Bauman G, Puderbach M, Deimling M, *et al.* Non-contrast-enhanced perfusion and ventilation assessment of the human lung by means of fourier decomposition in proton MRI. *Magn Reson Med* 2009;62:656-64.

(205) Zhang WJ, Niven RM, Young SS, *et al.* Dynamic oxygen-enhanced magnetic resonance imaging of the lung in asthma-initial experience. *Eur J Radiol* 2015;84:318-26.

(206) Ohno Y, Koyama H, Matsumoto K, *et al.* Oxygen-enhanced MRI vs. quantitatively assessed thin-section CT: pulmonary functional loss assessment and clinical stage classification of asthmatics. *Eur J Radiol* 2011;77:85-91.

(207) Ohno Y, Nishio M, Koyama H, *et al.* Asthma: comparison of dynamic oxygen-enhanced MR imaging and quantitative thin-section CT for evaluation of clinical treatment. *Radiology* 2014;273:907-16.

(208) Renne J, Hinrichs J, Schonfeld C, *et al.* Noninvasive quantification of airway inflammation following segmental allergen challenge with functional MR imaging: a proof of concept study. *Radiology* 2015;274:267-75.

(209) Sommer G, Bauman G, Koenigkam-Santos M, *et al.* Non-contrast-enhanced preoperative assessment of lung perfusion in patients with non-small-cell lung cancer using Fourier decomposition magnetic resonance imaging. *Eur J Radiol* 2013;82:e879-87.

(210) Lederlin M, Bauman G, Eichinger M, *et al.* Functional MRI using Fourier decomposition of lung signal: reproducibility of ventilation- and perfusion-weighted imaging in healthy volunteers. *Eur J Radiol* 2013;82:1015-22.

(211) Bauman G, Puderbach M, Heimann T, *et al.* Validation of Fourier decomposition MRI with dynamic contrast-enhanced MRI using visual and automated scoring of pulmonary perfusion in young cystic fibrosis patients. *Eur J Radiol* 2013;82:2371-7.

(212) Bianchi A, Ozier A, Ousova O, *et al.* Ultrashort-TE MRI longitudinal study and characterization of a chronic model of asthma in mice: inflammation and bronchial remodeling assessment. *NMR Biomed* 2013;26:1451-9.

(213) Albert MS, Cates GD, Driehuys B, *et al.* Biological magnetic resonance imaging using laser-polarized ^{129}Xe. *Nature* 1994;370:199-201.

(214) Kruger SJ, Nagle SK, Couch MJ, *et al.* Functional imaging of the lungs with gas agents. *J Magn Reson Imaging* 2015.

(215) Walker TG, Happer W. Spin-exchange optical pumping of noble-gas nuclei. *Reviews of Modern Physics* 1997;69:629-42.

(216) Cho A. Physics. Helium-3 shortage could put freeze on low-temperature research. *Science* 2009;326:778-79.

(217) Woods JC. Mine the moon for 3He MRI? Not yet. *J Appl Physiol (1985)* 2013;114:705-6.

(218) Lutey BA, Lefrak SS, Woods JC, *et al.* Hyperpolarized 3He MR imaging: physiologic monitoring observations and safety considerations in 100 consecutive subjects. *Radiology* 2008;248:655-61.

(219) Shukla Y, Wheatley A, Kirby M, *et al.* Hyperpolarized 129Xe magnetic resonance imaging: tolerability in healthy volunteers and subjects with pulmonary disease. *Acad Radiol* 2012;19:941-51.

(220) Kirby M, Heydarian M, Svenningsen S, *et al.* Hyperpolarized ^{3}He magnetic resonance functional imaging semiautomated segmentation. *Acad Radiol* 2012;19:141-52.

(221) He M, Kaushik SS, Robertson SH, *et al.* Extending semiautomatic ventilation defect analysis for hyperpolarized (129)Xe ventilation MRI. *Acad Radiol* 2014;21:1530-41.

(222) Tustison NJ, Avants BB, Flors L, *et al.* Ventilation-based segmentation of the lungs using hyperpolarized (3)He MRI. *J Magn Reson Imaging* 2011;34:831-41.

(223) Mathew L, Evans A, Ouriadov A, *et al.* Hyperpolarized 3He magnetic resonance imaging of chronic obstructive pulmonary disease: reproducibility at 3.0 tesla. *Acad Radiol* 2008;15:1298-311.

(224) Fain SB, Gonzalez-Fernandez G, Peterson ET, *et al.* Evaluation of structure-function relationships in asthma using multidetector CT and hyperpolarized He-3 MRI. *Acad Radiol* 2008;15:753-62.

(225) Woodhouse N, Wild JM, Paley MN, *et al.* Combined helium-3/proton magnetic resonance imaging measurement of ventilated lung volumes in smokers compared to never-smokers. *J Magn Reson Imaging* 2005;21:365-9.

(226) Tzeng YS, Lutchen K, Albert M. The difference in ventilation heterogeneity between asthmatic and healthy subjects quantified using hyperpolarized 3He MRI. *J Appl Physiol* 2009;106:813-22.

(227) Sheikh K, Paulin GA, Svenningsen S, *et al.* Pulmonary ventilation defects in older never-smokers. *J Appl Physiol* 2014;117:297-306.

(228) Kirby M, Svenningsen S, Ahmed H, *et al.* Quantitative evaluation of hyperpolarized helium-3 magnetic resonance imaging of lung function variability in cystic fibrosis. *Acad Radiol* 2011;18:1006-13.

(229) Kirby M, Mathew L, Heydarian M, *et al.* Chronic obstructive pulmonary disease: quantification of bronchodilator effects by using hyperpolarized ^{3}He MR imaging. *Radiology* 2011;261:283-92.

(230) Niles DJ, Kruger SJ, Dardzinski BJ, *et al.* Exercise-induced bronchoconstriction: reproducibility of hyperpolarized 3He MR imaging. *Radiology* 2013;266:618-25.

(231) de Lange EE, Altes TA, Patrie JT, *et al.* Changes in regional airflow obstruction over time in the lungs of patients with asthma: evaluation with ^{3}He MR imaging. *Radiology* 2009;250:567-75.

(232) de Lange EE, Altes TA, Patrie JT, *et al.* The variability of regional airflow obstruction within the lungs of patients with asthma: assessment with hyperpolarized helium-3 magnetic resonance imaging. *J Allergy Clin Immunol* 2007;119:1072-8.

(233) de Lange EE, Altes TA, Patrie JT, *et al.* Evaluation of asthma with hyperpolarized helium-3 MRI: correlation with clinical severity and spirometry. *Chest* 2006;130:1055-62.

(234) Kruger SJ, Niles DJ, Dardzinski B, *et al.* Hyperpolarized Helium-3 MRI of exercise-induced bronchoconstriction during challenge and therapy. *J Magn Reson Imaging* 2014;39:1230-7.

(235) Altes TA, Powers PL, Knight-Scott J, *et al.* Hyperpolarized ^{3}He MR lung ventilation imaging in asthmatics: preliminary findings. *J Magn Reson Imaging* 2001;13:378-84.

(236) Samee S, Altes T, Powers P, *et al.* Imaging the lungs in asthmatic patients by using hyperpolarized helium-3 magnetic resonance: assessment of response to methacholine and exercise challenge. *J Allergy Clin Immunol* 2003;111:1205-11.

(237) Costella S, Kirby M, Maksym GN, *et al.* Regional Pulmonary Response to a Methacholine Challenge using Hyperpolarized ^{3}He Magnetic Resonance Imaging. *Respirology* 2012;17:1237-46.

(238) Aysola R, de Lange EE, Castro M, *et al.* Demonstration of the heterogeneous distribution of asthma in the lungs using CT and hyperpolarized helium-3 MRI. *J Magn Reson Imaging* 2010;32:1379-87.

(239) Cadman RV, Lemanske RF, Jr., Evans MD, *et al.* Pulmonary 3He magnetic resonance imaging of childhood asthma. *J Allergy Clin Immunol* 2013;131:369-76 e1-5.

(240) Saam BT, Yablonskiy DA, Kodibagkar VD, *et al.* MR imaging of diffusion of (3)He gas in healthy and diseased lungs. *Magn Reson Med* 2000;44:174-79.

(241) Kauczor HU, Ebert M, Kreitner KF, *et al.* Imaging of the lungs using 3He MRI: preliminary clinical experience in 18 patients with and without lung disease. *J Magn Reson Imaging* 1997;7:538-43.

(242) Parraga G, Ouriadov A, Evans A, *et al.* Hyperpolarized 3He ventilation defects and apparent diffusion coefficients in chronic obstructive pulmonary disease: preliminary results at 3.0 Tesla. *Invest Radiol* 2007;42:384-91.

(243) Diaz S, Casselbrant I, Piitulainen E, *et al.* Hyperpolarized 3He apparent diffusion coefficient MRI of the lung: reproducibility and volume dependency in healthy volunteers and patients with emphysema. *J Magn Reson Imaging* 2008;27:763-70.

(244) Morbach AE, Gast KK, Schmiedeskamp J, *et al.* Diffusion-weighted MRI of the lung with hyperpolarized helium-3: a study of reproducibility. *J Magn Reson Imaging* 2005;21:765-74.

(245) Woods JC, Choong CK, Yablonskiy DA, *et al.* Hyperpolarized 3He diffusion MRI and histology in pulmonary emphysema. *Magn Reson Med* 2006;56:1293-300.

(246) Wang C, Altes TA, Mugler JP, 3rd, *et al.* Assessment of the lung microstructure in patients with asthma using hyperpolarized 3He diffusion MRI at two time scales: comparison with healthy subjects and patients with COPD. *J Magn Reson Imaging* 2008;28:80-8.

(247) Gonem S, Hardy S, Buhl N, *et al.* Characterization of acinar airspace involvement in asthmatic patients by using inert gas washout and hyperpolarized helium magnetic resonance. *J Allergy Clin Immunol* 2015.

CHAPTER 2

To better understand ventilation defects in asthma, here we quantitatively compared hyperpolarized ^{3}He and ^{129}Xe MRI in a small group of well-controlled asthmatics before and after bronchodilator administration.

The contents of this chapter were previously published in the Journal of Magnetic Resonance Imaging: S Svenningsen, M Kirby, D Starr, D Leary, A Wheatley, G Maksym, DG McCormack and G Parraga. Hyperpolarized ^{3}He and ^{129}Xe Magnetic Resonance Imaging Differences in Asthma prior to Bronchodilation. J Magn Reson Imaging 2013; 38(6):1521-1530. Permission to reproduce this article was granted by John Wiley & Sons and is provided in Appendix A.

2 HYPERPOLARIZED ^{3}HE AND ^{129}XE MRI: DIFFERENCES IN ASTHMA BEFORE BRONCHODILATION

2.1 Introduction

Asthma – a chronic inflammatory disease of the airways is characterized by acute intermittent attacks of airflow limitation resulting in symptoms of dyspnea, cough, chest tightness, and wheeze.[1,2] Reversible airflow obstruction occurs in response to external stimuli that trigger acute effects such as bronchoconstriction, plasma exudation, edema and mucus hypersecretion. It is believed that untreated chronic airway inflammation leads to airway remodeling, resulting in numerous physiological and functional consequences including airflow limitation and ventilation abnormalities.[3,4] The diagnosis and monitoring of asthma are commonly performed using the spirometry measurement[5,6] of the forced expiratory volume in 1s (FEV_1) -a global measure of airflow limitation that is relatively insensitive to changes in small airway structure and function.[7,8]

Multiple-breath-nitrogen washout (MBNW) studies have clearly shown that ventilation is heterogeneous in asthma[9,10] and that this heterogeneity is likely related to airway hyper-responsiveness,[11] although similar to FEV_1, MBNW measurements cannot provide regional information. Imaging studies including those using nuclear medicine scintigraphy,[12-14] positron emission tomography[15] and x-ray computed tomography (CT)[16-18] have provided a regional picture of heterogeneous ventilation abnormalities in asthma. Additionally, at our site[19] and other centres,[20-25] magnetic resonance imaging (MRI) using hyperpolarized helium-3 (^{3}He) has shown regional ventilation heterogeneity[20,21,25] and the surprising spatial-temporal persistence of ventilation abnormalities or defects[22,23] in

asthma. Moreover, in asthma, hyperpolarized ^{3}He ventilation defects have been correlated with disease severity[21] and ventilation defects become larger and/or more numerous after methacholine challenge and exercise.[19,24,25]

Hyperpolarized ^{3}He MRI remains a specialized imaging research tool, primarily because the restricted quantity and unpredictable cost of ^{3}He gas[26] has limited uptake in pulmonary medicine. These issues do not pertain to hyperpolarized ^{129}Xe MRI, an alternative contrast agent[27] that was used to obtain the first reported MR ventilation images.[28,29] With recent advances in polarization physics,[30-33] ^{129}Xe MRI has been further developed to provide high resolution measurements of both ^{129}Xe pulmonary ventilation and diffusion.[28,29,32,34-41] The safety and tolerability[38,42] of ^{129}Xe MRI was recently evaluated and a direct quantitative comparison with ^{3}He MRI was reported in COPD and healthy subjects.[43] This previous work showed significantly greater ^{129}Xe as compared to ^{3}He ventilation defects in COPD subjects, although in healthy volunteers there were no differences observed.[43] Similarly, previous work qualitatively compared ^{3}He and ^{129}Xe MRI gas distribution in subjects with cystic fibrosis (CF) and showed ^{3}He and ^{129}Xe ventilation defects were in good agreement for some subjects, but in other subjects, ^{129}Xe ventilation defects were larger and/or more numerous.[44] Although it is unclear what the structural determinants or mechanisms are behind the differences between ^{3}He and ^{129}Xe gas distribution, such differences are believed to reflect differences in the physical properties of the inspired gases and their interaction with pulmonary abnormalities that are not present in healthy volunteers. A potential mechanism responsible for the differences in ^{3}He and ^{129}Xe gas distribution is the effect of gas density and viscosity on flow resistance in the airways, which is dependent on airway lumen dimensions.[45] Structural narrowing of the airway lumen is a common feature in asthma and COPD, resulting in increased resistance to flow in the airways. Thus, the higher density and viscosity of ^{129}Xe gas may result in greater resistance to flow through narrowed airways, contributing to greater ^{129}Xe MRI as compared to ^{3}He MRI ventilation defects.

To our knowledge, the direct comparison of ^{129}Xe and ^{3}He MRI has not been performed in asthmatics. Accordingly, here we quantitatively compared hyperpolarized ^{3}He and ^{129}Xe MRI within a short 5-minute period before and 25-30 minutes after salbutamol administration in a small group of well-controlled asthmatic adults.

2.2 Materials and Methods

2.2.1 Subjects and Study Design

All subjects provided written informed consent to the study protocol approved by the local research ethics board and Health Canada, and the study was compliant with the Personal Information Protection and Electronic Documents Act (PIPEDA, Canada) and the Health Insurance Portability and Accountability Act (HIPAA, USA). Seven subjects were enrolled between the ages of 18 and 60 years of age (mean age=47±7 years; n=4 males) with a physician diagnosis of asthma and $FEV_1 \geq 60\%_{pred}$ **(Table 2-1)**. Before salbutamol administration, vital signs were recorded, pulmonary function tests completed, and MRI was performed. Post-bronchodilator imaging and pulmonary function tests were performed 25-30 minutes after administration of 200μg salbutamol (Apo-Salvent CRC Free Inhalation Aerosol; Apotex, Toronto, Ontario, Canada) delivered through a pressurized metered dose inhaler and *AeroChamber Plus* valved holding chamber (Trudell Medical International, London, Canada).

Spirometry and plethysmography were performed pre- and post-salbutamol using a *MedGraphics Elite Series* plethysmograph (MedGraphics, St. Paul, MN, USA). All manoeuvres were performed according to the American Thoracic Society (ATS) guidelines.[46] All subjects also underwent a previous imaging session 326±199 days prior to this study. At this time, hyperpolarized ^{3}He MRI and thoracic CT were performed prior to methacholine challenge and ^{3}He MRI was repeated following methacholine, as previously described.[19]

2.2.2 Image Acquisition

MRI was performed on a whole body 3.0 Tesla Discovery 750MR (General Electric Health Care, Milwaukee, WI, USA) MRI system with broadband imaging capability as previously described.[47] Subjects were instructed to inhale a gas mixture from a 1.0L Tedlar® bag (Jensen Inert Products, Coral Springs, FL, USA) from functional residual capacity (FRC), and image acquisition was performed in 8-15s under breath-hold conditions. To minimize the potential for differences or bias in the levels of inspiration between ^{3}He and ^{129}Xe MRI, extensive coaching was performed and the order of ^{3}He and ^{129}Xe MRI acquisition was

randomized. Conventional ^{1}H MRI was performed prior to hyperpolarized ^{3}He and ^{129}Xe MRI with subjects scanned during 1.0L breath-hold of ultrahigh purity, medical grade nitrogen (N_2) (Spectra Gases, Alpha, NJ) using the whole body radiofrequency (RF) coil and ^{1}H fast spoiled gradient-recalled-echo sequence (10s data acquisition, TR = 4.3ms, TE = 1.2ms, flip angle = 20 degrees, field of view (FOV) = 40cm x 40cm; matrix, 128 x 128; 14-17 slices; slice thickness = 15mm, 0mm gap) as previously described.[47]

Hyperpolarized ^{3}He MRI was enabled using a linear bird-cage transmit/receive chest coil (RAPID Biomedical GmbH, Wuerzburg Germany). A turn-key system (HeliSpin™) was used to polarize ^{3}He gas to 30—40% and doses (5mL/kg body weight) were administered in 1.0L Tedlar® bags diluted with N_2. ^{3}He MRI coronal static ventilation images were acquired using a fast gradient-recalled echo method (9s data acquisition, TR = 3.8ms, TE = 1ms, flip angle = 1 degree, FOV = 40cm x 40cm; matrix, 128 x 128; 14-17 slices; slice thickness = 15mm, 0mm gap) as previously described.[47]

Hyperpolarized ^{129}Xe MRI was enabled using a custom-made, unshielded quadrature-asymmetric bird-cage coil model tuned to 35.34MHz, as previously described.[48,49] ^{129}Xe gas (86% enriched) was polarized to 10—60% using a turn-key polarizer (XeBox-E10, Xemed LLC, New Hampshire, USA). Doses of hyperpolarized ^{129}Xe gas were dispensed directly into the pre-rinsed 1.0L Tedlar® bags pre-filled with ^{4}He to generate a 50/50 mixture. ^{129}Xe MRI coronal static ventilation images were acquired using a 3D fast gradient-recalled-echo sequence with centric phase-encoding ordering in the y direction and normal sampling in the z direction during a breath-hold of the 1.0L $^{129}Xe/^{4}He$ mixture (14s data acquisition, TR = 6.7ms, TE = 1.5ms, flip angle = variable, FOV = 40cm × 40cm; matrix, 128 x 128; 14-17 slices; 15mm slice thickness, 0 gap) as previously described.[43]

Thoracic CT was performed using a 64-slice Lightspeed VCT scanner (GEHC, Milwaukee, WI USA) using a detector configuration of 64×0.625mm, 120 kVp, 100 effective mA, tube rotation time of 500ms and a pitch of 1.0. In order to reduce the radiation dose delivered to each subject, CT images were acquired for 56 (versus a total of 400 possible) 1.25mm thick slices in a region-of-interest (ROI) spatially identified by ^{3}He MRI to contain ventilation defects. In order to spatially register CT and ^{3}He MRI breath-hold volumes and

anatomy, CT was acquired similar to MRI with subjects in breath-hold after inhalation of a 1.0L Tedlar® bag of N_2 from FRC.

2.2.3 Image Analysis

^{3}He and ^{129}Xe MRI semi-automated segmentation was performed to quantify lung volumes using custom software generated using MATLAB R2007b (The Mathworks Inc., Natick, MA, USA), as previously described.[50] To compare the distribution of both ^{3}He and ^{129}Xe gases within the lung, we segmented the ^{3}He and ^{129}Xe images based on pixel signal intensity. Briefly, ^{3}He and ^{129}Xe static ventilation images were segmented using a K-means approach that classified voxel intensity values into five clusters ranging from signal void (cluster 1 (C1) or ventilation defect volume (VDV)) and hypo-intense (cluster 2 (C2)) to hyper-intense signal (cluster 5 (C5)), and therefore generating a gas distribution cluster-map. For delineation of the ventilation defect boundaries, a seeded region-growing algorithm[51] was used to segment the ^{1}H MRI thoracic cavity for registration to the cluster-map. ^{3}He and ^{129}Xe VDP were generated using VDV normalized to the thoracic cavity volume. Similarly, for the remaining ventilation clusters, the segmented ^{1}H thoracic cavity volume was used to generate a cluster percentage representing a normalized cluster volume for the lung. All measurements were performed by the same observer (S.S.) with two years of experience performing semi-automated ^{3}He MR image segmentation. The reproducibility of the semi-automated method was previously determined[50] on the basis of intra-observer variability of five repeated ^{3}He MRI VDP measurements for five asthmatic subjects.

The signal-to-noise ratio (SNR) was calculated for each ^{3}He and ^{129}Xe static ventilation slice and then averaged to obtain a single SNR value for each subject image. Briefly, SNR was determined by calculating the mean voxel value within a 5 x 5 cm^2 voxel region of interest (ROI) for four representative ROI within the lung parenchyma, and dividing by the standard deviation of the voxel values for four representative ROI of the same size in the image background where there was no lung structure, as previously described.[43]

Ventilation heterogeneity was estimated according to previously described methods[25] using the coefficient of variation (COV). Briefly, a ventilated lung ROI was defined as gas

distribution cluster-map clusters C2-C5. For each voxel within the ventilated lung ROI a local ventilation heterogeneity value was calculated by computing the coefficient of variation of the signal intensity in the voxels 5 x 5 neighborhood. Mean COV for each slice was calculated for each ^{3}He and ^{129}Xe static ventilation slice and then averaged to obtain a single COV value for each subject.

Partial CT image analysis was performed using software (Pulmonary Workstation 2.0, VIDA Diagnostics; Iowa City, IA, USA) to generate wall area percent (WA%) and lumen area (LA). An automated airway tree segmentation algorithm (VIDA) was applied, however, a manual component was introduced to the algorithm if the trachea and main bronchus were not present in the image. Seed-points were manually placed within the lumen of the airway of interest to initiate manual segmentation of the airway. To confirm the spatial relationship between a ventilation defect and the corresponding airway of interest, the partial CT was manually registered to the corresponding MR image using 3D Slicer manual registration software (http://www.slicer.org).[52]

2.2.4 Statistical Analysis

In order to determine the statistical significance of the difference between pulmonary function tests and MRI measurements pre- and post-salbutamol we performed a multivariate analysis of variance (MANOVA) and repeated measures analysis of variance (ANOVA) using SPSS 20.0 (IBM, Armonk, NY, USA). Furthermore, in order to determine if the change observed following salbutamol inhalation using ^{129}Xe MRI was significantly greater than the change observed using ^{3}He MRI, we performed a three-way mixed-design repeated measures ANOVA, using SPSS 20.0. In this analysis subject was treated as a between-subjects factor, and treatment (pre- and post-salbutamol) and gas (^{3}He and ^{129}Xe) was treated as a within-subjects factor. Finally, because ^{3}He MRI often has higher SNR than ^{129}Xe MRI, there is the potential for regions of reduced signal intensity to appear as ventilation defects in low SNR ^{129}Xe images. Therefore, Pearson correlations (r) were performed to determine the relationship between the difference in ^{3}He and ^{129}Xe VDP with the difference between ^{3}He and ^{129}Xe SNR using GraphPad Prism version 4.00 (Graphpad Software Inc, San Diego, CA, USA). In all statistical analyses, results were

considered statistically significant when the probability of making a Type I error was less than 5% ($p < 0.05$).

2.3 Results

Table 2-1 shows demographic characteristics, pulmonary function, and MRI measurements for seven mild-to-moderate asthma subjects (four males) pre- and post-salbutamol. For all subjects, mean age was 47±7 years and mean body mass index was 27±4 kg/m^2. Pre-bronchodilator mean FEV_1 was 76±6%$_{pred}$ and mean FVC was 91±12%$_{pred}$. All subjects were considered to be well-controlled with ≤ 1 asthma exacerbation resulting in hospitalization in the calendar year prior to the study visit.

Table 2-1 Subject demographic characteristics, pulmonary function and MRI measurements.

	Pre-Salbutamol (n=7)	**Post-Salbutamol** (n=7)	**Significance of Difference** (p)*
Subject Demographics			
Age yrs (±SD)	47 (7)	-	-
Male Sex	4	-	-
BMI kg/m^2 (±SD)	27 (4)	-	-
Pulmonary Function Test			
FEV_1 %$_{pred}$ (±SD)	76 (6)	83 (10)	**0.01**
FVC %$_{pred}$ (±SD)	91 (12)	93 (13)	0.35
FEV_1/FVC % (±SD)	67 (7)	71 (6)	**0.01**
TLC %$_{pred}$ (±SD)	104 (8)	103 (10)	0.41
RV %$_{pred}$ (±SD)	136 (16)	123 (12)	0.17
RV/TLC (%)(±SD)	40 (8)	37 (6)	0.15
IC %$_{pred}$ (±SD)	101 (16)	112 (18)	**0.02**
FRC %$_{pred}$ (±SD)	108 (17)	95 (16)	**0.003**
Raw %$_{pred}$ (±SD)	184 (72)	133 (56)	**0.04**
MRI Measurements			
^{3}He VDP % (±SD)	6 (5)	4 (3)	**0.001**
^{129}Xe VDP % (±SD)	8 (5)	5 (4)	**<0.0001**
^{3}He COV (±SD)	0.282 (0.018)	0.269 (0.024)	**<0.0001**
^{129}Xe COV (±SD)	0.309 (0.028)	0.296 (0.036)	**0.002**

SD=Standard Deviation, BMI=Body Mass Index, FEV_1=Forced Expiratory Volume in 1s, %$_{pred}$=Percent Predicted, FVC=Forced Vital Capacity, TLC=Total Lung Capacity, RV=Residual Volume, IC=Inspiratory Capacity, FRC=Functional Residual Capacity, Raw=Airway resistance, VDP=Ventilation Defect Percent, COV=Coefficient of Variation.

*Significance of difference ($p<.05$) determined using a multivariate analysis of variance.

Figure 2-1 shows for two representative asthmatics (subject A and B), ^{3}He and ^{129}Xe MRI coronal slices before and after bronchodilator administration as well as signal intensity cluster maps and COV maps. For both subjects, there were visibly obvious regional ventilation abnormalities in the MRI and cluster maps. As shown, ^{129}Xe gas distribution was qualitatively more heterogeneous (COV maps) compared to ^{3}He MRI, with regions of patchy signal void (cluster and COV maps). As shown in **Figure 2-1**, following salbutamol administration, for both ^{129}Xe and ^{3}He MRI, some ventilation abnormalities disappeared whereas others persisted.

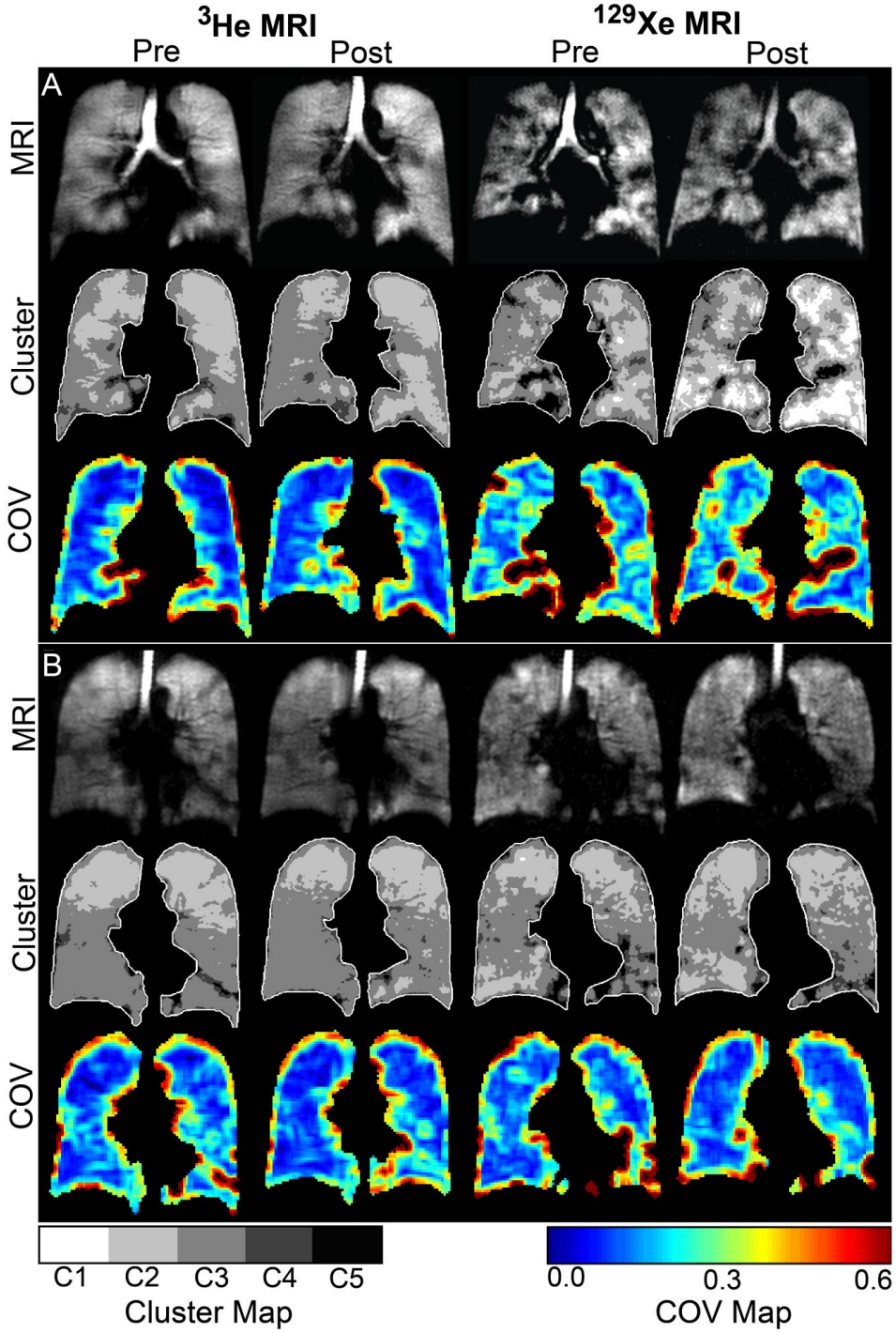

Figure 2-1 ^{3}He and ^{129}Xe MRI pre- and post-salbutamol.
Hyperpolarized ^{3}He and ^{129}Xe MRI for two representative subjects (Subjects A and B) pre- and post-salbutamol. Static ventilation MRI, corresponding cluster maps and coefficient of variation (COV) maps are shown for:

A) 43 yr old male, baseline FEV_1=82%$_{pred}$, baseline FEV_1/FVC=69%;

B) 50 yr old female, baseline FEV_1=71%$_{pred}$, baseline FEV_1/FVC=68%.

C1 = cluster 1, C2 = cluster 2, C3 = cluster 3, C4 = cluster 4, and C5 = cluster 5.

As shown in **Table 2-1**, for all subjects there was a significant improvement in mean $FEV_1\%_{pred}$ (p=0.01), FEV_1/FVC (p=0.01), IC $\%_{pred}$ (p=0.02), FRC $\%_{pred}$ (p=0.003), and airways resistance (Raw $\%_{pred}$ p=0.04) after the administration of salbutamol. Pre-bronchodilator ^{129}Xe VDP (8 ± 5%) was significantly greater than ^{3}He VDP (6 ± 5%, p=0.003); post-bronchodilator ^{3}He (4 ± 3%) and ^{129}Xe VDP (5 ± 4%) were not significantly different. SNR was significantly lower for ^{129}Xe MRI compared to ^{3}He MRI both pre- (^{3}He: 46±21, ^{129}Xe: 22±8, p=0.02) and post-bronchodilator (^{3}He: 36±16, ^{129}Xe: 22±10, p=0.005), importantly however, the difference between ^{3}He and ^{129}Xe VDP pre-bronchodilator (r=0.02, p=0.96) was not related to image SNR. The COV for ^{129}Xe MRI ventilation was significantly greater than for ^{3}He MRI ventilation, both pre- (p<0.0001) and post-bronchodilator (p<0.0001).

In **Table 2-1** and shown in more detail in **Figure 2-2**, there was a significant improvement post-salbutamol for ^{3}He (p=0.001) and ^{129}Xe MRI VDP (p<0.0001) with the improvement in ^{129}Xe MRI VDP significantly greater than for ^{3}He MRI VDP (p=0.008). Post-salbutamol, both ^{3}He (p<0.0001) and ^{129}Xe (p=0.002) COV were significantly decreased. There was no relationship for the difference in VDP post-salbutamol with SNR (^{3}He MRI, r=-0.30, p=0.51; ^{129}Xe MRI, r=-0.32, p=0.49). A subject listing of all MRI measurements is provided in **Table 2-2**.

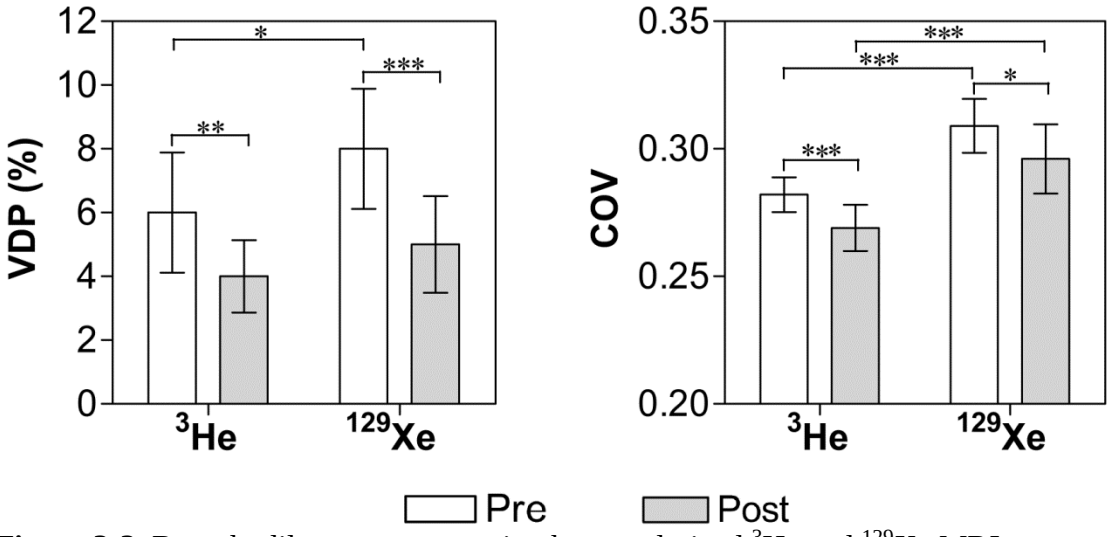

Figure 2-2 Bronchodilator response using hyperpolarized ^{3}He and ^{129}Xe MRI.
Mean hyperpolarized ^{3}He and ^{129}Xe ventilation defect percent (VDP) and ventilation coefficient of variation (COV) pre- (white) and post-salbutamol (grey). Values are means for all subject slices, and error bars are ± SD. *p ≤ 0.01, **p ≤ 0.001, ***p ≤ 0.0001.

Table 2-2 Pre- and post-salbutamol hyperpolarized ^{3}He and ^{129}Xe MRI measurements.

	Pre – Salbutamol									
	^{3}He MRI					**^{129}Xe MRI**				
Subject	VDP (%)	C2 (%)	C3 (%)	C4 (%)	C5 (%)	VDP (%)	C2 (%)	C3 (%)	C4 (%)	C5 (%)
1‡	3	12	40	29	16	4	9	35	36	16
2	1	10	37	33	19	3	9	28	40	21
3§	17	11	32	26	15	18	9	26	28	20
4*	6	12	39	29	15	8	15	19	36	23
5†	6	12	37	35	10	7	11	35	34	14
6	6	12	40	29	12	7	13	33	34	14
7	5	11	40	30	14	8	11	30	38	14
Mean (±SD)	6 (5)	11 (1)	38 (3)	30 (3)	14 (3)	8 (5)	11 (2)	29 (6)	35 (4)	17 (4)
	Post – Salbutamol									
	^{3}He MRI					**^{129}Xe MRI**				
Subject	VDP (%)	C2 (%)	C3 (%)	C4 (%)	C5 (%)	VDP (%)	C2 (%)	C3 (%)	C4 (%)	C5 (%)
1‡	2	10	44	30	14	2	9	32	40	17
2	1	10	41	30	18	1	6	17	45	31
3§	12	12	31	31	14	13	12	21	34	20
4*	4	10	35	32	19	4	10	27	37	23
5†	3	9	40	33	14	4	9	31	38	18
6	6	12	42	28	12	8	17	25	35	15
7	4	11	39	31	15	4	14	29	42	12
Mean(±SD)	4 (3)	11(1)	39(4)	31(2)	15(2)	5 (4)	11(4)	26(5)	39(4)	19(6)

VDP=ventilation defect percent (C1=Cluster 1), C2 =Cluster 2, C3=Cluster 3, C4=Cluster 4, C5=Cluster 5, SD=standard deviation. † Subject A, ‡ Subject B, § Subject C, * Subject D

To further investigate the difference in ^{3}He and ^{129}Xe gas distribution detected prior to salbutamol inhalation we evaluated the spatial relationship of airways and ventilation defects using thoracic CT. All subjects underwent a previous imaging session, 326±199 days prior to this study when hyperpolarized ^{3}He MRI and thoracic CT were acquired as previously described.[19] In **Figure 2-3**, we show the centre coronal slice ^{3}He and ^{129}Xe MRI and the corresponding centre slice ^{3}He MRI following methacholine challenge[19] for 2 subjects: Subject C, a 41yr old male, FEV_1=75% $_{pred}$; and Subject D, a 36 year old female, FEV_1=86%$_{pred}$. As shown with arrows in **Figure 2-3**, for Subject C, a large sub-segmental ventilation defect distal to the apical bronchus of the right upper lobe (RB1) was visualized using ^{129}Xe MRI and also using ^{3}He MRI but only after provocation with methacholine, at the PC_{20}. Thoracic CT for this subject revealed a 4th generation apical sub-segmental bronchus of the right upper lobe as the airway that was spatially proximal to this specific

ventilation defect. The CT-derived WA% and LA for this 4th generation airway were 78% and 2.9 mm^2 respectively, both of which are worse than previously reported values for a group of older asthmatic men (WA%=55-80% and LA=5-15mm^2).[53] For Subject D, there was no evidence of a right upper lobe ventilation abnormality and CT-derived measurements WA% and LA were 69% and 3.8 mm^2 respectively for the same 4th generation apical sub-segmental bronchus.

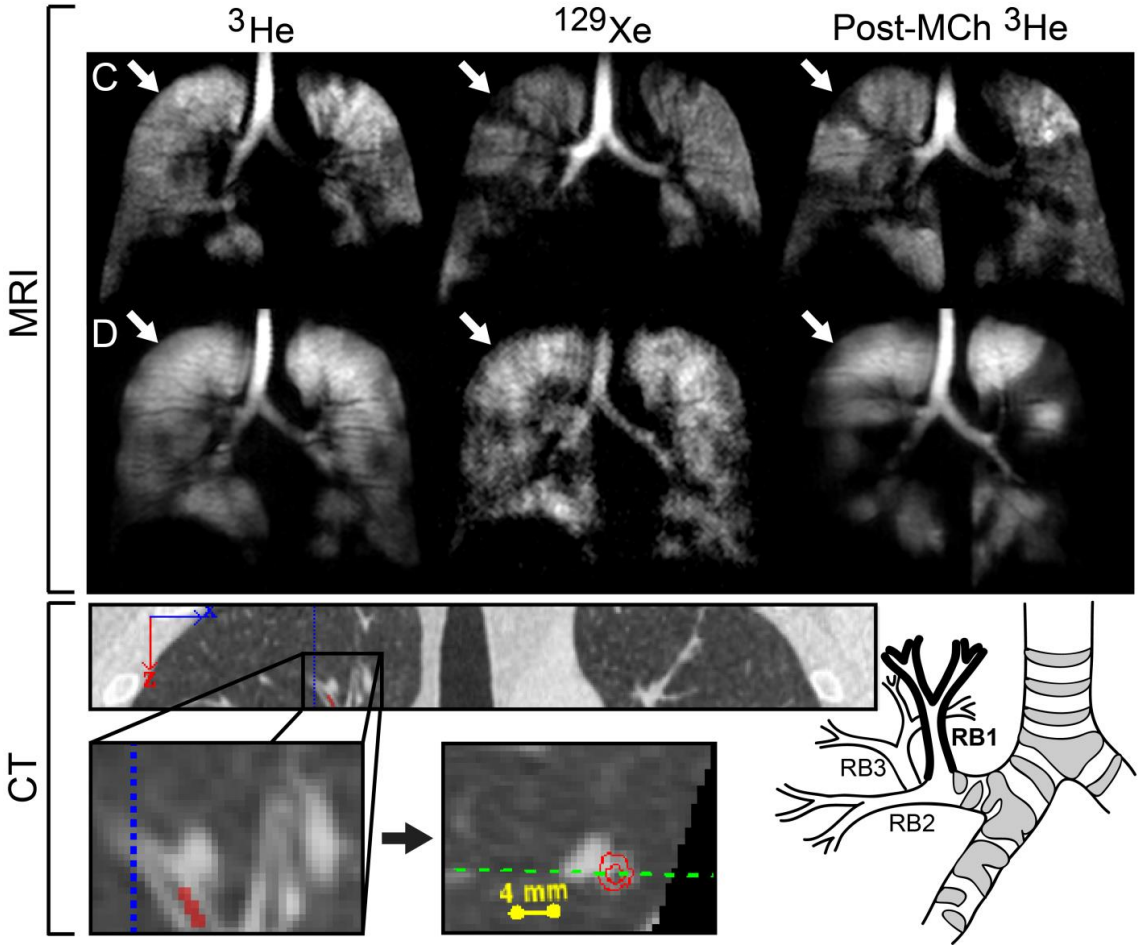

Figure 2-3 MRI and CT for two asthmatic subjects.
Hyperpolarized ^3He and ^{129}Xe MRI and post-methacholine ^3He MRI for two subjects (C and D)
C) 41 yr old male, FEV_1=75%$_{pred}$, FEV_1/FVC=66%. White arrows identify a right upper lobe ventilation defect visible using ^{129}Xe MRI, and for ^3He MRI, only post-methacholine at PC_{20}. Regional CT is shown with the apical segmental bronchus of the right upper lobe in red which is proximal to the ^{129}Xe and ^3He post-methacholine ventilation defect. The cross-sectional slice of the airway is shown and the airway of interest is identified in a schematic of the bronchial tree.
D) 36 yr old female, FEV_1=86%$_{pred}$, FEV_1/FVC=73% with no ventilation defect in the right upper lobe.

2.4 Discussion

Hyperpolarized ^{3}He MRI of asthma has been performed over the last 2 decades[19-25,54,55] and across numerous studies, asthma ventilation defects have been shown to be spatially and temporally persistent,[22,23] and some of these ventilation defects partially or fully resolve following inhaled or systemic therapy.[19,20,24,25] Unfortunately, we still do not have a full understanding of the structural or physiological determinants of such asthma ventilation abnormalities,[56] although armed with such an understanding there is the potential to use functional MRI to guide asthma therapy, to identify new therapeutic targets or at least, better understand regional pulmonary response to asthma therapy. A recent pilot study that compared ^{3}He and ^{129}Xe MRI in older healthy and COPD subjects[43] showed greater ^{129}Xe MRI ventilation defects in COPD suggesting that ^{129}Xe MRI may provide enhanced sensitivity to airway abnormalities in obstructive lung disease. In COPD there are multiple mechanisms that may be responsible for ^{3}He and ^{129}Xe ventilation differences including increased airways resistance and the presence of emphysema and the effects of collateral ventilation.[43,57] To try to get a better understanding of the structure-function relationships in the asthmatic lung, and to tease out the different contributing etiological factors that result in ventilation defects in asthma, here we directly compared hyperpolarized ^{3}He and ^{129}Xe MRI ventilation defects before and after salbutamol inhalation. We made a number of important observations: 1) ^{129}Xe VDP and COV were significantly greater than ^{3}He MRI VDP and COV before salbutamol inhalation, 2) there were significantly greater post-salbutamol improvements in ^{129}Xe MRI VDP such that ^{3}He and ^{129}Xe MRI were not significantly different post-salbutamol, and, 3) a remodeled sub-segmental airway was shown to be spatially related to a sub-segmental ^{129}Xe MRI ventilation defect that was not visible using ^{3}He MRI, except at $PC_{20,}$ after methacholine administration.

First, we directly compared hyperpolarized ^{3}He and ^{129}Xe MRI acquired within approximately five minutes of one another and observed that ^{129}Xe MRI VDP and COV were both qualitatively and quantitatively greater than ^{3}He MRI-derived VDP and COV. We note that in this study, the differences between ^{3}He and ^{129}Xe MRI VDP were not large – much smaller in fact than previously reported in COPD.[43] Although VDP was not large,

qualitatively, there certainly was evidence of increased ^{129}Xe ventilation heterogeneity compared to ^{3}He and these differences were quantified using the ^{3}He and ^{129}Xe ventilation COV. We note that SNR was lower for ^{129}Xe as compared to ^{3}He MRI, and therefore there is the potential for regions of the lung with reduced signal intensity to appear as ventilation defects in low SNR ^{129}Xe images. However, we observed that the difference between ^{3}He and ^{129}Xe SNR was not significantly correlated with the difference between ^{3}He and ^{129}Xe VDP. Therefore, VDP and COV differences might well reflect other differences in the physical properties of the inspired gases and perhaps their interactions with airway abnormalities present in the asthmatic lung. For example, in asthma, like COPD, the small airways (<2mm) are the major site of airflow obstruction and are believed to result in increased airways resistance.[58] ^{129}Xe gas has both a greater density and viscosity than ^{3}He (pure ^{129}Xe gas has approximately 40 times greater density and 1.5 times greater viscosity than pure ^{3}He gas)[57] and this has an effect on resistance to both turbulent and laminar flow in the airways, as previously described.[45] Importantly, we have previously estimated the density and viscosity of the inspired ^{3}He-N_2 (40/60) and ^{129}Xe-^{4}He gas mixtures (50/50).[57] The estimated density of the inspired ^{3}He-N_2 gas mixture and ^{129}Xe-^{4}He gas mixture was 0.61kg/m^3 and 2.65kg/m^3, respectively, and the estimated viscosity of the ^{3}He-N_2 mixture and ^{129}Xe-^{4}He mixture was $1.99\text{x}10^{-4}$P and $2.55\text{x}10^{-4}$P, respectively.[57] The increased density of ^{129}Xe gas would tend to increase the gas Reynold's number, thereby increasing the probability for turbulent flow with higher airflow resistance; laminar flow resistance would also increase proportionately to the change in viscosity according to Poiseulle's equation.[45] The increased density and viscosity of ^{129}Xe gas could lead to slower filling or decreased access to lung units distal to narrowed or obstructed airways, amplifying ventilation differences arising from airway abnormalities between the gases.

In COPD, emphysema may be an additional factor responsible for the differences in ^{3}He and ^{129}Xe MRI ventilation and may account for the larger ^{129}Xe/^{3}He MRI differences previously observed in COPD[43] compared to asthma. In emphysematous lung tissue, resistance to flow through collateral channels is low whereas in normal lung tissue, flow resistance through collateral channels is very high.[59] Regardless, the results observed here in asthma support further interrogation using dynamic imaging approaches such as recently reported in COPD.[60] It is also important to note that previous work has also shown that the

mixture of $^{129}Xe/^{4}He$ gas administered during image acquisition performed here better approximates the self-diffusion coefficient of room air in the lung,[43] as compared to $^{3}He/N_2$ or $^{3}He/^{4}He$ gas mixtures, supporting the notion that ^{129}Xe gas distribution might provide a better estimate of "ground truth" ventilation abnormalities.

Second, and as might be expected, we observed a significant regional improvement in both ^{3}He and ^{129}Xe MRI VDP following salbutamol administration, with the ^{129}Xe MRI improvement significantly greater than ^{3}He MRI. Regional improvements in ventilation have previously been reported following salbutamol inhalation using xenon-enhanced dual-energy CT in asthma.[61] However, to our knowledge this is the first study to report a change in ^{129}Xe MRI ventilation abnormalities following inhaled salbutamol. Beta-2 (β2) adrenergic receptor agonists promote smooth muscle relaxation and dilation, increasing airway caliber with concomitant decreased resistance to flow. Post-salbutamol, for all subjects, the global measurement of airways resistance was significantly decreased and this may have resulted in the improved and more similar regional distribution of ^{3}He and ^{129}Xe gas post-salbutamol. This suggests that increased airway caliber following bronchodilator administration allows for similar access of ^{3}He and ^{129}Xe to lung regions, as previously reported in healthy subjects.[43]

Finally, in a single asthmatic, we showed that a relatively large sub-segmental ventilation defect that was visualized using ^{129}Xe MRI, was also visible using ^{3}He MRI, but only after methacholine challenge at the PC_{20}. Thoracic CT acquired within a year of this study and contemporaneous to the methacholine challenge was used to locate the airway proximal to this defect. A 4^{th} generation apical segmental bronchus of the right upper lobe was identified as the significantly remodeled airway that was spatially related to this ventilation defect. Furthermore, in another asthmatic with a normally ventilated right upper lobe, the same 4^{th} generation airway showed more "normal" airway morphology. It is clear that airway diameters and wall thicknesses vary among individuals and we acknowledge that we do not believe that one defect in one subject confirms our hypothesis. However, these results support the hypothesis that in asthma, ^{3}He gas may penetrate lung regions through partially obstructed airways that ^{129}Xe gas cannot access during a short breath-hold scan; in other words ^{3}He MRI may mask clinically relevant airway abnormalities in asthma. This interesting finding warrants further investigation in a larger group of asthmatic subjects to

determine whether there is indeed a relationship between abnormal airway pathophysiology and the differences between ^{3}He and ^{129}Xe gas distribution.

We acknowledge that this work was limited by the small number of subjects evaluated and therefore caution should be exercised in generalizing these results to a more general asthma population. Indeed, the reported VDP in this small group of asthmatics was low and may be related to the nearly normal FVC for these subjects, reflecting the fact that these subjects (who were enrolled from a tertiary care asthma centre) were receiving optimal asthma therapy. The low baseline VDP also suggests that the differences in ^{3}He and ^{129}Xe VDP reported here might provide a conservative estimate of the differences that would be observed in a larger, less specialized asthma subject group. What is clear though, is that salbutamol effectively negated the differences observed between ^{3}He and ^{129}Xe VDP. Future studies should aim to evaluate a large group of healthy volunteers and asthmatic subjects with varying disease severity. Additionally, clinical tests such as dyspnea scores and measurements of exercise performance should be performed. The clinical relevance of the difference in ^{3}He and ^{129}Xe gas distribution detected could then be determined by direct comparison with established measures that are patient-centred and clinically relevant.

Over the last two decades, an international imaging physics research effort has been undertaken to develop non-invasive MRI methods, with the promise of direct and serial structure-function measurements of the lung without radiation burden or risk. Yet, the treatment and monitoring of patients with asthma is still mainly based on spirometry and some emerging inflammatory biomarkers.[62] Certainly, low accessibility and the high/unpredictable cost of ^{3}He gas has also limited its development and use.[26] It is important to note that the relatively low and predictable cost of ^{129}Xe gas provides the potential for greater accessibility of pulmonary functional imaging for research and patient care. One advantage of ^{129}Xe gas is that it is capable of passive transmembrane diffusion and it is soluble in tissues and blood. Hyperpolarized ^{129}Xe MRI dissolved phase imaging has shown good spatial agreement with the corresponding ventilation image.[34]. The differences between ^{3}He and ^{129}Xe MRI gas distribution shown here are unlikely to be related to transmembrane diffusion of ^{129}Xe gas as it has been estimated that only 1-2% of the inhaled ^{129}Xe gas dose is dissolved in the tissues and blood, during the 10-15s breath-

hold.[21] Regardless of the gas used for imaging, we think that the lack of a clear understanding of the clinical or physiological meaning of MRI ventilation defects will also impede its development as a clinical tool, necessitating more detailed physiological and modeling studies. In this study, we observed small but significant differences between ^{129}Xe and ^{3}He MRI VDP before salbutamol inhalation that suggested ^{129}Xe MRI may be more sensitive to airflow obstruction in asthma that is responsive to salbutamol. It is not clear which one of the currently available pulmonary functional MRI methods (including oxygen-enhanced MRI)[63,64] provides ventilation estimates that are closest to ground truth (ie. ventilation that occurs with molecular oxygen mixed in air). The availability of oxygen-enhanced and ^{129}Xe MRI will certainly facilitate the research that still needs to be done to investigate the fundamental anatomical and morphological determinants that govern the occurrence and location of a ventilation defect, including bronchoscopy with biopsy and histological assessment. MRI can be considered complementary to CT and endobronchial biopsy because the anatomical determinants of small airway ventilation defects may be beyond the resolution of CT and perhaps the reach of an endoscope or optical coherence tomography probe[65] as well.

In conclusion, we evaluated hyperpolarized ^{3}He and ^{129}Xe MRI ventilation defects in a small group of asthmatics before and after salbutamol inhalation and reported significantly greater (worse) ^{129}Xe compared to ^{3}He VDP and COV pre-salbutamol. We identified a remodeled airway that was spatially related to a sub-segmental ventilation defect visualized only with ^{129}Xe MRI. These results suggest that the higher density and viscosity of ^{129}Xe gas (which is more similar to molecular oxygen in air than ^{3}He gas) may help reveal ventilation abnormalities prior to bronchodilation that are not observed using ^{3}He MRI.

2.5 References

(1) Fanta CH. Asthma. *N Engl J Med* 2009;360:1002-14.

(2) Locksley RM. Asthma and allergic inflammation. *Cell* 2010;140:777-83.

(3) Lange P, Parner J, Vestbo J, *et al.* A 15-year follow-up study of ventilatory function in adults with asthma. *N Engl J Med* 1998;339:1194-200.

(4) Brown PJ, Greville HW, Finucane KE. Asthma and irreversible airflow obstruction. *Thorax* 1984;39:131-6.

(5) Busse WW. Asthma diagnosis and treatment: filling in the information gaps. *J Allergy Clin Immunol* 2011;128:740-50.

(6) Celli BR. The importance of spirometry in COPD and asthma: effect on approach to management. *Chest* 2000;117:15S-9S.

(7) Macklem P, Mead J. Resistance of central and peripheral airways measured by a retrograde catheter. *J Appl Physiol* 1967;22:395-401.

(8) Burgel PR. The role of small airways in obstructive airway diseases. *Eur Respir Rev* 2011;20:23-33.

(9) Bourdin A, Paganin F, Prefaut C, *et al.* Nitrogen washout slope in poorly controlled asthma. *Allergy* 2006;61:85-89.

(10) Farah CS, King GG, Brown NJ, *et al.* The role of the small airways in the clinical expression of asthma in adults. *J Allergy Clin Immunol* 2012;129:381-87.

(11) Downie SR, Salome CM, Verbanck S, *et al.* Ventilation heterogeneity is a major determinant of airway hyperresponsiveness in asthma, independent of airway inflammation. *Thorax* 2007;62:684-9.

(12) King GG, Eberl S, Salome CM, *et al.* Differences in airway closure between normal and asthmatic subjects measured with single-photon emission computed tomography and technegas. *Am J Respir Crit Care Med* 1998;158:1900-06.

(13) King GG, Eberl S, Salome CM, *et al.* Airway closure measured by a technegas bolus and SPECT. *Am J Respir Crit Care Med* 1997;155:682-88.

(14) Pellegrino R, Biggi A, Papaleo A, *et al.* Regional expiratory flow limitation studied with Technegas in asthma. *J Appl Physiol* 2001;91:2190-98.

(15) Venegas JG, Winkler T, Musch G, *et al.* Self-organized patchiness in asthma as a prelude to catastrophic shifts. *Nature* 2005;434:777-82.

(16) Grenier P, Mourey-Gerosa I, Benali K, *et al.* Abnormalities of the airways and lung parenchyma in asthmatics: CT observations in 50 patients and inter- and intraobserver variability. *Eur Radiol* 1996;6:199-206.

(17) King GG, Carroll JD, Muller NL, *et al.* Heterogeneity of narrowing in normal and asthmatic airways measured by HRCT. *Eur Respir J* 2004;24:211-18.

(18) Nitt-Gray MF, Goldin JG, Johnson TD, *et al.* Development and testing of image-processing methods for the quantitative assessment of airway hyperresponsiveness from high-resolution CT images. *J Comput Assist Tomogr* 1997;21:939-47.

(19) Costella S, Kirby M, Maksym GN, *et al.* Regional Pulmonary Response to a Methacholine Challenge using Hyperpolarized ^{3}He Magnetic Resonance Imaging. *Respirology* 2012;17:1237-46.

(20) Altes TA, Powers PL, Knight-Scott J, *et al.* Hyperpolarized ^{3}He MR lung ventilation imaging in asthmatics: preliminary findings. *J Magn Reson Imaging* 2001;13:378-84.

(21) de Lange EE, Altes TA, Patrie JT, *et al.* Evaluation of asthma with hyperpolarized helium-3 MRI: correlation with clinical severity and spirometry. *Chest* 2006;130:1055-62.

(22) de Lange EE, Altes TA, Patrie JT, *et al.* The variability of regional airflow obstruction within the lungs of patients with asthma: assessment with hyperpolarized helium-3 magnetic resonance imaging. *J Allergy Clin Immunol* 2007;119:1072-8.

(23) de Lange EE, Altes TA, Patrie JT, *et al.* Changes in regional airflow obstruction over time in the lungs of patients with asthma: evaluation with ^{3}He MR imaging. *Radiology* 2009;250:567-75.

(24) Samee S, Altes T, Powers P, *et al.* Imaging the lungs in asthmatic patients by using hyperpolarized helium-3 magnetic resonance: assessment of response to methacholine and exercise challenge. *J Allergy Clin Immunol* 2003;111:1205-11.

(25) Tzeng YS, Lutchen K, Albert M. The difference in ventilation heterogeneity between asthmatic and healthy subjects quantified using hyperpolarized 3He MRI. *J Appl Physiol* 2009;106:813-22.

(26) Cho A. Physics. Helium-3 shortage could put freeze on low-temperature research. *Science* 2009;326:778-79.

(27) Walker T, Happer W. Spin-exchange optical pumping of noble-gas nuclei. *Rev of Mod Phys* 1997;69:629-42.

(28) Mugler JP, III, Driehuys B, Brookeman JR, *et al.* MR imaging and spectroscopy using hyperpolarized 129Xe gas: preliminary human results. *Magn Reson Med* 1997;37:809-15.

(29) Albert MS, Cates GD, Driehuys B, *et al.* Biological magnetic resonance imaging using laser-polarized ^{129}Xe. *Nature* 1994;370:199-201.

(30) Hersman FW, Ruset IC, Ketel S, *et al.* Large production system for hyperpolarized 129Xe for human lung imaging studies. *Acad Radiol* 2008;15:683-92.

(31) Ruset IC, Ketel S, Hersman FW. Optical pumping system design for large production of hyperpolarized. *Phys Rev Lett* 2006;96:053002.

(32) Patz S, Hersman FW, Muradian I, *et al.* Hyperpolarized (129)Xe MRI: a viable functional lung imaging modality? *Eur J Radiol* 2007;64:335-44.

(33) Driehuys B, Pollaro J, Cofer GP. In vivo MRI using real-time production of hyperpolarized 129Xe. *Magn Reson Med* 2008;60:14-20.

(34) Cleveland ZI, Cofer GP, Metz G, *et al.* Hyperpolarized Xe MR imaging of alveolar gas uptake in humans. *PLoS One* 2010;5:e12192.

(35) Dregely I, Mugler JP, III, Ruset IC, *et al.* Hyperpolarized Xenon-129 gas-exchange imaging of lung microstructure: first case studies in subjects with obstructive lung disease. *J Magn Reson Imaging* 2011;33:1052-62.

(36) Dregely I, Ruset IC, Mata JF, *et al.* Multiple-exchange-time xenon polarization transfer contrast (MXTC) MRI: initial results in animals and healthy volunteers. *Magn Reson Med* 2012;67:943-53.

(37) Driehuys B, Cofer GP, Pollaro J, *et al.* Imaging alveolar-capillary gas transfer using hyperpolarized 129Xe MRI. *Proc Natl Acad Sci USA* 2006;103:18278-83.

(38) Driehuys B, Martinez-Jimenez S, Cleveland ZI, *et al.* Chronic obstructive pulmonary disease: safety and tolerability of hyperpolarized 129Xe MR imaging in healthy volunteers and patients. *Radiology* 2012;262:279-89.

(39) Kaushik SS, Cleveland ZI, Cofer GP, *et al.* Diffusion-weighted hyperpolarized 129Xe MRI in healthy volunteers and subjects with chronic obstructive pulmonary disease. *Magn Reson Med* 2011;65:1154-65.

(40) Mugler JP, III, Altes TA, Ruset IC, *et al.* Simultaneous magnetic resonance imaging of ventilation distribution and gas uptake in the human lung using hyperpolarized xenon-129. *Proc Natl Acad Sci USA* 2010;107:21707-12.

(41) Patz S, Muradian I, Hrovat MI, *et al.* Human pulmonary imaging and spectroscopy with hyperpolarized 129Xe at 0.2T. *Acad Radiol* 2008;15:713-27.

(42) Shukla Y, Wheatley A, Kirby M, *et al.* Hyperpolarized 129Xe magnetic resonance imaging: tolerability in healthy volunteers and subjects with pulmonary disease. *Acad Radiol* 2012;19:941-51.

(43) Kirby M, Svenningsen S, Owrangi A, *et al.* Hyperpolarized 3He and 129Xe MR imaging in healthy volunteers and patients with chronic obstructive pulmonary disease. *Radiology* 2012;265:600-10.

(44) Altes TA, Mugler JP, III, Meyer C, *et al.* A comparison of Hyperpolarized Helium-3 and Xenon-129 MR Ventilation Imaging in Cystic Fibrosis. *Proceedings of the 20th Annual Meeting of ISMRM, Melbourne* 2012.

(45) Wood LD, Engel LA, Griffin P, *et al.* Effect of gas physical properties and flow on lower pulmonary resistance. *J Appl Physiol* 1976;41:234-44.

(46) Miller MR, Hankinson J, Brusasco V, *et al.* Standardisation of spirometry. *Eur Respir J* 2005;26:319-38.

(47) Parraga G, Ouriadov A, Evans A, *et al.* Hyperpolarized 3He ventilation defects and apparent diffusion coefficients in chronic obstructive pulmonary disease: preliminary results at 3.0 Tesla. *Invest Radiol* 2007;42:384-91.

(48) De Zanche N, Chhina N, Teh K, *et al.* Asymmetric quadrature split birdcage coil for hyperpolarized 3He lung MRI at 1.5T. *Magn Reson Med* 2008;60:431-38.

(49) Farag A, Wang J, Ouriadov A, *et al.* Unshielded and Asymmetric RF Transmit Coil for Hyperpolarized 129Xe Human Lung Imaging at 3.0T. *Proceedings of the 20th Annual Meeting of ISMRM, Melbourne, Australia* 2012:Poster#1233.

(50) Kirby M, Heydarian M, Svenningsen S, *et al.* Hyperpolarized ^{3}He magnetic resonance functional imaging semiautomated segmentation. *Acad Radiol* 2012;19:141-52.

(51) Adams R, Bischof L. Seeded Region Growing. *IEEE Trans Pattern Anal and Mach Intell* 1994;16:641-47.

(52) Fedorov A, Beichel R, Kalpathy-Cramer J, *et al.* 3D Slicer as an image computing platform for the Quantitative Imaging Network. *Magn Reson Imaging* 2012;30:1323-41.

(53) Shimizu K, Hasegawa M, Makita H, *et al.* Comparison of airway remodelling assessed by computed tomography in asthma and COPD. *Respir Med* 2011;105:1275-83.

(54) Fain SB, Gonzalez-Fernandez G, Peterson ET, *et al.* Evaluation of structure-function relationships in asthma using multidetector CT and hyperpolarized He-3 MRI. *Acad Radiol* 2008;15:753-62.

(55) Campana L, Kenyon J, Zhalehdoust-Sani S, *et al.* Probing airway conditions governing ventilation defects in asthma via hyperpolarized MRI image functional modeling. *J Appl Physiol* 2009;106:1293-300.

(56) Pare PD, Nagano T, Coxson HO. Airway imaging in disease: Gimmick or useful tool? *J Appl Physiol* 2012;113:636-46.

(57) Kirby M, Svenningsen S, Kanhere N, *et al.* Pulmonary ventilation visualized using hyperpolarized helium-3 and xenon-129 magnetic resonance imaging: differences in COPD and relationship to emphysema. *J Appl Physiol* 2013;114:707-15.

(58) Hogg JC, Macklem PT, Thurlbeck WM. Site and nature of airway obstruction in chronic obstructive lung disease. *N Engl J Med* 1968;278:1355-60.

(59) Hogg JC, Macklem PT, Thurlbeck WM. The resistance of collateral channels in excised human lungs. *J Clin Invest* 1969;48:421-31.

(60) Marshall H, Deppe MH, Parra-Robles J, *et al.* Direct visualisation of collateral ventilation in COPD with hyperpolarised gas MRI. *Thorax* 2012;67:613-17.

(61) Kim WW, Lee CH, Goo JM, *et al.* Xenon-enhanced dual-energy CT of patients with asthma: dynamic ventilation changes after methacholine and salbutamol inhalation. *AJR Am J Roentgenol* 2012;199:975-81.

(62) Nair P, Dasgupta A, Brightling CE, *et al.* How to diagnose and phenotype asthma. *Clin Chest Med* 2012;33:445-57.

(63) Ohno Y, Chen Q, Hatabu H. Oxygen-enhanced magnetic resonance ventilation imaging of lung. *Eur J Radiol* 2001;37:164-71.

(64) Ohno Y, Hatabu H. Basics concepts and clinical applications of oxygen-enhanced MR imaging. *Eur J Radiol* 2007;64:320-28.

(65) Coxson HO, Quiney B, Sin DD, *et al.* Airway wall thickness assessed using computed tomography and optical coherence tomography. *Am J Respir Crit Care Med* 2008;177:1201-06.

CHAPTER 3

Hyperpolarized ^{3}He MRI previously revealed the temporal and spatial heterogeneity of ventilation defects in asthmatics, but these findings have not been used in treatment studies or to guide personalized treatment. Accordingly, here we generated personalized ^{3}He MRI temporal-spatial pulmonary function maps to regionally identify temporally persistent and intermittent ventilation defects that may be used to optimize, evaluate and guide asthma treatment.

The contents of this chapter were previously published in Academic Radiology: S Svenningsen, F Guo, M Kirby, S Choy, A Wheatley, DG McCormack and G Parraga. Pulmonary Functional Magnetic Resonance Imaging: Asthma Temporal-spatial Maps. Acad Radiol 2014; 21(11):1402-1410. Permission to reproduce this article was granted by Elsevier and is provided in Appendix A.

3 PULMONARY FUNCTIONAL MAGNETIC RESONANCE IMAGING: ASTHMA TEMPORAL-SPATIAL MAPS

3.1 Introduction

Asthma is a chronic pulmonary disease[1] characterized by acute and predominantly reversible episodes of airflow limitation and airway hyperresponsiveness that leads to airway remodeling[2,3] Currently used asthma measurements are largely dependent on spirometry measurements of airflow limitation made at the mouth. Such measurements tend to over-estimate large airway constriction and under-estimate small airways disease[4] and these measurements cannot regionally identify the airways responsible for airflow limitation, asthma symptoms or control.

Currently, pulmonary imaging techniques play a minor role in the clinical diagnosis and management of asthma, although quantitative measurements of regional structural and functional pulmonary abnormalities[5] can be derived using a number of imaging methods. For example, x-ray computed tomography (CT) has been used to show airway remodeling and evidence of gas trapping in asthmatics.[6,7] Single-photon emission computed tomography[8,9] and positron-emission tomography[10] have revealed the spatial distribution and extent of airway remodeling in asthmatics at rest and during exacerbations. Hyperpolarized noble gas magnetic resonance imaging (MRI), using either ^{3}He or ^{129}Xe, also provides a way to visualize and quantify lung regions that participate in ventilation and those that do not.[11,12] Longitudinal and interventional ^{3}He MRI studies have revealed

the regional and temporal nature of ventilation defects in asthma before and after provocation (exercise and methacholine) and therapy.[13-15] Previous work also showed that in asthma, ventilation defects are related to disease severity,[16] CT measurements of gas trapping[17] and airway morphological abnormalities.[18] Taken together, these studies suggest that in asthma, ventilation defects are related to airways disease, are regionally heterogeneous, temporally variable and responsive to therapy and provocation.[19-22] Asthma ventilation defects may be considered as therapy targets or intermediate endpoints as they are present in older asthmatics with more advanced or severe disease, increased indices of inflammation and more severely remodeled airways.[18]

There is enormous potential for imaging methods to improve the efficacy or cost-effectiveness of asthma therapy. However until now, the presence, location and/or variability of such defects has not yet been used to guide or interpret the efficacy of asthma therapy. The purpose of this proof-of-concept study, therefore, was to exploit the inherent temporal and spatial pulmonary function information provided by hyperpolarized ^{3}He MRI to identify temporally persistent and intermittent ventilation defects as potential targets for therapy.

3.2 Materials and Methods

3.2.1 Study Design

Subjects who were 18-55 years of age, with a physician diagnosis of asthma and forced expiratory volume in one second (FEV_1) $\geq$ 60%$_{pred}$ were recruited from a tertiary care asthma clinic. All subjects provided written informed consent to a study protocol that was in compliance with the Health Insurance Portability and Accountability Act and approved by the local Research Ethics Board and Health Canada. All subjects consented to three study visits, each 5±2 days apart, that took place between May 2007 and May 2008. At each visit, pre- and post-exercise challenge, spirometry was performed followed by ^{1}H and ^{3}He MRI. Spirometry was performed using an *ndd EasyOne* spirometer (ndd Medizintechnik AG, Zurich, Switzerland) and FEV_1, forced vital capacity (FVC) and FEV_1/FVC were obtained according to the American Thoracic Society guidelines.[23] The exercise challenge was performed according to American Thoracic Society guidelines.[24] Briefly the subject exercised (after a 2-minute warm-up) for 6 minutes on a treadmill, while

inhaling compressed, room temperature dry air, at a workload which increased the heart rate to 80-90% of the individual's age predicted maximum.

3.2.2 Magnetic Resonance Imaging

Following spirometry, MRI was performed using a whole body 3.0 Tesla Excite 12.0 MR system (GE Healthcare, Milwaukee, WI, USA), as previously described.[25] Subjects were in the supine position and all image acquisitions were performed under breath-hold conditions (15 sec) following inspiration of a 1.0 L gas mixture from functional residual capacity (FRC). To minimize the potential for differences in the level of inspiration between imaging sessions, extensive coaching was performed prior to and during each imaging session. To ensure that each inhalation was performed from FRC, subjects were instructed to take two tidal breaths before inhaling the gas mixture from the 1.0 L Tedlar® bag (Jensen Inert Products, Coral Springs, FL, USA).

Hyperpolarized ^{3}He MRI static ventilation imaging was enabled using a single-channel, rigid, transmit-receive elliptical chest coil (RAPID Biomedical GmbH, Wuerzburg, DEU) as previously described.[25] Hyperpolarized ^{3}He gas (30-40% polarization) was provided by a turnkey system (HeliSpin™, GE Healthcare, Durham, NC, USA) and administered to subjects (dose: 5mL/kg of body weight) in a $^{3}He/N_2$ mixture.[25] Hyperpolarized ^{3}He MRI static ventilation images were acquired following inspiration of the hyperpolarized $^{3}He/N_2$ gas mixture using a fast two-dimensional gradient echo sequence with the following parameters: repetition time, 4.3 msec; echo time, 1.4 msec; flip angle, 7°; field of view, 44 x 44 cm; matrix size, 128 x 128; slice gap, 0 mm; 14 contiguous slices; and slice thickness, 15 mm. Subsequent to hyperpolarized ^{3}He MRI, conventional ^{1}H MRI was performed during a 1.0 L breath-hold of $^{4}He/N_2$ to mimic the ^{3}He MRI breath-hold manoeuvre. For ^{1}H imaging, a fast spoiled gradient recalled echo sequence was applied with the following parameters: repetition time, 4.7 msec; echo time, 1.2 msec; flip angle, 30°; field of view, 44 x 44 cm; matrix size, 256 x 256; slice gap, 0 mm; 14 contiguous slices; and slice thickness, 15 mm.

3.2.3 Image Analysis

3.2.3.1 *Overview of Pipeline*

Figure 3-1 provides a summary of the registration and segmentation pipeline used to generate whole lung, two-dimensional, temporal-spatial pulmonary function maps. The inputs to the pipeline are N ^{3}He images acquired at visits $i \in \{1,2\ldots,N\}$, where $N \geq 2$, and an associated ^{1}H MR image acquired at an arbitrary visit j, $j \in \{1,2\ldots,N\}$. The pipeline consists of four steps: 1) Registration, 2) ^{1}H MRI Segmentation[26], 3) ^{3}He MRI Segmentation[26] and, 4) Temporal Map Generation and was developed using 3D Slicer 4.2 open source platform (http://www.slicer.org, Boston, MA, USA) and MATLAB R2013A (The Mathworks Inc. Natick, MA, USA). In this proof-of-concept demonstration, ^{3}He MR images were acquired at three visits ($N=3$), and an associated ^{1}H MR image was arbitrarily chosen at visit 2 ($j=2$).

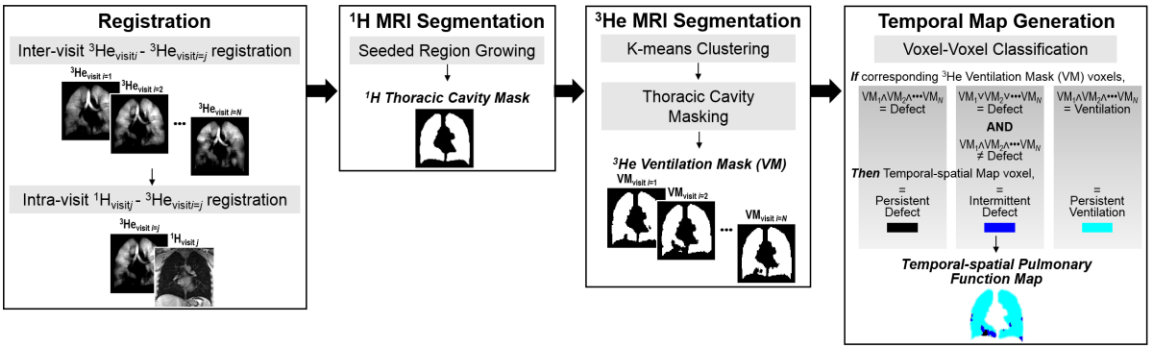

Figure 3-1 Pipeline to generate whole lung, two-dimensional, hyperpolarized ^{3}He MRI temporal-spatial pulmonary function maps.
The pipeline is divided into four steps: 1) Registration, 2) ^{1}H MRI Segmentation, 3) ^{3}He MRI Segmentation and, 4) Temporal Map Generation. The inputs to the pipeline are N ^{3}He MR images acquired at visits $i \in \{1,2\ldots,N\}$, where $N \geq 2$, and an associated ^{1}H MR image acquired at an arbitrary visit j, $j \in \{1,2\ldots,N\}$.

3.2.3.2 *Step 1: Registration*

As shown in **Figure 3-1**, using 3D Slicer, ^{3}He MR images acquired at each visit *i*, ^{3}He$_{visit i}$, $i \in \{1,2\ldots,N\}$, and the ^{1}H MR image acquired at visit *j*, are co-registered to ^{3}He$_{visit i=j}$ to generate temporal-spatial pulmonary function maps. ^{3}He$_{visit i=j}$, corresponding to the same visit at which the ^{1}H MR image was acquired, is used as the fixed image for each inter-

visit $^{3}He_{visit\,i}$-$^{3}He_{visit\,i=j}$ and intra-visit $^{1}H_{visit\,j}$-$^{3}He_{visit\,i=j}$ registration. Inter-visit $^{3}He_{visit\,i}$-$^{3}He_{visit\,i=j}$ registration is required to correct for misalignment between two ^{3}He MRI scans acquired at visit *i* and *j* due to inter-visit patient position variability on the scanner bed. $^{3}He_{visit\,i}$-$^{3}He_{visit\,i=j}$ co-registration is performed using an automated non-rigid deformable (B-spline) registration method. Intra-visit $^{1}H_{visit\,j}$-$^{3}He_{visit\,i=j}$ co-registration is employed using landmark-based affine registration with 4-7 corresponding anatomical fiducial markers, such the carina, trachea, primary bronchi and the diaphragm.

3.2.3.3 *Step 2: ^{1}H MRI Segmentation*

The thoracic cavity mask, which identifies the lung boundary and intern the thoracic cavity volume (TCV), is generated by segmenting $^{1}H_{visit\,j}$ using a seeded-region growing algorithm,[27] as previously described.[26] There is a subsequent manual editing option implemented to permit user modification of the automatically generated mask.

3.2.3.4 *Step 3: ^{3}He MRI Segmentation*

For each visit *i*, automated $^{3}He_{visit\,i}$ ventilation segmentation is achieved using a hierarchical K-means clustering method, as previously described.[26] The resulting ^{3}He cluster maps consist of five clusters that represent signal intensity classes ranging from no signal (cluster 1 (C1), or ventilation defect volume (VDV)), hypo-intense signal (C2) to hyper-intense signal (C5). Subsequently, ^{3}He clusters C2-C5 are merged and thoracic cavity masking was performed to generate corresponding ^{3}He ventilation masks (VM). ^{3}He MRI ventilation defect percent (VDP) was quantified by normalizing VDV to the TCV, as previously described.[28]

3.2.3.5 *Step 4: Temporal Map Generation*

To convey the short-term temporal behavior of ^{3}He gas distribution, temporal-spatial pulmonary function maps are generated from *N* ^{3}He ventilation masks and consist of three clusters: 1) persistent defect, 2) intermittent defect, and 3) persistent ventilation. Temporal-spatial pulmonary function map voxels are deemed as "persistent defect" if the corresponding ^{3}He MRI ventilation mask voxels were ventilation defect (C1) at each visit. Similarly, a voxel is deemed persistently ventilated if the corresponding ventilation mask voxels were ventilated (C2-C5) at each visit. A voxel is deemed as "intermittent defect" if the corresponding voxels were not consistently ventilation (C2-C5) or ventilation defect

(C1) at each visit. Persistent ventilation defect percent (VDP_P), intermittent ventilation defect percent (VDP_I) and persistent ventilation percent (PVP) were generated as the ratio of each volume to the ^{1}H MRI TCV.

3.2.4 Registration Performance Evaluation

Registration accuracy was estimated using the target registration error (TRE),[29] defined as the distance between corresponding fiducial points in the fixed image and the moving images after registration. Distinguishing anatomical landmarks that were readily apparent to the human observer, including the carina, trachea, primary bronchi and the diaphragm, were used as fiducials.

3.2.5 Statistical Analysis

Repeated-measures analysis of variance (ANOVA) were performed to evaluate changes in spirometry measurements, ^{3}He polarization, ^{3}He dose and ^{3}He MRI VDP across timepoints using IBM SPSS Statistics version 21.00 (SPSS Inc., Chicago, IL, USA). Paired two-tailed t-tests were used for statistical comparison of temporal-spatial pulmonary function map (VDP_P and VDP_I) anterior-centre-posterior (AP) and superior-middle-inferior (SI) differences, as previously described,[20] using GraphPad Prism version 6.02 (GraphPad Software, Inc., San Diego, CA, USA). Relationships between temporal-spatial pulmonary function maps (VDP_P and VDP_I) and spirometry were evaluated using Spearman correlation coefficients (r) and linear regressions (r^2) generated using GraphPad Prism. The mean of all spirometric measurements, acquired at visit 1, 2 and 3, were used to assess relationships. Results were considered statistically significant when the probability of making a Type I error was less than 5% ($p < 0.05$).

3.3 Results

Subject demographic characteristics are shown in **Table 3-1** for seven adults with asthma (n=4 males, mean age=28±9 years), all of whom completed three imaging sessions with a mean inter-visit interval of 5±2 days. In total there were 8 adverse events in 6 subjects. All adverse events were related to hypoxia, defined as a temporary decrease in SpO_2 below 88%, and these were temporally related to MRI breath-hold manoeuvres. **Table 3-2** shows

mean spirometry and hyperpolarized ^{3}He measurements acquired at each visit and **Table 3-3** provides a subject listing of all measurements.

Table 3-1 Subject demographic characteristics.

Parameter	**Asthma** (n=7) (±SD) [range]
Age years	28 (9) [21-47]
Male/Female	4/3
BMI kg/m^{-2}	26 (4) [21-33]
SaO_2	97 (2) [94-98]
FEV_1 $\%_{pred}$	88 (11) [65-99]
FVC $\%_{pred}$	104 (10) [89-120]
FEV_1/FVC %	72 (8) [61-81]

SD=Standard Deviation; BMI=Body Mass Index; SaO_2=Arterial Oxygen Saturation; FEV_1=Forced Expiratory Volume in 1s; $\%_{pred}$= Percent Predicted; FVC=Forced Vital Capacity.

Table 3-2 Repeated spirometry and hyperpolarized ^{3}He measurements.

	Time-point (n=7) (±SD)			**Sig of Diff (p)***
Parameter	**Visit 1**	**Visit 2**	**Visit 3**	
Spirometry				
FEV_1 $\%_{pred}$	88 (11)	86 (12)	84 (12)	0.22
FVC $\%_{pred}$	104 (10)	101 (15)	99 (14)	0.18
FEV_1/FVC %	72 (8)	71 (7)	72 (8)	0.76
Hyperpolarized ^{3}He				
Dose mL	386 (70)	380 (76)	386 (95)	0.74
Polarization %	13 (2)	12 (2)	12 (2)	0.31
MRI VDP %	4 (2)	4 (3)	4 (3)	0.93

Sig of Diff=Significance of difference; SD=Standard Deviation; FEV_1=Forced Expiratory Volume in 1s; $\%_{pred}$=Percent Predicted; FVC=Forced Vital Capacity; MRI=Magnetic Resonance Imaging; VDP=Ventilation Defect Percent.

*Significance of difference ($p<0.05$) determined using a repeated-measures analysis of variance.

Table 3-3 Subject listing of demographic, spirometry and hyperpolarized ^{3}He MRI measurements.

			Spirometry			*Hyperpolarized ^{3}He MRI*					
Subject	**Age**	**Sex**	**$FEV_1\%_{pred}$**	**$FVC\%_{pred}$**	**FEV_1/FVC%**	**Dose mL**	**Polarization%**	**VDP%**	**VDP_P%**	**VDP_I %**	**PVP%**
			V1/V2/V3	V1/V2/V3	V1/V2/V3	V1/V2/V3	V1/V2/V3	V1/V2/V3			
1	27	M	89/88/77	108/103/95	69/70/68	390/390/390	13/14/14	3/5/8	0.59	6.45	92.96
2	25	M	85/83/84	94/96/87	76//73/81	420/420/420	13/12/14	1/1/1	0.02	1.49	98.49
3	22	M	88/91/94	120/127/126	62/60/63	390/390/390	15/12/13	7/9/2	0.30	7.23	92.47
4	28	M	95/89/90	106/101/95	75/74/79	490/490/550	11/9/12	2/2/1	0.03	3.13	96.84
5	27	F	94/96/95	102/105/102	81/81/82	290/250/250	10/8/9	4/1/2	0.02	1.97	98.01
6	21	F	99/93/87	108/100/105	77/78/70	420/400/400	14/14/14	2/4/5	0.13	3.35	96.53
7	47	F	65/59/62	89/77/83	61/64/62	300/320/300	14/13/9	6/4/6	0.34	6.68	92.98
Mean	**28**	-	**88/86/84**	**104/101/99**	**72/71/72**	**386/380/386**	**13/12/12**	**4/4/4**	**0.20**	**4.33**	**95.47**
SD	**9**	-	**11/12/12**	**10/15/14**	**8/7/8**	**70/76/95**	**2/2/2**	**2/3/3**	**0.22**	**2.40**	**2.58**

V1=Visit 1; V2=Visit 2; V3=Visit 3; FEV_1=Forced Expiratory Volume in 1s; $\%_{pred}$=Percent Predicted; FVC=Forced Vital Capacity; VDP=Ventilation Defect Percent; VDP_P=Persistent Ventilation Defect Percent; VDP_I=Intermittent Ventilation Defect Percent; PVP=Persistent Ventilation Percent.

Figure 3-2 shows representative coronal hyperpolarized ^{3}He MRI slices, acquired at each visit, for each subject. All asthmatics evaluated had visually obvious ^{3}He MRI gas distribution abnormalities at one or more of their imaging timepoints and qualitative differences in the distribution of ^{3}He gas were observed between visits, as shown in **Figure 3-2**. However, despite regional gas distribution differences, as shown in **Table 3-2**, spirometry ($FEV_1\%_{pred}$, p=0.22; $FVC\%_{pred}$, p=0.18; FEV_1/FVC%, p=0.76) and whole lung ^{3}He MRI VDP (p=0.93) were not significantly different between visits. Additionally, ^{3}He dose (p=0.74) and polarization (p=0.31) was not different between imaging sessions.

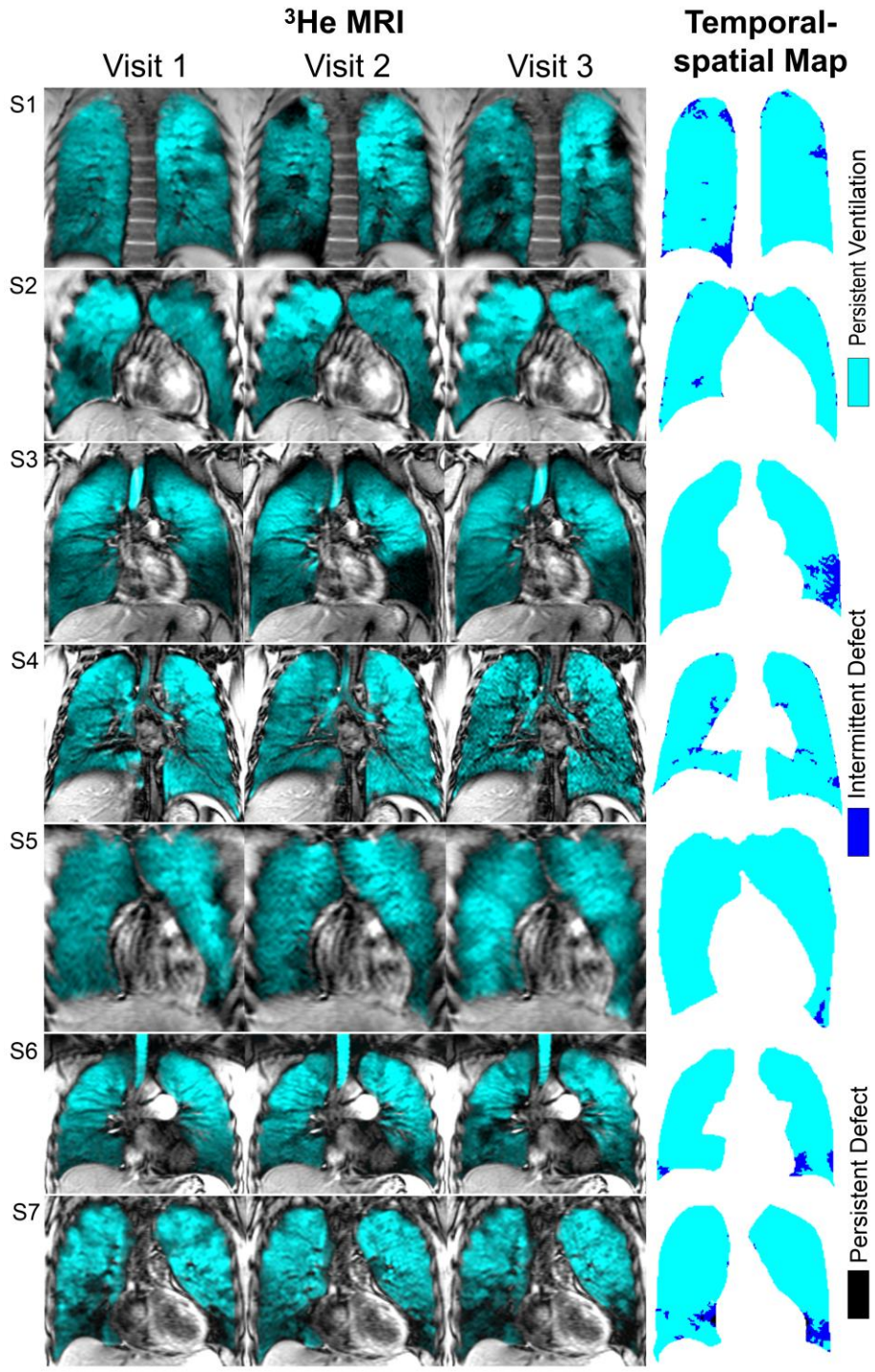

Figure 3-2 ^{3}He MRI co-registered to the corresponding ^{1}H MRI acquired at visit 1-3, and the corresponding temporal-spatial pulmonary function maps for seven asthmatic subjects. Regional differences in the spatial distribution of ^{3}He MRI ventilation defects are visually apparent between visits for each subject. This short-term temporal ^{3}He ventilation defect behaviour is shown in the corresponding two-dimensional temporal-spatial map for each subject.

3.3.1 Temporal-Spatial Pulmonary Function Maps

Temporal-spatial pulmonary function maps were generated from ^{3}He MR images acquired at three visits ($N = 3$), and an associated ^{1}H MR image was arbitrarily chosen at visit 2 ($j = 2$).

3.3.1.1 *Target Registration Error*

Four corresponding fiducials were marked on each image volume ($^{3}He_{visit1}$, $^{3}He_{visit2,}$ $^{3}He_{visit3}$ and $^{1}H_{visit2}$), for a total of 168 fiducials (24 per subject). The mean distance between corresponding fiducials in the ^{3}He-^{3}He and ^{1}H-^{3}He image sets was 22±12mm and 19±10mm, respectively. For inter-visit ^{3}He-^{3}He registration, the mean TRE value for all 112 fiducials (56 pairs) was 7±5mm (range: 1mm-29mm). For intra-visit ^{1}H-^{3}He registration, the mean TRE for all 56 fiducials (28 pairs) was 6±3mm (range: 2mm-14mm).

3.3.1.2 *Ventilation Defect Temporal Behavior*

Figure 3-2 shows temporal-spatial pulmonary function maps for each subject and these spatially quantified the short-term temporal behavior of ^{3}He MRI ventilation defects. Lung regions with persistent (black) and intermittent ventilation defects (blue) were identified, the remaining regions were persistently ventilated (cyan). For all subjects evaluated, the mean persistent ventilation defect percent was low (mean VDP_P=0.2±0.2%) as was mean intermittent ventilation defect percent (VDP_I=4±2%). Mean persistent ventilation percent was high (PVP=95±3%) across the three imaging sessions.

3.3.1.3 *Anatomic Differences*

As qualitatively shown in **Figure 3-3** and quantitatively described in **Figure 3-4**, VDP_P and VDP_I were evaluated in the AP and SI regions of interest. VDP_I was significantly greater in the posterior as compared to the centre (p=0.02) and anterior (p=0.04) lung regions but VDP_P was not different. In the inferior lung region, VDP_I was significantly greater (p=0.04) than the superior lung region, while VDP_P was not different.

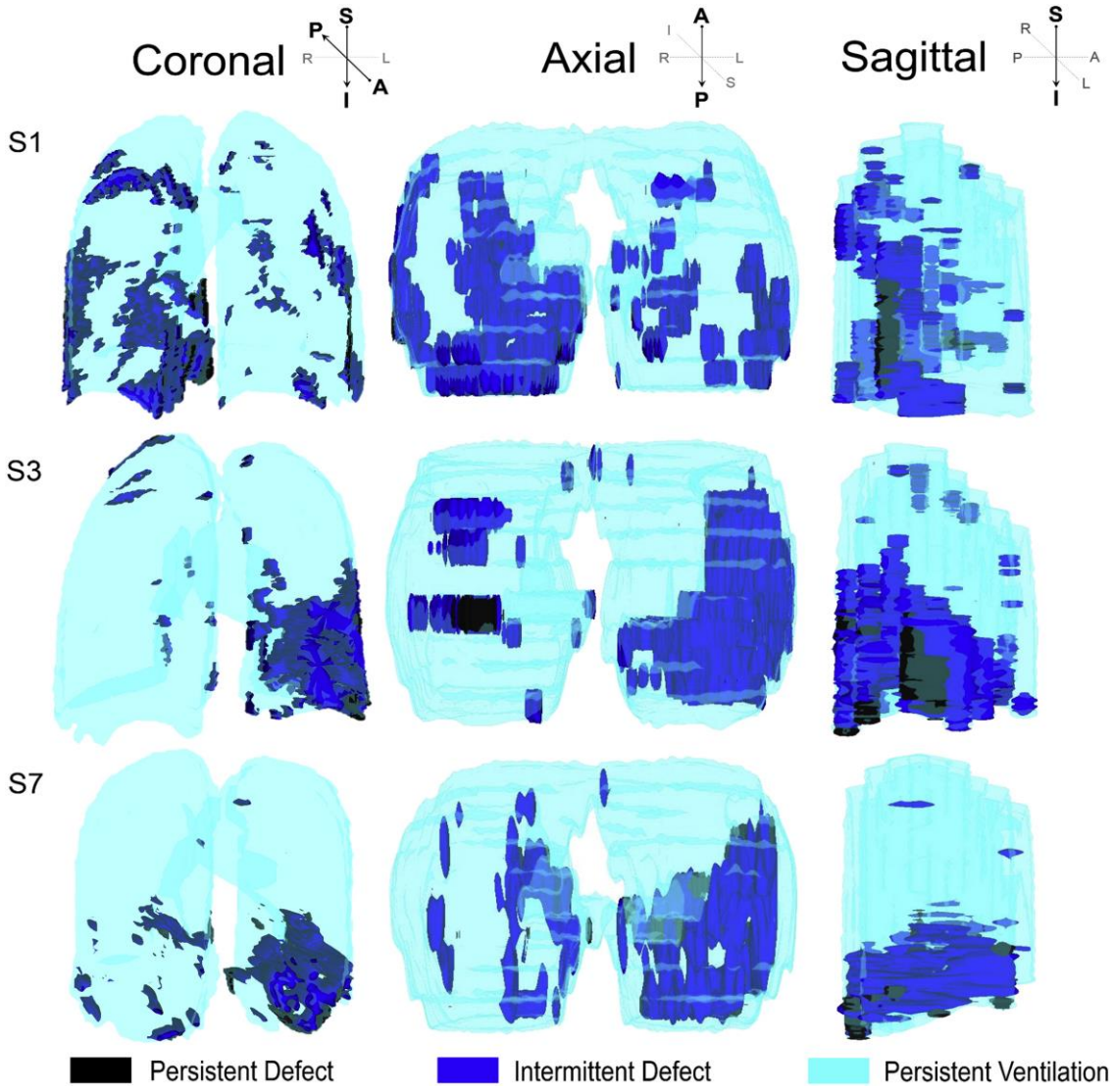

Figure 3-3 Three-dimensional ^{3}He MRI temporal-spatial pulmonary function maps for three representative asthmatic subjects.
3D ^{3}He MRI in the coronal, axial and sagittal view to qualitatively evaluate persistent and intermittent ventilation defects. Both persistent and intermittent ventilation defects are prominent in the gravity-dependent posterior and inferior lung regions.

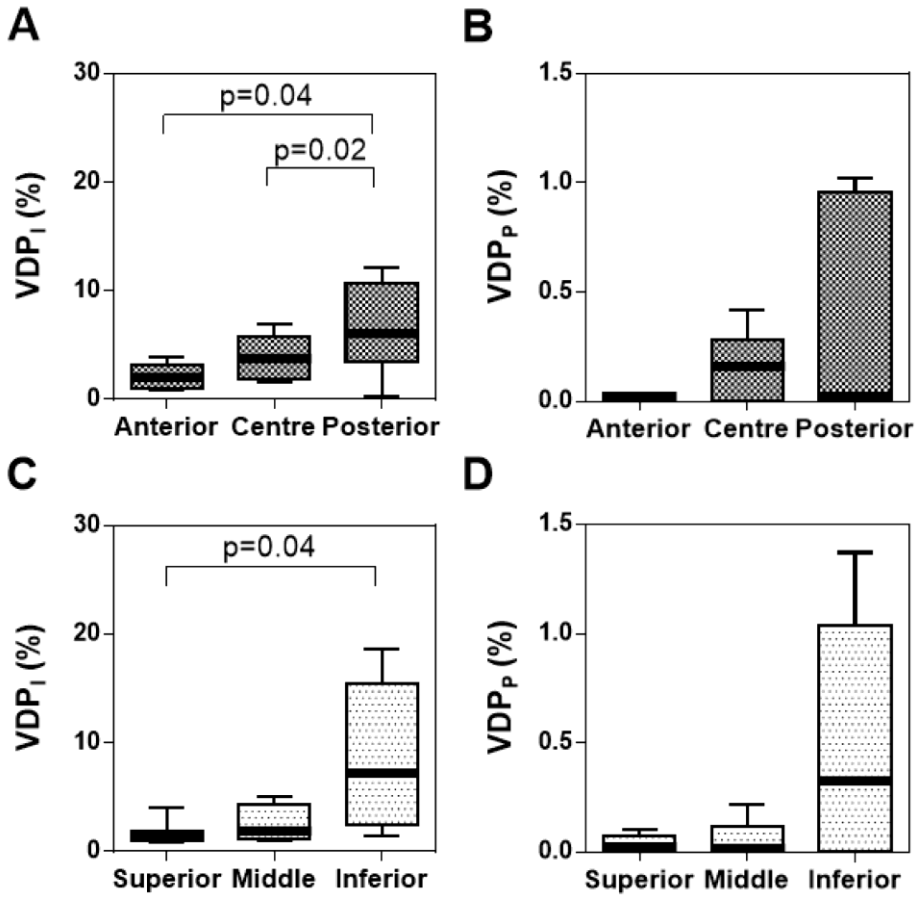

Figure 3-4 ^{3}He MRI intermittent ventilation defect percent (VDP_I) and persistent ventilation defect percent (VDP_P) anatomical differences.
Plots show anatomical differences in VDP_I and VDP_P for regions of interest in the anterior-centre-posterior (A, B) and superior-middle-inferior directions (C, D). Box and whisker plots represent: minimum, 25th percentile, median, 75th percentile, and maximum. Statistically significant differences between regions of interest are shown.

3.3.1.4 *Relationships with Spirometry*

Figure 3-5 shows correlations for VDP_P and VDP_I with baseline and post-exercise FEV_1/FVC. Both VDP_P and VDP_I were negatively correlated with baseline (VDP_P: r=-0.87, p=0.01; VDP_I: r=-0.96, p=0.0008) and post-exercise FEV_1/FVC (VDP_P: r=-0.79, p=0.04; VDP_I: r=-0.96, p=0.003). There were no significant correlations for VDP_P or VDP_I with $FEV_1\%_{pred}$ or $FVC\%_{pred}$.

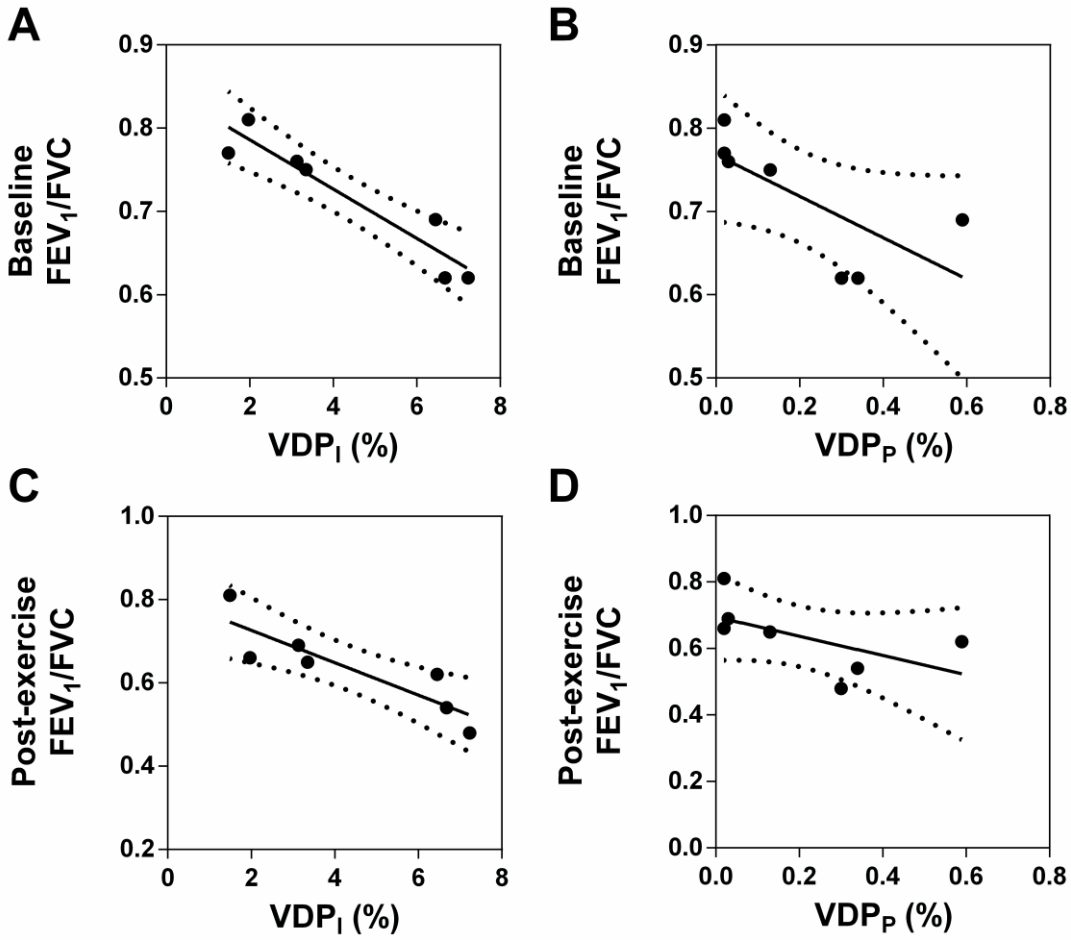

Figure 3-5 Relationship of ^{3}He MRI temporal-spatial pulmonary function with airflow obstruction at baseline and following exercise challenge.
Baseline FEV_1/FVC was significantly correlated with intermittent ventilation defect percent (VDP_I) (r=-0.96, p=0.0008) (A), and persistent ventilation defect percent (VDP_P) (r=-0.87, p=0.01) (B). Post-exercise FEV_1/FVC was significantly correlated with VDP_I (r=-0.96, p=0.003) (C), and VDP_P (r=-0.79, p=0.04) (D). Dotted lines indicate the 95% limits of agreement.

3.4 Discussion

We aimed to exploit ^{3}He MRI ventilation measurements to generate asthma temporal-spatial pulmonary function maps in acknowledgement of the paucity of real-time visualization/quantification tools available to identify temporal changes in regional ventilation, especially in response to therapy. Therefore, here we developed a registration-segmentation pipeline to generate ^{3}He MRI temporal maps in mild-to-moderate asthmatics in order to spatially quantify temporally persistent and intermittent ventilation defects.

First, we acquired ^{3}He MRI in seven asthmatic subjects, in whom there were no changes in pulmonary function tests or ^{3}He MRI VDP during a three-week data acquisition period. For most subjects however, there were visually obvious differences in the regional distribution of ^{3}He ventilation defects over the three-week time period. Previous studies have evaluated ^{3}He MRI ventilation defects following bronchoconstriction[13,20,21,30] and bronchodilation,[20,22] and these studies quantitatively described changes in the size and number of ventilation defects. Other studies[13,14,30] have evaluated ventilation defect reproducibility prior to and following bronchoconstriction and bronchodilation. These studies suggested that the location and the temporal occurrence of ventilation defects prior to broncho-provocation were heterogeneous.[30] We think that this important information can be quantified and simplified using multiple ^{3}He MRI time-points and that using a single snapshot in time would likely be insufficient to quantify the complex interactions between space, time and airway hyperresponsiveness. Persistent ventilation defects represented regions that were always abnormal, perhaps due to remodeled, narrowed and/or collapsed airways that altered the time constants for lung filling beyond the timeframe for MRI acquisition (15 sec). Intermittent defects may be related to a number of underlying physiological airway abnormalities such as variable airway lumen diameter, exposure to triggers of hyperresponsiveness or mucus plugging.

MRI temporal-spatial pulmonary function maps may be used to regionally locate the specific airways that are proximal to persistent or intermittent ventilation abnormalities as potential targets for localized airway treatment such as bronchial thermoplasty.[31] For example, as shown in **Figure 3-2** and **Figure 3-3**, for subject 3, the map provides evidence of highly localized disease. For this subject, measurements of response to therapy to localize treatment should be directed to the lower left lobe, and can avoid the upper left lobe and the right lung.

Second, we observed that intermittent ventilation defects and persistently ventilated lung showed regional differences or biases. All subjects were imaged in the supine position, and in the gravity-dependent lung regions (posterior and inferior) VDP_I was increased. This suggests that ventilation defects are more variable over time in dependent lung regions, a finding which must be further investigated. This finding is supported by previous quantitative findings in both asthmatic and healthy subjects[20] that VDP is greater

in the dependent lung regions. Although the physiological mechanism responsible for this observation is not known, airway collapse may be a plausible explanation.

Finally, we observed correlations for airflow obstruction (FEV_1/FVC) with VDP_I and VDP_P at baseline and following exercise-induced bronchoconstriction. Due to an increased sensitivity of asthmatic airways to a range of constrictor agonists, bronchial hyperresponsiveness is often referred to as the "hallmark" of asthma. Accordingly, intermittent defects were identified in an attempt to spatially identify hyperresponsive airways as potential therapy targets. We hypothesized that asthmatics with intermittent defects would show greater response to broncho-provocation and interestingly, we did observe a strong relationship between intermittent defects and post-exercise FEV_1/FVC ($r=-0.96$, $p=0.003$) in these seven asthmatics. This lends support to the notion that temporal-spatial measurements may be identifying hyper-responsive lung regions or ROI that are more likely to constrict during an exacerbation.

Although this preliminary demonstration provides promising proof-of-concept results, we must acknowledge several limitations. Importantly, a sample size of seven is small, therefore, our feasibility results should be considered a conservative estimate of VDP_P and VDP_I. In fact, the immediate application of our method may be better-suited to poorly-controlled and more severe asthma. Additionally, the maps generated here captured week-to-week lung function variability and not long-term ventilation defect persistence or disease progression. The temporal persistence of ventilation defects was previously shown to decrease with time,[14] therefore a longer inter-visit interval than used here might yield fewer persistent defect ROIs. Additionally, we recognize the importance of potential registration errors and the effect this has on map interpretation – especially on the lung periphery where sub-segmental defects tend to appear. In our experience, most registration errors are derived from scan-to-scan variability/differences in lung inflation levels, potentially due to gas trapping, and we therefore implemented a deformable registration method to minimize this. If the methodology developed here was extended to generate maps to display transient ROI in response to methacholine and/or salbutamol, the application of the non-rigid registration algorithm presented here would be even more essential to account for larger changes in lung volumes and shape. Finally, we must consider our approach as a precursor to temporal-spatial pulmonary function maps

generated using hyperpolarized ^{129}Xe gas[22] as these will certainly play a more prominent role in the future.[32] Clearly, prior to the clinical application of this potential pulmonary image-guidance tool extensive efficacy evaluations are required. Specifically, a randomized two-arm evaluation comparing the efficacy of conventional and image-guided treatment will be necessary to determine if similar changes in asthma control and quality-of-life can be achieved as those obtained following conventional therapy.

By "seeing" the disease and its variability over time, we can potentially help improve asthma treatments and outcomes, amounting to enormous clinical value. Therefore, this work must be viewed as a first necessary step towards the development of high resolution image-guidance maps to help target specific airway abnormalities in asthmatics who undergo localized asthma therapies, such as bronchial thermoplasty, that currently are not guided by imaging to abnormally functioning lung. In conclusion, personalized asthma temporal-spatial pulmonary function maps were generated from thoracic ^{3}He MRI to visualize and quantify regional ventilation defects observed over time.

3.5 References

(1) Global Initiative for Asthma: Global Strategy for Asthma Management and Prevention, 2012. http://www.ginasthma.org (accessed July 2014).

(2) Crimi E, Spanevello A, Neri M, *et al.* Dissociation between airway inflammation and airway hyperresponsiveness in allergic asthma. *Am J Respir Crit Care Med* 1998;157:4-9.

(3) Skold CM. Remodeling in asthma and COPD - differences and similarities. *Clin Respir J* 2010;4:20-27.

(4) Perez T, Chanez P, Dusser D, *et al.* Small airway impairment in moderate to severe asthmatics without significant proximal airway obstruction. *Respir Med* 2013;107:1667-74.

(5) Castro M, Fain SB, Hoffman EA, *et al.* Lung imaging in asthmatic patients: the picture is clearer. *J Allergy Clin Immunol* 2011;128:467-78.

(6) Niimi A, Matsumoto H, Amitani R, *et al.* Airway wall thickness in asthma assessed by computed tomography. Relation to clinical indices. *Am J Respir Crit Care Med* 2000;162:1518-23.

(7) Aysola RS, Hoffman EA, Gierada D, *et al.* Airway remodeling measured by multidetector CT is increased in severe asthma and correlates with pathology. *Chest* 2008;134:1183-91.

(8) King GG, Eberl S, Salome CM, *et al.* Airway closure measured by a technegas bolus and SPECT. *Am J Respir Crit Care Med* 1997;155:682-88.

(9) King GG, Eberl S, Salome CM, *et al.* Differences in airway closure between normal and asthmatic subjects measured with single-photon emission computed tomography and technegas. *Am J Respir Crit Care Med* 1998;158:1900-06.

(10) Venegas JG, Winkler T, Musch G, *et al.* Self-organized patchiness in asthma as a prelude to catastrophic shifts. *Nature* 2005;434:777-82.

(11) Albert MS, Cates GD, Driehuys B, *et al.* Biological magnetic resonance imaging using laser-polarized ^{129}Xe. *Nature* 1994;370:199-201.

(12) Altes TA, Powers PL, Knight-Scott J, *et al.* Hyperpolarized ^{3}He MR lung ventilation imaging in asthmatics: preliminary findings. *J Magn Reson Imaging* 2001;13:378-84.

(13) de Lange EE, Altes TA, Patrie JT, *et al.* The variability of regional airflow obstruction within the lungs of patients with asthma: assessment with hyperpolarized helium-3 magnetic resonance imaging. *J Allergy Clin Immunol* 2007;119:1072-8.

(14) de Lange EE, Altes TA, Patrie JT, *et al.* Changes in regional airflow obstruction over time in the lungs of patients with asthma: evaluation with ^{3}He MR imaging. *Radiology* 2009;250:567-75.

(15) Wheatley A, McKay S, Mathew L, *et al.* Hyperpolarized helium-3 magnetic resonance imaging of asthma: short-term reproducibility 2008:69161X-61X-8.

(16) de Lange EE, Altes TA, Patrie JT, *et al.* Evaluation of asthma with hyperpolarized helium-3 MRI: correlation with clinical severity and spirometry. *Chest* 2006;130:1055-62.

(17) Fain SB, Gonzalez-Fernandez G, Peterson ET, *et al.* Evaluation of structure-function relationships in asthma using multidetector CT and hyperpolarized He-3 MRI. *Acad Radiol* 2008;15:753-62.

(18) Svenningsen S, Kirby M, Starr D, *et al.* What are ventilation defects in asthma? *Thorax* 2014;69:63-71.

(19) Tzeng YS, Lutchen K, Albert M. The difference in ventilation heterogeneity between asthmatic and healthy subjects quantified using hyperpolarized 3He MRI. *J Appl Physiol* 2009;106:813-22.

(20) Costella S, Kirby M, Maksym GN, *et al.* Regional Pulmonary Response to a Methacholine Challenge using Hyperpolarized ^{3}He Magnetic Resonance Imaging. *Respirology* 2012;17:1237-46.

(21) Samee S, Altes T, Powers P, *et al.* Imaging the lungs in asthmatic patients by using hyperpolarized helium-3 magnetic resonance: assessment of response to methacholine and exercise challenge. *J Allergy Clin Immunol* 2003;111:1205-11.

(22) Svenningsen S, Kirby M, Starr D, *et al.* Hyperpolarized ^{3}He and ^{129}Xe MRI: Differences in asthma before bronchodilation. *J Magn Reson Imaging* 2013;38:1521-30.

(23) Miller MR, Hankinson J, Brusasco V, *et al.* Standardisation of spirometry. *Eur Respir J* 2005;26:319-38.

(24) Crapo RO, Casaburi R, Coates AL, *et al.* Guidelines for methacholine and exercise challenge testing-1999. This official statement of the American Thoracic Society was adopted by the ATS Board of Directors, July 1999. *Am J Respir Crit Care Med* 2000;161:309-29.

(25) Parraga G, Ouriadov A, Evans A, *et al.* Hyperpolarized 3He ventilation defects and apparent diffusion coefficients in chronic obstructive pulmonary disease: preliminary results at 3.0 Tesla. *Invest Radiol* 2007;42:384-91.

(26) Kirby M, Heydarian M, Svenningsen S, *et al.* Hyperpolarized ^{3}He magnetic resonance functional imaging semiautomated segmentation. *Acad Radiol* 2012;19:141-52.

(27) Adams R, Bischof L. Seeded Region Growing. *IEEE Trans Pattern Anal and Mach Intell* 1994;16:641-47.

(28) Mathew L, Kirby M, Etemad-Rezai R, *et al.* Hyperpolarized (3)He magnetic resonance imaging: preliminary evaluation of phenotyping potential in chronic obstructive pulmonary disease. *Eur J Radiol* 2011;79:140-6.

(29) Fitzpatrick JM, West JB. The distribution of target registration error in rigid-body point-based registration. *IEEE Trans Med Imaging* 2001;20:917-27.

(30) Niles DJ, Kruger SJ, Dardzinski BJ, *et al.* Exercise-induced bronchoconstriction: reproducibility of hyperpolarized 3He MR imaging. *Radiology* 2013;266:618-25.

(31) Cox G, Miller JD, McWilliams A, *et al.* Bronchial thermoplasty for asthma. *Am J Respir Crit Care Med* 2006;173:965-9.

(32) Cho A. Physics. Helium-3 shortage could put freeze on low-temperature research. *Science* 2009;326:778-79.

CHAPTER 4

Towards the goal of understanding the structural determinants and clinical consequences of MRI ventilation defects in asthma, we evaluated well-established clinical and emerging CT-derived airway morphology measurements in healthy volunteers and asthmatics with and without ventilation defects.

The contents of this chapter were previously published in the journal Thorax: S Svenningsen, M Kirby, D Starr, HO Coxson, NA Paterson, DG McCormack and G Parraga. What are Ventilation Defects in Asthma? Thorax 2014; 69(1):63-71. Permission to reproduce this article was granted by BMJ Publishing Group Ltd and is provided in Appendix A.

4 WHAT ARE VENTILATION DEFECTS IN ASTHMA?

4.1 Introduction

Asthma is typically diagnosed and characterized using the spirometry measurement[1,2] of the forced expiratory volume in 1 second (FEV_1). Although relatively simple and inexpensive, spirometry measurements provide a global estimate of the morphological changes in the small and medium-sized airways that are believed to be related to luminal inflammation, airway remodeling and constriction. We now realize using multiple breath nitrogen washout studies[3,4] and pulmonary imaging methods, that functional abnormalities in asthma are in fact regionally heterogeneous,[5-7] temporally persistent[8-10] and that these abnormalities regionally respond to broncho-provocation[7,11,12] and to bronchodilator therapy.[11,13] Thoracic x-ray computed tomography (CT) has been used for over a decade as a non-invasive method to investigate structure-function relationships of asthmatic airways and has shown strong relationships between CT-derived airway measurements with inflammation,[14,15] spirometry[14-21] and disease severity.[14,16,20,22] However, while these CT data are encouraging, they are still somewhat limited because it is well recognized that CT cannot resolve or measure airways beyond the 5th or 6th generation. Moreover, even using new lower dose and iterative reconstruction methods,[23] CT is not recommended for longitudinal studies and studies of young adults and children because of the potential risks associated with exposure to ionizing radiation. Other pulmonary imaging methods such as nuclear medicine scintigraphy[24-26] and positron emission tomography (PET)[27] are also limited clinically because of inherently low spatial resolution.

Hyperpolarized ^{3}He magnetic resonance imaging (MRI) has been previously used to visualize heterogeneous and abnormal gas distribution in asthma. Regions of signal void or ventilation defects have been shown to be temporally persistent[8-10] and to correlate significantly with spirometry,[6,28,29] disease severity[6] and CT measurements of gas trapping.[28] In addition, ^{3}He MRI also provides a way to perform intensive serial measurements due in part to its excellent safety profile,[30] and the speed with which imaging can be performed. More specifically, ^{3}He MRI ventilation defects have been shown to increase from baseline following both methacholine[7,11,12] and exercise[12] challenge, and decrease from baseline following salbutamol administration.[13] In asthma, the relationship between ventilation defects and patient outcomes such as exacerbation frequency and severity has not yet been evaluated, however this has been evaluated in chronic obstructive pulmonary disease (COPD).[31] Recently, there has been growing interest in the clinical application of hyperpolarized gas MRI to assess treatment efficacy and furthermore to guide localized airway treatments in asthma. Preliminary work in severe asthma has shown improved ^{3}He gas distribution following localized bronchial thermoplasty treatment.[32] While these results provide a strong foundation for the use of MRI in asthma research and patient care, a major drawback has been that we do not clearly understand the etiology of MRI ventilation defects.[33] It has been speculated that MRI ventilation defects reflect regional airway narrowing that may be the consequence of airway remodeling;[34] however, to our knowledge, the direct spatial and quantitative relationship between MRI ventilation defects and CT airway measurements has not been reported in asthmatics. Therefore, our objective was to determine the underlying structural and clinical determinants of asthma ventilation abnormalities by evaluating well-established clinical and emerging imaging (hyperpolarized ^{3}He MRI and CT) measurements in healthy volunteers and subjects with asthma.

4.2 Methods

4.2.1 Study Subjects

All subjects provided written informed consent to a study protocol approved by the local research ethics board, and the study was compliant with the Personal Information Protection and Electronic Documents Act (PIPEDA, Canada) and the Health Insurance

Portability and Accountability Act (HIPAA, USA). Subjects were enrolled between 18 and 60 years of age, including mild-to-moderate[35] asthmatics, and healthy subjects with no history or diagnosis of asthma or any other chronic or current acute respiratory illness. Asthmatic subjects were phenotyped from health records based on disease severity and symptoms from a tertiary care centre (interdisciplinary Allergy and Respirology asthma care centre); all asthma subjects had a current physician diagnosis of asthma, were currently under treatment for asthma and had a positive methacholine challenge within the past five years. At a single visit, spirometry, plethysmography, fractional exhaled nitric oxide (FeNO) breath analysis and pulmonary CT was performed within 30 minutes of MRI.

4.2.2 Pulmonary Function Tests

Spirometry and plethysmography were performed according to American Thoracic Society Guidelines[36] using an *ndd EasyOne* spirometer (ndd Medizintechnik AG, Zurich, Switzerland) and a *MedGraphics Elite Series* plethysmograph (MedGraphics, St. Paul, MN, USA), respectively. FeNO was measured using a *Niox Mino* (Aerocrine Inc. USA, New Providence, NJ, USA). Methacholine challenge was performed as previously described [11] and the provocative concentration causing a 20% decrease in FEV_1 (PC_{20}) was determined. Borg and modified Medical Research Council (mMRC) dyspnea scores were recorded.

4.2.3 Magnetic Resonance Imaging

MRI was performed on a whole body 3.0 Tesla Discovery 750MR (General Electric Health Care, Milwaukee, WI, USA) system with broadband imaging capability, as previously described.[37] Subjects were instructed to inhale a gas mixture from a 1.0L Tedlar® bag (Jensen Inert Products, Coral Springs, FL, USA) from functional residual capacity (FRC), and image acquisition was performed in 8-15s under breath-hold conditions. Conventional ^{1}H MRI was performed prior to hyperpolarized ^{3}He MRI, both methods are previously described.[37]

^{3}He MR images were qualitatively and quantitatively evaluated for ventilation abnormalities by a single trained observer. Upon qualitative inspection, asthmatic subjects were classified into two groups, 1) asthmatics with no ventilation defects (ND) and

asthmatics with ventilation defects (AD). If ^{3}He gas was homogenously distributed throughout the lung and there were no visible ventilation defects the subject was classified as belonging to the ND group. In contrast, if ^{3}He gas was heterogeneously distributed throughout the lung and/or there were visually obvious ventilation defects, the subject was classified as belonging to the AD group. Quantitative evaluation of ^{3}He MRI was performed to estimate ventilation defect percent (VDP) and ventilation heterogeneity using the coefficient of variation (COV). ^{3}He MRI semi-automated segmentation was performed to quantify lung volumes using custom software generated using MATLAB R2007b (The Mathworks Inc., Natick, MA, USA), as previously described.[38] As shown in **Figure 4-1**, ^{3}He static ventilation images were segmented using a K-means approach that classified voxel intensity values into five clusters ranging from signal void (cluster 1 (C1) or ventilation defect volume (VDV)) to hyper-intense signal (cluster 5 (C5)) to create a gas distribution cluster-map. ^{3}He MRI VDP was generated using VDV normalized to the thoracic cavity volume. Whole lung and regional VDP specific to the CT region-of-interest (ROI) were generated for each subject. Ventilation heterogeneity was estimated according to previously described methods[7] using the COV. Briefly, a ventilated lung ROI was defined as gas distribution cluster-map clusters C2-C5. For each voxel within the ventilated lung ROI a local ventilation heterogeneity value was calculated by computing the COV of the signal intensity in the voxels 5 x 5 neighborhood. Mean COV for each slice was calculated for each ^{3}He static ventilation slice and then averaged to obtain a single COV value for each subject.

4.2.4 Computed Tomography

Following ^{3}He MRI, thoracic CT was performed with the same inhalation breath-hold volume and manoeuvre used for MRI, in order to match CT and MRI lung volume and anatomy. CT imaging was performed in the supine position using a 64-slice Lightspeed VCT scanner (GEHC, Milwaukee, WI USA) using a detector configuration of 64×0.625 mm, 120 kVp, 100 mA, 0.5 second gantry rotation, and a pitch of 1.25. To reduce the radiation dose, CT was obtained for a 4cm axial ROI where there were visually obvious MRI ventilation defects. In the case where there were no visually obvious ventilation defects, the CT volume was acquired in the superior region of the lung. This approach

resulted in CT volumes consisting of 32-80 slices and a total effective dose ranging from 0.37 mSv to 0.14 mSv, (generated using the CT parameters and algorithm at www.impactscan.org).

CT image analysis was performed using Pulmonary Workstation 2.0, (VIDA Diagnostics; Iowa City, IA, USA) to generate bronchial wall area percent, wall thickness percent and lumen area for all 3rd-5th generation segmental bronchi analyzed and lumen area was normalized to body surface area.[39] As shown in **Figure 4-1**, an automated airway tree segmentation algorithm was applied with a manual seed-point in the airway lumen introduced if the trachea and main bronchus were not present in the image. For each subject, all airway segment measurements were averaged to report whole lung means. To identify potential spatial relationships between ^{3}He MRI ventilation defects and corresponding airways, CT-MRI co-registration was performed using 3D Slicer registration software (http://www.slicer.org).[40]

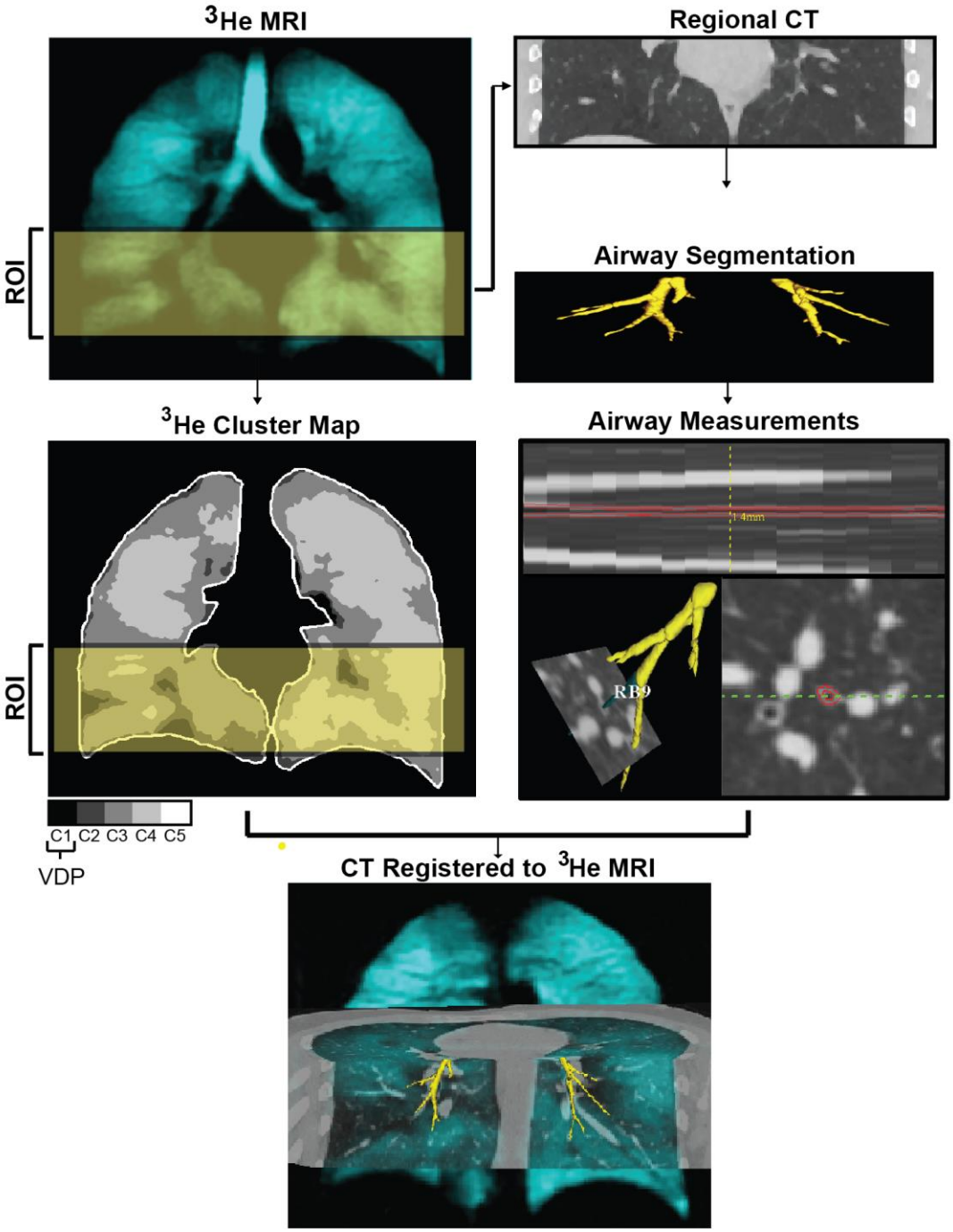

Figure 4-1 Schematic for ^{3}He MRI – Regional CT image acquisition, co-registration and analysis.

A region-of-interest (ROI) (green-yellow rectangle) with ventilation defects was located using ^{3}He MRI. Following MRI, regional CT was acquired in that specific ROI. Ventilation defect percent (VDP) was quantified for the whole lung and the CT-derived ROI and an automated airway tree segmentation algorithm (VIDA) was applied to obtain airway measurements. Using the carina and trachea as a landmark, the regional CT with rendered airways was rigidly co-registered with the corresponding MR image to confirm the spatial relationship between ventilation defects and corresponding airways.

4.2.5 Statistical Analysis

Pulmonary function tests, MRI and CT measurements were compared between subject groups using unpaired Student t-tests performed using SPSS 20.0 (IBM, Armonk, NY, USA). Linear regression (r^2) and Spearman rank correlation coefficients (r) were performed using GraphPad Prism version 4.00 (Graphpad Software Inc, San Diego, CA, USA). Results were considered statistically significant when the probability of making a Type I error was less than 5% ($p < 0.05$).

4.3 Results

We enrolled 34 subjects including 26 subjects with a clinical diagnosis of asthma and previous methacholine challenge results consistent with asthma, and 8 healthy volunteers. **Table 4-1** shows subject demographic data, pulmonary function measurements, and dyspnea scores for the two subgroups, and a subject listing of all data is provided in the online supplement, **Table 4-3S**.

Table 4-1 Subject demographic characteristics for asthmatics and healthy volunteers.

	Healthy (n=8)	**Asthmatics (n=26)**
Subject Demographics		
Age yrs (±SD)	34 (11)	35 (11)
Male/Female	4/4	12/14
BMI kg/m^2 (±SD)	23 (3)	25 (5)
Pulmonary Function Tests		
FEV_1 $\%_{pred}$(±SD)	102 (10)	84 (15)
FVC $\%_{pred}$ (±SD)	103 (10)	93 (11)
FEV_1/FVC % (±SD)	81 (6)	74 (11)
sRaw $cmH_2O \cdot s$ (±SD)	3.0 (0.5)	6.9 (4.7)
FeNO ppb (±SD)	18*	44 (45)
PC_{20} mg/ml (±SD)	42.3 (19.2)	5.9 (12.3)
Dyspnea Scores		
mMRC Score (±SD)	0 (0)	1 (1)
Borg Score (±SD)	0 (0)	0.5 (1)

SD=Standard Deviation, BMI=Body Mass Index, FEV_1=Forced Expiratory Volume in 1s, $\%_{pred}$= Percent Predicted, FVC=Forced Vital Capacity, sRaw=Specific Airway Resistance, FeNO=Fraction of Exhaled Nitric Oxide, PC_{20}= provocative concentration of methacholine sufficient to induce a 20% decrease in FEV_1, mMRC=modified Medical Research Council.
*n=1

Upon qualitative visual inspection, nine of the 26 asthmatics had no ventilation defects (ND) and 17 had visually obvious asthma ventilation defects (AD). **Figure 4-2** shows posterior, centre and anterior ^{3}He MRI static ventilation coronal slices (in blue) co-registered to the ^{1}H anatomical MRI (in grey-scale) for a representative healthy volunteer as well as ND and AD asthmatics with yellow arrows identifying ventilation defects. For both healthy volunteers and ND asthmatics, ^{3}He gas was homogeneously distributed throughout the lung whereas in contrast, AD asthmatics had visually obvious ventilation heterogeneity and ventilation defects. Of the 8 healthy volunteers and 26 asthmatics evaluated, 2 healthy volunteers and 12 asthmatics underwent imaging across multiple timepoints ranging from 4 years prior, to 2 years following the study session reported here. In accordance with the study visit data presented here, both healthy volunteers had no ventilation defects at their additional timepoint. All asthmatics who underwent multiple imaging timepoints were AD asthmatics and all of these subjects had ventilation defects at their additional timepoint and in the same spatial locations. Moreover, for all asthmatic subjects with repeated imaging measurements (n=12), VDP was not significantly different (p=0.49) from measurements acquired and reported in this study.

As shown in **Table 4-2**, AD subjects were significantly older than ND subjects (p=0.01) with significantly worse FEV_1/FVC (p=0.0003), specific airways resistance (sRaw) (p=0.004), FeNO (p=0.03), PC_{20} (p=0.008), COV (p=0.046), wall thickness percent (p=0.02) and lumen area normalized to body surface area (p=0.04), but importantly there was no mean difference for FEV_1 (p=0.08), FVC (p=0.71) or dyspnea (mMRC: p=0.79, Borg: p=0.12). As compared to healthy subjects, AD subjects had significantly worse FEV_1 (p=0.001), FEV_1/FVC (p=0.003), sRaw (p=0.003), PC_{20} (p<0.0001), COV (p=0.007) wall area percent (p=0.001), wall thickness percent (p=0.04), and lumen area normalized to body surface area (p=0.0003), but there was no significant difference for FVC (p=0.06). ND subjects had significantly worse FVC (p=0.04), PC_{20} (p=0.02) and wall area percent (0.03) compared to healthy volunteers, but no significant difference for FEV_1 (p=0.09), FEV_1/FVC (p=0.36), sRaw (p=0.36), COV (p=0.11), wall thickness percent (p=0.61) or lumen area normalized to body surface area (p=0.26).

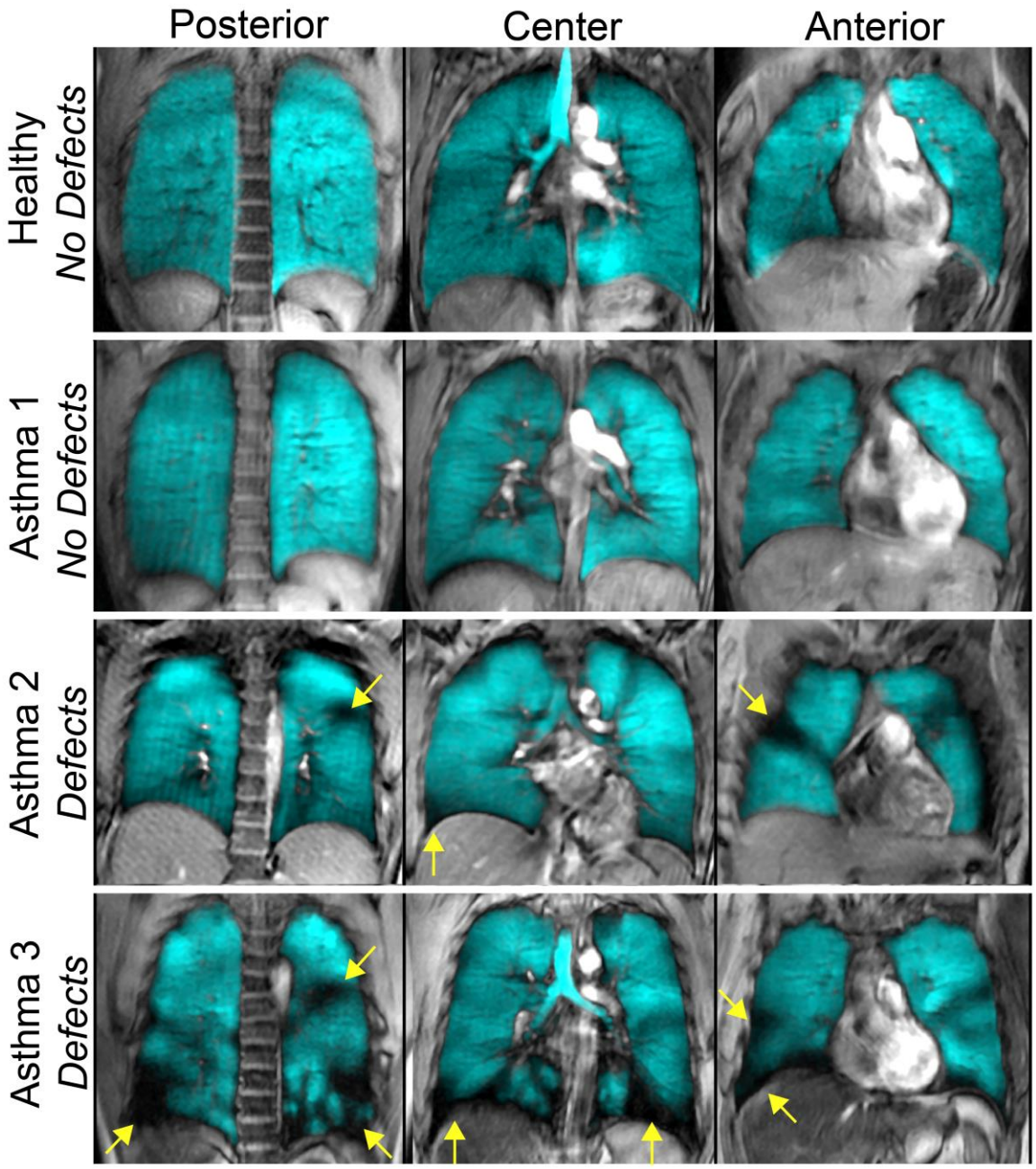

Figure 4-2 Hyperpolarized ^{3}He MRI of a representative healthy volunteer and asthmatic subjects.

^{3}He MRI gas distribution (in blue) registered to the ^{1}H MRI of the thorax (in grey-scale) for posterior, centre and anterior coronal slices for a representative healthy volunteer, an asthmatic with no ventilation defects**,** and two asthmatics with ventilation defects. Yellow arrows identify ventilation defects.

Healthy Volunteer: 27 yr old female, FEV_1=105%$_{pred}$, FEV_1/FVC=85%, sRaw=2.60 $cmH_2O{\cdot}s$; Asthmatic 1 No Defects: 23 yr old female, FEV_1=82%$_{pred}$, FEV_1/FVC=79%, sRaw=3.80 $cmH_2O{\cdot}s$; Asthmatic 2 Defects: 25 yr old female, FEV_1=87%$_{pred}$, FEV_1/FVC=69%, sRaw=5.36 $cmH_2O{\cdot}s$; Asthmatic 3 Defects: 42 yr old male, FEV_1=72%$_{pred}$, FEV_1/FVC=65%, sRaw=13.85 $cmH_2O{\cdot}s$.

Table 4-2 Subject demographic characteristics, pulmonary function, hyperpolarized ^{3}He MRI and x-ray CT airways measurements for asthmatics and healthy volunteers.

	Healthy (n=8)	**Asthma (n=26)**		**Significance of Difference* (p)**		
		ND (n=9)	AD (n=17)	HV vs. ND	HV vs. AD	ND vs. AD
Subject Demographics						
Age yrs (±SD)	34 (11)	27 (8)	39 (11)	0.19	0.29	**0.01**
Male/Female	4/4	2/7	10/7	-	-	-
Pulmonary Function Tests						
FEV_1 $\%_{pred}$(±SD)	102 (10)	91 (13)	81 (14)	0.09	**0.001**	0.08
FVC $\%_{pred}$ (±SD)	103 (10)	92 (10)	94 (11)	**0.04**	0.06	0.71
FEV_1/FVC % (±SD)	81 (6)	84 (7)	69 (10)	0.36	**0.003**	**0.0003**
sRaw $cmH_2O{\cdot}s$ (±SD)	2.96 (0.53)	3.42(1.22)	8.51(4.95)	0.36	**0.003**	**0.004**
FeNO ppb (±SD)	18[†]	17 (9)[‡]	60 (50)[δ]	-	-	**0.03**
PC_{20} mg/ml (±SD)	42.3 (19.2)	14.3(16.8)	1.4 (3.9)	**0.02**	**<0.0001**	**0.008**
Dyspnea						
mMRC Score (±SD)	0.0 (0.0)	0.7 (0.7)	0.8 (1.0)	**0.02**	**0.04**	0.79
Borg Score (±SD)	0.1 (0.2)	0.2 (0.3)	0.7 (0.8)	0.28	**0.047**	0.12
^{3}He MRI						
Whole Lung VDP% (±SD)	1.22 (0.19)	1.31(0.32)	4.26(3.28)	-	-	-
Regional VDP% (±SD)[¥]	0.94 (0.28)	0.95(0.40)	2.35(0.98)	-	-	-
Whole Lung COV (±SD)	0.22 (0.02)	0.23(0.01)	0.26(0.03)	0.11	**0.007**	**0.046**
Regional CT[¥]						
WA% (±SD)	62 (2)	66 (3)	69 (3)	**0.03**	**0.001**	0.08
WT% (±SD)	24 (4)	25 (2)	29 (4)	0.61	**0.04**	**0.02**
LA mm^2 (±SD)	18 (3)	14 (6)	11 (4)	0.19	**0.002**	0.12
LA/BSA mm^2/m^2 (±SD)	10 (2)	8 (3)	6 (2)	0.26	**0.0003**	**0.04**

ND=Asthmatics with No Defects, AD=Asthmatics with Defects, SD=Standard Deviation, FEV_1=Forced Expiratory Volume in 1s, $\%_{pred}$= Percent Predicted, FVC=Forced Vital Capacity, sRaw=Specific Airway Resistance, FeNO=Fraction of Exhaled Nitric Oxide, PC_{20}= provocative concentration of methacholine sufficient to induce a 20% decrease in FEV_1, mMRC=modified Medical Research Council, VDP=Ventilation Defect Percent, COV=Coefficient of Variation, WA%=Wall Area Percent, WT%=Wall Thickness Percent, LA=Lumen Area, BSA=Body Surface Area. *Significance of difference ($p<0.05$) determined using a t-test. [†]n=1; [‡]n=8; [δ]n=13; [¥]HV: n=5; ND: n=9; AD: n=9.

Figure 4-3 shows the correlations for FEV_1 and sRaw with whole lung VDP, regional VDP and wall area percent. FEV_1 was significantly correlated with both ^{3}He MRI VDP (whole lung: r=-0.61, p=0.0002; regional: r=-0.55, p=0.006) and wall area percent (r=-0.49, p=0.02). In addition, sRaw was significantly correlated with both ^{3}He MRI VDP (whole lung: r=0.77, p<0.0001; regional: r=0.81, p<0.0001) and wall area percent (r=0.48, p=0.02). Additionally, FEV_1 and sRaw were significantly correlated with whole lung ^{3}He MRI COV (FEV_1: r=-0.49, p=0.003; sRaw: r=0.59, p=0.0003). **Figure 4-4** demonstrates that for all subjects wall area percent was significantly correlated with whole lung (r=0.42, p=0.046) and regional VDP (r=0.43, p=0.04).

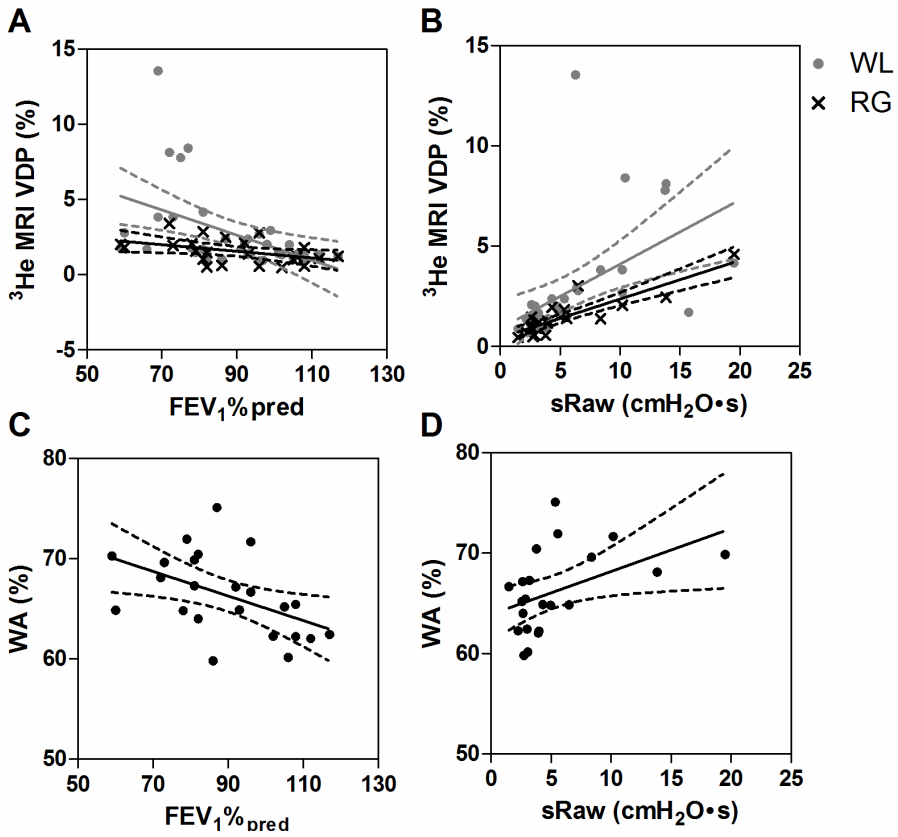

Figure 4-3 Relationships of MRI and CT measurements with FEV_1 and airways resistance.
(A) Negative relationship between ^{3}He MRI VDP and $FEV_1\%_{pred}$ (WL: r=-0.61, r^2=0.20, p=0.0002; RG: r=-0.55, r^2=0.26, p=0.006).
(B) Positive relationship between ^{3}He MRI VDP and specific airways resistance (sRaw) (WL: r=0.77, r^2=0.62, p<0.0001; RG: r=0.81, r^2=0.75, p<0.0001).
(C) Negative relationship between wall area percent and $FEV_1\%_{pred}$ (r=-0.49, r^2=0.23, p=0.02).
(D) Positive relationship between wall area percent and specific airways resistance (sRaw) (r=0.48, r^2=0.21, p=0.02).
WL=whole lung, RG=regional, WA%=wall area percent

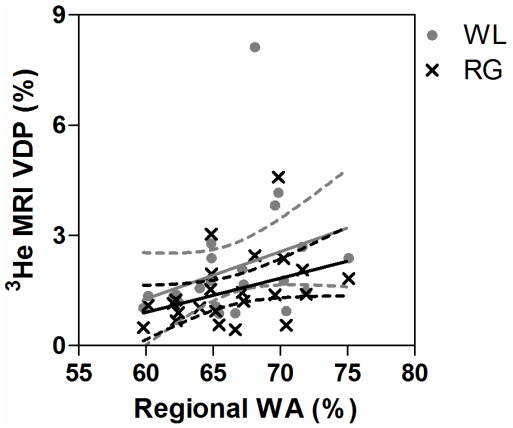

Figure 4-4 Relationship between ^{3}He MRI VDP and CT-derived wall area percent (WA%) WA% was significantly correlated with both whole lung ^{3}He MRI VDP ($r = 0.42$, $r^2 = 0.11$, $p = 0.046$) and regional ^{3}He MRI VDP ($r = 0.43$, $r^2 = 0.15$, $p = .04$).
Dashed lines represent the 95% confidence intervals of the regression line.

Figure 4-5 shows hyperpolarized ^{3}He MRI ventilation maps for four asthmatics with the ^{3}He MRI ventilation map in blue co-registered to the CT volume with the airway tree segmented in yellow. The qualitative spatial relationship between ventilation defects (yellow arrows) and remodeled airways (white arrows) is shown.

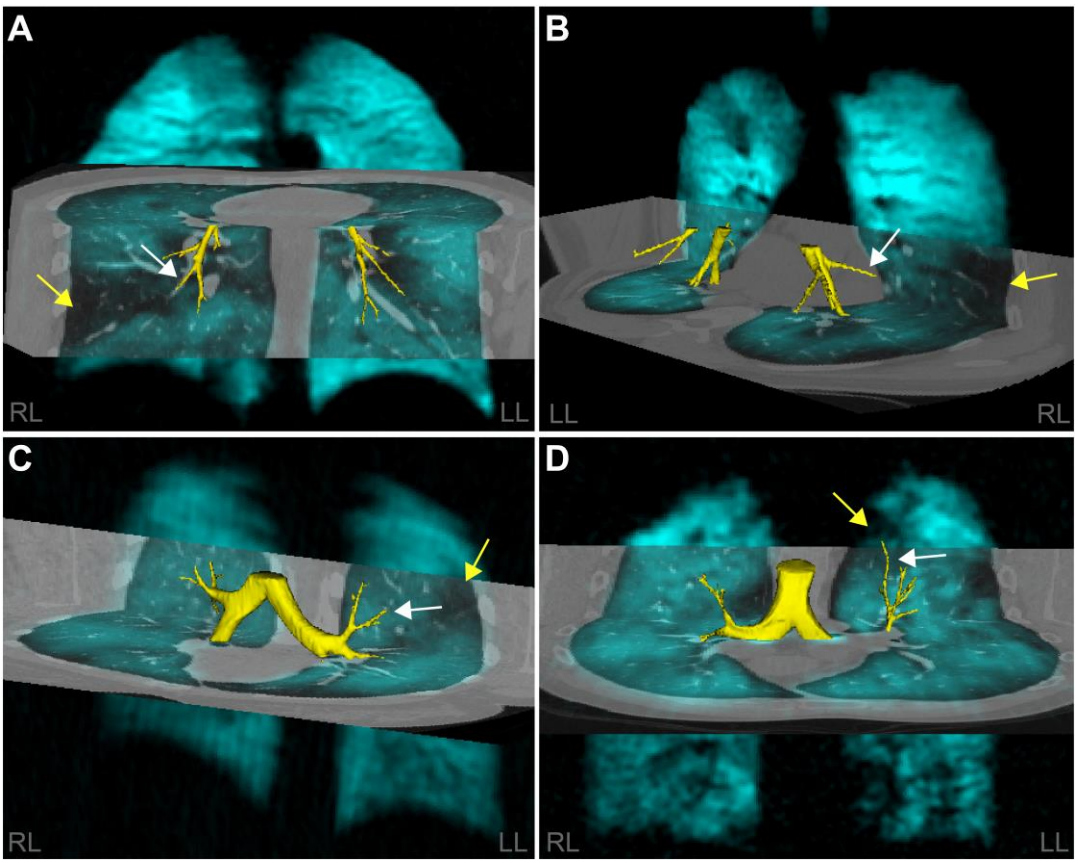

Figure 4-5 Spatial relationship between ventilation defects and airways for four representative asthmatics with ventilation defects.
^{3}He MRI gas distribution (in blue) registered to the regional CT of the thorax (in grey-scale) with the airway tree segmented in yellow. Airway measurements are for the specific airway (white arrow) spatially related to the ventilation defect (yellow arrow) of interest. Panel A is a 29 yr old male FEV_1=81%$_{pred}$, regional VDP=5%, wall area=71%, lumen area=5mm^2; Panel B is a 49 yr old male, FEV_1=60% $_{pred}$, regional VDP=3%, wall area =67%, lumen area=12mm^2 ; Panel C is a 25 yr old female, FEV_1=87% $_{pred}$, regional VDP=2%, wall area =75%, lumen area=5mm^2; Panel D is a 58 yr old male, FEV_1=73% $_{pred}$, regional VDP=1%, wall area=70%, lumen area=5mm^2.

4.4 Discussion

To better understand the structural and clinical determinants of MRI ventilation defects in asthma, and, in turn, what it might mean for an asthmatic to have ventilation defects, we evaluated well-established clinical measurements and emerging CT and ^{3}He MRI measurements of airway structure and function.

We think that it is interesting that 9/26 (35%) subjects with clinical findings and methacholine challenge results diagnostic of asthma had a ^{3}He MRI gas distribution that was qualitatively and quantitatively (VDP and COV) similar to healthy volunteers. It is important to note that all of the healthy volunteers had a homogenous gas distribution with no visual or quantitative evidence of ventilation defects, which is in agreement with previous work at our centre[11,41-43] and others.[5,7,44] In contrast, and as expected based on previous investigations,[5-9,11,12] the remaining 17/26 (65%) asthmatics had obvious ventilation abnormalities. This observation prompted us to ask the question: *Are asthmatics with ventilation defects different than asthmatics without ventilation defects?* The results here suggest that asthmatics with ventilation defects are older, with worse FEV_1/FVC, (but similar FEV_1), and greater airways resistance, airway responsiveness, and airway inflammation/remodeling. Such findings suggest that ventilation defects may reflect long-term or progressive airway remodeling in patients with a longer history of disease or perhaps more severe or advanced disease. Regardless, the constellation of clinical and imaging findings in these asthmatics suggest that more aggressive therapy or compliance to therapy is required. This is a hypothesis that can be tested in future imaging studies of older and/or more severe asthmatics.

A number of studies have quantitatively investigated asthma airway structure using CT and showed that bronchial wall thickness was related to asthma severity, duration of disease and airflow obstruction.[14-22] Similarly, ^{3}He MRI has previously shown that ventilation defects were related to asthma severity[6] and in a preliminary report,[45] half of a small group of asthmatics (7/15) showed no obvious ventilation defects, with significantly different bronchial wall thickness (but not bronchial wall area) compared to asthmatics with ventilation defects. Here, we prospectively acquired both MRI and CT within about 30 minutes using the same lung volume and breath-hold manoeuvre to try to mimic the same airway and parenchyma dimensions using both imaging methods. We must consider that because ^{3}He gas is itself, highly diffusive and may penetrate even narrowed airways, there is the possibility that even when bronchial wall thickness and lumen area are abnormal, some ^{3}He gas ventilation is possible. In support of this explanation, we note the recent report of indirect or collateral ventilation in COPD that was directly visualized using

hyperpolarized ^{3}He MRI[46] – likely possible only because the timeframe for imaging was relatively long and ^{3}He gas is highly diffusive.

We also observed that regional CT airway morphology and ^{3}He ventilation defect measurements were significantly correlated. This important finding suggests that there is a relationship between airways that are remodeled and/or constricted and ventilation defects. Previous studies have demonstrated that focal regions of hyperlucency on CT (likely related to gas trapping) were spatially correlated with ^{3}He MRI ventilation defects[28] and bronchoalveolar lavage had higher total and percent neutrophils in areas of the lung with greater ventilation defects, suggestive of increased inflammation. Although we observed significant relationships between airway dimensions and defects, these relationships were modest, perhaps because of the heterogeneity of asthma and the asthma patients evaluated here, or because of the relatively low dose partial CT region of interest that was utilized. It is important to acknowledge that in asthma, the airways from the large bronchi to the alveolar ducts may be involved,[47] thus using CT to measure airway dimensions has limitations because CT cannot spatially resolve the small airways (<2mm) sufficiently to provide accurate measurements. In addition to small and heterogeneously distributed ventilation defects, some of the asthmatics evaluated here presented large wedge shaped defects; these have previously been reported using single photon emission computed tomography (SPECT) imaging with Technegas[25] and are believed to be the result of segmental airway narrowing. Following MRI-CT registration we were able to identify and quantify segmental bronchi that were spatially related to ventilation defects. Larger 'segmental' ventilation defects may be the result of proximal remodeled sub-segmental airways feeding these regions of signal void. Unfortunately, due to the limitations of the spatial resolution of the CT images, we cannot comment on the structure of the smaller airways distal to the sub-segmental airways quantified here, which may further contribute to the abnormal gas distributions observed.

Large and temporally persistent ^{3}He ventilation defects, provide excellent targets for therapy and could potentially guide localized airway treatments such as bronchial thermoplasty. Although we have focused our attention on ventilation defects, areas of hyper-intense signal intensity are often observed in asthmatic subjects in conjunction with ventilation defects. Similar to regions of signal void, to our knowledge, the underlying

etiology of these regions has not been investigated. We hypothesize that hyper-intense signal may be due to hyperinflation and note that investigation of these regions is warranted in asthma.

We recognize and acknowledge that this work was limited by the relatively small number of subjects evaluated, although we note that this is the single largest prospective study that directly compared CT and ^{3}He MRI in asthmatics and healthy subjects. Furthermore, the subjects evaluated here were enrolled from a multi-disciplinary asthma care centre and therefore they represent a diverse group of asthmatics that have been mainly referred to improve asthma symptoms and control. As shown in **Figure 4-3**, there was a single subject with elevated VDP as compared to the other AD subjects and we confirmed that this 42 year old male had experienced an asthma exacerbation that required hospitalization approximately 5 months prior to hyperpolarized ^{3}He MRI performed here. This subject's asthma was previously well-controlled and the exacerbation was determined to be the result of sudden cessation of asthma medication. It is important to note that the relationships presented in **Figure 4-3** remain statistically significant when this outlier is removed from the analysis. Certainly, this is a hypothesis generating study and therefore marginally significant p-values should be interpreted with caution, and larger studies are required for more extensive phenotyping and characterization of asthmatics and to test the hypotheses generated here. We must also acknowledge that our analysis was limited because of the acquisition of partial CT thoracic volumes.

In summary, our results showed that asthmatics with ^{3}He MRI ventilation abnormalities were older, with greater airway hyperresponsiveness, and worse measurements of FEV_1/FVC and airways resistance/inflammation as well as abnormally remodeled airways in comparison to asthmatics without ventilation defects. Hyperpolarized ^{3}He ventilation abnormalities were spatially and quantitatively related to remodeled airways in asthmatics providing a better understanding of the etiology of heterogeneous ventilation abnormalities in asthma and the clinical meaning of these abnormalities in asthmatics with similar FEV_1.

4.5 References

(1) Busse WW. Asthma diagnosis and treatment: filling in the information gaps. *J Allergy Clin Immunol* 2011;128:740-50.

(2) Celli BR. The importance of spirometry in COPD and asthma: effect on approach to management. *Chest* 2000;117:15S-9S.

(3) Bourdin A, Paganin F, Prefaut C, *et al.* Nitrogen washout slope in poorly controlled asthma. *Allergy* 2006;61:85-89.

(4) Farah CS, King GG, Brown NJ, *et al.* The role of the small airways in the clinical expression of asthma in adults. *J Allergy Clin Immunol* 2012;129:381-87.

(5) Altes TA, Powers PL, Knight-Scott J, *et al.* Hyperpolarized ^{3}He MR lung ventilation imaging in asthmatics: preliminary findings. *J Magn Reson Imaging* 2001;13:378-84.

(6) de Lange EE, Altes TA, Patrie JT, *et al.* Evaluation of asthma with hyperpolarized helium-3 MRI: correlation with clinical severity and spirometry. *Chest* 2006;130:1055-62.

(7) Tzeng YS, Lutchen K, Albert M. The difference in ventilation heterogeneity between asthmatic and healthy subjects quantified using hyperpolarized 3He MRI. *J Appl Physiol* 2009;106:813-22.

(8) de Lange EE, Altes TA, Patrie JT, *et al.* The variability of regional airflow obstruction within the lungs of patients with asthma: assessment with hyperpolarized helium-3 magnetic resonance imaging. *J Allergy Clin Immunol* 2007;119:1072-8.

(9) de Lange EE, Altes TA, Patrie JT, *et al.* Changes in regional airflow obstruction over time in the lungs of patients with asthma: evaluation with ^{3}He MR imaging. *Radiology* 2009;250:567-75.

(10) Wheatley A, McKay S, Mathew L, *et al.* Hyperpolarized helium-3 magnetic resonance imaging of asthma: short-term reproducibility 2008:69161X-61X-8.

(11) Costella S, Kirby M, Maksym GN, *et al.* Regional Pulmonary Response to a Methacholine Challenge using Hyperpolarized ^{3}He Magnetic Resonance Imaging. *Respirology* 2012;17:1237-46.

(12) Samee S, Altes T, Powers P, *et al.* Imaging the lungs in asthmatic patients by using hyperpolarized helium-3 magnetic resonance: assessment of response to methacholine and exercise challenge. *J Allergy Clin Immunol* 2003;111:1205-11.

(13) Svenningsen S, Kirby M, Starr D, *et al.* Hyperpolarized ^{3}He and ^{129}Xe MRI: Differences in asthma before bronchodilation. *J Magn Reson Imaging* 2013;38:1521-30.

(14) Aysola RS, Hoffman EA, Gierada D, *et al.* Airway remodeling measured by multidetector CT is increased in severe asthma and correlates with pathology. *Chest* 2008;134:1183-91.

(15) Niimi A, Matsumoto H, Amitani R, *et al.* Airway wall thickness in asthma assessed by computed tomography. Relation to clinical indices. *Am J Respir Crit Care Med* 2000;162:1518-23.

(16) Awadh N, Muller NL, Park CS, *et al.* Airway wall thickness in patients with near fatal asthma and control groups: assessment with high resolution computed tomographic scanning. *Thorax* 1998;53:248-53.

(17) de Jong PA, Muller NL, Pare PD, *et al.* Computed tomographic imaging of the airways: relationship to structure and function. *Eur Respir J* 2005;26:140-52.

(18) Gono H, Fujimoto K, Kawakami S, *et al.* Evaluation of airway wall thickness and air trapping by HRCT in asymptomatic asthma. *Eur Respir J* 2003;22:965-71.

(19) Kosciuch J, Krenke R, Gorska K, *et al.* Relationship between airway wall thickness assessed by high-resolution computed tomography and lung function in patients with asthma and chronic obstructive pulmonary disease. *J Physiol Pharmacol* 2009;60 Suppl 5:71-76.

(20) Little SA, Sproule MW, Cowan MD, *et al.* High resolution computed tomographic assessment of airway wall thickness in chronic asthma: reproducibility and relationship with lung function and severity. *Thorax* 2002;57:247-53.

(21) Ueda T, Niimi A, Matsumoto H, *et al.* Role of small airways in asthma: investigation using high-resolution computed tomography. *J Allergy Clin Immunol* 2006;118:1019-25.

(22) Mitsunobu F, Tanizaki Y. The use of computed tomography to assess asthma severity. *Curr Opin Allergy Clin Immunol* 2005;5:85-90.

(23) Katsura M, Matsuda I, Akahane M, *et al.* Model-based iterative reconstruction technique for radiation dose reduction in chest CT: comparison with the adaptive statistical iterative reconstruction technique. *Eur Radiol* 2012;22:1613-23.

(24) King GG, Eberl S, Salome CM, *et al.* Airway closure measured by a technegas bolus and SPECT. *Am J Respir Crit Care Med* 1997;155:682-88.

(25) King GG, Eberl S, Salome CM, *et al.* Differences in airway closure between normal and asthmatic subjects measured with single-photon emission computed tomography and technegas. *Am J Respir Crit Care Med* 1998;158:1900-06.

(26) Pellegrino R, Biggi A, Papaleo A, *et al.* Regional expiratory flow limitation studied with Technegas in asthma. *J Appl Physiol* 2001;91:2190-98.

(27) Venegas JG, Winkler T, Musch G, *et al.* Self-organized patchiness in asthma as a prelude to catastrophic shifts. *Nature* 2005;434:777-82.

(28) Fain SB, Gonzalez-Fernandez G, Peterson ET, *et al.* Evaluation of structure-function relationships in asthma using multidetector CT and hyperpolarized He-3 MRI. *Acad Radiol* 2008;15:753-62.

(29) Tgavalekos NT, Musch G, Harris RS, *et al.* Relationship between airway narrowing, patchy ventilation and lung mechanics in asthmatics. *Eur Respir J* 2007;29:1174-81.

(30) Lutey BA, Lefrak SS, Woods JC, *et al.* Hyperpolarized 3He MR imaging: physiologic monitoring observations and safety considerations in 100 consecutive subjects. *Radiology* 2008;248:655-61.

(31) Kirby M, Kanhere N, Etemad-Rezai R, *et al.* Hyperpolarized helium-3 magnetic resonance imaging of chronic obstructive pulmonary disease exacerbation. *J Magn Reson Imaging* 2013;37:1223-7.

(32) Sheshadri A, Thomen R, Kozlowski J, *et al.* Ventilation Defects With Hyperpolarized ^{3}Helium MRI In Severe Asthma Before And After Bronchial Thermoplasty [abstract]. *Am J Respir Crit Care Med* 2013;187:A5443.

(33) Pare PD, Nagano T, Coxson HO. Airway imaging in disease: Gimmick or useful tool? *J Appl Physiol* 2012;113:636-46.

(34) Aysola R, de Lange EE, Castro M, *et al.* Demonstration of the heterogeneous distribution of asthma in the lungs using CT and hyperpolarized helium-3 MRI. *J Magn Reson Imaging* 2010;32:1379-87.

(35) Busse WW. National Asthma Education and Prevention Program Expert Panel Report 3: Guidelines for the Diagnosis and Management of Asthma, Summary Report 2007. *J Allergy Clin Immunol* 2007;120:S93-S140.

(36) Miller MR, Hankinson J, Brusasco V, *et al.* Standardisation of spirometry. *Eur Respir J* 2005;26:319-38.

(37) Parraga G, Ouriadov A, Evans A, *et al.* Hyperpolarized 3He ventilation defects and apparent diffusion coefficients in chronic obstructive pulmonary disease: preliminary results at 3.0 Tesla. *Invest Radiol* 2007;42:384-91.

(38) Kirby M, Heydarian M, Svenningsen S, *et al.* Hyperpolarized ^{3}He magnetic resonance functional imaging semiautomated segmentation. *Acad Radiol* 2012;19:141-52.

(39) King GG, Muller NL, Pare PD. Evaluation of airways in obstructive pulmonary disease using high-resolution computed tomography. *Am J Respir Crit Care Med* 1999;159:992-1004.

(40) Fedorov A, Beichel R, Kalpathy-Cramer J, *et al.* 3D Slicer as an image computing platform for the Quantitative Imaging Network. *Magn Reson Imaging* 2012;30:1323-41.

(41) Kirby M, Svenningsen S, Owrangi A, *et al.* Hyperpolarized Helium-3 and Xenon-129 Magnetic Resonance Imaging in Healthy Volunteers and Subjects with Chronic Obstructive Pulmonary Disease. *Radiology* 2012;265:600-10.

(42) Parraga G, Mathew L, Etemad-Rezai R, *et al.* Hyperpolarized 3He magnetic resonance imaging of ventilation defects in healthy elderly volunteers: initial findings at 3.0 Tesla. *AcadRadiol* 2008;15:776-85.

(43) Kirby M, Mathew L, Wheatley A, *et al.* Chronic obstructive pulmonary disease: longitudinal hyperpolarized ^{3}He MR imaging. *Radiology* 2010;256:280-89.

(44) Mata J, Altes T, Knake J, *et al.* Hyperpolarized 3He MR imaging of the lung: effect of subject immobilization on the occurrence of ventilation defects. *Acad Radiol* 2008;15:260-4.

(45) Peterson ET, Dattawadkar A, Samimi K, *et al.* Airway Measures on MDCT in Asthma at Locations of Ventilation Defect Identified by He-3 MRI. *Am J Respir Crit Care Med* 2010;181.

(46) Marshall H, Deppe MH, Parra-Robles J, *et al.* Direct visualisation of collateral ventilation in COPD with hyperpolarised gas MRI. *Thorax* 2012;67:613-17.

(47) Macklem PT. The physiology of small airways. *Am J Respir Crit Care Med* 1998;157:S181-S83.

4.6 Supplementary Material

Table 4-3S Subject listing of demographic characteristics, pulmonary function and dyspnea.

Subject	Age (yrs)	Gender	FEV_1 ($\%_{pred}$)	FVC ($\%_{pred}$)	FEV_1/FVC (%)	IC ($\%_{pred}$)	RV ($\%_{pred}$)	TLC ($\%_{pred}$)	sRaw ($cmH_2O \cdot s$)	FeNO (ppb)	PC_{20} (mg/ml)	mMRC	Borg	
													Baseline	Post-MCh
Healthy Volunteers (n=8)														
021	27	F	105	105	85	124	107	113	2.60	18	8.5	0	0	0.0
023	39	M	86	95	72	125	182	118	2.77	-	54.4	0	0	0.0
027	24	M	108	110	80	113	179	121	4.00	-	-	0	0.5	2.0
030	50	F	106	107	79	134	75	110	3.08	-	-	0	0	2.0
031	26	F	97	90	93	99	109	96	3.24	-	46.1	0	0	0.5
033	23	M	93	91	85	110	99	99	2.18	-	52.6	0	0	0.0
034	30	M	101	108	77	111	102	109	2.81	-	49.9	0	0	0.5
035	50	F	117	118	79	126	88	115	3.01	-	-	0	0	0.5
Mean(±SD)	34(11)	-	102(10)	103(10)	81(6)	118(11)	118(40)	110(9)	2.96(0.53)	-	42.3(19.2)	0(0)	0.1(0.2)	0.7(0.8)
Asthmatics with No Defects (n=9)														
005	45	F	78	87	72	124	108	102	4.97	-	2.4	2	0.5	4
006	23	F	96	91	92	107	104	97	1.50	8	16.9	1	1	7
007	24	M	81	85	81	86	111	94	3.22	12	27.9	0	0.5	3
008	34	M	82	79	84	110	105	91	2.67	16	55.2	0	0	3
010	30	F	102	101	87	135	82	96	2.25	21	3.4	1	0	2
017	23	F	112	102	96	128	164	122	3.95	12	13.2	0	0	3
018	22	F	79	83	82	90	115	91	5.58	37	0.4	0	0	3
020	23	F	82	91	79	104	69	87	3.80	17	0.3	1	0	2
024	20	F	108	110	86	138	85	99	2.88	10	9.1	1	0	4
Mean(±SD)	27(8)	-	91(13)	92(10)	84(7)	114(18)	105(25)	98(10)	3.42(1.22)	17(9)	14.3(16.8)	0.7(0.7)	0.2(0.3)	3.4(1.4)
Asthmatics with Defects (n=17)														
001	49	F	69	94	59	116	144	110	10.20	38	0.08	0	1	1
002	30	M	96	105	75	122	108	109	5.11	-	0.2	0	0	4
003	29	M	81	100	66	118	115	111	19.50	114	0.1	1	0.5	3
004	49	F	59	75	63	84	130	96	-	-	0.07	0	0	2
011	23	F	98	93	91	101	113	95	2.93	116	0.2	1	1	3
012	25	F	87	107	69	119	98	101	5.36	50	0.1	1	0	3
013	37	M	77	77	81	107	135	97	10.42	31	0.1	4	1	3
014	29	F	92	102	77	98	96	97	2.64	18	1.3	1	1	3
015	47	M	60	82	57	99	115	94	6.51	45	0.3	0	0.5	4
016	53	M	104	104	77	111	82	100	4.78	22	16.3	0	0	4
019	42	M	72	88	65	110	144	108	13.85	40	0.1	1	0	1
022	24	F	99	111	76	132	90	108	6.40	187	0.2	0	0	3
025	58	M	73	99	56	91	121	110	8.38	29	1.0	0	0.5	0
026	37	M	93	93	66	105	107	109	4.33	-	2.6	1	0.5	3
028	36	F	66	92	59	129	165	113	15.74	-	0.8	1	3	3
029	41	M	75	95	63	114	136	106	13.76	69	0.1	1	2	3
032	49	M	69	77	70	98	98	87	6.31	23	1.0	1	0.5	3
Mean(±SD)	39(11)	-	81(14)	94(11)	69(10)	109(13)	117(22)	103(8)	8.51(4.95)	60(50)	1.4(3.9)	0.8(1.0)	0.7(0.8)	2.7(1.1)

SD=Standard Deviation, FEV_1=Forced Expiratory Volume in 1s, $\%_{pred}$= Percent Predicted, FVC=Forced Vital Capacity, IC=Inspiratory Capacity, RV=Residual Volume, TLC=Total Lung Capacity, sRaw=Specific Airway Resistance, FeNO=Fraction of Exhaled Nitric Oxide, PC_{20}=provocative concentration of methacholine sufficient to induce a 20% decrease in FEV_1, mMRC=modified Medical Research Council.

CHAPTER 5

Improving asthma control is the primary treatment goal for asthmatics. Links between asthma control and ventilation defects have not been ascertained so we endeavoured to answer the question, "What is the relationship of asthma control with in vivo ventilation defects quantified and regionally visualized using MRI?"

The contents of this chapter are in preparation to be submitted to the journal Radiology: S Svenningsen, P Nair, DG McCormack and G Parraga. What do Ventilation Defects Reveal about Asthma Control? Radiology (To be submitted December 2015).

5 WHAT DO VENTILATION DEFECTS REVEAL ABOUT ASTHMA CONTROL?

5.1 Introduction

The primary goal of asthma treatment is the achievement and maintenance of disease control. Unfortunately, approximately 50% of asthmatics remain poorly controlled with up-to 10% of these patients experiencing severe and life-threatening exacerbations.[1] It is now well-understood that the clinical and pathophysiological characteristics of poorly-controlled asthma are heterogeneous which makes treatment decisions particularly complex. Because of this heterogeneity, sensitive and specific disease biomarkers are required to guide treatment decisions aimed at improving asthma control. Recent studies using multiple-breath-gas-washout techniques have suggested that poor asthma control may be related to ventilation heterogeneity.[2,3] Although the exact pathophysiological abnormalities responsible for ventilation heterogeneity are unclear, these may include regional variations in luminal accumulation of inflammatory cells, mucus, albumin and fibrin, thickening of the airway walls, smooth muscle hyperplasia and hypertrophy, sub-epithelial fibrosis and mucus cell metaplasia.

Ventilation heterogeneity measured using the lung clearance index (LCI), was first described over 65 years ago,[4] and has endured as a biomarker of obstructive lung disease. Ventilation heterogeneity in asthmatics is elevated in comparison to healthy controls,[5-7] is an independent determinant of airway hyperresponsiveness,[8] improves with bronchodilation[5,9] and inhaled corticosteroids[3,10] and worsens during exacerbations.[11] Although this mature body of research strongly supports the notion that LCI is sensitive to

ventilation heterogeneity in asthma, such measurements cannot localize the site of these functional abnormalities.

On the other hand ventilation defects may be regionally identified and visualized using pulmonary imaging methods[12,13] including noble gas magnetic resonance imaging (MRI).[14] It was previously established that in well-controlled asthmatics, focal MRI ventilation defects are associated with worse lung function, increased airway inflammation, airway hyperresponsiveness and greater airway wall thickness.[15] Furthermore, MRI ventilation defects are temporally and spatially persistent,[16] worsen in response to bronchoconstriction and improve following bronchodilation.[17]

Until now however, the relationship between ventilation defects and asthma control and exacerbations has not been ascertained. Therefore, the purpose of this small study in severe asthmatics was to investigate MBNW and MRI measurements of ventilation heterogeneity to better understand their relationship with asthma control. We hypothesized that MRI ventilation defects and the lung clearance index would be correlated, and that both would be biomarkers of poor asthma control. Given the relative lack of therapy options for severe asthma, this is important because regional ventilation defects and the lung clearance index provide endpoints that might be helpful in guiding treatment decisions aimed at improving asthma control.

5.2 Methods

5.2.1 Study Participants and Design

Participants provided written informed consent to a study protocol approved by a local research ethics board, and the study was compliant with the Personal Information Protection and Electronic Documents Act (PIPEDA, Canada) and the Health Insurance Portability and Accountability Act (HIPAA, USA). Patients between 18 and 70 years of age with a diagnosis of severe asthma, according to the Global Initiative of Asthma (GINA) treatment step criteria [18] and under the care of a respirologist were recruited from two academic tertiary care centres (McMaster and Western Universities, Canada).

During a single 2-hour visit, all participants performed pre- and post-bronchodilator spirometry, MBNW and MRI. Asthma-control and quality-of-life was assessed using the

Asthma-Control-Questionnaire (ACQ; 7-item version)[19] and Standardized-Asthma-Quality-of-Life-Questionnaire (AQLQ(S)),[20] respectively. Borg and modified Medical Research Council dyspnea scores were recorded. Clinical history of severe asthma exacerbations, emergency department (ED) visits and hospitalizations for respiratory symptoms were self-reported. As previously defined,[21] a severe asthma exacerbation was a worsening of symptoms requiring treatment with oral or intravenous corticosteroids, OR a doubling of inhaled corticosteroid (ICS) dose for ≥ 3 days, OR any temporary increase in the dosage of oral corticosteroids (OCS) for subjects taking maintenance OCS. Methacholine challenge was performed within 6 months previous to the MRI visit to determine the provocative concentration resulting in a ≥20% decrease in FEV_1 (PC_{20}).

5.2.2 Pulmonary Function Tests and Bronchial Challenge

Spirometry was performed according to American Thoracic Society Guidelines [22] using a *MedGraphics Elite Series* plethysmograph (MedGraphics; St. Paul, MN, USA). For post-bronchodilator measurements, four 100μg doses of *Novo-Salbutamol® HFA* (Teva Novopharm Ltd.; Toronto, ON, Canada) were delivered through a pressurized meter dose inhaler using an *AeroChamber Plus* spacer (Trudell Medical International; London, ON, Canada). All participants were instructed to withhold their short-acting beta-agonists 12 hours prior to their visit (overnight).

5.2.3 Lung Clearance Index

The multiple breath washout manoeuvre was performed using 100% oxygen (O_2) for nitrogen washout and the *ndd EasyOne Pro® LAB* system (ndd Medical Technologies; AG, Zurich, Switzerland) equipped with an ultrasonic flow and molar mass sensor. With the volunteer seated upright and breathing through a mouth piece while wearing nose clips, the washout phase was initiated after several breaths of room air by switching from room air to 100% O_2 at end expiration. Tidal breathing of 100% O_2 was performed until washout was complete (expired N_2 concentration <2.5% of test start). Functional residual capacity (FRC) was calculated from the cumulative volume of expired N_2 divided by the difference between the end-tidal concentration at the start and end of the washout. The cumulative expired volume (CEV) was the cumulative volume of expired air during the washout. The

lung clearance index (LCI) was the number of FRC lung turnovers required to reach N_2 concentration<2.5% of test start and was generated as CEV divided by FRC as previously described.[23] The washout manoeuvre was performed in duplicate and LCI was reported as the mean of two washout manoeuvres.

5.2.4 Magnetic Resonance Imaging

MRI was performed on a whole body 3.0 Tesla Discovery MR750 (General Electric Health Care, Milwaukee, WI, USA) system with broadband imaging capability, as previously described.[24] Subjects were instructed to inhale a gas mixture from a 1.0L Tedlar® bag (Jensen Inert Products; Coral Springs, FL, USA) from FRC, and image acquisition was performed in 8-15s under breath-hold conditions. Conventional ^{1}H MRI was performed 5 minutes prior to hyperpolarized ^{3}He MRI and both methods were previously described.[24]

Quantitative evaluation was performed by a single trained observer (S.S) using custom semi-automated segmentation software generated using MATLAB R2007b (The Mathworks Inc.; Natick, MA, USA), as previously described.[25] ^{3}He MRI ventilation defect percent (VDP) was generated and defined as the ventilation defect volume normalized to the thoracic cavity volume.[25]

5.2.5 Statistical Analysis

Data were tested for normality using the Shapiro-Wilk normality test and when data were not normal, non-parametric tests were performed. Univariate relationships were evaluated using linear regressions (r^2), Pearson correlations (r) and when the data were not normal, Spearman correlations (ρ). Paired two-tailed t-tests and Wilcoxon matched-pairs signed rank tests were used to evaluate the effect of bronchodilator therapy on ventilation heterogeneity. Unpaired t-tests and Mann-Whitney tests were performed to compare ventilation heterogeneity in subjects stratified by ACQ ($\leq$2 or >2) and AQLQ scores ($\geq$5 or <5) and previous 6-month exacerbation history (<1 or $\geq$1). All statistical analyses were performed using GraphPad Prism version 6.02 (GraphPad Software Inc.; La Jolla, CA, USA) and results were considered statistically significant when the probability of making a Type I error was < 5% ($p < 0.05$).

5.3 Results

5.3.1 Study Participants

Table 5-1 provides a summary of demographic and asthma characteristics for 18 participants (6 males/12 females, 46±12 years) with severe asthma. The mean duration of asthma was 31±15 years (range=7-57), pre-bronchodilator FEV_1 was 68±24%$_{pred}$ (range=33-103%$_{pred}$) and pre-bronchodilator FEV_1/FVC was 65±15% (range=35-88%). A participant listing provided in **Table 5-3** (supplement) shows there was abnormal ventilation heterogeneity (both VDP and LCI) for 13 participants and there was normal VDP/LCI or normal VDP/abnormal LCI for five subjects.

Table 5-1 Participant demographics and asthma measurements.

Parameter (±SD)	**Severe Asthma (n=18)**	
	Pre-bronchodilator	**Post-bronchodilator**
Age years	46 (12)	-
Male/Female	6/12	-
Duration of asthma years	31 (15)	-
BMI kg/m^2	29 (5)	-
FEV_1 L	2.2 (0.8)	2.5 (0.8)
FEV_1 %$_{pred}$	68 (24)	75 (26)
FVC L	3.5 (1.0)	3.6 (1.0)
FVC %$_{pred}$	83 (19)	88 (17)
FEV_1/FVC %	65 (15)	68 (16)
PC_{20} mg/mL	1.4 (2.8)*	-
Lung clearance index	10.5 (3.0)	9.5 (2.6)†
Ventilation defect percent %	12 (11)	8 (8)

SD=standard deviation; BMI=body mass index; FEV_1=forced expiratory volume in 1 second; %$_{pred}$=percent predicted; FVC=forced vital capacity; PC_{20}=methacholine concentration for 20% decrease in FEV_1. *n=5; †n=17

Asthma medications and control parameters are summarized in **Table 5-2**. A participant listing of these data is also provided in **Table 5-4** (supplement). Despite receiving medium-to-high dose inhaled corticosteroids (ICS) and long-acting beta-agonists (GINA treatment step 4-5),[18] all 18 participants had poorly-controlled disease as evidenced by mean ACQ score (2.3±0.9, range=1.0-4.3). Eight (44%) participants were prednisone-dependent (dosage ranging from 2.5 to 50 mg/day). One or more severe asthma exacerbations were

reported by nine (50%) and 15 (83%) participants in the previous 6- and 12-months respectively.

Table 5-2 Asthma medication and control.

	Severe Asthma (n=18)
Asthma Medications	
Inhaled corticosteroid n (%)	18 (100%)
Long-acting β_2-agonist n (%)	18 (100%)
Long-acting anticholinergic n (%)	7 (39%)
Oral corticosteroid n (%)	8 (47%)
Leukotriene receptor antagonist n (%)	9 (53%)
Anti-immunoglobulin E n (%)	1 (6%)
Asthma Control	
ACQ score*	2.3 (0.9)
AQLQ total score*	4.6 (1.2)
mMRC dyspnea score*	1.3 (1.0)
Borg dyspnea score*	2.5 (2.3)
Severe exacerbation previous 6 months n (%)	9 (50%)
Severe exacerbation previous year n (%)	15 (83%)
ED visit previous 6 months n (%)	1 (6%)
ED visit previous year n (%)	4 (22%)
Hospitalization previous 6 months n (%)	0 (0%)
Hospitalization previous year n (%)	1 (6%)

Values are mean (±SD) except when indicated otherwise. ACQ=asthma control questionnaire; AQLQ=asthma quality-of-life questionnaire; mMRC=modified Medical Research Council; ED=emergency department. *n=16

5.3.2 Ventilation Heterogeneity

Figure 5-1 shows pre-bronchodilator coronal ^{3}He MRI ventilation (in blue) co-registered to ^{1}H anatomical MRI (in grey-scale) for six representative participants. As shown qualitatively in **Figure 5-1**, there was a greater number and volume of ^{3}He MRI ventilation abnormalities in participants with worse ACQ. For example, in subject S17 there was a relatively homogeneous ventilation pattern, normal LCI and relatively good asthma control whereas for subjects S16, S06, S13 and S04, there was qualitatively abnormal ventilation that was concomitant with worse asthma control.

Table 5-1 shows that both VDP (pre-salbutamol=12±11%, post-salbutamol=8±8%, p=0.008) and LCI (pre-salbutamol=10.5±3.0, post-salbutamol=9.5±2.6, p=0.02) significantly improved following bronchodilation. One participant (S12) could not

complete the post-bronchodilator MBNW manoeuvre due to fatigue and was excluded from this evaluation.

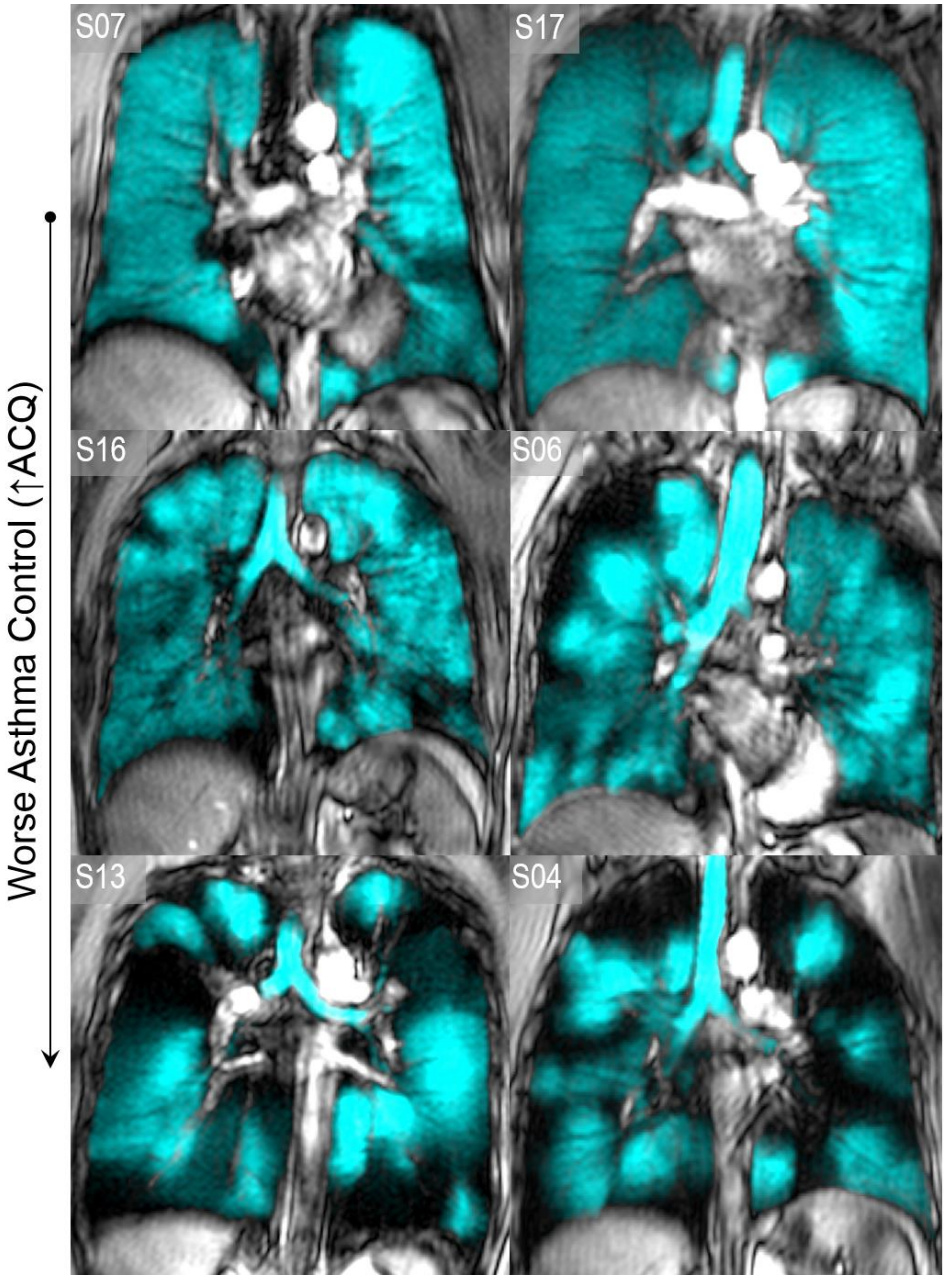

Figure 5-1 Hyperpolarized ^{3}He MRI of representative patients with severe asthma. Centre coronal slice ^{3}He MRI ventilation in blue co-registered to anatomical ^{1}H MRI in grey-scale for six representative severe asthmatics. S07: 55 year-old female, FEV_1=77%$_{pred}$, ACQ=1.4, LCI=9.7, VDP=2%; S17: 39 year-old female, FEV_1=66%$_{pred}$, ACQ=1.7, LCI=6.7, VDP=3%; S16: 48 year-old male, FEV_1=78%$_{pred}$, ACQ=2.3, LCI=8.6, VDP=8%; S06: 45 year-old male, FEV_1=34%$_{pred}$, ACQ=2.7, LCI=11.5, VDP=14%; S13: 56 year-old male, FEV_1=34%$_{pred}$, ACQ=3.1, LCI=17.5, VDP=33%; S04: 60 year-old female, FEV_1=47%$_{pred}$, ACQ=4.3, LCI=14.0, VDP=35%.

5.3.3 Ventilation Heterogeneity and Asthma Control

Figure 5-2 shows VDP and LCI in participants stratified by ACQ score (ACQ≤2, n=7 and ACQ>2, n=9), AQLQ score (AQLQ≥5, n=7 and AQLQ<5, n=9) and by the number of self-reported exacerbations in the past 6 months (exacerbations <1, n=9 and exacerbations ≥1, n=9). As shown in **Figure 5-2A**, there was significantly worse VDP (18±13% versus 6±5%; p=0.04), but not LCI (11.2±3.6 versus 9.4±2.4; p=0.3), in the subgroup of asthmatics with ACQ scores >2. There was also significantly worse VDP (18±13% versus 6±5%; p=0.04), but not LCI (11.4±3.3 versus 9.1±2.6; p=0.2), in the subgroup of asthmatics with AQLQ scores <5. **Figure 5-2C** also shows that there was a trend towards worse VDP (17±13% versus 8±5%; p=0.053), but not LCI (11.2±3.8 versus 9.7±1.8; p=0.3), in asthmatics reporting ≥1 exacerbation in the past 6-months. There were 15 subjects with exacerbations in the previous 12-months (VDP=13±12%; LCI=10.3±3.2).

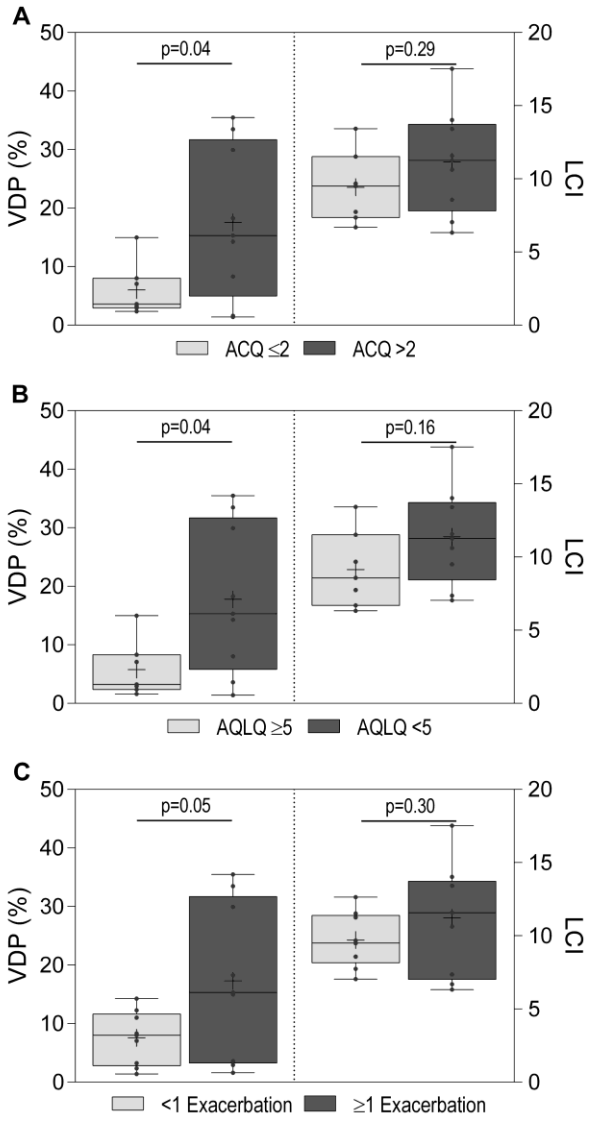

Figure 5-2 Ventilation heterogeneity stratified by ACQ and AQLQ scores and self-reported exacerbations.

A) Significantly worse VDP (>2 ACQ, VDP=18±13%; ≤2 ACQ, VDP=6±5, p=0.04), but not LCI (>2 ACQ, LCI=11.2±3.6; ACQ≤2, LCI=9.4±2.4, p=0.29) for subjects with ACQ >2.

B) Significantly worse VDP (AQLQ<5, VDP=18±13; AQLQ≥5, VDP=6±5, p=0.04), but not LCI (AQLQ<5, LCI=11.4±3.3; AQLQ≥5, LCI= 9.1±2.6, p=0.16), for subjects with AQLQ total scores <5.

C) There was a trend towards greater VDP (exacerbations ≥1, VDP=17±13%; exacerbations<1, VDP=8±5%; p=0.053), but not LCI (exacerbations ≥1, LCI=11.2±3.8 exacerbations<1, LCI= 9.7±1.8; p=0.3), for subjects with ≥1 exacerbation in past 6-months.

Box-and-whiskers plots show minimum, 25th percentile, median, 75th percentile, and maximum with each individual value superimposed on the graph. += mean. ACQ=asthma control questionnaire; AQLQ=asthma quality-of-life questionnaire; LCI=lung clearance index; VDP=ventilation defect percent.

5.3.4 Relationships

Given the different results for the ACQ and AQLQ subgroups with VDP and LCI measurements, we also evaluated the bilateral relationships for LCI and VDP and their post-salbutamol changes. **Figure 5-3** qualitatively shows some of these relationships in individual participants. For example, for subjects S11, S03 and S15, there was significantly improved VDP, with minimal post-salbutamol change in LCI. In contrast, for subjects S02, S13 and S05, there was significantly improved LCI with a minimal post-salbutamol change in VDP. **Figure 5-4A** shows that there were strong VDP-LCI correlations pre- ($r=0.86$, $r^2=0.74$, $p<0.0001$) and post-bronchodilator ($r=0.93$, $r^2=0.86$, $p<0.0001$). However, as shown in **Figure 5-4B**, the post-bronchodilator change in VDP was not correlated with the post-bronchodilator change in LCI ($r=0.44$, $r^2=0.01$, $p=0.08$). As shown in **Figure 5-4C and D**, VDP ($r=0.62$, $r^2=0.38$, $p=0.01$) was correlated with ACQ score and LCI ($r=0.49$, $r^2=0.24$, $p=0.052$) showed a similar trend. VDP and LCI were not related to AQLQ score (VDP: $r=-0.34$, $r^2=0.11$, $p=0.20$; LCI: $r=-0.22$, $r^2=0.05$, $p=0.40$) or exacerbations in the past 6 (VDP: $r=0.31$, $r^2=0.02$, $p=0.21$; LCI: $r=0.08$, $r^2=0.0001$, $p=0.77$) and 12-months (VDP: $r=0.03$, $r^2=0.003$, $p=0.92$; LCI: $r=-0.21$, $r^2=0.06$, $p=0.41$).

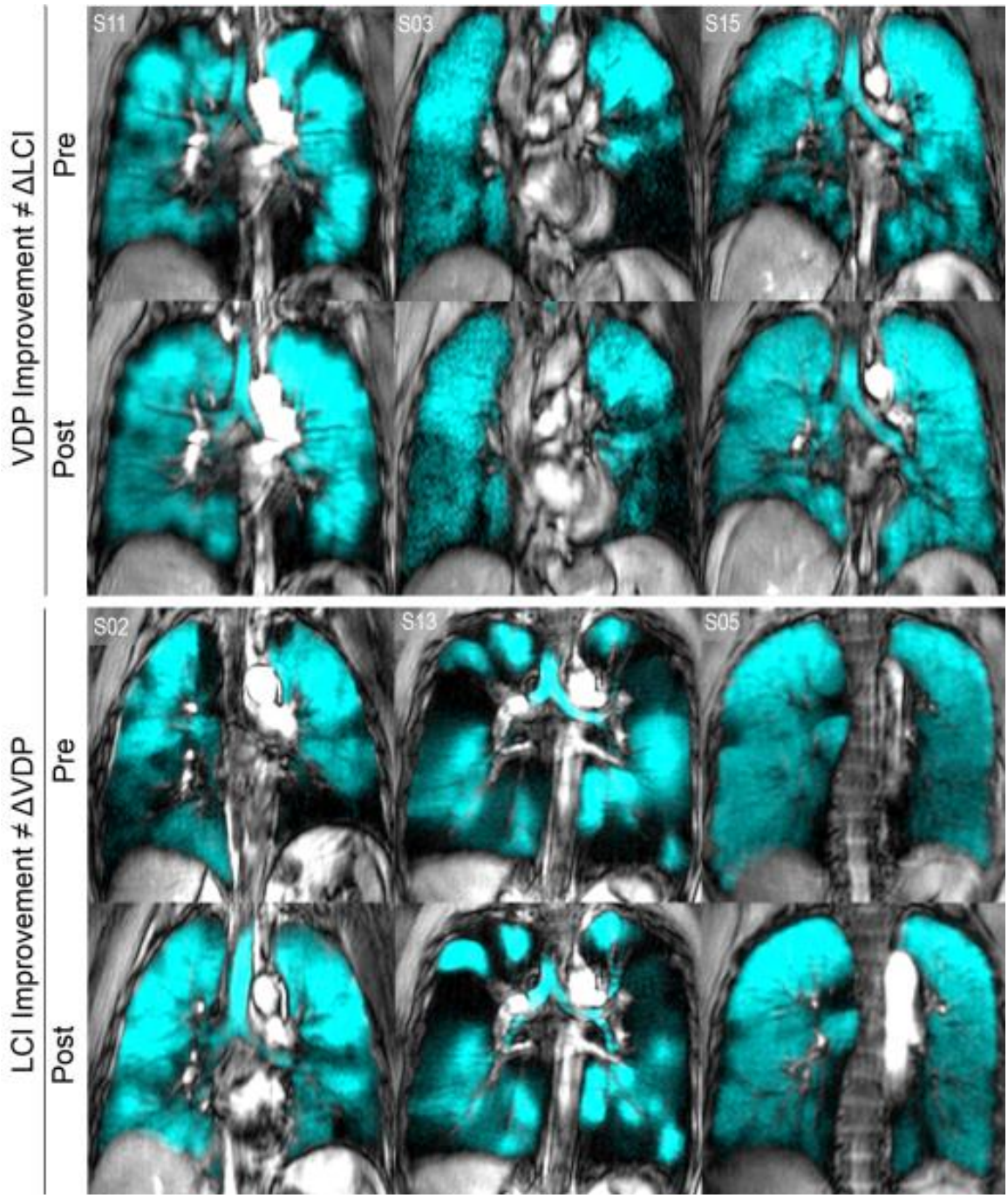

Figure 5-3 Pre- and post-bronchodilator ^{3}He ventilation MRI.
S11: 40 year-old female, ACQ=2.3, ΔLCI=-0.8, ΔVDP=-11%; S03: 61 year-old male, ACQ=2.1, ΔLCI=-1.4, ΔVDP=-13; S15: 42 year-old male, ACQ=1.4, ΔLCI=0.6, ΔVDP=-4%; S02: 67 year-old male, ACQ=NA, ΔLCI=-3.8, ΔVDP=-5%; S13: 56 year-old male, ACQ=3.1, ΔLCI=-2.1, ΔVDP=-5%; S05: 38 year-old female, ACQ=1.9, ΔLCI=-2.2, ΔVDP=-1%.

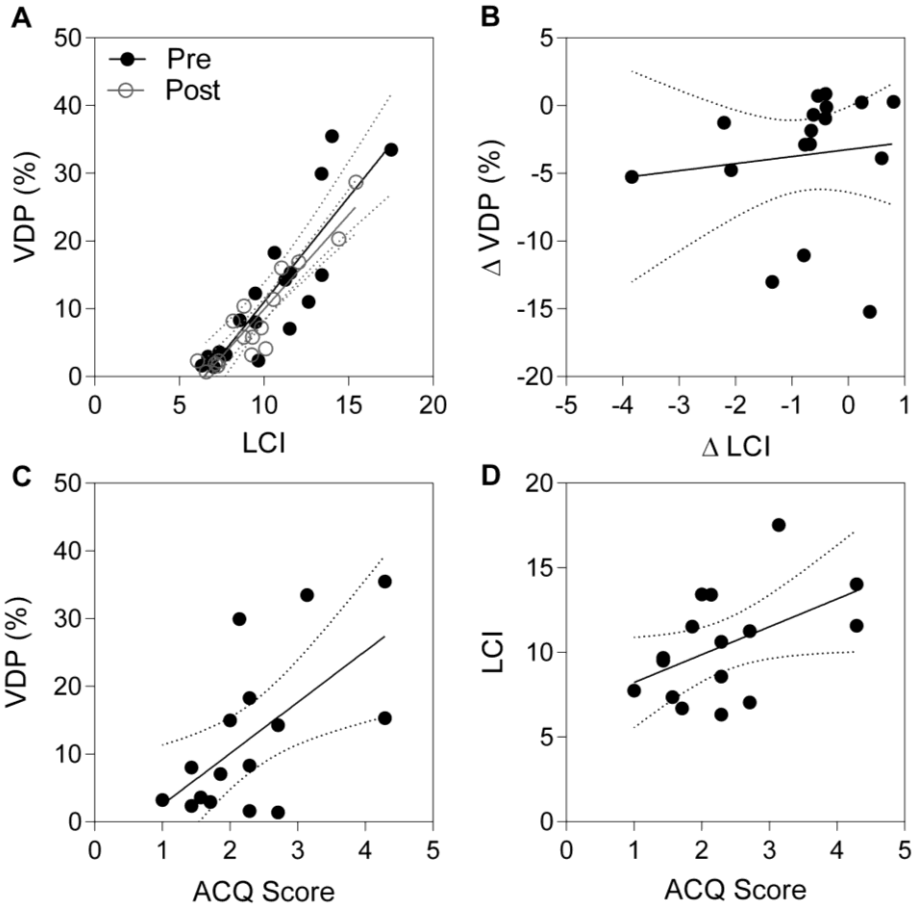

Figure 5-4 Relationship for ventilation heterogeneity and asthma control.

A) VDP was significantly correlated with LCI pre- (r=0.86, r^2=0.74, p<0.0001, y=3.1x-20.0) and post-bronchodilator (r=0.93, r^2=0.86, p<0.0001).
B) The change in VDP and LCI post-bronchodilator was not correlated (r=0.44, r^2=0.01, p=0.08).
C) VDP was significantly correlated with ACQ (r=0.62, r^2=0.38, p=0.01).
D) There was a trend for an LCI–ACQ correlation (r=0.49, r^2=0.24, p=0.052).

Dotted lines=95% confidence intervals; ACQ=asthma control questionnaire; LCI=lung clearance index; VDP=ventilation defect percent.

5.4 Discussion

In an endeavour to answer the question: *Are MRI ventilation defects related to asthma control?*, we evaluated MRI and LCI measurements in 18 severe asthmatics. We observed: 1) abnormal VDP and LCI were strongly correlated but there were different responses to salbutamol, 2) there was significantly worse VDP but not LCI in asthmatics with an ACQ score >2 and AQLQ score <5, which was supported by a significant VDP-ACQ correlation,

and, 3) there was a trend towards greater VDP, but not LCI, in asthmatics with ≥1 exacerbation in the past 6-months.

To our knowledge, this is the first direct evaluation of MRI and LCI ventilation heterogeneity and their relationship with asthma control. Similar to previous imaging[17,26] and multiple-breath washout studies[27] we observed abnormally heterogeneous ventilation that improved post-bronchodilator. The strong correlation for LCI and VDP was not surprising. The fact that there was no relationship for the post-bronchodilator change in VDP and LCI was not expected, but may be explained by a number of mechanistic differences in the measurements themselves.

The temporal resolution of both approaches relative to the time constants for lung segment filling and emptying are important to consider. For example, inert gas washout measurements are made over a time-course of many minutes of normal tidal breathing and based on the time needed to exchange N_2 with O_2 in lung regions accessible to inhaled gas. In contrast, MRI ventilation defects are typically measured during a single 8-10s inhalation breath-hold; hence, inhaled-gas MRI provides a rapid visual snapshot of where the inhaled gas goes when inhaled from FRC. In the case of airway narrowing or gas trapping that are both common in severe asthma, long time constants for lung filling and emptying are expected and this may explain some of the differences for VDP and LCI observed here.

In addition to temporal resolution differences, there may be differences in the apparent spatial resolution of the MBNW and MRI methods used. In principle, LCI measurements may be influenced by any or all of the conducting and acinar lung zones.[27] For ventilation MRI, there is somewhat coarse spatial resolution (3x3x15mm) and this may result in an underestimation of very small ventilation defects. Supporting this notion, subjects S07 and S14 reported relatively well-controlled disease (ACQ=1.4 and 1.0) but abnormal LCI and relatively homogeneous MRI ventilation. Another explanation, previously proposed,[27] suggests that even small ventilation defects may increase LCI well beyond the upper-limit of normal, resulting in an overestimation of disease severity. Supporting this view, subject 07 had an abnormal LCI (9.7) and only a single small hypo-ventilated region (VDP=2%). Importantly, this 55 yr old female was prescribed oral prednisone (7.5mg/day) and ICS (Budesonide > 1000μg), and was relatively well-controlled (ACQ=1.4). We also observed

post-bronchodilator imaging improvements in patients in whom LCI did not change, such as in subject S04. This 60 year old female reported very poor control (ACQ=4.3) and highly heterogeneous ventilation (VDP=35%; LCI=14.0) despite high-dose OCS maintenance therapy (prednisone 50mg/day) and ICS (Fluticasone propionate dose>1000μg). Similar VDP responses have been reported in COPD patients with little or no bronchodilator reversibility measured using FEV_1.[28]

The most important observation stemming from this study was the finding of significantly worse VDP in asthmatics with ACQ>2 and AQLQ<5 and a trend toward worse VDP in asthmatics with more frequent exacerbations. These findings were not observed using LCI measurements, perhaps because of the small sample size and/or because LCI is a less sensitive measure of the underlying pathophysiology responsible for asthma control. This novel imaging result was also supported by a significant relationship for VDP (and a trend for a significant relation for LCI) with ACQ score. It is worth noting that a previous ventilation imaging study using single photon emission computerized tomography (SPECT), reported no relationship for ACQ score and ventilation.[29] This discordant result may stem from the inherently low spatial resolution of SPECT or small sample size, or perhaps because the asthmatics in the previous study were well-controlled. Previous seminal studies point to the clinical importance of airflow obstruction,[30] airway inflammation,[31] respiratory system reactance[32] and inert-gas washout ventilation heterogeneity measurements of asthma.[2,3] Yet, some of these measurements underestimate asthma pathophysiology because of their relative insensitivity to the peripheral airway abnormalities directly responsible for asthma symptoms and control. In view of the limitations of conventional clinical asthma measurements, we think our results strongly support the use of pulmonary MRI in clinical research and in the management of severe asthmatics in whom control is difficult to achieve.

We recognize a number of study limitations including the small number of study participants. However, pulmonary imaging measurements are quite sensitive and therefore significant differences may be detected using small sample sizes. Nonetheless, caution should be exercised in generalizing our results to a general asthma population. We also acknowledge that asthma patients were recruited from two major tertiary care centres, so FeNO and sputum inflammometry were not available for the majority of patients. If these

were available, we could try to tease out the relative contribution of luminal inflammation to ventilation heterogeneity and asthma control. Furthermore, we did not (for logistical reasons) evaluate a comparator group of well-controlled asthmatics or asthmatics with more moderate disease. Because of this, we could not ascertain the relative contribution of asthma severity to ventilation heterogeneity in this study, but this relationship was previously explored in well-controlled patients with mild to moderate asthma.[15] It is noteworthy that there was no difference in ventilation heterogeneity for participants prescribed oral prednisone versus those who were not prednisone-dependent. Postural effects should also be considered when comparing MRI and MBNW measurements of ventilation heterogeneity because imaging was performed supine, whereas MBNW was performed upright. In one previous study, gas trapping was increased in supine asthmatic children but this was not the case for MBNW ventilation heterogeneity measurements.[33] Regardless, to mitigate and minimize postural effects including atelectasis, imaging was completed within 5 minutes, limiting the time that patients remained supine, which limits atelectasis.[34]

While there is strong evidence that poor asthma control is associated with an increased risk for future severe asthma events[35] and exacerbations,[36] biomarkers that identify the source and regional location of poor control are generally lacking and many are not readily available except in highly specialized care centres, beyond the reach of the vast majority of asthma patients. In this context, we note that MBNW biomarkers are more universally available and previously revealed the efficacy of aerosolized ultrafine steroid particles in a subset of asthma patients with abnormal acinar airways.[10] Moreover, emerging biomarkers of airway inflammation have been proposed[37] and used as therapy targets to significantly decrease asthma exacerbations.[38-40] The results of our study argue for the continued development and use of novel and conventional ventilation heterogeneity biomarkers and measurements of asthma.

In conclusion, in a small group of poorly-controlled severe asthmatics, MRI ventilation defects were significantly worse in the subgroup of patients with worse asthma control and quality-of-life. Hence, regional ventilation defects may be considered as intermediate endpoints of asthma that can be used to evaluate therapies in relatively small studies that target improved asthma control and quality-of-life.

5.5 References

(1) Partridge MR, van der Molen T, Myrseth SE, *et al.* Attitudes and actions of asthma patients on regular maintenance therapy: the INSPIRE study. *BMC Pulm Med* 2006;6:13.

(2) Farah CS, King GG, Brown NJ, *et al.* The role of the small airways in the clinical expression of asthma in adults. *J Allergy Clin Immunol* 2012;129:381-87.

(3) Farah CS, King GG, Brown NJ, *et al.* Ventilation heterogeneity predicts asthma control in adults following inhaled corticosteroid dose titration. *J Allergy Clin Immunol* 2012;130:61-8.

(4) Becklake MR. A new index of the intrapulmonary mixture of inspired air. *Thorax* 1952;7:111-6.

(5) Gustafsson PM. Peripheral airway involvement in CF and asthma compared by inert gas washout. *Pediatr Pulmonol* 2007;42:168-76.

(6) Zwitserloot A, Fuchs SI, Muller C, *et al.* Clinical application of inert gas Multiple Breath Washout in children and adolescents with asthma. *Respir Med* 2014;108:1254-9.

(7) Macleod KA, Horsley AR, Bell NJ, *et al.* Ventilation heterogeneity in children with well controlled asthma with normal spirometry indicates residual airways disease. *Thorax* 2009;64:33-7.

(8) Downie SR, Salome CM, Verbanck S, *et al.* Ventilation heterogeneity is a major determinant of airway hyperresponsiveness in asthma, independent of airway inflammation. *Thorax* 2007;62:684-9.

(9) Verbanck S, Schuermans D, Paiva M, *et al.* Nonreversible conductive airway ventilation heterogeneity in mild asthma. *J Appl Physiol* 2003;94:1380-6.

(10) Verbanck S, Schuermans D, Paiva M, *et al.* The functional benefit of anti-inflammatory aerosols in the lung periphery. *J Allergy Clin Immunol* 2006;118:340-6.

(11) Thompson BR, Douglass JA, Ellis MJ, *et al.* Peripheral lung function in patients with stable and unstable asthma. *J Allergy Clin Immunol* 2013;131:1322-8.

(12) King GG, Eberl S, Salome CM, *et al.* Airway closure measured by a technegas bolus and SPECT. *Am J Respir Crit Care Med* 1997;155:682-88.

(13) Venegas JG, Winkler T, Musch G, *et al.* Self-organized patchiness in asthma as a prelude to catastrophic shifts. *Nature* 2005;434:777-82.

(14) Altes TA, Powers PL, Knight-Scott J, *et al.* Hyperpolarized ^{3}He MR lung ventilation imaging in asthmatics: preliminary findings. *J Magn Reson Imaging* 2001;13:378-84.

(15) Svenningsen S, Kirby M, Starr D, *et al.* What are ventilation defects in asthma? *Thorax* 2014;69:63-71.

(16) de Lange EE, Altes TA, Patrie JT, *et al.* Changes in regional airflow obstruction over time in the lungs of patients with asthma: evaluation with ^{3}He MR imaging. *Radiology* 2009;250:567-75.

(17) Samee S, Altes T, Powers P, *et al.* Imaging the lungs in asthmatic patients by using hyperpolarized helium-3 magnetic resonance: assessment of response to methacholine and exercise challenge. *J Allergy Clin Immunol* 2003;111:1205-11.

(18) Global Initiative for Asthma: Global Strategy for Asthma Management and Prevention, 2015. http://www.ginasthma.org (accessed July 2015).

(19) Juniper EF, O'Byrne PM, Guyatt GH, *et al.* Development and validation of a questionnaire to measure asthma control. *Eur Respir J* 1999;14:902-7.

(20) Juniper EF, Buist AS, Cox FM, *et al.* Validation of a standardized version of the Asthma Quality of Life Questionnaire. *Chest* 1999;115:1265-70.

(21) Wechsler ME, Laviolette M, Rubin AS, *et al.* Bronchial thermoplasty: Long-term safety and effectiveness in patients with severe persistent asthma. *J Allergy Clin Immunol* 2013;132:1295-302.

(22) Miller MR, Hankinson J, Brusasco V, *et al.* Standardisation of spirometry. *Eur Respir J* 2005;26:319-38.

(23) Robinson PD, Latzin P, Verbanck S, *et al.* Consensus statement for inert gas washout measurement using multiple- and single- breath tests. *Eur Respir J* 2013;41:507-22.

(24) Parraga G, Ouriadov A, Evans A, *et al.* Hyperpolarized 3He ventilation defects and apparent diffusion coefficients in chronic obstructive pulmonary disease: preliminary results at 3.0 Tesla. *Invest Radiol* 2007;42:384-91.

(25) Kirby M, Heydarian M, Svenningsen S, *et al.* Hyperpolarized ^{3}He magnetic resonance functional imaging semiautomated segmentation. *Acad Radiol* 2012;19:141-52.

(26) de Lange EE, Altes TA, Patrie JT, *et al.* Evaluation of asthma with hyperpolarized helium-3 MRI: correlation with clinical severity and spirometry. *Chest* 2006;130:1055-62.

(27) Verbanck S, Paiva M, Schuermans D, *et al.* Relationships between the lung clearance index and conductive and acinar ventilation heterogeneity. *J Appl Physiol* 2012;112:782-90.

(28) Kirby M, Mathew L, Heydarian M, *et al.* Chronic obstructive pulmonary disease: quantification of bronchodilator effects by using hyperpolarized ^{3}He MR imaging. *Radiology* 2011;261:283-92.

(29) Farrow CE, Salome CM, Harris BE, *et al.* Airway closure on imaging relates to airway hyperresponsiveness and peripheral airway disease in asthma. *J Appl Physiol* 2012;113:958-66.

(30) Aburuz S, McElnay J, Gamble J, *et al.* Relationship between lung function and asthma symptoms in patients with difficult to control asthma. *J Asthma* 2005;42:859-64.

(31) Sippel JM, Holden WE, Tilles SA, *et al.* Exhaled nitric oxide levels correlate with measures of disease control in asthma. *J Allergy Clin Immunol* 2000;106:645-50.

(32) Kelly VJ, Sands SA, Harris RS, *et al.* Respiratory system reactance is an independent determinant of asthma control. *J Appl Physiol* 2013;115:1360-9.

(33) Gustafsson PM. Pulmonary gas trapping increases in asthmatic children and adolescents in the supine position. *Pediatr Pulmonol* 2003;36:34-42.

(34) Mata J, Altes T, Knake J, *et al.* Hyperpolarized 3He MR imaging of the lung: effect of subject immobilization on the occurrence of ventilation defects. *Acad Radiol* 2008;15:260-4.

(35) Sullivan SD, Wenzel SE, Bresnahan BW, *et al.* Association of control and risk of severe asthma-related events in severe or difficult-to-treat asthma patients. *Allergy* 2007;62:655-60.

(36) Meltzer EO, Busse WW, Wenzel SE, *et al.* Use of the Asthma Control Questionnaire to predict future risk of asthma exacerbation. *J Allergy Clin Immunol* 2011;127:167-72.

(37) Nair P, Hargreave FE. Measuring bronchitis in airway diseases: clinical implementation and application: Airway hyperresponsiveness in asthma: its measurement and clinical significance. *Chest* 2010;138:38S-43S.

(38) Nair P, Pizzichini MM, Kjarsgaard M, *et al.* Mepolizumab for prednisone-dependent asthma with sputum eosinophilia. *N Engl J Med* 2009;360:985-93.

(39) Green RH, Brightling CE, McKenna S, *et al.* Asthma exacerbations and sputum eosinophil counts: a randomised controlled trial. *Lancet* 2002;360:1715-21.

(40) Jayaram L, Pizzichini MM, Cook RJ, *et al.* Determining asthma treatment by monitoring sputum cell counts: effect on exacerbations. *Eur Respir J* 2006;27:483-94.

5.6 Supplementary Material

Table 5-3S Participant listing of demographic and other measurements.

	Demographics			Questionnaires and Exacerbation History									Spirometry			Ventilation heterogeneity	
	Age	Sex	BMI	Duration	ACQ	AQLQ Scores		Dyspnea Scores		Exacerbations	ED visits	Hospitalizations	FEV_1	FVC	FEV_1/FVC	LCI	VDP
Subject	(yrs)	(M/F)	(kg/m^2)	(yrs)	Score	Tota	Acti	mMRC	Borg	(n)*	(n)*	(n)*	Pre/Post(L)	Pre/Post(L)	Pre/Post(%)	Pre/Post	Pre/Post(%)
001	34	F	40	16	-	-	-	-	-	0/2	0/0	0/0	2.2/2.5	3.0/3.2	74/80	9.5/8.8	12/10
002	67	M	28	7	-	-	-	-	-	0/0	0/0	0/0	3.1/3.4	4.8/5.0	66/68	12.6/8.8	11/6
003	61	M	33	7	2.1	4.6	4.6	0.0	4.0	1/3	0/0	0/0	2.7/3.4	5.0/5.8	54/59	13.4/12.1	30/17
004	60	F	33	39	4.3	3.2	2.7	3.0	9.0	2/4	0/2	0/0	1.0/0.9	2.1/2.0	46/46	14.0/14.4	35/20
005	38	F	30	36	1.9	5.9	6.0	1.0	1.0	0/1	0/0	0/0	1.4/1.6	1.7/2.0	82/79	11.5/9.3	7/6
006	45	M	25	44	2.7	4.7	4.6	1.0	1.0	0/0	0/0	0/0	1.5/1.6	3.3/3.4	44/47	11.5/10.6	14/11
007	55	F	33	20	1.4	5.0	5.1	1.0	3.0	0/1	0/0	0/0	2.1/2.3	2.9/3.1	71/76	9.7/9.3	2/3
008	47	F	30	34	2.3	5.3	5.3	2.0	2.0	2/5	1/1	0/0	3.0/3.0	3.7/3.6	80/83	6.3/7.1	2/2
009	21	F	20	18	2.7	3.1	3.6	2.0	5.0	0/5	0/0	0/0	3.4/3.5	3.8/3.7	88/94	7.0/7.3	1/2
010	45	F	31	41	1.6	4.0	4.9	0.0	0.5	4/18	0/0	0/0	3.0/3.3	3.8/3.8	78/86	7.4/6.6	4/1
011	40	F	29	27	2.3	4.8	4.7	1.0	1.0	6/12	0/0	0/0	2.1/2.4	3.3/3.4	65/72	10.6/9.8	18/7
012	31	F	37	28	2.0	5.8	5.8	2.0	1.0	3/4	0/3	0/1	0.9/1.4	2.3/3.1	42/46	13.4/NA	15/5
013	56	M	25	55	3.1	4.2	4.4	-	-	2/3	0/0	0/0	1.5/1.5	4.4/4.2	35/37	17.5/15.5	33/29
014	44	F	27	23	1.0	5.6	5.6	1.0	0.5	0/1	0/0	0/0	2.9/3.0	3.8/3.9	74/79	7.7/7.3	3/2
015	42	M	33	28	1.4	4.6	5.5	1.0	2.0	0/0	0/0	0/0	2.7/3.1	4.0/4.4	67/71	9.5/10.1	8/4
016	48	M	30	46	2.3	5.5	6.4	0.0	3.0	0/1	0/0	0/0	2.9/3.2	4.2/4.4	69/72	8.6/8.2	8/8
017	39	F	22	36	1.7	6.1	6.2	1.0	0.5	5/7	0/0	0/0	2.2/2.4	4.0/3.9	56/62	6.7/6.1	3/2
018	59	F	23	57	4.3	1.7	2.4	3.0	4.0	4/8	0/1	0/0	1.4/1.6	1.9/2.7	71/58	11.6/11.0	15/16
Mean	46	12F/	29	31	2.3	4.6	4.9	1.3	2.5	9(50%)/	1(6%)/	0(0%)/	2.2(0.8)/	3.5(1.0)/	65(15)/	10.5(3.0)/	12(11)/
(±SD)	(12)	6M	(5)	(15)	(0.9)	(1.2)	(1.2)	(1.0)	(2.3)	15(83%)	4(22%)	1(6%)	2.5(0.8)	3.6(1.0)	68(16)	9.5(2.7)	8(8)

SD=standard deviation; M=Male; F=Female; BMI=body mass index; ACQ=asthma control questionnaire; AQLQ=asthma quality-of-life questionnaire; Tota=Total; Acti=Activity; mMRC=modified Medical Research Council; ED=emergency department; FEV_1=forced expiratory volume in 1 second; BD=bronchodilator; FVC=forced vital capacity; LCI=lung clearance index; VDP=ventilation defect percent. *in previous 6 months/in previous year.

Table 5-4S Participant listing of asthma medications.

	SABA	LABA		LAAC		ICS		OCS		LTRA		Anti-IgE	
Subject	Generic	Generic	Dose(µg/d)	Generic	Dose(µg/d)	Generic	Dose(µg/d)	Generic	Dose(mg/d)	Generic	Dose(mg/d)	Generic	Dose(mg)
001	Salbutamol	Formoterol	12	--	--	Budesonide	400	Prednisone	4	--	--	--	--
002	Salbutamol	Formoterol	24	--	--	Budesonide	800	Prednisone	12.5	--	--	--	--
003	Salbutamol	Formoterol	24	Tiotropium	18	Budesonide	800	Prednisone	20	Montelukast	10	--	--
004	Salbutamol	Salmeterol	100	Tiotropium	18	Fluticasone	2500	Prednisone	50	Montelukast	10	--	--
005	Salbutamol	Formoterol	36	--	--	Budesonide/Beclometasone	1200/800	Prednisone	2.5	--	--	--	--
006	Salbutamol	Formoterol	20	Tiotropium	18	Mometasone furoate/Fluticasone	800/1000	--	--	Montelukast	10	--	--
007	Salbutamol	Formoterol	24	Tiotropium	18	Budesonide	1600	Prednisone	7.5	--	--	--	--
008	Salbutamol	Salmeterol	100	--	--	Fluticasone	1000	--	--	Montelukast	10	--	--
009	Terbutaline	Formoterol	24	--	--	Budesonide	800	--	--	Montelukast	10	--	--
010	Salbutamol	Salmeterol	100	--	--	Fluticasone	1500	--	--	Montelukast	10	--	--
011	Salbutamol	Formoterol	24	--	--	Budesonide/Ciclesonide	800/800	Prednisone	7.5	Montelukast	10	--	--
012	Salbutamol	Salmeterol	100	Tiotropium	18	Fluticasone/Ciclesonide	1000/400	Prednisone	3	Montelukast	10	--	--
013	Salbutamol	Salmeterol	100	Tiotropium	18	Fluticasone	1000	--	--	--	--	--	--
014	Salbutamol	Formoterol	24	--	--	Budesonide	800	--	--	--	--	--	--
015	Salbutamol	Formoterol	24	--	--	Budesonide	1200	--	--	--	--	--	--
016	Salbutamol	Formoterol	24	--	--	Budesonide/Ciclesonide	800/800	--	--	--	--	Omalizumab	150
017	Salbutamol	Formoterol	24	--	--	Budesonide	800	--	--	Montelukast	10	--	--
018	Salbutamol	Formoterol	20	Aclidinium bromide	800	Mometasone furoate/Ciclesonide	800/800	--	--	--	--	--	--

SABA=Short-acting beta-agonist; LABA=Long-acting beta-agonist; LAAC=Long-acting anticholinergics; ICS=Inhaled Corticosteroids; OCS=Oral corticosteroids; LTRA=Leukotriene Receptor Antagonists; Anti-IgE=Anti-immunoglobulin E.

CHAPTER 6

6 Conclusions and Future Directions

The final chapter of this thesis revisits our rationale and research objectives and provides a summary of the important findings and conclusions of Chapters 2-5. Subsequently, study specific limitations, general limitations and potential solutions are presented. Finally, a roadmap for future studies in asthma motivated by the work presented in this thesis will be outlined.

6.1 Overview of Rationale and Research Questions

The forced expiratory volume in one second (FEV_1) currently plays an important role in the diagnosis and management of asthma; and it is also universally used as a primary endpoint of lung function in the majority of asthma clinical trials.[1,2] However, FEV_1 is a global measurement made at the mouth that cannot be used to ascertain regional lung function and it is relatively insensitive to subtle changes and peripheral airway pathology in asthma.[3] For decades, the concept of regionally heterogeneous airway abnormalities in asthma has been acknowledged. This regional heterogeneity was first noted in cadavers using post mortem *ex vivo* gross sections and histology.[4] Shortly after, single-breath and multiple-breath washout studies in living patients were also indicative of ventilation heterogeneity in asthma, but due to the limitations of this technique, the regional site of functional abnormalities could not be ascertained.[5] Accordingly, beyond specialized academic centres, it has been difficult to investigate asthmatics based on the suggested regional nature of their underlying pathology. There has therefore been an urgent need for non-invasive and quantitative imaging methods to regionally evaluate asthma.

In response to this demand, numerous imaging methods have been developed and are currently available to non-invasively evaluate asthma regionally,[6] however, they are not all well-suited for serial and longitudinal investigations. While CT is widely available and provides high spatial and temporal resolution images of lung structure[7,8] and function,[9] it is burdened by radiation exposure, a particular concern when evaluating asthmatic children and young adults. Similarly, nuclear medicine methods are burdened by ionizing radiation exposure and are further limited by relatively poor spatial resolution.[10-12]

In contrast, functional MRI using hyperpolarized ^{3}He and ^{129}Xe is not limited by radiation exposure. The recent development of this approach has demonstrated promise for functional imaging of asthma[13] as it provides an opportunity to visualize, with high spatial and temporal resolution, those areas of the lung that participate in gas distribution and those that do not. In healthy young adults, inhalation of hyperpolarized gas results in homogeneous signal suggesting that all areas of the lung are participating equally in ventilation.[14-17] In contrast, characteristic ventilation defects are observed in asthma, corresponding to areas of the lung that are not ventilated within the time-course of a breath-hold scan.[13,18-27] Previous work using this technique provides a strong foundation for its use in asthma research and patient care; however, a major drawback is that the clinical and physiological meaning of MRI-derived ventilation defects is poorly understood. Furthermore, the heterogeneity of asthma is under appreciated by the medical community. Regardless of the gas used for imaging, a clear understanding of ventilation defects is absolutely necessary prior to the clinical translation of hyperpolarized gas imaging methods. Therefore, in spite of the well-demonstrated potential for pulmonary imaging to provide a better understanding of the regional aspects of asthma, it currently takes on an insignificant role in asthma clinical care and treatment evaluation and guidance.

Accordingly, the overarching objective of this thesis was to develop and apply novel pulmonary imaging methods to better understand asthma and to provide a foundation for functional imaging to guide clinical decisions and therapy in patients with asthma. The specific research questions investigated here included: 1) Do the different properties of ^{129}Xe and ^{3}He gas result in significant differences in ^{129}Xe compared to ^{3}He gas distribution before and after bronchodilator administration in well-controlled asthmatics? **(CHAPTER 2)**; 2) Can the inherent temporal and spatial pulmonary function information provided by hyperpolarized ^{3}He MRI be used to visualize and quantify temporally persistent and intermittent ventilation defects as potential targets for therapy? **(CHAPTER 3)**; 3) Are asthmatics with ^{3}He MRI ventilation defects different from asthmatics without ventilation defects with respect their airway structure and standard clinical measurements of disease? **(CHAPTER 4)** and, 4) What is the relationship of asthma control with ventilation defects quantified and regionally visualized using ^{3}He MRI? **(CHAPTER 5)**.

6.2 Summary and Conclusions

In Chapter 2, we quantitatively compared hyperpolarized ^{3}He and ^{129}Xe MRI in a small group of seven asthmatics before and after salbutamol inhalation. Prior to salbutamol inhalation, ^{129}Xe VDP (8±5%) was significantly greater than ^{3}He VDP (6±5%, p=0.003). Post-salbutamol, there was a significant improvement in both ^{129}Xe (5±4%, p<0.0001) and ^{3}He (4±3%, p=0.001) VDP, but the improvement in ^{129}Xe VDP was significantly greater (p=0.008). For a single asthmatic, a sub-segmental ^{129}Xe MRI ventilation defect that was visible only prior to salbutamol inhalation but not visible using ^{3}He MRI was spatially related to a remodeled airway (WA%=78%, LA=2.9 mm^2). These results indicate that hyperpolarized ^{129}Xe MRI may help reveal ventilation abnormalities prior to bronchodilation that are not observed using hyperpolarized ^{3}He MRI.

In Chapter 3, we exploited the temporal and spatial information inherent to ^{3}He MRI to generate pulmonary ventilation temporal-spatial maps that could be used to measure, optimize and guide asthma therapy. In this proof-of-concept study, seven asthmatics underwent spirometry and ^{3}He MRI on three occasions, each 5±2 days apart. A registration and segmentation pipeline was developed to generate temporal-spatial pulmonary function maps. This enabled the regional mapping of temporally persistent and intermittent ventilation defects that were normalized to the ^{1}H MRI thoracic cavity volume to generate VDP_P and VDP_I. Persistent and intermittent ventilation defects were identified and were strongly correlated with FEV_1/FVC (VDP_P: r=-0.87, p=0.01; VDP_I: r=-0.96, p=0.0008). These findings suggest that temporal-spatial pulmonary maps generated from ^{3}He MRI can be used to quantify temporally persistent and intermittent ventilation defects as asthma intermediate endpoints and targets for therapy.

In Chapter 4, we evaluated well-established clinical as well as ^{3}He MRI and x-ray CT airway measurements in eight healthy and 26 asthmatic subjects to better understand the determinants of ^{3}He MRI ventilation defects in asthma. Prior to broncho-provocation, 17 asthmatics (17/26=65%) had visually obvious evidence of ventilation defects and nine asthmatics had no ventilation defects (9/26=35%). Asthmatics with defects were older (p=0.01) with worse FEV_1/FVC (p=0.0003), airways resistance (p=0.004), FeNO (p=0.03), lower PC_{20} (p=0.008), and wall thickness percent (p=0.02), compared to asthmatics without

defects. We also identified a moderate correlation for wall area percent with VDP (r=0.43, p=0.04). These results indicate that asthmatics with ^{3}He MRI ventilation defects are older with significantly worse airway hyperresponsiveness, inflammation and airway remodeling in comparison to asthmatics without defects; and that hyperpolarized ^{3}He ventilation abnormalities are spatially and quantitatively related to abnormally remodeled airways.

In Chapter 5, we evaluated MBNW and MRI measurements of ventilation heterogeneity and their relationship with asthma control in 18 severe asthmatics. Mean VDP was 12±11% and LCI was 10.5±3.0 with both VDP (p=0.008) and LCI (p=0.02) improving post-bronchodilator. While VDP was strongly correlated with LCI (r=0.86, p<0.0001), the post-bronchodilator change in VDP and LCI was not correlated (p=0.08). There was significantly worse VDP but not LCI in asthmatics with ACQ >2 (p=0.04) and AQLQ<5 (p=0.04). Notably, VDP (but not LCI, p=0.052) was correlated with ACQ score (r=0.62, p=0.01). MRI ventilation defects were significantly worse in severe asthma patients with poor asthma control and poor quality-of-life. This is important, because as an intermediate endpoint, ventilation defects may be used to target therapy to improve clinically-important asthma outcomes.

In summary, we have provided: 1) evidence that hyperpolarized ^{129}Xe MRI may be more sensitive than ^{3}He MRI to ventilation abnormalities; 2) a new method to quantify temporally persistent and intermittent ventilation defects that may be used as intermediate endpoints and targets for therapy; 3) evidence that asthmatics with ^{3}He ventilation defects are older with significantly worse airway hyperresponsiveness, inflammation and airway remodeling in comparison to asthmatics without defects; and, 4) evidence that ventilation defects are significantly worse in severe asthmatics with poor asthma control and poor quality-of-life.

6.3 Limitations

In this section, some of the most significant limitations of the studies presented in Chapters 2-5 are discussed. It should be noted that a description of the study specific limitations are also presented within the discussion section of the respective Chapters. In addition to

Chapter specific limitations, this section includes a description of general limitations common to Chapters 2-5.

6.3.1 Study Specific Limitations

Hyperpolarized ^{3}He and ^{129}Xe MRI: Differences in Asthma before Bronchodilation (Chapter 2)

In the study presented in Chapter 2, thoracic CTs were not contemporaneously acquired and this limited our ability to investigate the relationship between lung structure and function. However, for two of the seven asthmatics evaluated, partial thoracic CTs were acquired approximately one year before ^{3}He and ^{129}Xe MRI. In a single asthmatic, we observed a large wedge shaped ventilation defect at baseline using ^{129}Xe MRI but not using ^{3}He MRI; the defect was spatially related to a partially obstructed airway. This serendipitous finding led us to hypothesize that ^{3}He gas may penetrate lung regions through partially obstructed airways that ^{129}Xe gas cannot access during a short breath-hold scan. Unfortunately, without whole lung thoracic CTs for all seven subjects we were unable to further investigate, and statistically evaluate, the relationship between abnormal airway pathophysiology and the differences between ^{3}He and ^{129}Xe gas distribution.

Another limitation was that ventilation abnormalities, quantified as VDP, for the small group of mild-to-moderate asthmatics with well-controlled disease evaluated in this study were not large. The mean pre-salbutamol VDP was low as compared to a previous study of asthma,[22] but importantly was higher than previously reported values observed for healthy volunteers of a similar age.[22] Accordingly, the differences in ^{3}He and ^{129}Xe ventilation defects reported here might be a conservative estimate of the differences that would be observed in a larger group of asthmatics with a range of disease severity. Ideally, a range of mild, moderate and severe asthmatics would have been evaluated to ascertain if the differences observed between the two gases were dependent on disease severity.

Similarly, we were unable to ascertain the clinical relevance of the improvement in both ^{3}He and ^{129}Xe VDP following salbutamol inhalation. This endeavor was not possible as clinically-relevant measurements such as dyspnea or exercise capacity were not collected at the time of study. Importantly, however, the smallest detectable difference (SDD), defined as the smallest difference that can be measured with prospectively determined

confidence not due to measurement error (variability) has been previously calculated for ^{3}He MRI and the mean change in the ^{3}He (0.11L) and ^{129}Xe MRI (0.14L) ventilation defect volume measured in this study was greater than the SDD (0.05L).[28] Although the SDD is not a measure of clinical relevance, this confirms that the changes detected were not due to measurement variability. In future attempts to determine the clinical relevance of the changes detected using ^{3}He and ^{129}Xe MRI, we will evaluate the degree of dyspnea and/or exercise capacity in study participants.

Pulmonary Functional Magnetic Resonance Imaging: Asthma Temporal-Spatial Maps (Chapter 3)

In the longitudinal study presented in Chapter 3, we did not obtain well-established clinical measurements of asthma or x-ray CT, and therefore questions regarding the clinical relevance of our data could not be investigated. Importantly, between visits we observed qualitative regional differences in the distribution of ^{3}He gas within the lung. These temporal differences, termed "intermittent defects" were quantified and visualized using the temporal-spatial pulmonary function maps. Unfortunately, we were unable to ascertain whether these asthmatics experienced symptomatic worsening over the two weeks that could be attributed to their variable ventilation heterogeneity. Furthermore, it would have been important to investigate the differences in CT-derived airway morphology for airways spatially related to intermittent defects, persistent defects and persistently-ventilated lung regions.

The maps generated in this study captured the week-to-week lung function variability in a small group of seven asthmatics. Previous work by de Lange and colleagues have demonstrated that the persistence of ventilation defects in asthma decreases with time.[20] Accordingly, it would be very important to evaluate these subjects over a longer period of time to determine whether the variability captured over a short two-week period is representative of the ventilation variability over longer periods of time, in the absence of an exacerbation. Before these temporal abnormalities are used as therapy targets or as an intermediate endpoint, this concept will first need to be investigated.

Another limitation of this study is that we currently do not know what "type" of ventilation defect, if any, is the best target for localized airway treatment in asthma. For example, in

addition to the persistent and intermittent ventilation defects identified in this study, dynamic ROI that respond to broncho-provocation (methacholine/exercise) or bronchodilation (salbutamol) could potentially be excellent targets for localized treatment. It is important to note however that this study provided proof-of-concept results; with this segmentation and registration pipeline, the methodology can subsequently be uniquely tailored to probe a wide variety of ventilation defect behaviours over time or in response to treatment. For example, the pipeline has been subsequently tailored to regionally quantify and visualize the temporal behaviour of ventilation defects in cystic fibrosis patients who underwent ^{3}He MRI on two occasions over four years.[29]

As a technical limitation, the temporal-spatial pulmonary function maps are susceptible to image registration errors that can have an effect on map interpretation. Scan-to-scan variability/differences in lung volume and patient position in the MRI scanner, particularly patient tilting, make registration across visits particularly challenging. Rotations out of plane are particularly cumbersome since our voxels have anisotropic dimensions (3.125 mm x 3.125 mm, slice thickness 15 mm). However, despite this limitation, we were able to achieve sufficient registrations between visits. We do acknowledge, however, that there were a few regions identified along the periphery of the maps with intermittent ventilation that may be attributed purely to mismatches in image registration. However, these occurrences were acknowledged and represent a very small percentage of the overall thoracic cavity volume.

What are Ventilation Defects in Asthma? (Chapter 4)

In the study presented in Chapter 4, we evaluated a relatively broad range of asthmatics who were not enrolled based on disease severity or symptoms. Importantly, however, they were patients from an interdisciplinary (Allergy and Respirology) asthma care centre, were between 18 and 60 years of age and had a physician diagnosis of asthma and a positive methacholine challenge within the past five years. The strength of this study would have been considerably improved if at least severity was documented based on the GINA treatment step score. Furthermore, it would have been advantageous to quantify asthma control using one of the many asthma control questionnaires. Unfortunately, the GINA

step score and asthma control questionnaires were not utilized in the asthma care clinic, nor the research study, and therefore could not be evaluated in this study.

Another limitation of this study was the use of partial thoracic CTs that reduced the number of airways that could be quantified. However, we strongly believe that whenever possible, lower dose partial CTs should be acquired and be used to quantify airway morphology in young subjects, in whom the benefit-risk ratio does not support more extensive CT imaging. In spite of the partial and lower dose CT volume, we were able to generate quantitative information and showed there was a significant relationship between CT airway measurements and ^{3}He MRI overall, and for specific defects and airways in certain cases.

What do Ventilation Defects Reveal about Asthma Control? (Chapter 5)

In the study presented in Chapter 5, we evaluated severe asthmatics who were poorly controlled but we did not include a control group of patients with less severe asthma but with the same degree of poor asthma control. Accordingly, we could not ascertain the relative contribution of asthma severity and asthma control to ventilation defects. In other words, we could not address the important question, "Is the same ventilation heterogeneity observed in milder asthmatics who are poorly controlled?" Future studies are necessary to investigate this important question.

Another limitation of this study was that MRI and MBNW measurements of ventilation heterogeneity were obtained in different positions, introducing the potential for postural effects. Imaging was performed supine, whereas MBNW was performed upright and this may have influenced the strength of the demonstrated relationships between MRI and MBNW measurements of ventilation heterogeneity. From previous experience, we have observed that MBNW measurements of ventilation heterogeneity are significantly worse when performed supine as compared to when performed upright. Regardless, we took necessary steps to mitigate and minimize potential postural effects in this study. Specifically, imaging was completed within five minutes to limit the time that the patients had to remain supine, which has been shown to limit atelectasis.[30]

6.3.2 General Limitations

One limitation to the studies presented in Chapters 2-5 was the small number of subjects evaluated, therefore, caution should be exercised in generalizing these results to the broader asthma population. Importantly, however, hyperpolarized gas MRI measurements are quite sensitive and therefore, as demonstrated in these studies and many others, significant differences may be detected using small sample sizes. Moreover, at the time of study initiation for the majority of these investigations, there was little prior MRI data in asthma available to help generate power calculations and so these were not performed. Regardless, future studies should aim to evaluate larger groups of asthmatics to confirm the results observed in these studies.

Pertinent to both Chapters 2 and 4, we acknowledge that the quantitative measurement of ventilation heterogeneity employed here, the COV, is likely affected by partial volumes inherent to both ^{3}He and ^{129}Xe MR images. Errors induced by partial volumes have the potential to influence the accuracy of the COV estimations reported in Chapters 2 and 4. Our objective was not to develop a novel quantitative metric to evaluate ventilation heterogeneity; instead, a previously published method developed by Tzeng and colleagues was adopted.[27] Edge and/or partial volume effects can be visualized in the cluster and COV maps of ventilation **(Figure 2-1)**. With respect to Chapter 2, in accordance with Tzeng and colleagues, we made the assumption that the elevated COV values observed toward the edges cancel out when images are compared, as this effect is present both pre- and post-salbutamol.[27] Therefore, although we acknowledge that edge and/or partial volume effects likely influence our COV maps, this does not influence or alter our overall conclusions which interrogated relative change.

In Chapters 2-5 our attention was directed towards ventilation defects; however, it is well-understood that ventilation visualized using hyperpolarized gas MRI is not binary. The studies presented in this thesis have overlooked the potential clinical significance of lung regions in asthma that have signal hyper-intensity. Many of the asthmatics evaluated in these studies have had a very heterogeneous MRI gas distribution with regions of hyper-intense signal intensity in addition to ventilation defects. We are interested in these regions of hyper-intense signal intensity and the physiological mechanisms that may cause them.

These regions may be due to hyperinflation and therefore may indicate underlying structural abnormalities within the asthmatic lung. The same semi-automated segmentation image analysis software employed in these studies to quantify VDP can be used to quantify the gradation of signal intensity observed in hyperpolarized gas MR images.[28] This analysis method segments static ventilation images using a k-means clustering algorithm that classifies voxel signal intensity values into five clusters and is therefore able to quantify hyper-intense signal regions. In future studies, it will be important to investigate these regions in addition to ventilation defects.

Another important limitation to this work in general is the limited ^{3}He access, and the high cost of ^{3}He gas that has thus far restricted translation of this imaging method beyond specialized MR physics centres. As previously discussed, this shortage is forcing the noble gas MRI community to transition to ^{129}Xe gas, a less expensive and more readily available contrast agent. While both ^{3}He and ^{129}Xe MRI were acquired within a five-minute period for the study presented in Chapter 2, the remaining study designs (Chapters 3-5) did not include ^{129}Xe MRI. In Chapter 2, significantly greater ^{129}Xe as compared to ^{3}He ventilation defects were observed in asthma, suggesting that ^{129}Xe gas may be more sensitive to airway abnormalities than ^{3}He gas. Although this increased sensitivity is advantageous moving forward, the observed difference suggests that our findings presented in Chapters 3-5 using ^{3}He gas may not be a direct reflection of what would be observed using ^{129}Xe gas. For example, in Chapter 4 we observed that 65% of well-controlled asthmatics had ^{3}He ventilation defects. If this study were to be repeated using ^{129}Xe MRI, one might hypothesize that ventilation defects would be visually obvious in nearly 100% of the same asthmatics. Similarly, in Chapter 3, one might hypothesize that ^{129}Xe MRI temporal-spatial pulmonary function maps of the same asthmatics would have increased intermittent and persistent ventilation defects. Regardless of this speculation, future ^{129}Xe MRI studies are required to validate the results presented here using ^{3}He MRI. Moreover, future research and potential clinical applications of noble gas MRI will most definitely utilize ^{129}Xe gas. In accordance with this trajectory, relevant studies that are currently underway at the Robarts Research Institute are now using ^{129}Xe MRI.

6.4 Future Directions

6.4.1 Functional MRI of Ventilation in Asthma: Sensitivity, Specificity and Comparison with FEV_1

Our results presented in Chapters 4 and 5 indicate that asthmatics with worse MRI ventilation, but not FEV_1, have worse asthma control, greater airways resistance and greater airway hyperresponsiveness. These results strongly support the notion that MRI ventilation defects may be more sensitive than FEV_1 to structural and functional changes in the asthmatic lung. Moreover, it is well-understood that FEV_1 is relatively insensitive to structural and functional changes in the small airways <2mm.[31] Taken together, the work presented in this thesis and previous work of others using hyperpolarized ^{3}He and ^{129}Xe MRI provides a strong foundation for the use of MRI in asthma research and clinical care. To accelerate clinical translation and regulatory approval of hyperpolarized gas MRI, studies must be performed to validate MRI-derived measurements of ventilation against clinical gold-standards, such as FEV_1.

We have performed preliminary analysis in a small proof-of-concept study in which spirometry, hyperpolarized ^{3}He MRI and a methacholine challenge were performed in a single visit. We wanted to evaluate and compare the performance of FEV_1 and ^{3}He MRI VDP to discriminate:

1. *Patients with a clinical diagnosis of asthma from healthy volunteers*
2. *Patients with and without bronchial hyperresponsiveness*

We speculated that MRI ventilation defects may be a more accurate predictor of asthma and bronchial hyperresponsiveness than FEV_1. Preliminary data was obtained for 34 subjects (Asthma: n=25, Healthy: n=9) who performed spirometry, hyperpolarized ^{3}He MRI, and a methacholine challenge during a single study visit. Receiver-operating characteristic (ROC) curves were used to characterize the performance of FEV_1 and MRI VDP as predictors of asthma and bronchial hyperresponsiveness **(Figure 6-1)**. Optimum diagnostic cut-offs were determined according to the maximum Youden's index value (J=sensitivity+specificity-1) and the corresponding sensitivity, specificity, positive and negative likelihood ratios were calculated.

As shown in **Figure 6-1**, similar to FEV_1, MRI measurements of ventilation discriminated: 1) patients with a clinical diagnosis of asthma from healthy volunteers (AUC_{FEV1}=0.82, p=0.006; $AUC_{MRI\ VDP}$=0.79, p=0.01); and 2) patients with and without bronchial hyperresponsiveness (AUC_{FEV1}=0.83, p=0.0009; $AUC_{MRI\ VDP}$=0.88, p=0.0002). Importantly, estimated likelihood ratios suggested that the most accurate diagnosis of asthma and bronchial hyperresponsiveness was established using ^{3}He MRI, not FEV_1. These preliminary results validated functional MRI against FEV_1, a clinically-accepted measurement of asthma, and this is a necessary step towards clinical translation and regulatory approval. As demonstrated in Chapter 2 of this thesis, ^{129}Xe MRI is more sensitive to ventilation abnormalities in asthma than ^{3}He MRI. Accordingly, next steps require a similar but larger scale validation study of ^{129}Xe MRI in asthma.

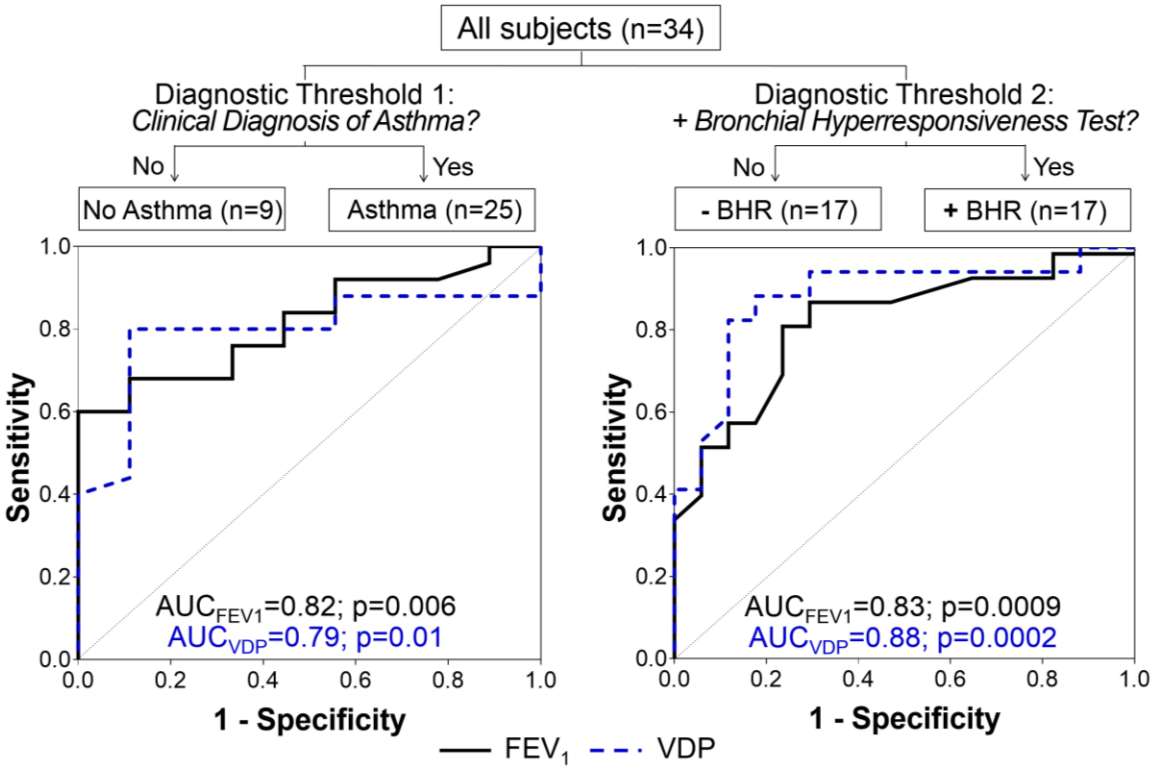

Figure 6-1 Performance of FEV_1 and ^{3}He MRI VDP as predictors of asthma (left plot) and bronchial hyperresponsiveness (right plot).
Receiver-operating characteristic curves show the sensitivity, specificity and area under the curve for FEV_1 (solid black line) and ^{3}He MRI VDP (broken blue line).

6.4.2 Efficacy of Functional MRI Guided Bronchial Thermoplasty

We now have an understanding of the underlying structural determinants of regional ventilation defects observed using MRI in asthma. The proof-of-concept results presented in Chapter 4 strongly support the notion that MRI ventilation defects are directly related to abnormally remodeled airways that are regionally heterogeneous in the asthmatic lung. Therefore, we speculate that abnormally remodeled airways, proximal to MRI ventilation defects, may be excellent targets for localized asthma treatment. In a similar fashion, normally functioning airways, proximal to well or normally-ventilated lung regions could be avoided during localized treatment. Current asthma treatments aim to treat all accessible airways.

Bronchial thermoplasty (BT), an established localized asthma treatment, aims to permanently reduce smooth muscle mass in the lobar and segmental bronchi with the goal of improving symptoms and asthma control.[32] To date, the effectiveness and safety of BT has been evaluated in four clinical trials,[33-36] and this work has demonstrated persistent improvement in asthma control, quality-of-life and fewer exacerbations following treatment in some patients. Despite its demonstrated safety and efficacy, BT is a time-consuming procedure. The current conventional whole-lung treatment approach targets all accessible airways throughout the lungs during three bronchoscopy sessions, each separated by approximately three weeks. Accordingly, the treatment assumes that all airways in the asthmatic lung are homogeneously remodeled, which may result in treatment of normally functioning airways. If a personalized, image-guided treatment approach were to be adopted that targeted only abnormally functioning airways, treatment time, cost and adverse effects might be reduced while patient outcomes may be improved.

In a study currently underway, we aim to use pulmonary functional MRI to guide BT treatment, evaluate BT treatment response and to generate new knowledge required to better understand airway-targeted therapy in severe asthma. All participants will have severe asthma and will undergo up to three pre-therapy MRIs to evaluate ventilation reproducibility and post-prednisone effects, and there will also be two longitudinal post-therapy MRIs to evaluate treatment effect. All participants will be randomized to MRI-directed or conventional BT and we will measure airway function and treatment response

using conventional and imaging tests as well as questionnaires that capture how well asthma is controlled and how patients are feeling.

For those participants randomized to the MRI-directed treatment arm, patient-specific BT treatment plans will be developed to identify specific airways to be targeted during a single-session BT treatment procedure. Briefly, low-dose thoracic CT will be used to generate a detailed three-dimensional model of the airway tree. Following CT, all subjects will undergo further MR imaging following methacholine challenge or salbutamol inhalation. As shown for a representative subject in **Figure 6-2**, the post-challenge MRI will be co-registered to the low-dose CT with airway rendering to enable spatial comparisons between ventilation defects and airways. Patient-specific treatment plans will identify target airways, prioritized in order of importance and grouped by lobe to be targeted. Airways demonstrating dynamic or static bronchoconstriction will be targeted based on their spatial proximity to ventilation defects.

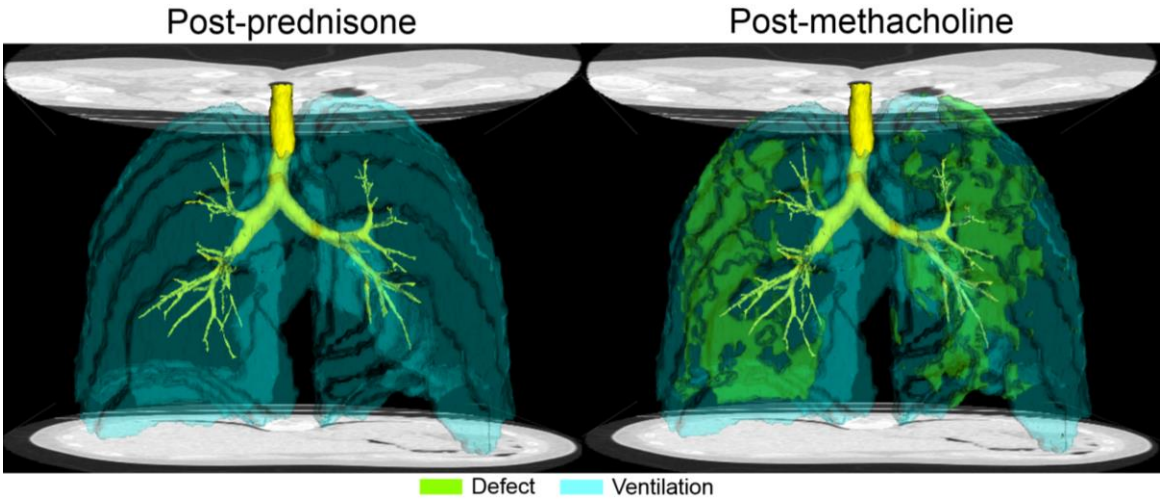

Figure 6-2 Spatial relationship between ^{3}He MRI ventilation (blue), ventilation defects (green) and airways (yellow) for a representative subject with severe asthma three days prior to BT while on 50 mg of prednisone.
^{3}He MRI registered to the CT of the thorax (in grey-scale) with the airways segmented in yellow to identify airways demonstrating dynamic bronchoconstriction following methacholine challenge to be targeted for treatment based on their spatial proximity to ventilation defects.

This study will address the following research questions:

1) *Do regional ventilation defects resolve following BT?*

2) *What is the relationship between ventilation defects and patient outcomes following BT?*

3) *Can MRI-guided BT treatment to specific abnormal airways result in improved asthma control and quality-of-life?*

4) *Are patient outcomes related to image-guided BT significantly different than those achieved using the conventional treatment approach?*

5) *Can MRI identify characteristic ventilation defects that predict BT response?*

One functional MRI study, evaluating seven severe asthmatics, has provided promising preliminary evidence supporting the notion that MRI ventilation defects decrease after BT treatment.[37] Our study will be the first to evaluate the effect of a localized airway intervention on regional ventilation visualized using MRI in asthma. The use of functional MRI in this context will provide a better understanding of BT treatment, providing a foundation of knowledge for studies aimed at assessing the ability of imaging methods to guide localized treatment to only abnormally-functioning airways. We hypothesize that treatment of only specific abnormal airways, proximal to MRI ventilation defects, will result in improved MRI gas distribution, airway hyperresponsiveness, asthma control and quality-of-life that is not significantly different from patients in the conventional therapy group. We also hypothesize that improved ventilation will be related to improvements in well-established clinical measurements of asthma.

6.4.3 Imaging Exercise-induced and Methacholine-induced Bronchoconstriction using Hyperpolarized Gas MRI: Same Ventilation Defects or Not?

Airway hyperresponsiveness is a universal defining feature of asthma.[38] It is currently measured clinically to aid in the diagnosis and management of asthma, and is often employed in clinical trials to evaluate the effectiveness of novel asthma therapies. Airway hyperresponsiveness can be assessed using both direct and indirect stimuli which induce bronchoconstriction via different mechanistic pathways; however, these differences are poorly understood.[39] A better understanding of airway hyper-responsiveness and the

mechanisms that contribute to this process in asthma is required to achieve better patient outcomes.

^{3}He MRI has been used to visualize regionally heterogeneous ventilation in response to both exercise-[23] and methacholine-induced[22,23] bronchoconstriction, suggesting that not all airways respond to provocation equally. However, the spatial relationship between exercise- and methacholine-induced ventilation defects has not been investigated in the same asthmatics. In other words, it is currently unknown if the same airways in asthma respond in a similar manner to both indirect and direct stimuli. It has been hypothesized that clinical assessments of airway hyperresponsiveness induced by indirect methods correlate better with the clinical features of asthma.[40] This hypothesis has not been tested using MRI, therefore it is unknown whether indirect or direct stimuli induced ventilation defects correlate more strongly with the clinical features of asthma. If non-invasive imaging measurements are going to be used as intermediate endpoints in clinical trials of new therapies, we think future MRI studies should investigate these concepts.

By acquiring pulmonary CT and well-established clinical measurements of asthma in addition to performing MRI following both exercise and methacholine challenge in the same asthmatics, the following research questions can be addressed:

1) *Are MRI ventilation defects observed in the same focal lung regions following exercise- and methacholine-induced bronchoconstriction in asthma?*
2) *Are exercise- or methacholine-induced MRI ventilation defects more strongly correlated with well-established clinical measurements of asthma?*
3) *Are CT-derived measurements of airway structure different for those airways proximal to ventilation defects observed following methacholine and exercise induced bronchoconstriction?*

Comparative imaging studies have the potential to provide a better understanding of the underlying mechanisms involved in airway hyperresponsiveness, and in turn provide a better understanding of potential treatment targets in asthma. So far at our centre, four asthmatics have undergone MR imaging prior to and following both exercise- and methacholine-induced bronchoconstriction. Imaging results from one of the four asthmatics is shown in **Figure 6-3**. Preliminary data suggests that exercise and

methacholine-induced bronchoconstriction will induce a similar decrease in well-established clinical measurements of asthma; however, visually obvious regional differences in gas distribution will be observed using MRI that cannot be detected by spirometry.

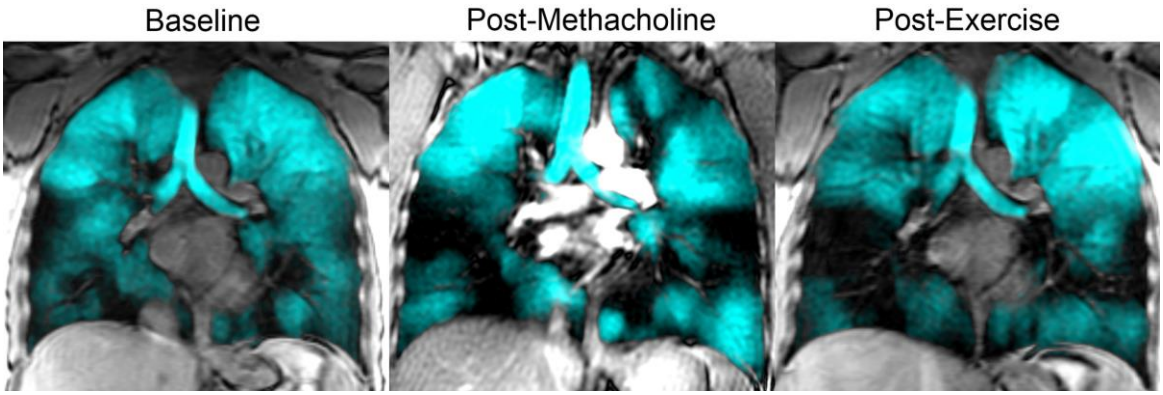

Figure 6-3 Representative coronal centre slice hyperpolarized ^{3}He MRI of an asthmatic subject at baseline and following both methacholine and exercise-induced bronchoconstriction.
^{3}He MRI gas distribution (in blue) registered to the ^{1}H MRI of the thorax (in grey-scale). Ventilation abnormalities are present at baseline that become worse following methacholine- and exercise-induced bronchoconstriction.

6.4.4 Functional MRI of Asthma: Alternative Approaches

It is well-established that direct visualization of the lung airspaces using functional MRI is important and that it and provides numerous advantages over clinically available tools. Motivating the work presented in Chapter 2, ^{3}He MRI is not well-suited to be a widely available clinical tool due to the limited availability of ^{3}He gas.[41] This roadblock has initiated further development of ^{129}Xe MRI and oxygen enhanced MRI,[42] as well as motivated the need for alternative approaches to visualize lung function using non-polarized inhaled gases and ^{1}H MRI. These emerging methods come with tradeoffs regarding cost, access and importantly, image quality.

Fluorine-19 (^{19}F) MRI of the lungs uses inert fluorinated gases (e.g. tetrafluoromethane (CF_4), sulfur hexafluoride (SF_6), perfluoropropane (C_3F_8 or PFP)) and may offer comparable regional lung function information to hyperpolarized gas MRI, but at a much lower cost.[43-46] This approach to functional lung imaging has the advantage of using gases that are inexpensive, abundant and do not need to be polarized prior to their use. Halaweish

and colleagues have been the first to apply this approach in patients with asthma, demonstrating its sensitivity to ventilation defects in two subjects.[44]

Free-breathing pulmonary ^{1}H MRI is another approach currently being developed with the ability to evaluate lung function.[47-50] Fourier decomposition of the ^{1}H signal intensity acquired during tidal breathing was introduced by Bauman and colleagues to generate ventilation and perfusion images.[47] This unique approach does not require a contrast agent and can be implemented on the majority of clinical scanners without the requirement for specialized multi-nuclear hardware; however, it is limited by cumbersome post-processing. Unlike ^{19}F MRI, this approach has not yet been evaluated in patients with asthma.

With these promising alternative functional MRI approaches in the pipeline, future studies are required to investigate their utility in the asthmatic population. Specifically, initial investigations should be focused towards direct qualitative and quantitative comparisons of ventilation abnormalities derived from these alternative approaches with those identified using hyperpolarized gas MRI. Such proof-of-concept demonstrations are currently underway in COPD[51] and should be emulated in asthma. One major advantage of these alternative functional MRI approaches is their direct translational ability as they can be implemented in most medical imaging centres with access to a clinical MRI scanner. This advantage is fundamentally important, making these alternative functional MRI approaches more likely to find a place in the clinical setting.

6.5 Significance and Impact

Even though it is well-understood that FEV_1 does not reflect the regional nature of asthma, the assessment of novel therapies and disease management continues to depend on this global metric. Using hyperpolarized gas MRI, heterogeneous ventilation defects are observed and the regional, patient-specific nature of asthma can be safely and non-invasively visualized – providing information that is not available using alternative clinical methods. This thesis significantly advances our understanding of the structural determinants of MRI ventilation defects identified in asthma and what it means clinically to be an asthmatic with ventilation defects. The studies presented in this thesis provide strong evidence that ventilation defects in asthma are not random, but are heterogeneously distributed in the lungs, spatially related to airway abnormalities and are related to worse

clinical characteristics of asthma including airway hyperresponsiveness, airway inflammation, airflow obstruction and disease control. It is also now well-understood that ^{129}Xe MRI is more sensitive to airway abnormalities in asthma than ^{3}He MRI, which is important for future clinical translation of this imaging method beyond specialized academic centres.

This thesis confirms that regional ventilation defects are a clinically relevant imaging-based biomarker of asthma and provides a foundation of knowledge supporting the need for clinical integration of functional MRI. Armed with this understanding, there is enormous potential for MRI ventilation defects to be used as intermediate endpoints of asthma that can be used to evaluate novel treatments and to better inform treatment decisions. Furthermore, the development of novel asthma treatments may be directed towards focal ventilation defects. Hence, there is the potential for functional MRI to guide validated localized airway treatments, such as bronchial thermoplasty, to abnormal airways that lead to ventilation defects. These advances in our understanding of asthma may very likely impact asthma management and how new treatment will be developed and evaluated. By "seeing" asthma and how it regionally responds to treatment and provocation, and how it changes over time, there is increased potential for more effective treatments, reduced treatment time, and improved patient outcomes.

6.6 References

(1) Celli BR. The importance of spirometry in COPD and asthma: effect on approach to management. *Chest* 2000;117:15S-9S.

(2) Reddel HK, Taylor DR, Bateman ED, *et al.* An official American Thoracic Society/European Respiratory Society statement: asthma control and exacerbations: standardizing endpoints for clinical asthma trials and clinical practice. *Am J Respir Crit Care Med* 2009;180:59-99.

(3) Macklem PT. The physiology of small airways. *Am J Respir Crit Care Med* 1998;157:S181-S83.

(4) Dunnill MS. The pathology of asthma, with special reference to changes in the bronchial mucosa. *JClinPathol* 1960;13:27-33.

(5) Macleod KA, Horsley AR, Bell NJ, *et al.* Ventilation heterogeneity in children with well controlled asthma with normal spirometry indicates residual airways disease. *Thorax* 2009;64:33-7.

(6) Castro M, Fain SB, Hoffman EA, *et al.* Lung imaging in asthmatic patients: the picture is clearer. *J Allergy Clin Immunol* 2011;128:467-78.

(7) Newman KB, Lynch DA, Newman LS, *et al.* Quantitative computed tomography detects air trapping due to asthma. *Chest* 1994;106:105-9.

(8) Gono H, Fujimoto K, Kawakami S, *et al.* Evaluation of airway wall thickness and air trapping by HRCT in asymptomatic asthma. *Eur Respir J* 2003;22:965-71.

(9) Jung JW, Kwon JW, Kim TW, *et al.* New insight into the assessment of asthma using xenon ventilation computed tomography. *Ann Allergy Asthma Immunol* 2013;111:90-95 e2.

(10) Venegas JG, Winkler T, Musch G, *et al.* Self-organized patchiness in asthma as a prelude to catastrophic shifts. *Nature* 2005;434:777-82.

(11) King GG, Eberl S, Salome CM, *et al.* Differences in airway closure between normal and asthmatic subjects measured with single-photon emission computed tomography and technegas. *Am J Respir Crit Care Med* 1998;158:1900-06.

(12) Engel LA, Landau L, Taussig L, *et al.* Influence of bronchomotor tone on regional ventilation distribution at residual volume. *J Appl Physiol* 1976;40:411-16.

(13) Altes TA, Powers PL, Knight-Scott J, *et al.* Hyperpolarized ^{3}He MR lung ventilation imaging in asthmatics: preliminary findings. *J Magn Reson Imaging* 2001;13:378-84.

(14) Parraga G, Ouriadov A, Evans A, *et al.* Hyperpolarized 3He ventilation defects and apparent diffusion coefficients in chronic obstructive pulmonary disease: preliminary results at 3.0 Tesla. *Invest Radiol* 2007;42:384-91.

(15) Kirby M, Svenningsen S, Owrangi A, *et al.* Hyperpolarized 3He and 129Xe MR imaging in healthy volunteers and patients with chronic obstructive pulmonary disease. *Radiology* 2012;265:600-10.

(16) Kauczor HU, Hofmann D, Kreitner KF, *et al.* Normal and abnormal pulmonary ventilation: visualization at hyperpolarized He-3 MR imaging. *Radiology* 1996;201:564-8.

(17) Mugler JP, III, Driehuys B, Brookeman JR, *et al.* MR imaging and spectroscopy using hyperpolarized 129Xe gas: preliminary human results. *Magn Reson Med* 1997;37:809-15.

(18) de Lange EE, Altes TA, Patrie JT, *et al.* The variability of regional airflow obstruction within the lungs of patients with asthma: assessment with hyperpolarized helium-3 magnetic resonance imaging. *J Allergy Clin Immunol* 2007;119:1072-8.

(19) de Lange EE, Altes TA, Patrie JT, *et al.* Evaluation of asthma with hyperpolarized helium-3 MRI: correlation with clinical severity and spirometry. *Chest* 2006;130:1055-62.

(20) de Lange EE, Altes TA, Patrie JT, *et al.* Changes in regional airflow obstruction over time in the lungs of patients with asthma: evaluation with ^{3}He MR imaging. *Radiology* 2009;250:567-75.

(21) Fain SB, Gonzalez-Fernandez G, Peterson ET, *et al.* Evaluation of structure-function relationships in asthma using multidetector CT and hyperpolarized He-3 MRI. *Acad Radiol* 2008;15:753-62.

(22) Costella S, Kirby M, Maksym GN, *et al.* Regional Pulmonary Response to a Methacholine Challenge using Hyperpolarized ^{3}He Magnetic Resonance Imaging. *Respirology* 2012;17:1237-46.

(23) Samee S, Altes T, Powers P, *et al.* Imaging the lungs in asthmatic patients by using hyperpolarized helium-3 magnetic resonance: assessment of response to methacholine and exercise challenge. *J Allergy Clin Immunol* 2003;111:1205-11.

(24) Cadman RV, Lemanske RF, Jr., Evans MD, *et al.* Pulmonary 3He magnetic resonance imaging of childhood asthma. *J Allergy Clin Immunol* 2013;131:369-76 e1-5.

(25) Kruger SJ, Niles DJ, Dardzinski B, *et al.* Hyperpolarized Helium-3 MRI of exercise-induced bronchoconstriction during challenge and therapy. *J Magn Reson Imaging* 2014;39:1230-7.

(26) Niles DJ, Kruger SJ, Dardzinski BJ, *et al.* Exercise-induced bronchoconstriction: reproducibility of hyperpolarized 3He MR imaging. *Radiology* 2013;266:618-25.

(27) Tzeng YS, Lutchen K, Albert M. The difference in ventilation heterogeneity between asthmatic and healthy subjects quantified using hyperpolarized 3He MRI. *J Appl Physiol* 2009;106:813-22.

(28) Kirby M, Heydarian M, Svenningsen S, *et al.* Hyperpolarized ^{3}He magnetic resonance functional imaging semiautomated segmentation. *Acad Radiol* 2012;19:141-52.

(29) Paulin GA, Svenningsen S, Jobse BN, *et al.* Differences in hyperpolarized (3) He ventilation imaging after 4 years in adults with cystic fibrosis. *J Magn Reson Imaging* 2015;41:1701-7.

(30) Mata J, Altes T, Knake J, *et al.* Hyperpolarized 3He MR imaging of the lung: effect of subject immobilization on the occurrence of ventilation defects. *Acad Radiol* 2008;15:260-4.

(31) Burgel PR. The role of small airways in obstructive airway diseases. *Eur Respir Rev* 2011;20:23-33.

(32) Cox PG, Miller J, Mitzner W, *et al.* Radiofrequency ablation of airway smooth muscle for sustained treatment of asthma: preliminary investigations. *Eur Respir J* 2004;24:659-63.

(33) Castro M, Rubin AS, Laviolette M, *et al.* Effectiveness and safety of bronchial thermoplasty in the treatment of severe asthma: a multicenter, randomized, double-blind, sham-controlled clinical trial. *Am J Respir Crit Care Med* 2010;181:116-24.

(34) Pavord ID, Cox G, Thomson NC, *et al.* Safety and efficacy of bronchial thermoplasty in symptomatic, severe asthma. *Am J Respir Crit Care Med* 2007;176:1185-91.

(35) Cox G, Thomson NC, Rubin AS, *et al.* Asthma control during the year after bronchial thermoplasty. *N Engl J Med* 2007;356:1327-37.

(36) Cox G, Miller JD, McWilliams A, *et al.* Bronchial thermoplasty for asthma. *Am J Respir Crit Care Med* 2006;173:965-9.

(37) Thomen RP, Sheshadri A, Quirk JD, *et al.* Regional ventilation changes in severe asthma after bronchial thermoplasty with ^{3}He MR imaging and CT. *Radiology* 2015;274:250-9.

(38) Busse WW. The relationship of airway hyperresponsiveness and airway inflammation: Airway hyperresponsiveness in asthma: its measurement and clinical significance. *Chest* 2010;138:4S-10S.

(39) Cockcroft DW. Direct challenge tests: Airway hyperresponsiveness in asthma: its measurement and clinical significance. *Chest* 2010;138:18S-24S.

(40) Pauwels R, Joos G, Van der Straeten M. Bronchial hyperresponsiveness is not bronchial hyperresponsiveness is not bronchial asthma. *Clin Allergy* 1988;18:317-21.

(41) Cho A. Physics. Helium-3 shortage could put freeze on low-temperature research. *Science* 2009;326:778-79.

(42) Edelman RR, Hatabu H, Tadamura E, *et al.* Noninvasive assessment of regional ventilation in the human lung using oxygen-enhanced magnetic resonance imaging. *Nat Med* 1996;2:1236-9.

(43) Couch MJ, Ball IK, Li T, *et al.* Pulmonary ultrashort echo time 19F MR imaging with inhaled fluorinated gas mixtures in healthy volunteers: feasibility. *Radiology* 2013;269:903-9.

(44) Halaweish AF, Moon RE, Foster WM, *et al.* Perfluoropropane gas as a magnetic resonance lung imaging contrast agent in humans. *Chest* 2013;144:1300-10.

(45) Couch MJ, Ball IK, Li T, *et al.* Inert fluorinated gas MRI: a new pulmonary imaging modality. *NMR Biomed* 2014;27:1525-34.

(46) Ouriadov AV, Fox MS, Couch MJ, *et al.* In vivo regional ventilation mapping using fluorinated gas MRI with an x-centric FGRE method. *Magn Reson Med* 2015;74:550-7.

(47) Bauman G, Puderbach M, Deimling M, *et al.* Non-contrast-enhanced perfusion and ventilation assessment of the human lung by means of fourier decomposition in proton MRI. *Magn Reson Med* 2009;62:656-64.

(48) Bauman G, Puderbach M, Heimann T, *et al.* Validation of Fourier decomposition MRI with dynamic contrast-enhanced MRI using visual and automated scoring of pulmonary perfusion in young cystic fibrosis patients. *Eur J Radiol* 2013;82:2371-7.

(49) Lederlin M, Bauman G, Eichinger M, *et al.* Functional MRI using Fourier decomposition of lung signal: reproducibility of ventilation- and perfusion-weighted imaging in healthy volunteers. *Eur J Radiol* 2013;82:1015-22.

(50) Sommer G, Bauman G, Koenigkam-Santos M, *et al.* Non-contrast-enhanced preoperative assessment of lung perfusion in patients with non-small-cell lung cancer using Fourier decomposition magnetic resonance imaging. *Eur J Radiol* 2013;82:e879-87.

(51) Capaldi DP, Sheikh K, Guo F, *et al.* Free-breathing pulmonary 1H and Hyperpolarized 3He MRI: comparison in COPD and bronchiectasis. *Acad Radiol* 2015;22:320-9.

APPENDIX

APPENDIX A – Permission for Reproduction of Scientific Articles

JOHN WILEY AND SONS LICENSE TERMS AND CONDITIONS

May 04, 2015

This Agreement between Sarah Svenningsen ("You") and John Wiley and Sons ("John Wiley and Sons") consists of your license details and the terms and conditions provided by John Wiley and Sons and Copyright Clearance Center.

License Number	3622100120683
License date	May 04, 2015
Licensed Content Publisher	John Wiley and Sons
Licensed Content Publication	Journal of Magnetic Resonance Imaging
Licensed Content Title	Hyperpolarized 3He and 129Xe MRI: Differences in asthma before bronchodilation
Licensed Content Author	Sarah Svenningsen,Miranda Kirby,Danielle Starr,Del Leary,Andrew Wheatley,Geoffrey N. Maksym,David G. McCormack,Grace Parraga
Licensed Content Date	Apr 15, 2013
Pages	10
Type of use	Dissertation/Thesis
Requestor type	Author of this Wiley article
Format	Print and electronic
Portion	Full article
Will you be translating?	No
Title of your thesis / dissertation	Evaluation of Regional Pulmonary Structure and Function in Asthma using Hyperpolarized Noble Gas Magnetic Resonance Imaging
Expected completion date	Jan 2016
Expected size (number of pages)	250
Requestor Location	Sarah Svenningsen 1151 Richmond Street North London , ON N6A 5B7 Canada Attn: Sarah Svenningsen
Billing Type	Invoice
Billing Address	Sarah Svenningsen 1151 Richmond Street North London , ON N6A 5B7 Canada Attn: Sarah Svenningsen
Total	0.00 CAD
Terms and Conditions	

ELSEVIER ORDER DETAILS

May 04, 2015

This is an Agreement between Sarah Svenningsen ("You") and Elsevier ("Elsevier"). It consists of your order details, the terms and conditions provided by Elsevier ("Elsevier"), and the payment terms and conditions.

Order Number	501005990
Order Date	May 04, 2015
Licensed content publisher	Elsevier
Licensed content publication	Academic Radiology
Licensed content title	Pulmonary Functional Magnetic Resonance Imaging Asthma Temporal–Spatial Maps
Licensed content author	None
Licensed content date	November 2014
Licensed content volume number	21
Licensed content issue number	11
Number of pages	9
Start Page	1402
End Page	1410
Type of Use	reuse in a thesis/dissertation
Intended publisher of new work	other
Portion	full article
Format	both print and electronic
Are you the author of this Elsevier article?	Yes
Will you be translating?	No
Title of your thesis/dissertation	Evaluation of Regional Pulmonary Structure and Function in Asthma using Hyperpolarized Noble Gas Magnetic Resonance Imaging
Expected completion date	Jan 2016
Estimated size (number of pages)	
Elsevier VAT number	GB 494 6272 12
Permissions price	Not Available
VAT/Local Sales Tax	Not Available
Total	Not Available

BMJ PUBLISHING GROUP LTD. LICENSE TERMS AND CONDITIONS

Jul 23, 2015

This Agreement between Sarah Svenningsen ("You") and BMJ Publishing Group Ltd. ("BMJ Publishing Group Ltd.") consists of your license details and the terms and conditions provided by BMJ Publishing Group Ltd. and Copyright Clearance Center.

License Number	3674890801814
License date	Jul 23, 2015
Licensed Content Publisher	BMJ Publishing Group Ltd.
Licensed Content Publication	Thorax
Licensed Content Title	What are ventilation defects in asthma?
Licensed Content Author	Sarah Svenningsen, Miranda Kirby, Danielle Starr, Harvey O Coxson, Nigel A M Paterson, David G McCormack, Grace Parraga
Licensed Content Date	Jan 1, 2014
Licensed Content Volume Number	69
Licensed Content Issue Number	1
Volume number	69
Issue number	1
Type of Use	Dissertation/Thesis
Requestor type	Author of this article
Format	Print and electronic
Portion	Figure/table/extract
Number of figure/table /extracts	5
Descriptionof figure/table /extracts	Figure 1 Figure 2 Figure 3 Figure 4 Figure 5 Table 1 Table 2
Will you be translating?	No
Circulation/distribution	1
Title of your thesis / dissertation	Pulmonary Imaging of Asthma to Better understand the Asthmatic Lung and Guide Asthma Therapy
Expected completion date	Nov 2015
Estimated size(pages)	250
BMJ VAT number	674738491
Billing Type	Invoice
Billing Address	Sarah Svenningsen 1151 Richmond Street North London , ON N6A 5B7

APPENDIX B – Health Science Research Ethics Board Approval Notices

Office of Research Ethics

The University of Western Ontario
Room 00045 Dental Sciences Building, London, ON, Canada N6A 5C1
Telephone: (519) 661-3036 Fax: (519) 850-2466 Email: ethics@uwo.ca
Website: www.uwo.ca/research/ethics

Use of Human Subjects - Ethics Approval Notice

Principal Investigator: Dr. D. McCormack

Review Number: 13109 **Review Date:** February 20, 2007 **Revision Number:**

Protocol Title: A 3 Period, Double-Blind, Randomized Crossover Study to Evaluate the Effects of a Single Dose of Montelukast Compared with Placebo on Exercise-Induced Bronchoconstriction as Assessed by Hyperpolarized Gas Magnetic Resonance Imaging

Department and Institution: Respirology, London Health Sciences Centre

Sponsor: MERCK & CO. INC.

Ethics Approval Date: March 21, 2007 **Expiry Date:** June 30, 2007

Documents Reviewed and Approved: UWO Protocol, Letter of Information and Consent dated 28 February 2007

Documents Received for Information: Protocol, 31-Jan-2007; IB, ed 6, 09 Sept 2005; Prod Mon, July 21, 2006

This is to notify you that The University of Western Ontario Research Ethics Board for Health Sciences Research Involving Human Subjects (HSREB) which is organized and operates according to the Tri-Council Policy Statement and the Health Canada/ICH Good Clinical Practice Practices: Consolidated Guidelines; and the applicable laws and regulations of Ontario has reviewed and granted full board approval to the above named research study on the approval date noted above. The membership of this REB also complies with the membership requirements for REB's as defined in Division 5 of the Food and Drug Regulations.

This approval shall remain valid until the expiry date noted above assuming timely and acceptable responses to the HSREB's periodic requests for surveillance and monitoring information. If you require an updated approval notice prior to that time you must request it using the UWO Updated Approval Request Form.

During the course of the research, no deviations from, or changes to, the protocol or consent form may be initiated without prior written approval from the HSREB except when necessary to eliminate immediate hazards to the subject or when the change(s) involve only logistical or administrative aspects of the study (e.g. change of monitor, telephone number). Expedited review of minor change(s) in ongoing studies will be considered. Subjects must receive a copy of the signed information/consent documentation.

Investigators must promptly also report to the HSREB:

a) changes increasing the risk to the participant(s) and/or affecting significantly the conduct of the study;

b) all adverse and unexpected experiences or events that are both serious and unexpected;

c) new information that may adversely affect the safety of the subjects or the conduct of the study.

If these changes/adverse events require a change to the information/consent documentation, and/or recruitment advertisement, the newly revised information/consent documentation, and/or advertisement, must be submitted to this office for approval.

Members of the HSREB who are named as investigators in research studies, or declare a conflict of interest, do not participate in discussion related to, nor vote on, such studies when they are presented to the HSREB.

Chair of HSREB: Dr. John W. McDonald

Deputy Chair: Susan Hoddinott

This is an official document. Please retain the original in your files.

Western

Office of Research Ethics

The University of Western Ontario
Room 5150 Support Services Building, London, ON, Canada N6A 3K7
Telephone: (519) 661-3036 Fax: (519) 850-2466 Email: ethics@uwo.ca
Website: www.uwo.ca/research/ethics

Use of Human Subjects - Ethics Approval Notice

Principal Investigator: Dr. G. Parraga
Review Level: Expedited
Review Number: 15928
Revision Number: 6
Review Date: January 06, 2011
Approved Local # of Participants: 34
Protocol Title: Hyperpolarized Helium-3 Magnetic Resonance Ventilation Heterogeneity and Airway Hyper-Responsiveness in Asthma
Department and Institution: Imaging, Robarts Research Institute
Sponsor: INTERNAL RESEARCH FUND-UWO
Ethics Approval Date: January 07, 2011
Expiry Date: March 31, 2011
Documents Reviewed and Approved: Addition of healthy volunteers (10), revised study methodology, revised inclusion criteria and revised letter of information & consent form dated Nov.25/10
Documents Received for Information:

This is to notify you that The University of Western Ontario Research Ethics Board for Health Sciences Research Involving Human Subjects (HSREB) which is organized and operates according to the Tri-Council Policy Statement: Ethical Conduct of Research Involving Humans and the Health Canada/ICH Good Clinical Practice Practices: Consolidated Guidelines; and the applicable laws and regulations of Ontario has reviewed and granted approval to the above referenced revision(s) or amendment(s) on the approval date noted above. The membership of this REB also complies with the membership requirements for REB's as defined in Division 5 of the Food and Drug Regulations.

The ethics approval for this study shall remain valid until the expiry date noted above assuming timely and acceptable responses to the HSREB's periodic requests for surveillance and monitoring information. If you require an updated approval notice prior to that time you must request it using the UWO Updated Approval Request Form.

During the course of the research, no deviations from, or changes to, the protocol or consent form may be initiated without prior written approval from the HSREB except when necessary to eliminate immediate hazards to the subject or when the change(s) involve only logistical or administrative aspects of the study (e.g. change of monitor, telephone number). Expedited review of minor change(s) in ongoing studies will be considered. Subjects must receive a copy of the signed information/consent documentation.

Investigators must promptly also report to the HSREB:

a) changes increasing the risk to the participant(s) and/or affecting significantly the conduct of the study;
b) all adverse and unexpected experiences or events that are both serious and unexpected;
c) new information that may adversely affect the safety of the subjects or the conduct of the study.

If these changes/adverse events require a change to the information/consent documentation, and/or recruitment advertisement, the newly revised information/consent documentation, and/or advertisement, must be submitted to this office for approval.

Members of the HSREB who are named as investigators in research studies, or declare a conflict of interest, do not participate in discussion related to, nor vote on, such studies when they are presented to the HSREB.

Chair of HSREB: Dr. Joseph Gilbert
FDA Ref. #: IRB 00000940

This is an official document. Please retain the original in your files.

cc: ORE File
LHRI

Research Western

Use of Human Participants - Ethics Approval Notice

Principal Investigator: Dr. Grace Parraga
Review Number: 18130
Review Level: Full Board
Approved Local Adult Participants: 100
Approved Local Minor Participants: 0
Protocol Title: A Single-center Study Evaluating Hyperpolarized 129Xenon Magnetic Resonance Imaging in Subjects with Chronic Lung Disease
Department & Institution: Imaging,Robarts Research Institute
Sponsor: Canadian Institutes of Health Research

Ethics Approval Date: August 12, 2011 **Expiry Date:** August 31, 2016

Documents Reviewed & Approved & Documents Received for Information:

Document Name	Comments	Version Date
UWO Protocol		
Letter of Information & Consent		2011/07/13
Advertisement		2011/07/13
Protocol	Received for information only	2011/06/22

This is to notify you that the University of Western Ontario Health Sciences Research Ethics Board (HSREB) which is organized and operates according to the Tri-Council Policy Statement: Ethical Conduct of Research Involving Humans and the Health Canada/ICH Good Clinical Practice Practices: Consolidated Guidelines; and the applicable laws and regulations of Ontario has reviewed and granted approval to the above referenced study on the approval date noted above. The membership of this HSREB also complies with the membership requirements for REB's as defined in Division 5 of the Food and Drug Regulations.

The ethics approval for this study shall remain valid until the expiry date noted above assuming timely and acceptable responses to the HSREB's periodic requests for surveillance and monitoring information. If you require an updated approval notice prior to that time you must request it using the UWO Updated Approval Request form.

Member of the HSREB that are named as investigators in research studies, or declare a conflict of interest, do not participate in discussions related to, nor vote on, such studies when they are presented to the HSREB.

The Chair of the HSREB is Dr. Joseph Gilbert. The UWO HSREB is registered with the U.S. Department of Health & Human Services under the IRB registration number IRB 00000940.

This is an official document. Please retain the original in your files.

The **University** *of* **Western Ontario**
Office of Research Ethics
Support Services Building Room 5150 • London, Ontario • CANADA - N6G 1G9
PH: 519-661-3036 • F: 519-850-2466 • ethics@uwo.ca • www.uwo.ca/research/ethics

Use of Human Participants - Initial Ethics Approval Notice

Principal Investigator: Dr. Grace Parraga
File Number:104200
Review Level: Full Board
Protocol Title: Hyperpolarized Magnetic Resonance Imaging in Asthma Pre- and Post-Bronchial Thermoplasty
Department & Institution: Schulich School of Medicine and Dentistry\Imaging,Robarts Research Institute
Sponsor: Lawson Health Research Institute

Ethics Approval Date: January 03, 2014
Ethics Expiry Date: February 28, 2017

Documents Reviewed & Approved & Documents Received for Information:

Document Name	Comments	Version Date
Instruments	Asthma Quality of Life Questionnaire with Standardized Activities (AQLQ(S))	2013/08/15
Instruments	Asthma Control Questionnaire	2013/08/15
Instruments	Modified Borg Scale Questionnaire	2013/08/15
Instruments	mMRC Dyspnea Score Questionnaire	2013/08/15
Protocol	Robarts Protocol-Received for Information	2013/12/19
Letter of Information & Consent	version 2	2013/12/19
Western University Protocol	including Study Design diagram	

This is to notify you that the University of Western Ontario Health Sciences Research Ethics Board (HSREB) which is organized and operates according to the Tri-Council Policy Statement: Ethical Conduct of Research Involving Humans and the Health Canada/ICH Good Clinical Practice Practices: Consolidated Guidelines; and the applicable laws and regulations of Ontario has reviewed and granted approval to the above referenced study on the approval date noted above. The membership of this HSREB also complies with the membership requirements for REB's as defined in Division 5 of the Food and Drug Regulations.

The ethics approval for this study shall remain valid until the expiry date noted above assuming timely and acceptable responses to the HSREB's periodic requests for surveillance and monitoring information. If you require an updated approval notice prior to that time you must request it using the University of Western Ontario Updated Approval Request form.

Member of the HSREB that are named as investigators in research studies, or declare a conflict of interest, do not participate in discussions related to, nor vote on, such studies when they are presented to the HSREB.

The Chair of the HSREB is Dr. Joseph Gilbert. The HSREB is registered with the U.S. Department of Health & Human Services under the IRB registration number IRB 00000940.

This is an official document. Please retain the original in your files.

Western Research

Use of Human Participants - Ethics Approval Notice

Principal Investigator: Dr. Grace Parraga
File Number:103516
Review Level: Full Board
Approved Local Adult Participants:200
Approved Local Minor Participants:0
Protocol Title: Structure and Function MRI of Asthma
Department & Institution: Schulich School of Medicine and Dentistry\Imaging,Robarts Research Institute
Sponsor:
Ethics Approval Date: April 08, 2013
Ethics Expiry Date: March 31, 2020

Documents Reviewed & Approved & Documents Received for Information:

Document Name	Comments	Version Date
Protocol	Robarts Protocol - Received for information only	2013/02/06
Instruments	Telephone Script	2013/03/14
Letter of Information & Consent	ROB0037 ICF March 13 2013	2013/03/13
Western University Protocol	(including study instruments & questionnaires)	

This is to notify you that the University of Western Ontario Health Sciences Research Ethics Board (HSREB) which is organized and operates according to the Tri-Council Policy Statement: Ethical Conduct of Research Involving Humans and the Health Canada/ICH Good Clinical Practice Practices: Consolidated Guidelines; and the applicable laws and regulations of Ontario has reviewed and granted approval to the above referenced study on the approval date noted above. The membership of this HSREB also complies with the membership requirements for REB's as defined in Division 5 of the Food and Drug Regulations.

The ethics approval for this study shall remain valid until the expiry date noted above assuming timely and acceptable responses to the HSREB's periodic requests for surveillance and monitoring information. If you require an updated approval notice prior to that time you must request it using the University of Western Ontario Updated Approval Request form.

Member of the HSREB that are named as investigators in research studies, or declare a conflict of interest, do not participate in discussions related to, nor vote on, such studies when they are presented to the HSREB.

The Chair of the HSREB is Dr. Joseph Gilbert. The HSREB is registered with the U.S. Department of Health & Human Services under the IRB registration number IRB 00000940.

This is an official document. Please retain the original in your files.

Western University, Research, Support Services Bldg., Rm. 5150
London, ON, Canada N6A 3K7 t. 519.661.3036 f. 519.850.2466 www.uwo.ca/research/services/ethics

APPENDIX C – Curriculum Vitae

EDUCATION

September 2007 – April 2011	Bachelor of Medical Science Honours Specialization Medical Biophysics (Medical Science Concentration) The University of Western Ontario, London, Ontario, Canada
September 2011 – November 2015	Doctor of Philosophy Department of Medical Biophysics, The University of Western Ontario, London, Ontario, Canada *Supervisor:* Dr. Grace Parraga *Thesis:* "Pulmonary Imaging of Asthma to Better understand the Asthmatic Lung and Guide Asthma Therapy"

RESEARCH POSITIONS

May 2009 – August 2009	**Undergraduate Research Assistant, Summer Research Assistantship** London Regional Cancer Program & Robarts Research Institute, London, Canada *Supervisor:* Dr. Brian Yaremko & Dr. Grace Parraga *Project:* Optimizing Radiation Treatment Plans for Lung Cancer Patients
September 2010 – April 2011	**Fourth Year Undergraduate Honours Thesis Student** Robarts Research Institute, London, Canada *Supervisor:* Dr. Grace Parraga *Project:* Quantitative Evaluation of Hyperpolarized ^{3}He Magnetic Resonance Imaging of Lung Function Variability in Cystic Fibrosis
May 2011 – August 2011	**Research Assistant, Summer Research Assistantship** Robarts Research Institute, London, Canada *Supervisor:* Dr. Grace Parraga *Project:* Hyperpolarized ^{3}He and ^{129}Xenon Magnetic Resonance Imaging of Asthma
September 2011 – November 2015	**Graduate Research Assistant, Doctoral** Department of Medical Biophysics**,** The University of Western Ontario, London, Canada *Supervisor:* Dr. Grace Parraga *Thesis:* Pulmonary Imaging of Asthma to Better understand the Asthmatic Lung and Guide Asthma Therapy

RESEARCH–SPECIFIC HONOURS, SCHOLARSHIPS AND AWARDS

2011 Western Graduate Research Scholarship, The University of Western Ontario

Awarded to a full time graduate student for stipend support who has maintained an average of 80% or more.

Institutional
$7,645 CAD

2012 Educational Stipend Award, International Society for Magnetic Resonance in Medicine (ISMRM)

Awarded to support the attendance of students, postdoctoral and clinical trainees to present abstracts at the international scientific meeting held in Melbourne, Australia.
International
$540 USD

2012 Natural Sciences and Engineering Research Council of Canada (NSERC), Canadian Graduate Scholarship – Masters (CGS-M)

Awarded to high-caliber scholars who are engaged in Master's programs, CGS is offered to the top-ranked applicants.
National
$17,500 CAD

2012 Ontario Graduate Scholarship *(Declined)*

A merit based scholarship (based on academic standing) that encourages excellence in graduate studies and is available to students in all disciplines of academic study.
Provincial
$15,000 CAD

2012 Western Graduate Research Scholarship, The University of Western Ontario

Awarded to a full time graduate student for stipend support who has maintained an average of 80% or more.
Institutional
$7,867 CAD

2013 Educational Stipend Award, International Society for Magnetic Resonance in Medicine (ISMRM)

Awarded to support the attendance of students, postdoctoral and clinical trainees to present abstracts at the international scientific meeting held in Salt Lake City, Utah, USA.
International
$440 USD

2013 London Health Research Day Poster Award (1st place), Schulich School of Medicine and Dentistry, The University of Western Ontario

Awarded to the top poster presenter in the Imaging category.
Institutional
$500 CAD

Lawson Internal Research Fund Spring 2013 Studentship Award

2013 *Successful grant application reviewed and awarded by the Lawson Health Research Institute (LHRI).*

Institutional

$15,000

2013 Radiological Society of North America (RSNA) Trainee Research Prize Competition Finalist

Awarded to the highest ranked abstracts submitted for the RSNA Trainee Research Prize.
International
$0

2013 Western Graduate Research Scholarship, The University of Western Ontario

Awarded to a full time graduate student for stipend support who has maintained an average of 80% or more.
Institutional
$7,975

2013 Dean's MSc Transfer to PhD Stipend for Graduate Research, Schulich School of Medicine and Dentistry, The University of Western Ontario

Awarded to two students annually by Dean Michael Strong. Recipients must have successfully transferred from the MSc to PhD program, have an outstanding academic record and have demonstrate research excellence.
Institutional
$15,000

2014 Educational Stipend Award, International Society for Magnetic Resonance in Medicine (ISMRM)

Awarded to support the attendance of students, postdoctoral and clinical trainees to present abstracts at the international scientific meeting held in Milan, Italy.
International
$435 USD

2014 London Health Research Day Platform Presentation Award (2nd place), Schulich School of Medicine and Dentistry, The University of Western Ontario

Awarded to the top platform presenters who presented first author original research abstracts.
Institutional
$600

2014 Canadian Institutes of Health Research (CIHR) National Student Research Poster Competition Participant

Nominated by the University of Western Ontario as being within the top 5% of doctoral students in the field of health sciences.
National
$0

2014 International Society of Magnetic Resonance in Medicine (ISMRM) Merit Award Summa Cum Laude

Awarded to those whose abstract score was in the top 5% of those submitted for review to be presented at the annual international meeting.
International

$0

2014 Ontario Graduate Scholarship

A merit based scholarship (based on academic standing) that encourages excellence in graduate studies and is available to students in all disciplines of academic study.
Provincial
$15,000 CAD

2014 Canadian Institutes of Health Research (CIHR) Canadian Student Health Research Forum Funding Competition

Selected by CIHR to receive funding to reimburse travel and accommodations for participation in the 2014 Canadian Student Health Research Forum in Winnipeg, Canada.
National
$833

2014 Award of Excellence (Silver category) in the Canadian Institutes of Health Research (CIHR) National Research Poster Competition

Awarded to the top poster presenters who presented first author original research abstracts.
National
$250

2014 Nellie Farthing Fellowship in Medical Sciences, Schulich School of Medicine and Dentistry, The University of Western Ontario

Established in 1960 to recognize a full-time doctoral student in the Medical Sciences, selection for this award is based on research excellence. One fellowship is awarded annually.
Institutional
$3,000

2014 Canadian Respiratory Research Network (CRRN) PhD Fellowship, Canadian Lung Association/Canadian Thoracic Society

Awarded to PhD candidates based on their grant proposal, academic excellence & research potential. Up to two fellowships are awarded annually.
National
$22,000 CAD

2015 Ontario Institute for Cancer Research (OICR) Imaging Translation Program Poster Presentation Winner (2nd Place), Imaging Network Ontario Symposium

Awarded to the top poster presenters at the 13th annual Imaging Network of Ontario Symposium.
National
$300 CAD

2015 National Emphysema Foundation Abstract Scholarship honouring Claude Lenfant, 2015 American Thoracic Society (ATS) International Conference

Awarded to the first author of the top ranked abstract presented at the annual international meeting held in Denver, Colorado, USA.
International
$500 USD

2015 International Society of Magnetic Resonance in Medicine (ISMRM) Merit Award Magna Cum Laude

Awarded to those whose abstract score was in the top 15% of those submitted for review to be presented at the annual international meeting.
International

2015 Drs. Madge and Charles Macklin Fellowship for Publication in Medical Sciences

Awarded based on the significance of the candidate's 1st author publication in a high impact peer reviewed journal. Up to two fellowships are awarded annually.
Institutional
$4,250 CAD

OTHER HONOURS, SCHOLARSHIPS AND AWARDS

2007 Western Scholarship of Excellence, The University of Western Ontario

Awarded upon admission to Western students who have an entrance average of 90-94.9%.
Institutional
$2,000

PUBLICATIONS and PRESENTATIONS

A. Refereed Journal Manuscripts (17 published, 1 in press, 1 in preparation)

Published (17)

1. M Kirby, **S Svenningsen**, H Ahmed, NAM Paterson and G Parraga. Quantitative Evaluation of Hyperpolarized Helium-3 Magnetic Resonance Imaging of Lung Function Variability in Cystic Fibrosis. *Acad Radiol.* 2011 Aug; 18(8):1006-13. doi: 10.1016/j.acra.2011.03.005.

2. M Kirby, M Heydarian, **S Svenningsen,** A Wheatley, DG McCormack, R Etemad-Rezai and G Parraga. Hyperpolarized ^{3}He Magnetic Resonance Functional Imaging Semiautomated Segmentation. *Acad Radiol.* 2012 Feb; 19(2):141-52. doi: 10.1016/j.acra.2011.10.007.

3. Y Shukla, A Wheatley, M Kirby, **S Svenningsen**, A Farag, G Santyr, NAM Paterson, DG McCormack and G Parraga. Hyperpolarized ^{129}Xe Magnetic Resonance Imaging: Tolerability in Healthy Volunteers and Subjects with Pulmonary Disease. *Acad Radiol.* 2012 Aug; 19(8):941-51. doi: 10.1016/j.acra.2012.03.018.

4. M Kirby, **S Svenningsen**, A Owrangi, A Wheatley, A Farag, A Ouriadov, GE Santyr, R Etemad-Rezai, HO Coxson, DG McCormack and G Parraga. Hyperpolarized Helium-3 and Xenon-129 Magnetic Resonance Imaging in Healthy

Volunteers and Subjects with Chronic Obstructive Pulmonary Disease. *Radiology.* 2012 Nov; 265(2):600-10. doi: 10.1148/radiol.12120485.

5. M Kirby, **S Svenningsen**, N Kanhere, A Owrangi, A Wheatley, HO Coxson, GE Santyr, NAM Paterson, DG McCormack and G Parraga. Pulmonary Ventilation Visualized using Hyperpolarized Helium-3 and Xenon-129 Magnetic Resonance Imaging: Differences in COPD and Relationship to Emphysema. *J Appl Physiol.* 2013 Mar 15;114(6):707-15. doi: 10.1152/japplphysiol.01206.2012.
6. **S Svenningsen,** M Kirby, D Starr, D Leary, A Wheatley, GN Maksym, DG McCormack and G Parraga. Hyperpolarized ^{3}He and ^{129}Xe MRI: Differences in asthma before bronchodilation. *J Magn Reson Imaging.* 2013 Dec;38(6):1521-30. doi: 10.1002/jmri.24111.
7. M Kirby, A Owrangi, **S Svenningsen**, A Wheatley, HO Coxson, NAM Paterson, DG McCormack and G Parraga. On the role of abnormal DLCO in ex-smokers without airflow limitation: symptoms, exercise capacity and hyperpolarised helium-3 MRI. *Thorax*. 2013 Aug;68(8):752-9. doi: 10.1136/thoraxjnl-2012-203108.
8. **S Svenningsen,** M Kirby, D Starr, HO Coxson, NAM Paterson, DG McCormack and G Parraga. What are ventilation defects in asthma? *Thorax*. 2014 Jan;69(1):63-71. doi: 10.1136/thoraxjnl-2013-203711. ***This manuscript was editorialized and featured on the cover of the journal.
9. W Ma, K Sheikh, **S Svenningsen**, D Pike, F Guo, R Etemad-Reza, J Leipsic, HO Coxson, DG McCormack and G Parraga. Ultra-short Echo-time Pulmonary Magnetic Resonance Imaging: Evaluation and Reproducibility in COPD subjects with and without Bronchiectasis. *J Magn Reson Imaging.* 2014 June 26. doi: 10.1002/jmri.24680.
10. K Sheikh, G Paulin, **S Svenningsen**, M Kirby, NAM Paterson, DG McCormack and G Parraga. Pulmonary Ventilation Defects in Older Never-Smokers. *J Appl Physiol.* 2014 Aug 1;117(3):297-306. doi: 10.1152/japplphysiol.00046.2014.
11. M Kirby, A Ouriadov, **S Svenningsen,** A Owrangi, A Wheatley, R Etemad-Rezai, GE Santyr, DG McCormack and G Parraga. Hyperpolarized 3He and 129Xe Magnetic Resonance Imaging Apparent Diffusion Coefficients: Physiological Relevance in Older Never- and Ex-smokers. *Physio Rep.* 2014 Jul 16;2(7). Pii: e12068. doi: 10.14814/phy2.12068.
12. GA Paulin, **S Svenningsen**, B Jobse, S Mohan, M Kirby, J Lewis and G Parraga. Longitudinal Hyperpolarized ^{3}He Magnetic Resonance Imaging of Cystic Fibrosis. *J Magn Reson Imaging.* 2014 Aug 30. doi: 10.1002/jmri.24744.
13. **S Svenningsen**, F Guo, M Kirby, S Choy, DG McCormack and G Parraga. Pulmonary Functional Magnetic Resonance Imaging: Asthma Temporal-Spatial Maps. *Acad Radiol.* 2014 Nov;21(11):1402-10. doi: 10.1016/j.acra.2014.08.002.
14. DPI Capaldi, K Sheikh, F Guo, **S Svenningsen,** R Etemad-Rezai, J Leipsic, HO Coxson, DG McCormack and G Parraga. Free-breathing Pulmonary ^{1}H and

Hyperpolarized ^{3}He MRI: Comparison in COPD and Bronchiectasis. *Acad Radiol.* 2015 Mar;22(3):320-9. doi: 10.1016/j.acra.2014.10.003.

15. F Guo, J Yuan, M Rajchl, **S Svenningsen**, DPI Capaldi, K Sheikh, A Fenster and G Parraga. Globally Optimal Co-Segmentation of Three-dimensional Pulmonary ^{1}H and Hyperpolarized ^{3}He MRI with Spatial Consistence Prior. *Medical Image Analysis*. 2015 July;23(1):43-55. doi: 10.1016/j.media.2015.04.001.

16. **S Svenningsen**, GA Paulin, K Sheikh, F Guo, A Hasany, M Kirby, R Etemad-Rezai, DG McCormack and G Parraga. Oscillatory Positive Expiratory Pressure in Chronic Obstructive Pulmonary Disease. *COPD.* 2015 Oct:1-9. doi: 10.3109/15412555.2015.1043523.

17. N Zha, D Pike, **S Svenningsen**, DPI Capaldi, DG McCormack and G Parraga. Second-order Texture Measurements of ^{3}He Ventilation MRI: Proof of Concept Evaluation of Asthma Bronchodilator Response. *Acad Radiol.* 2015 Nov. doi: 10.1016/j.acra.2015.10.010.

In Press (1)

1. C Davis, D Pike, **S Svenningsen**, DG McCormack, D O'Donnell, A Neder and G Parraga. Ventilation Heterogeneity in Never-smokers and COPD: Comparison of Pulmonary Functional Magnetic Resonance Imaging with Poorly Communicating Fraction derived from Plethysmography. *Acad Radiol.* ***(Accepted 16/09/2015, Manuscript ID: Wed-15529)***

In Preparation (1)

1. **S Svenningsen,** P Nair, DG McCormack and G Parraga. What do Ventilation Defects Reveal about Asthma Control? *Radiology* (December 2015).

B. Published Refereed Conference Papers (3)

1. F Guo, D Pike, **S Svenningsen**, HO Coxson, JJ Drozd, J Yuan, A Fenster and G Parraga. Development and application of pulmonary structure-function registration methods: towards pulmonary image-guidance tools for improved airway targeted therapies and outcomes. *Proc SPIE*. 9038, Medical Imaging 2014: Biomedical Applications in Molecular, Structural, and Functional Imaging, 90380Y. (March 13, 2014) doi: 10.1117/12.2043534. (Conference Proceeding Publication)

2. F Guo, S **Svenningsen,** E Bluemke, M Rajchl, J Yuan, A Fenster and G Parraga. Automated pulmonary lobar ventilation measurements using volume-matched thoracic CT and MRI. *Proc SPIE*. 9417, Medical Imaging 2015: Biomedical Applications in Molecular, Structural, and Functional Imaging, 9417A. (March 17, 2015) doi: 10.1117/12.2076398. (Conference Proceeding Publication)

3. DPI Capaldi, **S Svenningsen,** IA Cunningham and G Parraga. Fourier-based linear systems description of free-breathing pulmonary magnetic resonance imaging. *Proc SPIE*. 9417, Medical Imaging 2015: Biomedical Applications in Molecular,

Structural, and Functional Imaging, 94171A. (March 17, 2015) doi: 10.1117/12.2081503. (Conference Proceeding Publication)

C. Peer Reviewed Published Conference Abstracts (39)

1. **S Svenningsen**, M Kirby, H Ahmed, NAM Paterson and G Parraga. Evaluation of Short Term Reproducibility of Hyperpolarized Helium-3 Magnetic Resonance Imaging in Adult Cystic Fibrosis using a Semi-Automated Segmentation Tool.
   International Society for Magnetic Resonance in Medicine Proceedings 2011:19, A907
2. **S Svenningsen**, M Kirby, A Wheatley, A Farag, A Ouriadov, GE Santyr, DG McCormack and G Parraga. Anatomical Distribution of Hyperpolarized ^{3}He and ^{129}Xe MRI Apparent Diffusion Coefficients in Asthma.
   International Society for Magnetic Resonance in Medicine Proceedings 2012:20, A4004
3. **S Svenningsen**, M Kirby, A Wheatley, A Ouriadov, GE Santyr, DG McCormack and G Parraga. Hyperpolarized ^{3}He and ^{129}Xe Magnetic Resonance Imaging of Asthma.
   American Journal of Respiratory and Critical Care Medicine, Vol. 185, Meeting Abstracts 2012: A5586, 10.1164/ajrccm-conference.2012.185.1_MeetingAbstracts.A5586
4. DG McCormack, S Halko, S McKay, M Kirby, **S Svenningsen**, A Wheatley, A Farag, GE Santyr and G Parraga. Hyperpolarized ^{129}Xe MRI Feasibility, Subject Safety and Tolerability: At the doorstep of Clinical Translation?
   American Journal of Respiratory and Critical Care Medicine, Vol. 185, Meeting Abstracts 2012: A2031, 10.1164/ajrccm-conference.2012.185.1_MeetingAbstracts.A2031
5. **S Svenningsen**, D Starr, HO Coxson, NAM Paterson, DG McCormack, M Kirby and G Parraga. Asthma Airway Morphology and Hyperpolarized ^{3}He Magnetic Resonance Imaging Ventilation Defects.
   International Society for Magnetic Resonance in Medicine Proceedings 2013:21, A1460
6. M Kirby, **S Svenningsen**, A Ouriadov, GE Santyr, DG McCormack and G Parraga. Diffusion-weighted Hyperpolarized ^{3}He and ^{129}Xe Magnetic Resonance Imaging of Elderly Never-smokers and Ex-smokers with Chronic Obstructive Pulmonary Disease.
   International Society for Magnetic Resonance in Medicine Proceedings 2013:21, A0819
7. K Sheikh, **S Svenningsen**, M Kirby, DG McCormack and G Parraga. Hyperpolarized ^{3}He Magnetic Resonance Imaging ADC Gradients in Healthy Elderly Never-Smokers.
   International Society for Magnetic Resonance in Medicine Proceedings 2013:21, A1462
8. **S Svenningsen**, M Kirby, S Choy, A Wheatley, DG McCormack and G Parraga. Temporal-Spatial Maps of Asthma Ventilation to Identify Therapy Targets.

American Journal of Respiratory and Critical Care Medicine, Vol. 187, Meeting Abstracts 2013: A1049, 10.1164/ajrccm-conference.2013.187.1_MeetingAbstracts.A1049

9. K Sheikh, **S Svenningsen**, M Kirby, DG McCormack and G Parraga. Hyperpolarized ^{3}He MRI Ventilation Defects in Healthy Elderly Never-Smokers: Response to Deep Inspiration and Salbutamol.
   American Journal of Respiratory and Critical Care Medicine, Vol. 187, Meeting Abstracts 2013: A3734, 10.1164/ajrccm-conference.2013.187.1_MeetingAbstracts.A3734
10. K Sheikh, **S Svenningsen**, M Kirby, NAM Paterson, A Wheatley, DG McCormack and G Parraga. What is the Relationship between Hyperpolarized ^{3}He MRI Measurements, Airborne Toxin Exposure, and Exercise Capacity in Healthy Elderly Never-Smokers?
    American Journal of Respiratory and Critical Care Medicine, Vol. 187, Meeting Abstracts 2013: A4893, 10.1164/ajrccm-conference.2013.187.1_MeetingAbstracts.A4893
11. **S Svenningsen,** M Kirby, J Suggett, N Kanhere, A Hasany, DG McCormack and G Parraga. Oscillatory Positive Expiratory Pressure (oPEP) Treatment in Chronic Obstructive Pulmonary Disease.
    Chest 2013;144(4_MeetingAbstracts):741A. doi:10.1378/chest.1698587
12. **S Svenningsen,** M Kirby, A Wheatley, DG McCormack and G Parraga. Hyperpolarized ^{3}He Magnetic Resonance Imaging Temporal-spatial Maps of Asthma to Guide Endobronchial Thermo-ablation.
    Radiological Society of North America 2013 Scientific Assembly and Annual Meeting, Chicago IL, USA. http://archive.rsna.org/2013/13020527.html
13. D Pike, M Kirby, **S Svenningsen**, HO Coxson, DG McCormack and G Parraga. Are Hyperpolarized ^{3}He Magnetic Resonance Imaging Ventilation Defects Clinically Relevant in Ex-smokers without Airflow Limitation?
    Radiological Society of North America 2013 Scientific Assembly and Annual Meeting, Chicago IL, USA. http://archive.rsna.org/2013/13016112.html
14. **S Svenningsen**, GA Paulin, M Kirby, N Kanhere, R Etemad-Rezai, DG McCormack and G Parraga. Pulmonary Functional MRI to Phenotype COPD and Evaluate Treatment Efficacy: Intermediate Endpoints and Predictors of Efficacy when Conventional endpoints fail?
    International Society for Magnetic Resonance in Medicine Proceedings 2014:22, A0772
15. K Sheikh, W Ma, F Guo, **S Svenningsen**, TM Peters, HO Coxson, DG McCormack, R Etemad-Rezai and G Parraga. Two Dimensional Radial Pulmonary Ultra-short Echo Time ^{1}H MRI: Reproducibility in COPD and Bronchiectasis.
    International Society for Magnetic Resonance in Medicine Proceedings 2014:22, A2280
16. DPI Capaldi, F Guo, **S Svenningsen**, W Ma, K Sheikh, R Etemad-Rezai, J Leipsic, HO Coxson, DG McCormack and G Parraga. Comparison of Pulmonary ^{1}H non-contrast and Hyperpolarized ^{3}He MRI Ventilation Abnormalities in Bronchiectasis and COPD.

International Society for Magnetic Resonance in Medicine Proceedings 2014:22, A2281

17. **S Svenningsen**, GA Paulin, D Pike, S Mohan, DG McCormack and G Parraga. Pulmonary Functional Imaging of Bronchiectasis: A First Look at Ventilation Abnormalities and their Relationship with Pulmonary Function and Symptoms.
    American Journal of Respiratory and Critical Care Medicine, Vol. 189, Meeting Abstracts 2014: A3619, 10.1164/ajrccm-conference.2014.189.1_MeetingAbstracts.A3619
18. **S Svenningsen**, GA Paulin, DG McCormack and G Parraga. Ventilation Abnormalities in Chronic Bronchitis and Bronchiectasis: Is there a difference?
    American Journal of Respiratory and Critical Care Medicine, Vol. 189, Meeting Abstracts 2014: A3570, 10.1164/ajrccm-conference.2014.189.1_MeetingAbstracts.A3570
19. M Stankiewicz, **S Svenningsen**, GA Paulin, G Maksym, DG McCormack and G Parraga. Respiratory Resistance in Bronchiectasis and COPD using the Forced Oscillation Technique.
    American Journal of Respiratory and Critical Care Medicine, Vol. 189, Meeting Abstracts 2014: A3621, 10.1164/ajrccm-conference.2014.189.1_MeetingAbstracts.A3621
20. GA Paulin, **S Svenningsen**, S Mohan, BN Jobse, M Kirby, JF Lewis and G Parraga. Longitudinal Hyperpolarized ^{3}He Magnetic Resonance Imaging of Adult Cystic Fibrosis: Pilot Study results.
    American Journal of Respiratory and Critical Care Medicine, Vol. 189, Meeting Abstracts 2014: A2833, 10.1164/ajrccm-conference.2014.189.1_MeetingAbstracts.A2833
21. GA Paulin, **S Svenningsen**, JF Lewis, DG McCormack and G Parraga. Hyperpolarized ^{3}He MRI Ventilation Abnormalities of Cystic Fibrosis and Non-Cystic Fibrosis Bronchiectasis.
    American Journal of Respiratory and Critical Care Medicine, Vol. 189, Meeting Abstracts 2014: A2834, 10.1164/ajrccm-conference.2014.189.1_MeetingAbstracts.A2834
22. S Mohan, GA Paulin, **S Svenningsen**, JF Lewis and G Parraga. Can Pulmonary Functional Imaging Guide Therapy of Cystic Fibrosis Pulmonary Exacerbations?
    American Journal of Respiratory and Critical Care Medicine, Vol. 189, Meeting Abstracts 2014: A2831, 10.1164/ajrccm-conference.2014.189.1_MeetingAbstracts.A2831
23. W Ma, K Sheikh, D Pike, **S Svenningsen**, HO Coxson, DG McCormack and G Parraga. Conventional Pulmonary MRI and CT of Bronchiectasis and Emphysema: Tissue Density Measurements and Relationship to Pulmonary Function Tests.
    American Journal of Respiratory and Critical Care Medicine, Vol. 189, Meeting Abstracts 2014: A2399, 10.1164/ajrccm-conference.2014.189.1_MeetingAbstracts.A2399
24. DPI Capaldi, K Sheikh, GA Paulin, **S Svenningsen**, HO Coxson, DG McCormack and G Parraga. Conventional non-contrast MRI of Ventilation Abnormalities in Bronchiectasis: New Tools and Measurements for an old Disease.

American Journal of Respiratory and Critical Care Medicine, Vol. 189, Meeting Abstracts 2014: A2400, 10.1164/ajrccm-conference.2014.189.1_MeetingAbstracts.A2400

25. D Pike, M Kirby, **S Svenningsen**, DD Sin, DG McCormack, HO Coxson and G Parraga. Pulmonary Computed Tomography and ^{3}He Magnetic Resonance Imaging of GOLD Unclassified Ex-smokers: Does Imaging Matter?
    American Journal of Respiratory and Critical Care Medicine, Vol. 189, Meeting Abstracts 2014: A5956, 10.1164/ajrccm-conference.2014.189.1_MeetingAbstracts.A5956
26. **S Svenningsen,** GA Paulin, A Wheatley, D Pike, J Suggett, DG McCormack and G Parraga. Oscillating Positive Expiratory Pressure Therapy in Chronic Obstructive Pulmonary Disease and Bronchiectasis.
    European Respiratory Journal 2014; 44: Suppl. 58 A3679
27. DPI Capaldi, F Guo, **S Svenningsen**, DG McCormack and G Parraga. Fourier-decomposition Pulmonary Magnetic Resonance Imaging Ventilation Defects in Ex-smokers: Relationship to Emphysema and ^{3}He ventilation defects.
    Radiological Society of North America 2014 Scientific Assembly and Annual Meeting, Chicago IL, USA. http://archive.rsna.org/2014/14018829.html
28. **S Svenningsen,** DPI Capaldi, E Bluemke, GA Paulin, C Davis, K Sheikh, DG McCormack and G Parraga. Lung Clearance Index and Hyperpolarized ^{3}He MRI Ventilation Heterogeneity Measurements in Non-CF Bronchiectasis and COPD.
    American Journal of Respiratory and Critical Care Medicine, Vol. 191, Meeting Abstracts 2015: A2255, 10.1164/ajrccm-conference.2015.191.1_MeetingAbstracts.A2255
29. K Sheikh, GA Paulin, **S Svenningsen,** DG McCormack, JA Neder and G Parraga. How do Exercise Responses Relate to ^{3}He Magnetic Resonance Imaging Apparent Diffusion Coefficients in Older Never-Smokers?
    American Journal of Respiratory and Critical Care Medicine, Vol. 191, Meeting Abstracts 2015: A2124, 10.1164/ajrccm-conference.2015.191.1_MeetingAbstracts.A2124
30. DPI Capaldi, **S Svenningsen,** P Nair, DG McCormack and G Parraga. Ventilation Heterogeneity in Severe Asthma: Effects of Prednisone and Salbutamol before Bronchial Thermoplasty.
    American Journal of Respiratory and Critical Care Medicine, Vol. 191, Meeting Abstracts 2015: A1213, 10.1164/ajrccm-conference.2015.191.1_MeetingAbstracts.A1213
31. C Davis, D Pike, **S Svenningsen,** DG McCormack, D O'Donnell, JA Neder and G Parraga. Ventilation Heterogeneity in Older Never-Smokers and GOLD stage I-IV COPD: Poorly Communicating Fraction and MRI Ventilation defects in the TINCan Cohort.
    American Journal of Respiratory and Critical Care Medicine, Vol. 191, Meeting Abstracts 2015: A2274, 10.1164/ajrccm-conference.2015.191.1_MeetingAbstracts.A2274

32. E Bluemke, **S Svenningsen,** K Sheikh, GA Paulin, DG McCormack and G Parraga. Relationship of Ventilation Heterogeneity in the Conducting and Acinar Airway Zones with ^{3}He MRI in Elderly Never-Smokers.
    American Journal of Respiratory and Critical Care Medicine, Vol. 191, Meeting Abstracts 2015: A3515, 10.1164/ajrccm-conference.2015.191.1_MeetingAbstracts.A3515

33. **S Svenningsen,** F Guo, R Etemand-Rezai, DG McCormack and G Parraga. Automated Registration-Segmentation Pipeline to Generate Lobar Ventilation Measurements in Diffuse and Localized Bronchiectasis.
    International Society for Magnetic Resonance in Medicine Proceedings 2015:23, A3970

34. DPI Capaldi, K Sheikh, **S Svenningsen**, D Pike, DG McCormack and G Parraga. MRI Measurements of Regional Ventilation Heterogeneity: Ventilation Defect Clusters.
    International Society for Magnetic Resonance in Medicine Proceedings 2015:23, A3986

35. K Sheikh, DPI Capaldi, **S Svenningsen,** DG McCormack and G Parraga. Ultra-short Echo Time MRI Measurements of Emphysema using Principal Component Analysis.
    International Society for Magnetic Resonance in Medicine Proceedings 2015:23, A1479

36. F Guo, **S Svenningsen,** A Fenster and G Parraga. Three-Dimensional Pulmonary ^{1}H MRI Multi-Region Segmentation Using Convex Optimization.
    International Society for Magnetic Resonance in Medicine Proceedings 2015:23, A0851

37. **S Svenningsen,** B Driehuys, DG McCormack and G Parraga. Functional MRI Ventilation Discriminates Asthmatic and Healthy Subjects: Sensitivity, Specificity and Comparison with $FEV_{1.}$
    International Society for Magnetic Resonance in Medicine Proceedings 2015:23, A3989

38. **S Svenningsen**, DPI Capaldi, P Nair, DG McCormack and G Parraga. Linking Ventilation Heterogeneity and Asthma Control: Out with the Old and in with the New?
    7th International Workshop on Pulmonary Functional Imaging Proceedings 2015

39. F Guo, **S Svenningsen**, A Fenster and G Parraga. Automated Identification of Spatial Relationship between CT Airway and ^{3}He MRI Ventilation Defects: Towards Airway-Targeted Asthma Bronchial Thermoplasty.
    7th International Workshop on Pulmonary Functional Imaging Proceedings 2015

D. Peer Reviewed Oral Presentations (10) **presenter*

1. **S Svenningsen***, M Kirby, H Ahmed, NAM Paterson and G Parraga. Hyperpolarized Helium-3 Magnetic Resonance Imaging of Cystic Fibrosis Lung Function

Variability. 10th Imaging Network Ontario Symposium, Toronto, Ontario, Canada (02/12)

2. **S Svenningsen*,** D Starr, HO Coxson, NAM Paterson, DG McCormack, M Kirby and G Parraga. Asthma Airway Morphology and Hyperpolarized ^{3}He Magnetic Resonance Imaging Ventilation Defects**.** 11th Imaging Network Ontario Symposium, Toronto, Canada (02/13)

3. **S Svenningsen***, M Kirby, S Choy, A Wheatley, DG McCormack and G Parraga. Temporal-Spatial Maps of Asthma Ventilation to Identify Therapy Targets. International Conference of the American Thoracic Society Meeting, Philadelphia, Pennsylvania, USA (05/13)

4. **S Svenningsen*,** M Kirby, J Suggett, N Kanhere, A Hasany, DG McCormack and G Parraga. Oscillatory Positive Expiratory Pressure (oPEP) Treatment in Chronic Obstructive Pulmonary Disease. CHEST Annual Meeting, Chicago, IL, USA (10/13)

5. **S Svenningsen*,** M Kirby, A Wheatley, DG McCormack and G Parraga. Hyperpolarized ^{3}He Magnetic Resonance Imaging Temporal-spatial Maps of Asthma to Guide Endobronchial Thermo-ablation. Radiological Society of North America (RSNA) Annual Meeting, Chicago, IL, USA (12/13)

6. **S Svenningsen***, GA Paulin, D Pike, S Mohan, DG McCormack and G Parraga. Pulmonary Functional Imaging of Bronchiectasis: A First Look at Ventilation Abnormalities and their Relationship with Pulmonary Function and Symptoms. 12th Imaging Network Ontario Symposium, Toronto, Canada (03/14)

7. **S Svenningsen***, GA Paulin, D Pike, S Mohan, DG McCormack and G Parraga. Pulmonary Functional Imaging of Bronchiectasis: A First Look at Ventilation Abnormalities and their Relationship with Pulmonary Function and Symptoms. London Health Research Day, London, Canada (03/14)

8. **S Svenningsen***, GA Paulin, M Kirby, N Kanhere, R Etemad-Rezai, DG McCormack and G Parraga. Pulmonary Functional MRI to Phenotype COPD and Evaluate Treatment Efficacy: Intermediate Endpoints and Predictors of Efficacy when Conventional endpoints fail? International Society for Magnetic Resonance in Medicine Meeting, Milan, Italy (05/14)

9. **S Svenningsen***, GA Paulin, D Pike, S Mohan, DG McCormack and G Parraga. Pulmonary Functional Imaging of Bronchiectasis: A First Look at Ventilation Abnormalities and their Relationship with Pulmonary Function and Symptoms. International Conference of the American Thoracic Society Meeting, San Diego, California, USA (05/14)

10. **S Svenningsen***, DPI Capaldi, P Nair, DG McCormack and G Parraga. Linking Ventilation Heterogeneity and Asthma Control: Out with the Old and in with the New? 7th International Workshop on Pulmonary Functional Imaging, Edinburgh, Scotland (09/15)

E. Peer Reviewed Poster Presentations (15) **presenter*

1. **S Svenningsen***, M Kirby, H Ahmed, NAM Paterson and G Parraga. Evaluation of Short Term Reproducibility of Hyperpolarized Helium-3 Magnetic Resonance Imaging in Adult Cystic Fibrosis using a Semi-Automated Segmentation Tool. International Society for Magnetic Resonance in Medicine, Montreal, Quebec, Canada (05/11)

2. **S Svenningsen***, M Kirby, H Ahmed, NAM Paterson and G Parraga. Hyperpolarized ^{3}He MRI of Cystic Fibrosis Lung Function Variability. London Imaging Discovery Day, London, Ontario, Canada (07/11)

3. **S Svenningsen***, M Kirby, A Wheatley, A Ouriadov, GE Santyr, DG McCormack and G Parraga. Comparison of Hyperpolarized ^{3}He and ^{129}Xe Magnetic Resonance Imaging of Asthma: Pre- and Post-Salbutamol. London Health Research Day, London, Ontario, Canada (03/12)

4. **S Svenningsen***, M Kirby, A Wheatley, A Farag, A Ouriadov, GE Santyr, DG McCormack and G Parraga. Anatomical Distribution of Hyperpolarized ^{3}He and ^{129}Xe MRI Apparent Diffusion Coefficients in Asthma. International Society for Magnetic Resonance in Medicine, Melbourne, Australia (05/12)

5. **S Svenningsen***, M Kirby, A Wheatley, A Ouriadov, GE Santyr, DG McCormack and G Parraga. Hyperpolarized ^{3}He and ^{129}Xe Magnetic Resonance Imaging of Asthma. International Conference of the American Thoracic Society Meeting, San Francisco, California, USA (05/12)

6. **S Svenningsen***, M Kirby, A Wheatley, A Ouriadov, GE Santyr, DG McCormack and G Parraga. Comparison of Hyperpolarized ^{3}He and ^{129}Xe Magnetic Resonance Imaging of Asthma: Pre- and Post-Salbutamol. London Imaging Discovery Day, London, Ontario, Canada (06/12)

7. **S Svenningsen***, M Kirby, D Starr, HO Coxson, NAM Paterson, DG McCormack and G Parraga. Asthma Airway Morphology and Hyperpolarized ^{3}He Magnetic Resonance Imaging Ventilation Defects. London Healthy Research Day, London, Ontario, Canada (03/13)

8. **S Svenningsen***, D Starr, HO Coxson, NAM Paterson, DG McCormack, M Kirby and G Parraga. Asthma Airway Morphology and Hyperpolarized ^{3}He Magnetic Resonance Imaging Ventilation Defects. International Society for Magnetic Resonance in Medicine Meeting, Salt Lake City, Utah, USA (05/13)

9. **S Svenningsen***, GA Paulin, DG McCormack and G Parraga. Ventilation Abnormalities in Chronic Bronchitis and Bronchiectasis: Is there a difference? International Conference of the American Thoracic Society Meeting, San Diego, California, USA (05/14)
10. **S Svenningsen*,** GA Pauline, A Wheatley, D Pike, J Suggett, DG McCormack and G Parraga. Oscillating Positive Expiratory Pressure Therapy in Chronic Obstructive Pulmonary Disease and Bronchiectasis. European Respiratory Society International Congress Meeting, Munich, Germany (09/14)

11. **S Svenningsen*,** DPI Capaldi, E Bluemke, GA Paulin, C Davis, K Sheikh, DG McCormack and G Parraga. Lung Clearance Index and Hyperpolarized ^{3}He MRI Ventilation Heterogeneity Measurements in Non-CF Bronchiectasis and COPD. International Conference of the American Thoracic Society Meeting, Denver, Colorado, USA (05/15)

12. E Bluemke, **S Svenningsen*,** K Sheikh, GA Paulin, DG McCormack and G Parraga. Relationship of Ventilation Heterogeneity in the Conducting and Acinar Airway Zones with ^{3}He MRI in Elderly Never-Smokers. International Conference of the American Thoracic Society Meeting, Denver, Colorado, USA (05/15)

13. DPI Capaldi, **S Svenningsen*,** P Nair, DG McCormack G Parraga. Ventilation Heterogeneity in Severe Asthma: Effects of Prednisone and Salbutamol before Bronchial Thermoplasty. International Conference of the American Thoracic Society Meeting, Denver, Colorado, USA (05/15)

14. **S Svenningsen*,** B Driehuys, DG McCormack and G Parraga. Functional MRI Ventilation Discriminates Asthmatic and Healthy Subjects: Sensitivity, Specificity and Comparison with $FEV_{1.}$ International Society for Magnetic Resonance in Medicine Meeting, Toronto, Canada (06/15)

15. **S Svenningsen*,** F Guo, R Etemand-Rezai, DG McCormack and G Parraga. Automated Registration-Segmentation Pipeline to Generate Lobar Ventilation Measurements in Diffuse and Localized Bronchiectasis. International Society for Magnetic Resonance in Medicine Meeting, Toronto, Canada (06/15)

POST-GRADUATE EDUCATIONAL DEVELOPMENT

January 2013 – May 2013	**Graduate Teaching Assistant** 9550 Principles of Communication and Knowledge Translation for Biomedical Engineers Graduate Program in Biomedical Engineering The University of Western Ontario, London, Canada
March 2013 – June 2015	**Graduate Marking Assistant** Respiration and Airways (Year 1) Department of Medicine The University of Western Ontario, London, Canada
May 2012-November 2015	**Graduate Student Supervisor** Danielle Starr, B.Eng. *Summer Student (May 2012-August 2012)* *Project: Measurement of CT Airways in Asthma* Michal Stankiewicz, 4th year Medical Biophysics, UWO *Undergraduate Student (May 2013-May 2014)* *Project: Forced Oscillation Measurements of Respiratory Resistance in COPD* Gregory Paulin, B.MSc., Medical Biophysics MSc Candidate, UWO

Masters Student (May 2013-May 2014)
Project: Differences in Hyperpolarized ^{3}He Ventilation Imaging after 4 years in Cystic Fibrosis

Emma Bluemke, 2nd year Medical Biophysics, UWO
Undergraduate Student (May 2014-May 2015)
Project: Relating Multiple Breath Nitrogen Washout and ^{3}He MRI

Megan Fennema, 4th year Biomedical Engineering, UOG
Co-op Student (May 2015-November 2015)
Project: On the role of airways disease as a predictor of asthma control in severe asthmatics using FOT and MRI

Rachel Eddy, B.Eng., Medical Biophysics MSc Candidate, UWO
Masters Student (May 2015-November 2015)
Project: Image-guided asthma treatment

RESEARCH FUNDING APPLICATIONS

Grants

Canadian Lung Association National Grant Review *(Unsuccessful)*
Proposal: Pulmonary Functional Imaging of Asthma Pre- and Post-Bronchial Thermoplasty
December 2013

Lawson Health Research Institute Spring 2013 Internal Research Fund *(Successful)*
Hyperpolarized Gas Magnetic Resonance Imaging of Severe Asthma: The Effect of Bronchial Thermoplasty on Regional Lung Function
May 2013

PROFESSIONAL MEMBERSHIPS

2008 – 2015	Canadian Organization of Physicists in Medicine *Student Member*
2010 – 2015	American Thoracic Society *Student Member*
2010 – 2015	International Society of Magnetic Resonance in Medicine *Student Member*
2012 – 2015	Canadian Thoracic Society *Student Member*